Studies Towards Sustainable Syntheses of *Schisandra* Triterpenes



Pavle Kravljanac

Merton College

University of Oxford

A thesis submitted to the Board of the Faculty of Physical Sciences

in partial fulfilment of the requirements for the degree of

Doctor of Philosophy

Trinity 2024

Abstract

Triterpenes from the *Schisandraceae* family, have attracted the attention of the synthetic community due to their intricate structures and potential anti-HIV bioactivity. However, the previous syntheses of these molecules were hampered by lengthy routes, inefficient strategies, toxic and hazardous chemicals and excessive protecting groups and chromatographic purifications. Here we describe efforts to address these limitations by employing strategies that achieve efficient, scalable and sustainable syntheses of the key building blocks towards lancifodilactone I and rubriflordilactones A and B.

Our AB ring synthesis introduces a novel paradigm for tetrahydrofuran ring formation through a strategic ring expansion rearrangement of a cyclobutanol, which is derived from a cyclobutene-containing terpene chiral pool starting material. This resulted in a highly efficient scalable synthesis of the AB rings in only 7 steps, devoid of chromatographic separations, with just two crystallisations required.

Our FG ring synthesis explored the reactivity of an unusual vinylogous ester within a locked cis-decalin system, obtained via concise synthetic sequence from a carbohydrate chiral pool. However, the unanticipated challenges of ketone alpha-methylation in this bicyclic system hindered the continuation of this approach.

Our diyne fragment features the use of organogermanium chemistry to distinguish between two similar alkynes. This streamlined approach resulted in the synthesis of the diyne fragment in 9 steps. Unification of the AB rings and the diyne fragment constitutes a formal synthesis of rubriflordilactone A in 17 steps (LLS).

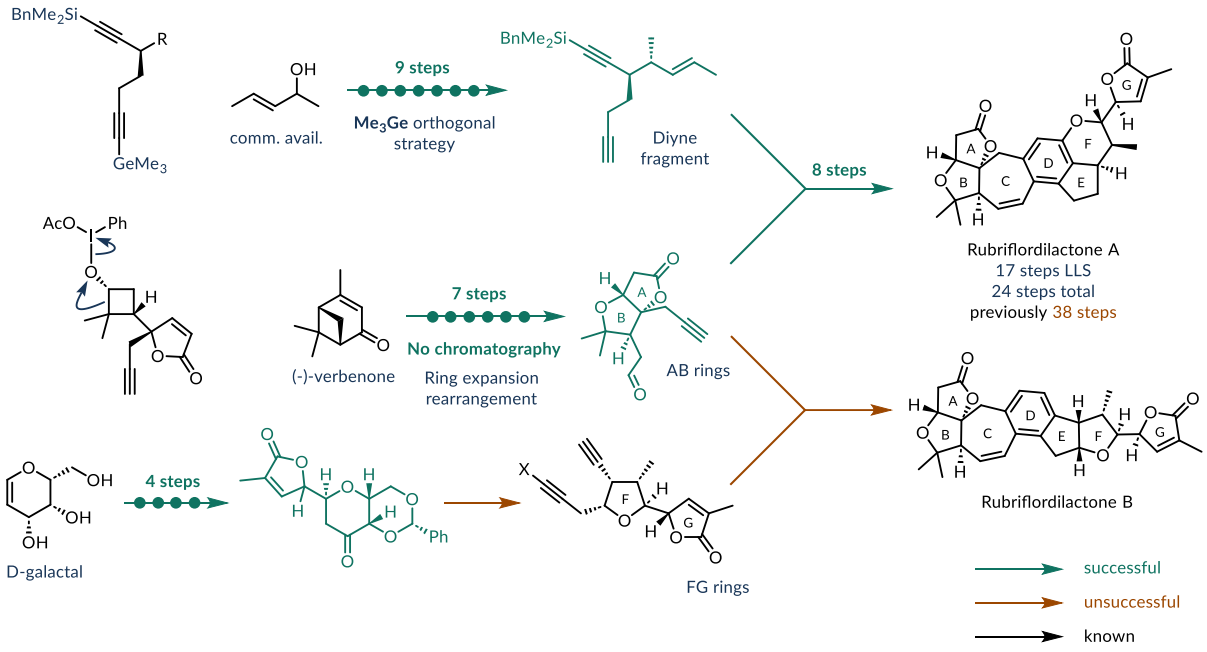

BnMe2Si
R
GeMe3
OH
comm. avail.
9 steps
Me3Ge orthogonal strategy
BnMe2Si
Diyne fragment
8 steps
Rubriflordilactone A
17 steps LLS
24 steps total
previously 38 steps
AcO
Ph
(-)-verbenone
7 steps
No chromatography
Ring expansion rearrangement
AB rings
D-galactal
4 steps
FG rings
Rubriflordilactone B
successful
unsuccessful
known

Table of contents

Acknowledgements ..... **i**
Abbreviations and legend ..... **ii**
Chapter 1: Introduction **1**
1.1 Thesis summary 1
1.2 Overview of synthetic efficiency, scalability and sustainability 3
1.3 Our approach to total synthesis 5
1.4 Overview of Schisandra triteprenes 8
1.5 Previous syntheses and synthetic studies 9
1.6 Z. Yang's racemic synthesis of schindilactone A (2011) 11
1.6.1 Overview of the strategy *11*
1.6.2 Forward synthesis *12*
1.7 A. Li's synthesis of rubriflordilactone A (2014) 17
1.7.1 Overview of the strategy *17*
1.7.2 Synthesis of the ABC fragment *18*
1.7.3 Synthesis of the EF fragment *19*
1.7.4 Fragments unification and completion of the synthesis *20*
1.8 E. Anderson's synthesis of rubriflordilactone A (2015) 22
1.8.1 Overview of the strategy *22*
1.8.2 Synthesis of the AB rings *23*
1.8.3 Synthesis of the diyne fragment *24*
1.8.4 Fragment unification and completion of the synthesis *25*
1.9 X. Chen's racemic synthesis of rubriflordilactone A (2024) 27
1.9.1 Overview of the strategy *27*
1.9.2 Forward synthesis *28*
1.10 A. Li's synthesis of rubriflordilactone B (2016) 31
1.10.1 Overview of the strategy *31*
1.10.2 Synthesis of the EFG fragment *32*
1.10.3 Completion of the synthesis *33*
1.11 E. Anderson's synthesis of rubriflordilactone B (2019) 34
1.11.1 Overview of the strategy *34*
1.11.2 Synthesis of the FG fragment *35*
1.11.3 Completion of the synthesis *37*
1.12 A. Hoveyda's synthesis of the AB rings (2020) 38
1.13 Our approach to the *Schisandra* triterpenes 40

Chapter 2: Cyclisation cascade toward lancifodilactone I 42
2.1 Carbopalladation, Suzuki coupling and electrocyclisation cascade 42
2.2 Synthesis of 5,6-fused systems 44
2.3 Synthesis of 5,8-fused systems 46
2.4 Selective Functionalisation of 5,6- and 5,8-Fused Ring Systems 46
2.5 Attempted synthesis of 7,6- and 7,8-fused ring systems 48
2.6 Attempted application of the cascade towards the ABCD rings of Schisandra triterpenes 49
2.7 Conclusion 50
Chapter 3: Synthesis of the *Schisandra* AB ring system 51
3.1 Introduction 51
3.2 C-H activation strategy 51
3.3 Cyclobutane opening strategy 54
3.4 Ring expansion rearrangement strategy 55
3.5 Final route to the AB rings 57
3.6 Comparative analysis of different routes to the AB rings 60
3.7 Conclusion 61
Chapter 4: FG rings synthesis 63
4.1 Introduction and retrosynthesis 63
4.2 Diels-Alder or Mukaiyama-Michael strategies 64
4.3 Methylation tactics 68
4.3.1 From ketone 68
4.3.2 From silyl enol ether: Silver-mediated alkylation 69
4.3.3 From silyl enol ether: Fluoride-mediated 70
4.3.4 From silyl enol ether: Miscellaneous 73
4.4 Methylation at earlier stage 75
4.5 Conclusion 77
Chapter 5: Towards rubriflordilactone B synthesis 78
5.1 Introduction and retrosynthesis 78
5.2 Synthesis of ABCDE rings of rubriflordilactone B 78
5.3 Radical cyclisation via 1,5-HAT 81
5.5 Conclusion 84
Chapter 6: Synthesis of the diyne fragment and rubriflordilactone A 85
6.1 Introduction and retrosynthesis of the diyne fragment 85
6.2 Darzens acylation strategy 87
6.3 Carboxylic acid to alkyne strategy 89

6.3 Alternative carboxylic acid to alkyne approach 91
6.4 Masked alkyne equivalents 92
6.4.1 Bromoalkyne 92
6.4.2 Chloroacetylene 94
6.4.3 Germylacetylene 95
6.5 Improvement of the diyne fragment synthesis 98
6.5.1 Overview of the initial diyne fragment synthesis 98
6.5.2 Enzymatic kinetic resolution via alcohol acylation 99
6.5.3 Early-stage germylation 102
6.5.4 Telescoped phosphate elimination and alkyne silylation 103
6.5.5 Alternative to organolithium-induced phosphate elimination 103
6.6 Final route to the diyne fragment 105
6.6.1 Overview of the final route 105
6.6.2 Comparative analysis of different routes to the diyne fragment 106
6.7 Conclusion 108
Chapter 7: Experimental 110
7.1 Experimental considerations 110
7.2 Process-mass-intensity calculations 110
7.3 Computational details 111
7.4 Procedures and characterisation from Chapter 2 119
7.5 Procedures and characterisation from Chapter 3 139
7.6 Procedures and characterisation from Chapters 4 and 5 156
7.7 Procedures and characterisation from Chapter 6 175
References 202

Acknowledgements

I would like to express my deepest gratitude to my family for their unwavering support, love, and encouragement throughout this journey.

I am immensely grateful to the Clarendon Fund and the Merton Chemistry Scholarship for their generous financial support, without which this endeavour would not have been possible.

A special thank you goes to my friends at Merton, who have been a source of joy and inspiration, creating cherished memories that will always stay with me. Finally, I would like to thank all wonderful colleagues and friends from F10 and F9, who shared the struggle of chemistry and provided a positive and supportive environment that greatly benefited me.

Abbreviations and legend

Legend:

Yield (**%**, black)	Yield for the reactions reported in the literature
Yield (**%**, green)	Yield for the reactions reported in this thesis
decomp.	Decomposition, complete conversion of the starting material without formation of isolable product
n.r.	No reaction, the starting material remained unchanged
mixture	Complete conversion of the starting material into (complex) mixture of products

Abbreviations:

AIBN	Azobisisobutyronitrile
bpy	2,2′-Bipyridine
CSA	Camphorsulfonic acid
Cy	Cyclohexyl
DAST	Diethylaminosulfur trifluoride
DBU	Diazabicycloundecene
DMAP	4-Dimethylaminopyridine
DME	Dimethoxyethane
DMPU	N,N′-Dimethylpropyleneurea
DNPH	Dinitrophenylhydrazine
HAT	Hydrogen atom transfer
HFIP	1,1,1,3,3,3-Hexafluoropropan-2-ol
HPLC-UV	High performance liquid chromatography with a UV detector
HVI	Hypervalent iodine

HWE	Horner-Wadsworth-Emmons reaction
LLS	Longest linear sequence
MoOPh	Oxodiperoxymolybdenum(pyridine)-(hexamethylphosphoric triamide)
MTBE	Methyl *tert*-butyl ether
NBO	Natural bond orbital
NOESY	Nuclear Overhauser effect spectroscopy (2D)
PC	Photocatalyst
PG	Protecting group
PIDA	Phenyliodine(III) diacetate, bis(acetoxy)iodobenzene
PMI	Process-mass-intensity
p-TSA	*p*-Toluenesulfonic acid
py	Pyridine
TFAA	Trifluoroacetic anhydride
TfOH	Triflic acid, trifluoromethanesulfonic acid
TMEDA	*N*,*N*,*N*′,*N*′-Tetramethylethane-1,2-diamine

Chapter 1: Introduction

1.1 Thesis summary

This thesis aims to develop strategies towards the total synthesis of three different triterpenes from the *Schisandraceae* plant family, with a particular focus on efficient, scalable and sustainable synthesis. This section provides an overview of the chapters that follow.

Chapter 1 begins with an introduction of the key concepts for understanding and measuring efficiency, scalability and sustainability of a synthetic route. This is followed by an exposition of our approach to achieve the stated goals and metrics. After a brief introduction of the triterpenes from *Schisandraceae* plant family, a historical overview of the synthetic efforts towards these natural products is presented. Detailed strategic analysis and forward synthesis of seven total syntheses is provided. This includes synthesis of schindilactone A by Yang; rubriflordilactone A by Li, Anderson and Chen; rubriflordilactone B by Li and Anderson; and the 'AB rings' by Hoveyda. For the first time in the literature, these syntheses are presented in full, with steps that are properly shown and correctly counted.[1] Rather than merely describing synthesis figures, this treatment puts emphasis on strategy and points to strengths and weaknesses of each synthesis. Forward syntheses are accompanied by comments explaining the purpose and rationale behind the outcome of all important reactions, especially regarding stereochemistry. Finally, our strategy towards the collective total synthesis of the *Schisandra* triterpenes is outlined.

Chapter 2 begins by proposing a cascade reaction involving alkyne (ynamide) carbopalladation, Suzuki coupling and electrocyclization to form the central 7,8-fused rings of lancifodilactone I. Initial sections describe the development of this cascade reaction using different model systems to form 5,6-, 5,8-, 7,5-, and 7,8- fused rings. Subsequent sections describe further functionalisation of the 5,6- and 5,8-fused cores and examination of different alkyne

substituents. Finally, attempted application towards a synthesis of lancifodilactone I is described.

Chapter 3 focuses on the AB rings synthesis in the wider context of *Schisandra* triterpenes. It describes the emergence of a successful route via lessons learned from prior unsuccessful attempts. This is followed by efforts to improve efficiency, scalability and sustainability of the synthesis. Finally, a comparative analysis is provided with key metrics including process-mass-intensity for this and previous AB rings syntheses by Anderson and Hoveyda.

Chapter 4 focuses on the FG ring synthesis in the context of rubriflordilactone B synthesis. The chapter begins with a retrosynthetic analysis, which is followed by exploration of Diels-Alder and Mukaiyama-Michael strategies. The rest of the chapter describes efforts to install the required methyl group via various tactics and at different stages of the synthesis.

Chapter 5 explores the use of a simpler diyne fragment instead of the FG rings in the context of rubriflordilactone B synthesis. The chapter begins with a retrosynthetic analysis. This is followed by the construction of the ABCDE core. The subsequent section describes the development of a radical cascade cyclisation involving 1,5-HAT using a model system, with the goal of the F ring construction with the correct stereochemistry.

Chapter 6 focuses on the diyne fragment synthesis in the context of rubriflordilactone A synthesis. The chapter begins with exploration of Darzens acylation strategy. This is followed by direct carboxylic acid to alkyne approaches using modern methodologies and alternative strategies. Subsequent sections deal with the problem of finding an adequate alkyne equivalent. Final sections describe efforts towards improving efficiency, scalability and sustainability of the diyne fragment synthesis. Finally, a comparative analysis is provided for this and previous diyne fragment synthesis.

1.2 Overview of synthetic efficiency, scalability and sustainability

Throughout the 20th century, synthetic chemists have advanced the field of total synthesis by pushing the boundaries of chemical synthesis, successfully synthesising natural products of previously unimaginable complexity. This historic phase, termed 'the age of feasibility',[2] is best illustrated in the first volume of Nicolaou's Classics in Total Synthesis.[3] The last decade has witnessed growing recognition of the importance of how a target molecule is synthesised, rather than synthesising the target molecule at any cost.[4] The number of perspective articles on efficiency, scalability, and sustainability in synthesis has grown significantly.[2, 5-7] The following paragraphs will cover the most discussed principles and metrics designed to achieve these goals.

Retrosynthesis. During the second half of the 20th century, a framework for systematic exploration of possible synthetic pathways leading to complex targets was developed. This framework, known as retrosynthesis, was developed by E. J. Corey and published in his book The Logic of Chemical Synthesis.[8] Along with the concepts of synthon, transform and retron, it introduced five high-level strategies in retrosynthesis:

1. Transform-based strategies: search for a powerful, simplifying transform.
2. Structure-goal strategies: search for a favourable starting material or intermediate.
3. Topological strategies: identification of bond disconnections that simplify connectivity.
4. Stereochemical strategies: removal of stereocentres with stereocontrol.
5. Functional group-based strategies: identification of suitable disconnections based on functional group relations.

The most important, overarching principle stated that the concurrent use of as many of these independent strategies as possible ultimately provides superior solutions. Examination of syntheses covered in sections 1.7-1.12 indeed supports the validity of this principle.

Redox economy. Introduced by Baran and Hoffmann[9] in 2009, redox economy recognises the efficiency benefit of minimising the number of non-strategic redox steps. These are the steps that involve oxidation or reduction that do not set stereochemistry or do not construct skeleton-forming bonds. Implementation of redox economy means that each skeleton-forming or strategic redox reaction generates the functionality required to carry out the next skeleton-forming or strategic redox reaction. Minimising adjustment of oxidation levels of the molecule in between strategic steps leads to a more efficient synthesis.

Ideality. Although the concept of an ideal synthesis dates back to 1975,[10] the practical, quantitative metric was proposed in 2010.[11] Ideality was defined as the ratio of the number of strategic steps to the total number of steps in a synthesis. Strategic steps include skeleton-forming reactions and redox reactions that set stereochemistry or lead to an oxidation state found in the target molecule. Non-strategic steps include all other redox reactions, functional group interconversions and protecting group manipulations. Defined in this way, ideality serves as a quantitative metric for assessing synthetic efficiency.

Scalability. Advantages of pursuing synthesis with scalability in mind was highlighted by Baran[12] in 2013. Scalability was defined as a weighted sum of factors: step count, level of complexity of chemistry used, stereochemical complexity and control, chemical stability of intermediates, overall yield and operational complexity, with the weights dependent on the specific application. Taking these factors into account leads to the development of robust and universally applicable chemistry, which has an immediate impact on real-world applications.

Sustainability. Published in 1998, the 12 principles of green chemistry[13] were formulated as guidelines to minimise environmental and health impact of chemical processes. However, the principles have some drawbacks as they fail to encompass process economics, life cycle analysis and feedstock supply, and it could be debatable whether their status as guidelines is beneficial.[14] A more holistic approach to sustainability focuses on environmental, economic, and social impacts. In organic synthesis, this would manifest itself in reduction in environmental,

chemical and health hazards, and the use of renewable feedstocks while simultaneously lowering the cost of chemical processes.

Process-mass-intensity. Process-mass-intensity (PMI) is defined as a ratio of mass of all input materials (substrates, reagents and solvents) to the mass of the pure product. A lower PMI value is indicative of a more efficient process, as it suggests that less waste is produced per mass unit of product. It has been shown that PMI positively correlates with the global warming potential (CO_2 kg-equivalent).[15] For a process with a PMI of 1000, for each kilogram of mass not used through a more efficient process, one can avoid the production of 5 kg of CO_2 equivalents.

A synthetic route cannot be adequately judged through a single metric. Rather, it is best judged through a combination of metrics, with particular emphasis on the specific context and purpose of the synthesis. These metrics include total and longest linear sequence (LLS) number of steps, overall yield, ideality, operational simplicity, robustness, number of chromatographic separations, PMI, scalability, cost, material supply chain, and the use of environmentally, chemically or health hazardous materials.

1.3 Our approach to total synthesis

It is our view that contemporary academic total synthesis should provide strategic and tactical ideas for efficient, scalable and sustainable construction of general complex structural motifs underutilised in commercial applications. Choosing a natural product as a synthetic target provides a good setting for this kind of work, as long as the natural product is complex or demonstrated to be synthetically challenging through previous synthetic studies or total syntheses. This work adheres to the following principles and guidelines, with a belief that such adherence would result in the realisation of the stated goals of contemporary total synthesis.

Asymmetric synthesis. The only synthesis that should ever be pursued is an asymmetric one. Racemic synthesis is equivalent to a model study of an asymmetric synthesis. Chiral auxiliaries, chiral separation and expensive and overengineered catalysts should not be used.

Retrosynthesis. Retrosynthesis should articulate the strategic thinking behind the chosen approach. It should incorporate all concepts from the previous section.

No chromatography. A synthesis should not require chromatographic separation at all. Chromatography solvent is by far the largest contributor to waste in a chemical reaction. Crystallisation or distillation should be preferred instead. Reactions likely to produce difficult-to-separate by-products should be avoided. It is preferred to plan for intermediates that could be isolated in high purity just by workup (e.g. acids via acid-base extractions). Taking advantage of physico-chemical properties of products and impurities (e.g. differential solubility in a particular solvent) should always be looked for. Robust reactions that could tolerate impure starting materials should be preferred. Planning for synthetic intermediates that have higher chance of being crystalline (e.g. a free alcohol compared to a silylated alcohol) increases the chance of simplifying purifications and avoiding chromatography.

Toxic reagent is not a solution. Employing a toxic reagent to achieve a transformation may be considered just as problematic as not achieving the desired transformation at all. A synthesis should not be planned around transformations requiring toxic compounds, such as organotin, chromium(VI), organoselenium, organomercury and others. Solvents like HMPA, CH_2Cl_2, CCl_4, and benzene should be avoided. Toxic chemicals are and will be regulated by laws and as such will become unavailable as starting materials, reagents or solvents. Carbon tetrachloride has already been discontinued from Sigma Aldrich catalogue. Just at the time of this writing, the US Environmental Protection Agency has issued a ban on most uses of dichloromethane.[16]

Every step is strategic. Every step should be 'strategic' (skeleton-forming or redox step that sets stereochemistry or leads to an oxidation state found in the target molecule). To achieve an efficient synthesis, each strategic step should lead into the next one. Strategic steps that do not prepare the molecule for the next strategic step should be avoided, because they would have to be followed by a non-strategic step. At the design stage, an ideal synthesis should be planned. Planning an ideal synthesis may not result in an ideal synthesis, but planning an

inefficient synthesis guarantees an inefficient synthesis in execution. To pursue an ideal synthesis, it is preferred to look beyond obvious disconnections. It is also preferred to think in terms of oxidation states, and not specific functional groups (e.g. aldehyde, acetal, alkyne, and vinyl-heteroatom are the same species).

Best transformations. The best transformations are those where every part of the molecule constructively contributes to a reaction outcome. This allows simple reagents to achieve complex and otherwise challenging transformations. The prime examples are the Grignard addition and the skeletal rearrangement steps in the AB rings synthesis (Section 3.5). Thinking in terms of isolated functional groups should be avoided. Instead, a holistic understanding of molecular reactivity should be adopted to allow identification of substrate specific powerful transformations, such as Mukaiyama-Michael step in the FG rings synthesis (Section 4.2).

Intelligent control of stereochemistry. Setting the correct stereochemistry should be planned from the beginning. Leaving it to chance would likely require extensive black box optimisation and likely result in a diastereomeric product mixture. Generating diastereomers with less than 5:1 dr would require a difficult chromatographic separation as well, which is both inefficient and not sustainable. A single diastereomer product is more likely when every part of the molecule constructively contributes to the desired stereochemical outcome, as exemplified by the Grignard addition step in the AB rings synthesis (Section 3.5) and benzylidene acetal formation in the FG rings synthesis (Section 4.2).

Multi-step detour is not a solution. If a planned strategic reaction fails, a multi-step detour that involves more than one non-strategic step should be avoided. Pursuing multi-step detours at the first sign of difficulty unnecessarily introduces inefficiency and overlooks the opportunity to find a creative solution to a synthetic problem that is likely to be common. Instead, an alternative tactic that achieves the same transformation should be sought. When introducing a non-strategic step in a detour, a reaction that could be telescoped should be preferred.

Operational simplicity. The more factors influencing a reaction, the greater the potential for failure. A reaction that mixes more than four chemicals (starting materials, solvents, reagents, catalysts, additives) is too complex and efforts should be put towards its simplification. Anhydrous solvents should never be used unless absolutely necessary. Nitrogen atmosphere should be avoided. Glovebox should be avoided. Active effort should be put towards minimising total number of operations (e.g. reagent addition, cooling, extraction, filtration, evaporation).

These guidelines set the standard for our total synthesis approach, focusing on efficiency, sustainability scalability, and strategy, while avoiding reliance on chromatography or toxic reagents. They are not intended as a critique of past or present syntheses, but rather as a framework to shape future synthetic efforts.

1.4 Overview of Schisandra triteprenes

Schisandraceae is a family of vine plants native to China, Russia, Korea and USA that has been used in traditional Chinese medicine for two millennia. Triterpenes from the *Schisandraceae* family represent a fascinating class of natural products due to their unique complex structures and biological activities. Structures, isolation, proposed biosynthetic pathways and biological activities of this terpene family have been summarised in three excellent reviews. The first review[17] covers a period between 1974 and 2008, the second review[18] covers a period between 2008 and 2014, and the third review[19] covers a period between 2014 and 2022. In total, 432 triterpenes have been covered, with the second and third reviews providing a tabular summary of antiviral (mostly anti-HIV), antitumor and neuroprotective activities.

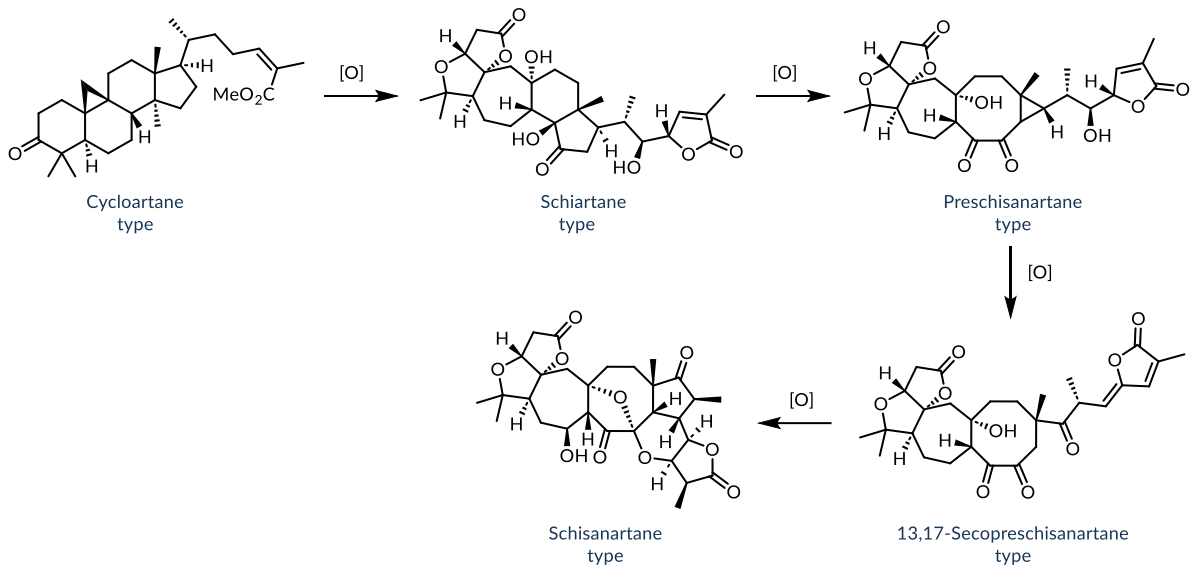


Figure 1. Different types of triterpenes from *Schisandraceae* family

These triterpenes can be categorised into different types according to the carbon skeleton and biosynthesis stage (Figure 1). Starting from a cycloartane type, a series of oxidation and rearrengements take place to arrive at a schiartane type. The central 6-membered ring could aromatise if a methyl group is lost via enzymatic decarboxylation, leading to a norshiartane type. Further increase in oxidation levels and skeletal rearrangement leads to preschisanartane type with a unique 7,8-fused system, secopreschisanartane type and finally the most complex schisanartane type.

1.5 Previous syntheses and synthetic studies

Triterpenes from *Schisandraceae* family have gained significant attention in the synthetic community since their isolation in early 2000s, with the first successful synthesis achieved in 2011 (Figure 2). Initial synthetic studies by Yang,[20, 21] Theodorakis[22] and Ghosh[23] focused on micrandilactone A. Synthetic studies by Paquette[24-26] and Anderson[27] focused on lancifodilactone G, while studies by Chen[28] focused on lancifodilactone F and studies by Mehta[29] focused on lancifodilactone C. In 2011, Yang[30] achieved a racemic synthesis of schindilactone A, representing the first synthesis of any *Schisandra* triterpene. This was followed by synthetic studies towards rubriflordilactones A and B by Ghosh[31] and Anderson,[32, 33] Peng,[34] Nicewicz,[35] Xie[36, 37] and Hoveyda.[38] In 2014, Li[39] successfully synthesised

rubriflordilactone A (Figure 2), the second *Schisandra* triterpene to be synthesised. This was soon followed by total syntheses by Anderson[40] in 2015 and Chen[41] in 2024. Its close relative, rubriflordilactone B was synthesised by Li[42] in 2016 and Anderson[43] in 2019. A number of successful syntheses of Schisandra triterpenes were published around this time: propindilactone G by Yang[44] and Gui,[45] lancifodilactone G by Yang,[46] schilancidilactone B by Tang[47, 48] and pre-schisanartanin C by Yang[49] (Figure 2).

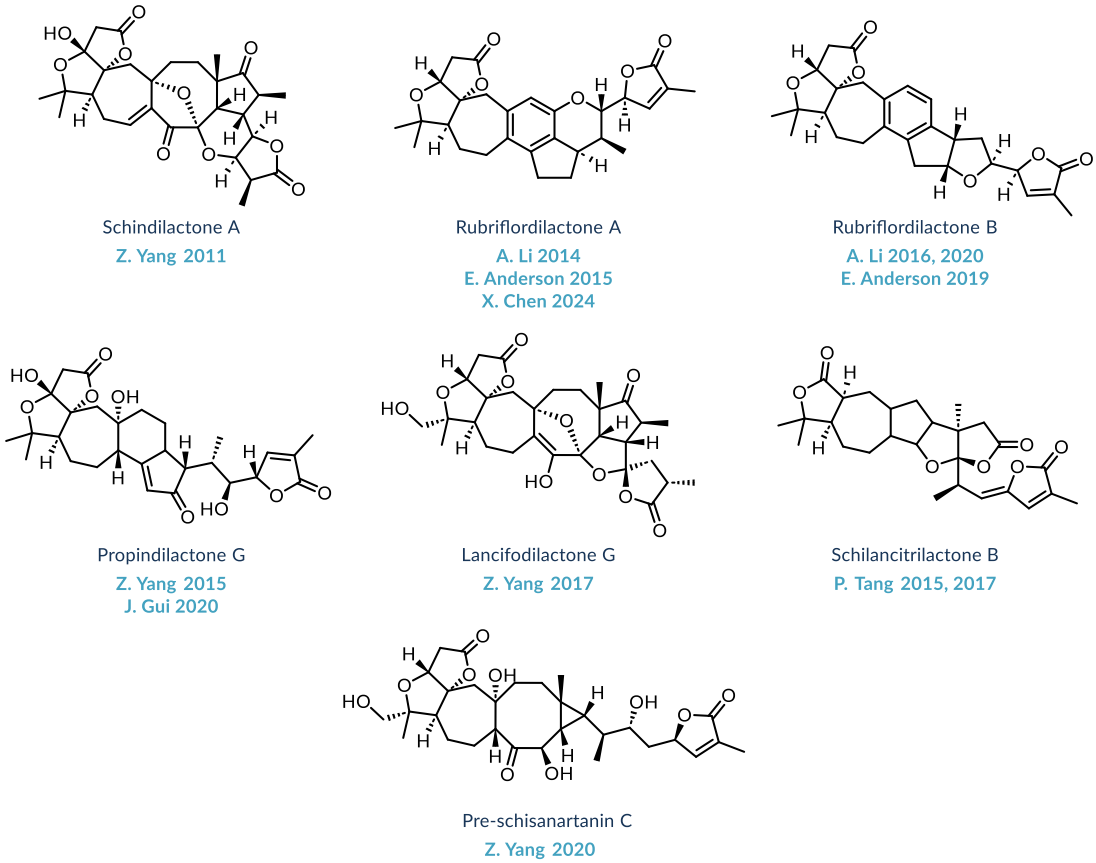


Figure 2. Previous total syntheses of Schisandra triterpenes

Next sections will cover the most instructive and relevant syntheses for this work:

1. Schindilactone A by Yang
2. Rubriflordilactone A by Li, Anderson and Chen
3. Rubriflordilactone B by Li and Anderson
4. AB rings synthesis by Hoveyda

Of importance has also been Xie's attempt at the AB rings synthesis[37] and Nicewicz's study[35] towards rubriflordilactone B.

1.6 Z. Yang's racemic synthesis of schindilactone A (2011)

1.6.1 Overview of the strategy

Schindilactone A was the first member from *Schisandraceae* triterpenes family to be synthesised. Although the synthesis was racemic, this presented a groundbreaking work and was achieved by Zhen Yang's group in 2011,[30] after more than 7 years of synthetic studies.[20, 21, 50]

Schindilactone A features a complex and stereochemically dense 5/5/7/8/5/6/5 carbo-and oxacyclic framework (Figure 3). The central 7,8-fused system (including its oxygen bridge) presents the greatest challenge in the synthesis. After examination of several strategies, Yang's group found a ring closing metathesis solution to form the 8-membered ring. Ring closing metathesis typically struggles with the closure of medium-sized rings,[51] however, Yang's group successfully constrained the molecule into an appropriate conformation to enable this challenging cyclisation. The GH rings were synthesised using palladium-catalysed carbonylative annulation.[21] The densely substituted cyclopentanone ring F was constructed via previously optimised challenging Pauson-Khand reaction.[50] The ABC rings were synthesised using the template of the C ring to sequentially construct the A and B rings with the correct stereochemistry.

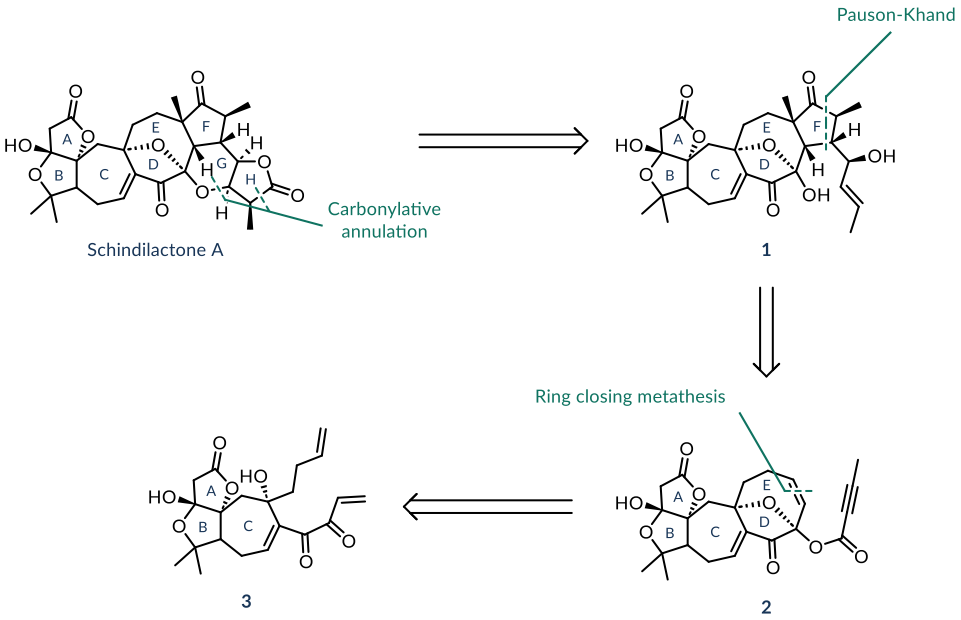


Figure 3. Yang's strategy for schindilactone A synthesis

1.6.2 Forward synthesis

The forward synthesis was reported from substances not commercially available, with no literature reference provided. To avoid this somewhat misleading practice, we present the synthesis of schindilactone A from the most meaningful commercially available precursors **4** and **6** (Figure 4). Literature reported[52] bromination of ketoester **4**, followed by bromide elimination produced enone **5**. In another literature reported reaction,[53] deprotonation of methyl vinyl ketone **6** and treatment with silyl triflate gave silyl enol ether **7**.

Lewis acid-mediated Diels-Alder cycloaddition between diene **7** and enone **5** selectively produced ketoester **8** as a single diastereomer, as a result of the alkene geometry. Addition of methylmagnesium bromide to this ketone resulted in formation of tertiary alcohol which immediately cyclised to form lactone **9**. This lactone was deprotonated and captured with oxygen to form a hydroperoxide that was *in situ* reduced with phosphite to give the corresponding alcohol, which was protected as a TES ether in the following step. The stereochemical outcome was a result of oxygen approaching the convex face of the substrate enolate.

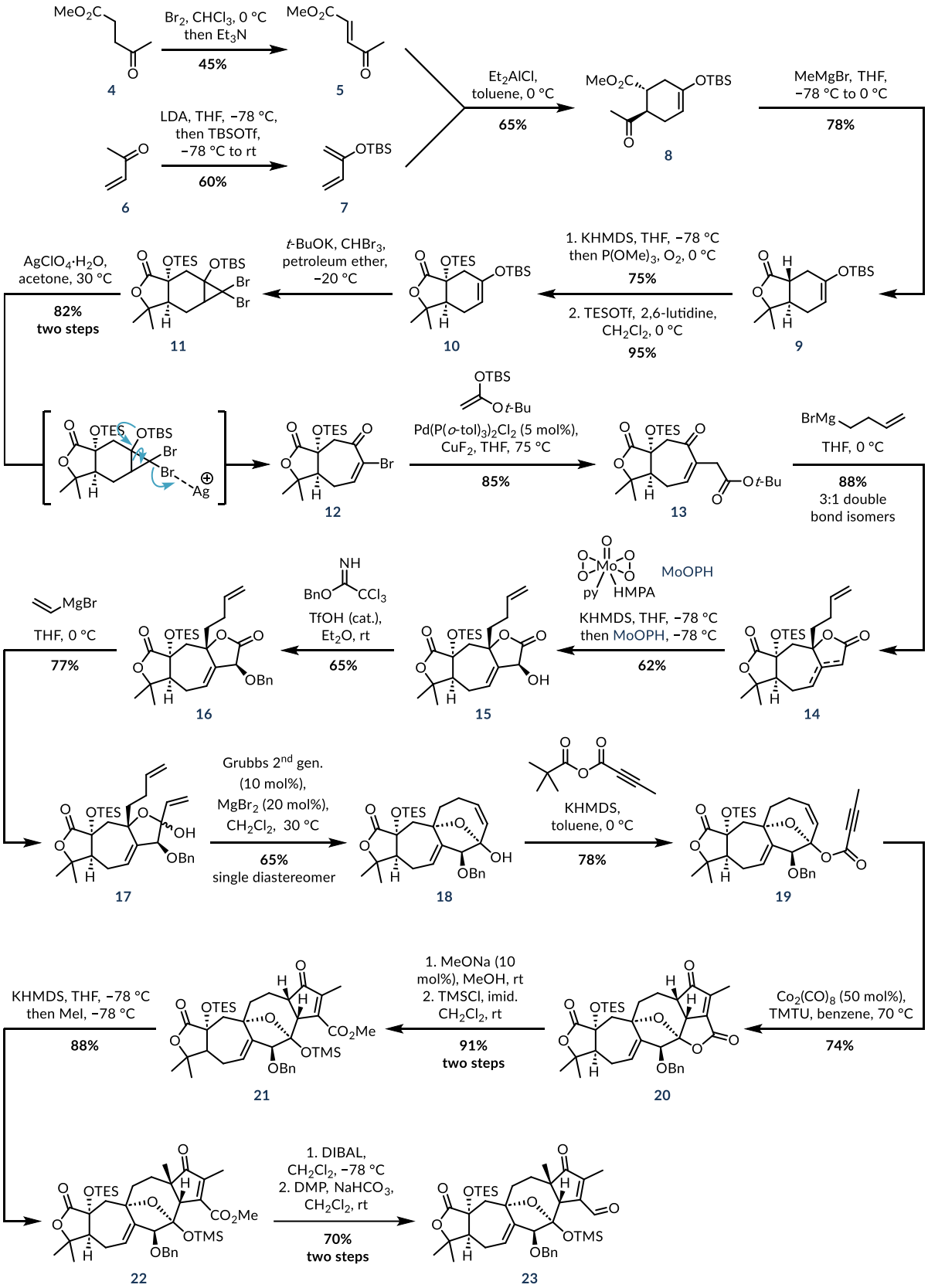


Figure 4. Yang's synthesis of schindilactone A

In this approach, all stereocentres necessary for the construction of the AB ring system were set using the existing stereochemistry of the C ring formed through Diels-Alder reaction and convex/concave face control of the fused BC rings system. As shall be seen later, without the C ring in place, synthesis of the AB ring system with the correct stereochemistry becomes increasingly difficult.

Continuing with the synthesis, a tactical combination to expand the C ring takes place. Cyclopropanation of silyl enol ether **10** with dibromocarbene gave dibromocyclopropane **11**, followed by silver-mediated ring expansion to form the seven membered ring **12** found in the natural product. Yang's group likely recognised both the difficulties in constructing the AB rings without the C ring in place and constructing the AB rings from a seven-membered C ring. Consequently, they used a six-membered C ring, efficiently synthesised via Diels-Alder reaction, to establish the necessary functionality for the AB rings before expanding it to form the desired seven-membered ring.

To construct the central 8-membered ring, bromide **12** was coupled with a silyl ketene acetal to deliver ketoester **13**. Addition of butenyl Grignard reagent to this ketone produced a tertiary alcohol which immediately cyclised to form lactone **14** as a mixture of double bond regioisomers. The position of the double bond was inconsequential for the next step, as deprotonation of the mixture **14** formed the same extended enolate, which was kinetically trapped with an oxygen electrophile (MoOPh). Benzylation of alcohol **15**, followed by vinyl Grignard addition produced hemiacetal **16** as a mixture of diastereomers. The hemiacetal form of **16** brings the two alkene-termini closer together compared to an open form, enabling the otherwise challenging ring closing metathesis to proceed efficiently. Furthermore, the authors found that addition of a catalytic amount of magnesium bromide produced the desired product **18** as a single isomer via acetal equilibration. This concluded the synthesis of the central 8-membered ring.

To complete the synthesis of the right-hand side of the molecule, hemiacetal **18** was acylated to give ester **19**. The previously studied and optimised Pauson-Khand reaction[21] with tetramethyl thiourea (TMTU) was employed to construct the cyclopentanone ring in **20**. The acetal was used as a handle to tether the alkyne, enabling the Pauson-Khand reaction to proceed intramolecularly and from the sterically more accessible side of the smaller bridge. After conversion of lactone to methyl ester and hemiacetal silylation, ketone **21** was methylated in the α-position from the convex side of the molecule. Conversion of ester **22** into aldehyde **23** via a two step reduction-oxidation sequence set the stage for the final phase of the synthesis.

Addition of vinyl Grignard reagent to aldehyde **23** (Figure 5) produced allylic alcohol **24** as a single diastereomer. Although the correct isomer was obtained, this selectivity could likely not have been anticipated before the reaction. After silyl deprotection, different reducing agents were screened for reduction of the double bond in enone **24**. $LiAlH_2(OMe)_2$ proved the most effective, with hydride delivery from the top face. The authors attributed this stereochemical outcome to the hydroxy-directed conjugate reduction, although it was not clear how an alcohol attached to a rotationally flexible acyclic chain could have exhibited preference for one face over the other. Product **25** was formed as a single diastereomer, with the correct stereochemistry at the methyl group position, though the reason for this outcome remained unexplained.

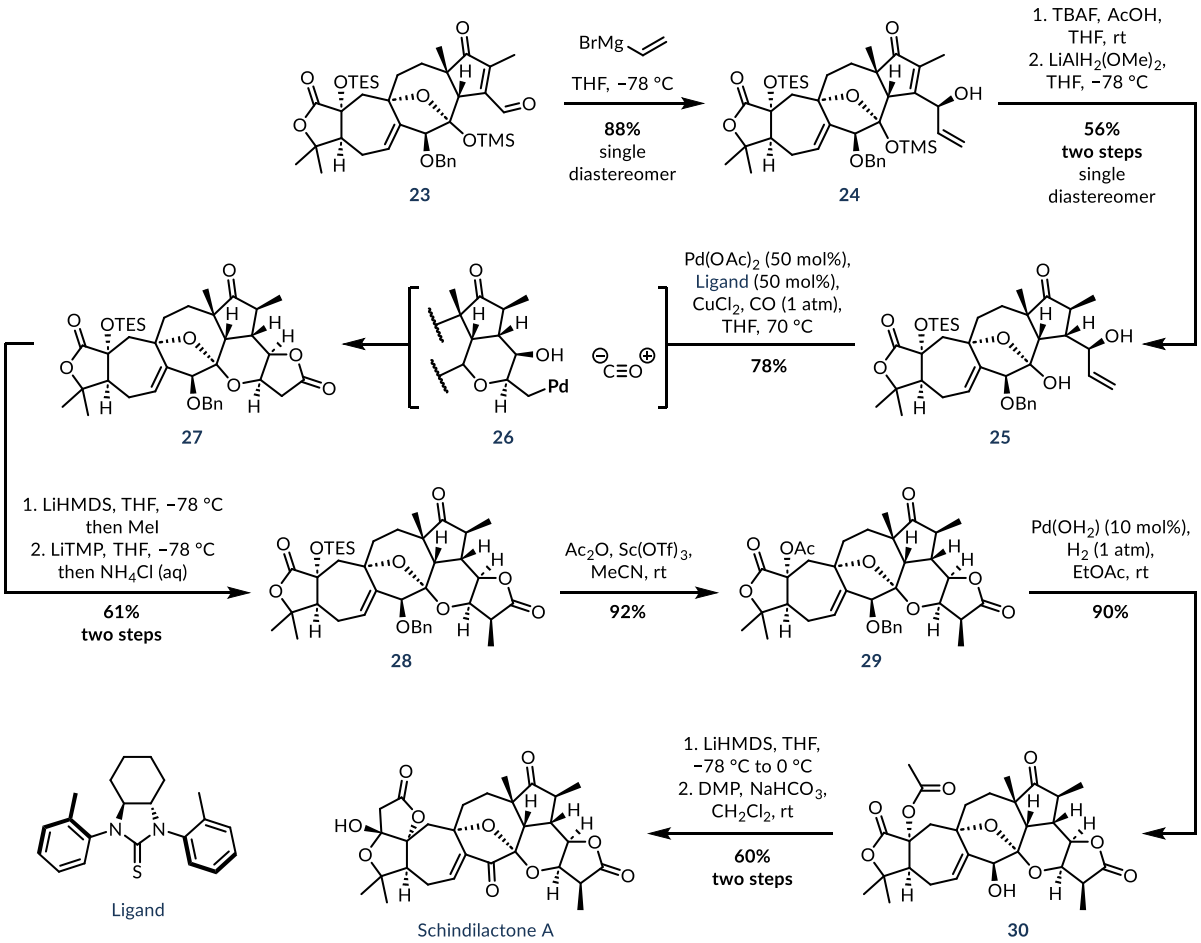


Figure 5. Final stages of Yang's synthesis of schindilactone A

Palladium catalysed carbonylative annulation was employed to simultaneously form the GH rings. Oxypalladation of olefin **25** produced alkylpalladium species **26**, which underwent a carbonyl migratory insertion to form an acylpalladium species (not shown). Subsequently, palladium was displaced by the neighbouring alcohol, resulting in the formation of lactone **27**. This lactone was methylated in the α-position, initially giving the undesired diastereomer, which was corrected via a deprotonation and protonation sequence to give the correct diastereomer **28**. This compound **28** was converted into an acetate **29** at the BC ring junction tertiary alcohol using scandium triflate, setting the stage for the final A ring construction. After debenzylation by hydrogenolysis, acetate **30** was deprotonated and the resulting enolate reacted in a Dieckmann condensation with the neighbouring lactone to form the A ring. Finally, oxidation of the secondary alcohol completed the racemic synthesis of schindilactone A in 31 steps and 0.05% overall yield.

After more than seven years of research, Yang's group achieved the first synthesis of any triterpene from *Schisandraceae* family. Although the synthesis was racemic, inefficient, and involved numerous toxic and unscalable solutions, it was based on sound strategic considerations such as building the AB rings from an established C ring, using a conformatinally constrained substrate for the ring closing metathesis to form the 8-membered ring, and using a tethered Pauson-Khand to form the cyclopentanone F ring. Yang's seminal work on schindilactone A has proven instructive for syntheses of other triterpenes from *Schisandraceae* family that followed.

1.7 A. Li's synthesis of rubriflordilactone A (2014)

1.7.1 Overview of the strategy

The key to the Li group's approach was the concurrent application of topological and structure-goal strategies. The butenolide G ring was disconnected first (Figure 6), based on the presence of favourable functional groups, however without a clear stereochemical strategy. Disconnecting bonds in a stereochemically complex environment without a clear strategy invites complications and ultimately results in an inferior synthesis, as will be shown in this and subsequent *Schisandra* triterpene syntheses. Cleavage of the central benzene ring in **31** would split the molecule into roughly similar fragments **33** and **34**. In a forward sense, the benzene ring would be constructed by a sequence of Stille coupling, followed by 6π-electrocyclisation and aromatisation. At the same time, Li's group recognised a close resemblance between the ABC fragment **34** and the ABC fragment used by Yang[30] in the schindilactone A synthesis (Section 1.6.2). Indeed, the ABC rings **34** were synthesised by deploying several steps from Yang's BC ring synthesis, while improving Yang's initial steps and rendering the synthesis asymmetric.

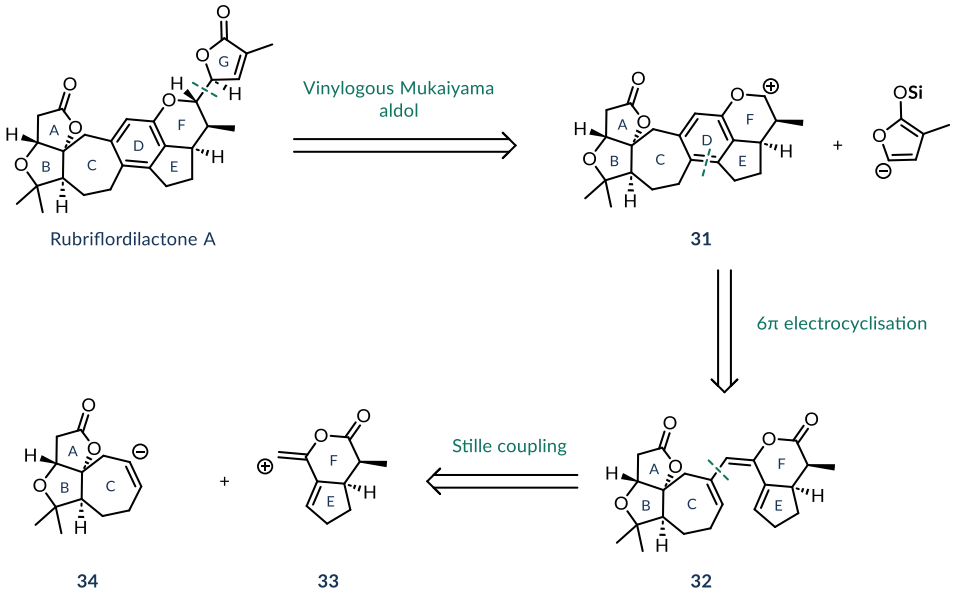


Figure 6. Li's retrosynthesis of rubriflordilactone A

1.7.2 Synthesis of the ABC fragment

As noted, the forward synthesis of the ABC fragment relied on the previously established synthesis of schindilactone A. Known compounds **36**[54] and **7**[53] were synthesised using literature procedures from commercially available materials (Figure 7). An asymmetric copper-catalysed Diels-Alder reaction was previously used by Ishihara[55] to synthesise an analogue of cyclohexenone **37**. Li's group used these conditions to synthesise cyclohexanone **37** with 76% ee. Removing the auxiliary with ethanethiolate formed a thioester that was subsequently coupled with ethylzinc iodide[56] to give ketone **38**. A five-step sequence previously established by Yang[30] followed: methyl Grignard addition, lactone α-hydroxylation, hydroxy group protection, cyclopropanation and ring expansion, ultimately producing bromoketone **42**. Bromide was removed by hydrogenation, and the corresponding enone was converted to vinyl triflate **43** via conjugate hydride addition, followed by enolate trapping with phenyl triflimide. Next, a two-step sequence from Yang's synthesis was applied to construct the A ring: scandium-mediated silyl to acetate exchange and Dieckmann condensation. Finally, acetal ionic reduction and palladium-catalysed stannylation completed the ABC fragment **46** synthesis.

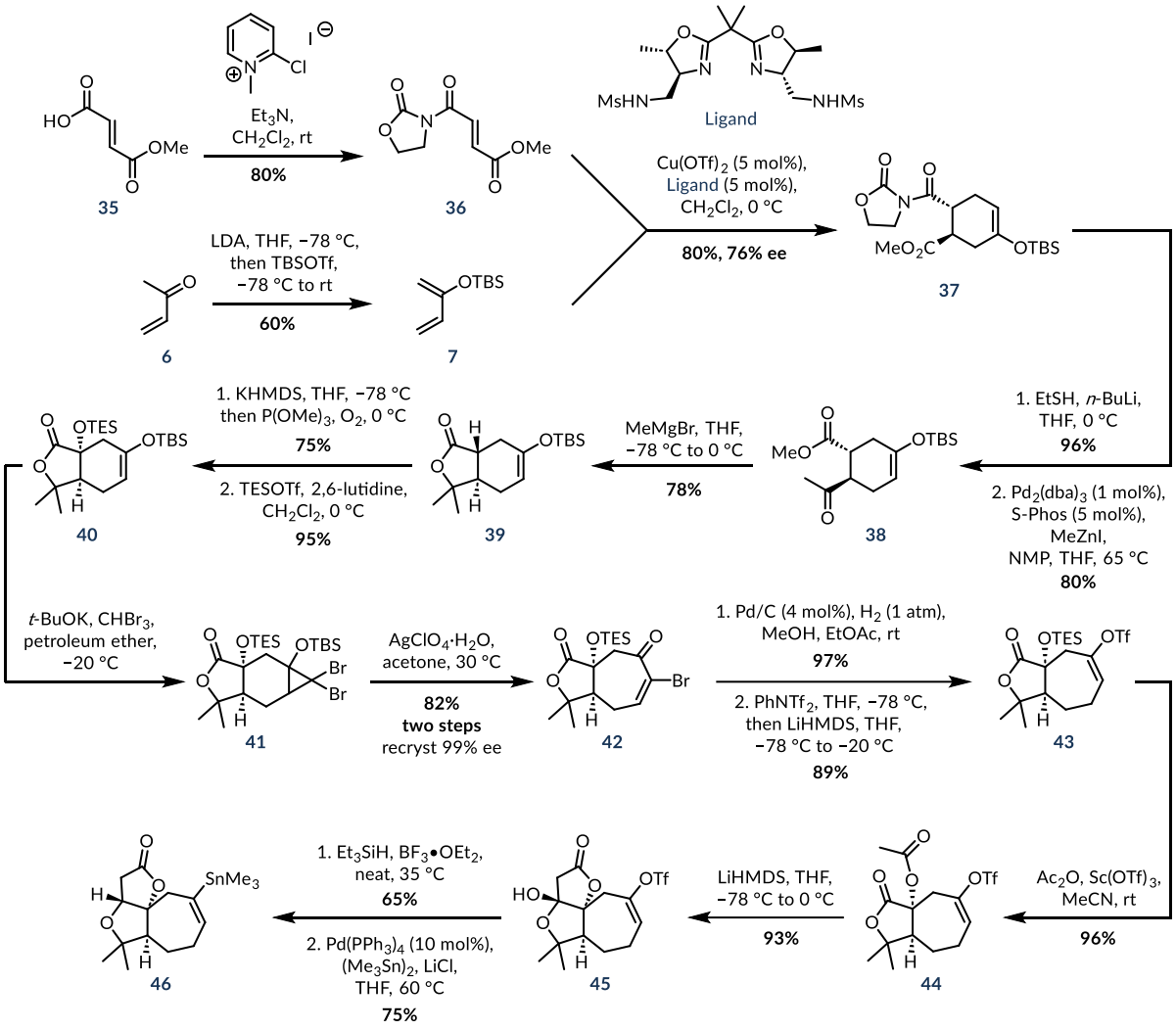


Figure 7. Synthesis of the ABC fragment

1.7.3 Synthesis of the EF fragment

To synthesise the EF fragment required for the rubriflordilactone A synthesis, iodoketone **48** was synthesised following a literature procedure[57] (Figure 8). Corey-Bakshi-Shibata reduction of this ketone resulted in the formation of cyclopentanol **49** with 99% ee. After alkyne introduction via Sonogashira coupling, allylic alcohol **50** participated in a diastereoselective Johnson-Claisen rearrangement. The alcohol configuration ensured the rearrangement took place on the top face of the molecule. While the favourable stereochemistry of the methyl-bearing carbon in **51** remained unexplained, it could have resulted either from an *E*-enol ether and a chair-like rearrangement transition state, or a *Z*-enol ether and boat-like transition state.

Acid hydrolysis, followed by electrophilic iodine-induced cyclisation delivered the required EF fragment **53**.

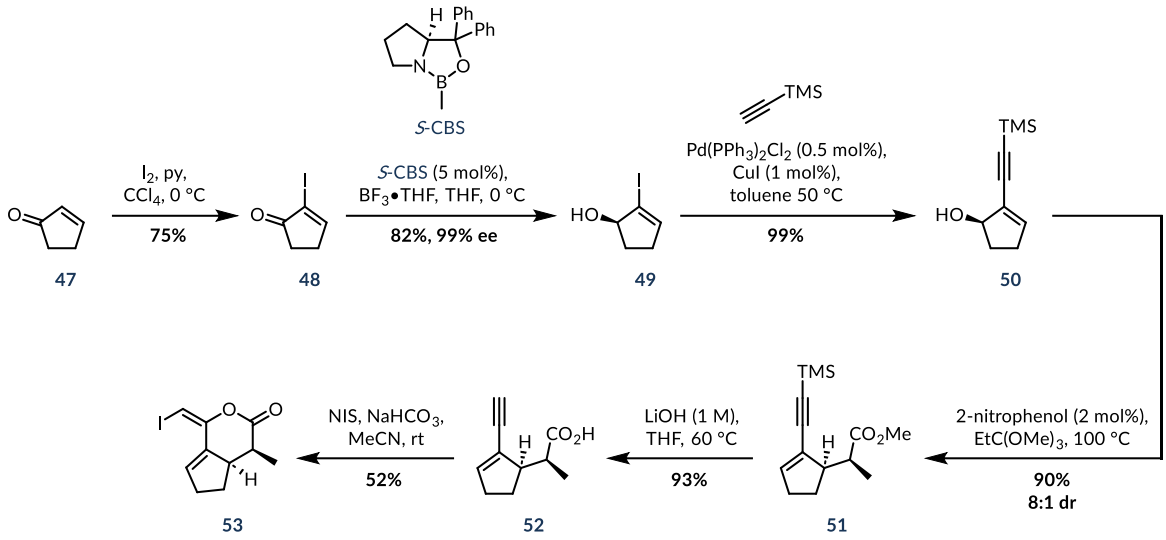


Figure 8. Synthesis of the EF fragment

1.7.4 Fragments unification and completion of the synthesis

By establishing a route to ABC rings **46** and EF rings **53**, the stage was set for their unification and completion of the rubriflordilactone A synthesis. Stille coupling unified the two fragments to give triene **54**. It is unclear why Stille coupling was chosen for fragment unification, given its requirement for handling of highly toxic organotin intermediates and stoichiometric production of toxic waste both at the stannylation and Stille coupling steps. Since both coupling partners could be potentially converted to a boronic acid equivalent, the same strategy could have been executed using Suzuki coupling, however no such attempts were reported.

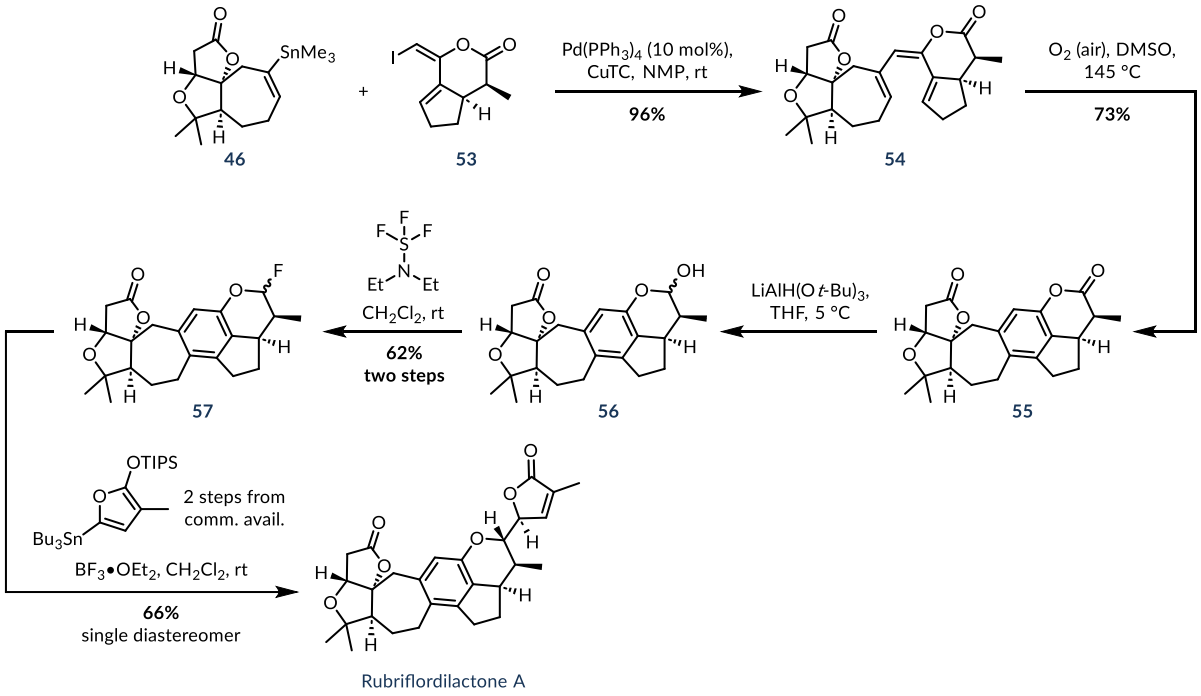


Figure 9. Completion of rubriflordilactone A

Exposure of triene **54** to high temperature and air resulted in 6π-electrocyclisation, and subsequent cyclohexadiene oxidation to form the central benzene ring in **55**. Li's group found they could selectively reduce the six membered lactone in **55** in the presence of a five membered lactone with lithium tri-*tert*-butoxyaluminum hydride, likely due to steric differentiation by a bulky reducing reagent. Acetal **56** was formed as a mixture of acetal and open-chain aldehyde form. The fact that this compound existed as a mixture of open and close-chain forms complicated further functionalisation and use of oxocarbenium chemistry with siloxyfuran to install the butenolide ring G. Ultimately, a solution was found that relied on conversion of acetal-aldehyde **56** to fluoride **57**, which reacted with oxyfurylstannane, available in two steps[58] from commercially available materials. Rubriflordilactone A was formed as a single diastereomer, although this stereoselectivity remained unexplained.

Li's group completed the first synthesis of rubriflordilactone A in 29 steps (20 LLS) and 1.9% overall yield. The key step of the synthesis, 6π-electrocyclisation followed by oxidation/aromatisation, enabled a convergent approach from two roughly equally sized fragments. The asymmetric synthesis of a suitable building block derived from an intermediate

in Yang's synthesis of schindilactone A simplified the efforts towards enantiopure rubriflordilactone A. Li's group employed a viable strategy based on molecular topology and starting material identification, however the use of multiple toxic organotin compounds makes their solutions less appealing due to safety and environmental concerns.

1.8 E. Anderson's synthesis of rubriflordilactone A (2015)

1.8.1 Overview of the strategy

Anderson's retrosynthesis of rubriflordilactone A consists of topological and transform-based strategies. After disconnection of the butenolide ring G (Figure 10), the central benzene ring was recognised as a strategic disconnection that would enable convergent synthesis. At the same time, the densely substituted benzene ring was recognised as a retron for (2+2+2) alkyne cyclotrimerisation. In the context of rubriflordilactone A synthesis, this powerful (2+2+2) formal cycloaddition would simultaneously form three rings, including the 7-membered C ring, from triyne precursor **59**. Triene **59** was designed with a secondary alcohol in place, enabling its synthesis through organometallic addition to an aldehyde of two similarly sized fragments: the AB rings and the diyne fragment.

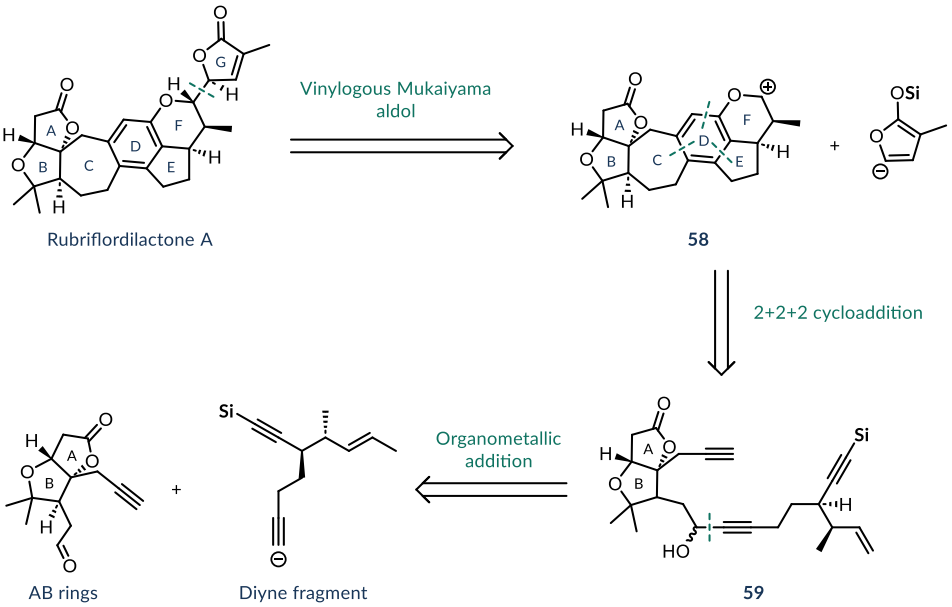


Figure 10. Anderson's retrosynthesis of rubriflordilactone A

1.8.2 Synthesis of the AB rings

Towards the AB rings, propargyl alcohol was first converted into allylic alcohol **62** via a four-step sequence (Figure 11). Sharpless asymmetric epoxidation this allylic alcohol **62** gave epoxide **63** with 92% ee. Opening of this epoxide with allylmagnesium bromide formed diol **64**. This tactical combination involving asymmetric epoxidation, followed by stereospecific epoxide opening was at the core of Anderson's approach to the AB rings. In this way, a challenging quaternary alcohol stereocentre was set enantioselectively, while also enabling the synthesis of the adjacent tertiary carbon centre with complete diastereoselectivity. With all stereocentres in place, the remainder of the synthesis involved steps to elaborate **64** into the AB rings.

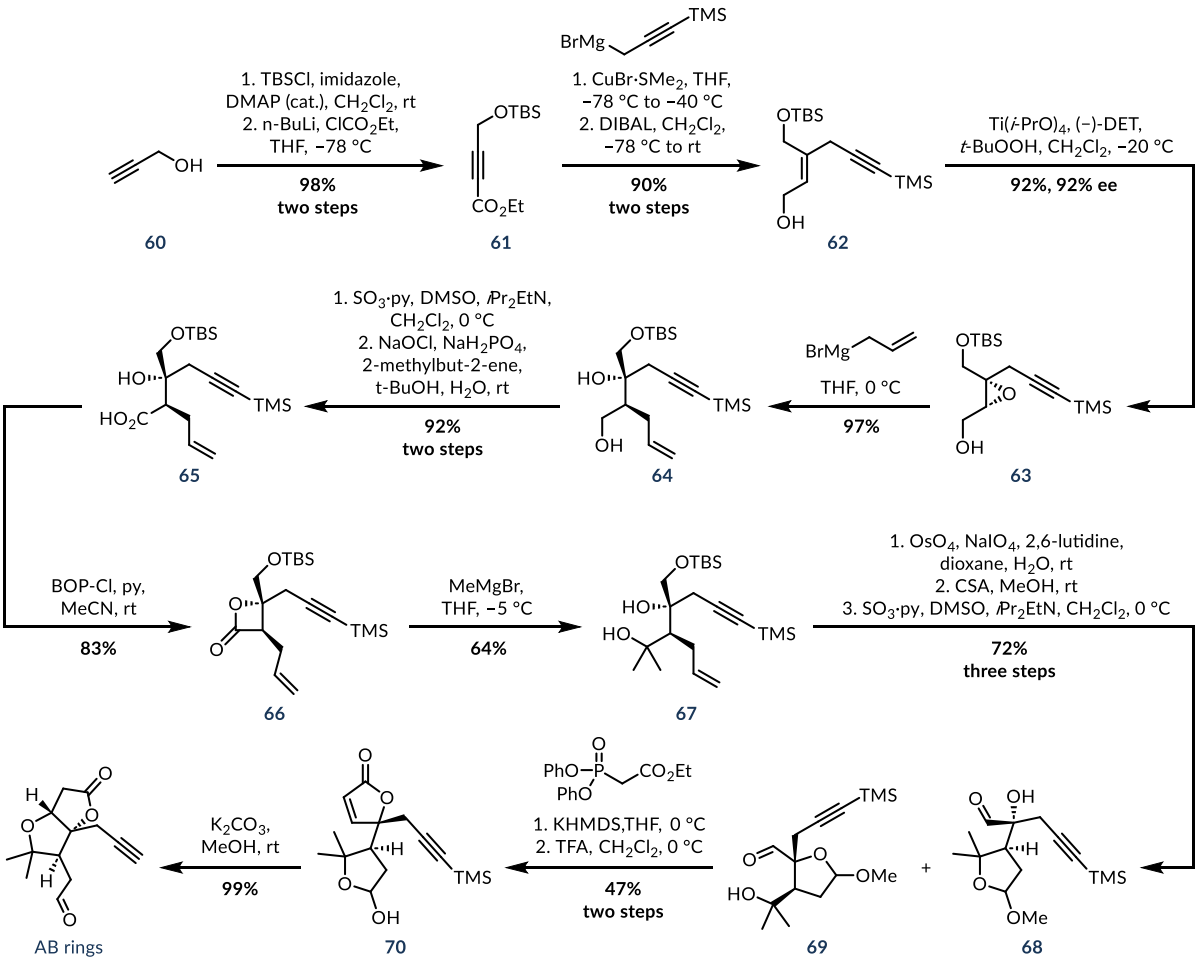


Figure 11. Anderson's synthesis of the AB rings

As such, the primary alcohol in **64** was functionalised with two additional carbon atoms in a reaction sequence involving Parikh-Doering oxidation, Pinnick oxidation, lactone **66** formation,

and methyl Grignard lactone-opening to give tertiary alcohol **67**. Oxidative cleavage of the double bond in **67** was followed by simultaneous methyl acetal formation and alcohol deprotection by camphorsulfonic acid. This alcohol was then oxidised to an aldehyde oxidation state, forming a mixture of acetals **68** and **69**. This mixture was subjected to the Ando variation[59] of the Horner–Wadsworth–Emmons reaction to form a butenolide ring, followed by acetal hydrolysis by trifluoroacetic acid to give hemiacetal **70**. With all functionalities in place, hemiacetal **70** was treated with potassium carbonate to cleave the trimethylsilyl group and release a tertiary alcohol that immediately cyclised onto a double bond, completing the synthesis of the AB rings in 16 steps and 15% overall yield.

Anderson's synthesis of the AB rings relied on a stereochemical strategy, using Sharpless asymmetric epoxidation / ring-opening to set the adjacent quaternary and tertiary stereocentres. Because the allylic alcohol substructure required for asymmetric epoxidation did not map well onto the AB rings, the group had to undertake many steps and functional group interconversions to introduce the functionality required for the AB rings. Out of 16 steps, 8 steps involved non-strategic redox and protecting group manipulations.

1.8.3 Synthesis of the diyne fragment

To synthesise the diyne fragment required for the planned rubriflordilactone A synthesis, 1,5-pentanediol **71** was monoprotected and oxidised to carboxylic acid **73** (Figure 12). At the same time, racemic alcohol **74** was subjected to enzymatic kinetic resolution[60] to give enantiopure alcohol **75**. After EDC-mediated ester formation, ester **76** was subjected to Ireland-Claisen rearrangement. In this reaction, the stereocentre present in substrate **76** controlled the formation of two new adjacent stereocentres in product **77** via an (*E*)-enolate / chair-like transition state. The product acid **77** was converted to aldehyde **78** in a sequence involving methylation, reduction and oxidation. Aldehyde **78** was homologated to alkyne **79** in a one-pot Stork-Zhao iodoolefination / elimination reaction. After installing the benzyldimethylsilyl group required for later Tamao-Fleming oxidation, protected alcohol **80** was converted into an alkyne

in a four-step sequence involving deprotection, oxidation and Corey-Fuchs reaction. These events completed the synthesis of the diyne fragment in 14 steps and 12% overall yield.

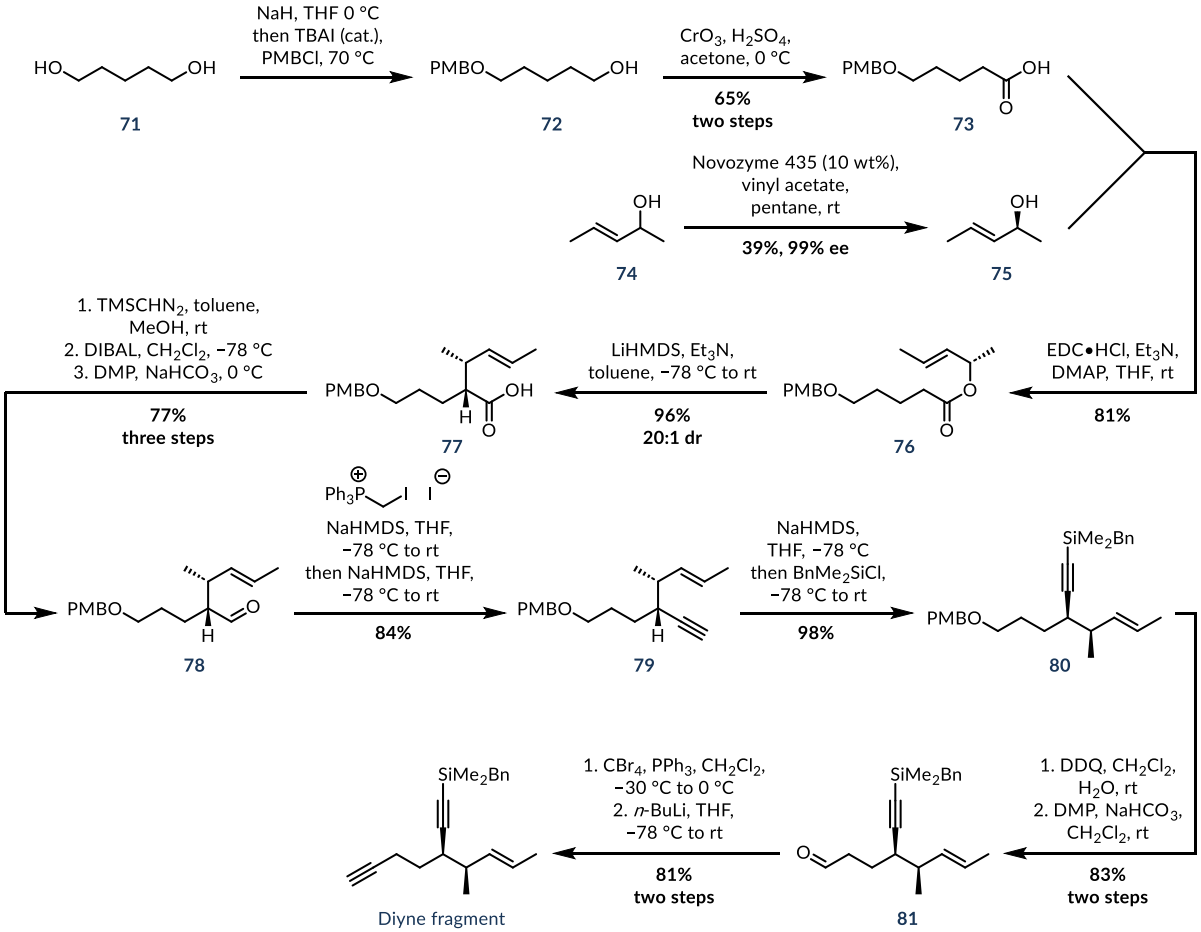


Figure 12. Anderson's synthesis of the diyne fragment

Anderson's synthesis of the diyne fragment relied on stereochemical and structure-goal strategies, using a Claisen rearrangement to set challenging stereocentres from an easily accessible, enantiopure starting material. However, subsequent conversion of the carboxylic acid and protected alcohol into two different alkynes required many additional steps. Out of 14 steps, 7 steps involved non-strategic redox and protecting group manipulations.

1.8.4 Fragment unification and completion of the synthesis

The two fragments were unified via addition of the lithiated diyne fragment to the AB ring aldehyde (Figure 13). The resulting triyne **82** was perfectly positioned to undergo the key (2+2+2) cyclotrimerisation to give **83**, generating three rings in one step. The arylsilane **83** was

converted to the corresponding phenol by Tamao-Fleming oxidation. The benzyldimethylsilyl group was chosen specifically for this step because of its ease of oxidation and stability.[61] Ionic reduction of the benzylic alcohol in **84**, followed by alkene oxidative cleavage produced hemiacetal **86**, the same intermediate from Li's synthesis (Section 1.7.4).

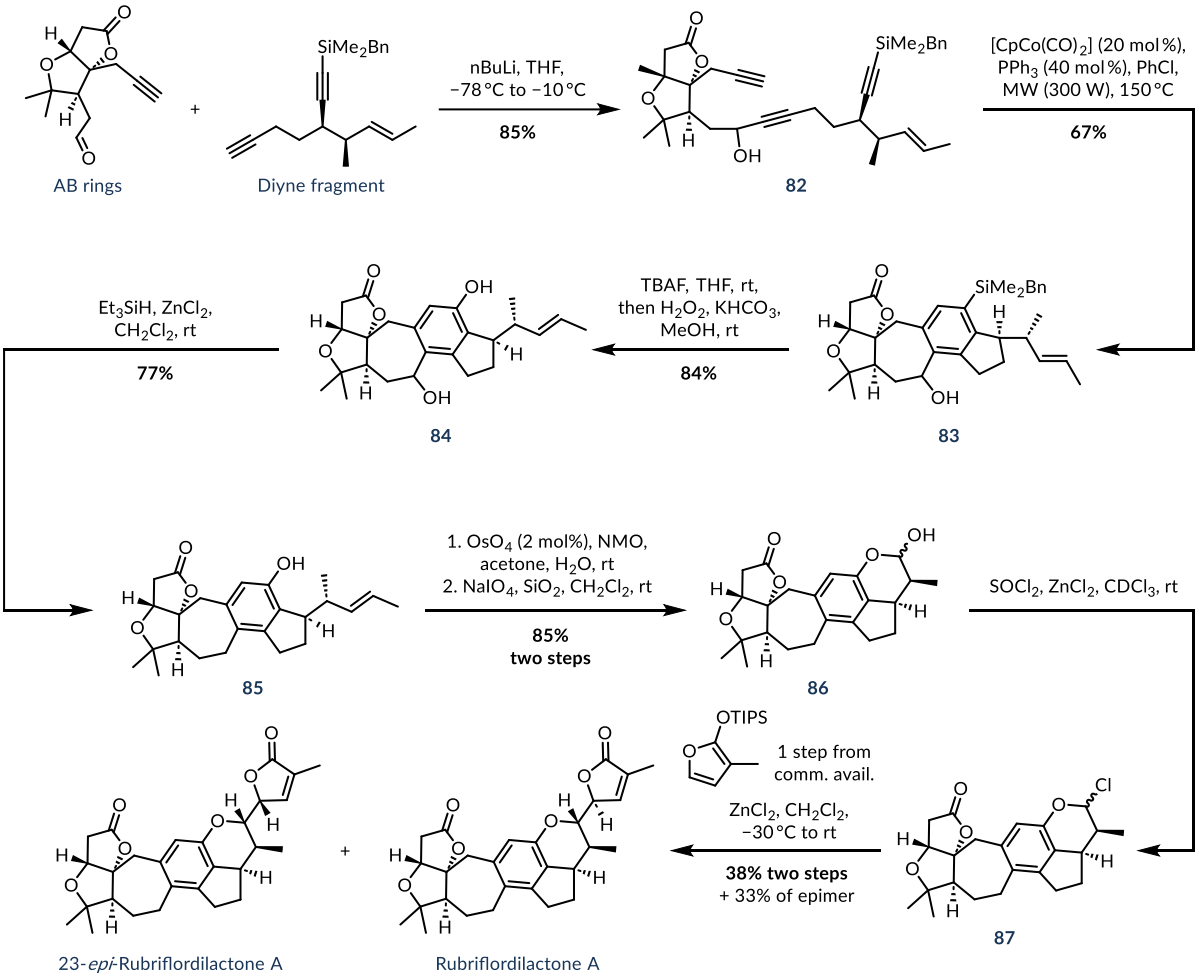


Figure 13. Completion of the rubriflordilactone A synthesis

To avoid use of the toxic furylstannane used by Li's group, a new way of converting acetal **86** to rubriflordilactone A was developed. Treatment with thionyl chloride formed chloropyran **87**, which was reacted with a siloxyfuran under Lewis acid conditions to give a mixture of rubriflordilactone A and its epimer at the butenolide stereocentre. Despite lacking stereocontrol at the butenolide carbon, the siloxyfuran addition occurred exclusively from the bottom face, opposite the adjacent methyl group and the cyclopentane ring of the relatively

flat oxonium ion. Rubriflordilactone A was thus completed in 38 steps (24 LLS) and 1.4% overall yield.

Anderson's synthesis of rubriflordilactone A employed an impressive (2+2+2) cycloaddition to simultaneously form three rings: the densely substituted benzene, cycloheptane and cyclopentane, while at the same time enabling a convergent strategy from two similarly sized building blocks. This represents a prime example of the power of combining topological and transform-based strategies effectively. High step count, on the other hand, resulted mostly from inefficiencies in constructing the AB rings and the diyne fragment building blocks. It was therefore improvements in these areas that were later pursued by Xie,[37] Hoveyda[38] and ultimately this thesis.

1.9 X. Chen's racemic synthesis of rubriflordilactone A (2024)

1.9.1 Overview of the strategy

Chen's strategy[41] towards racemic rubriflordilactone A prioritised connectivity, with surprisingly minimal consideration of stereochemistry. Disconnection across the F ring was seen as strategic (Figure 14), enabling unification of the ABCDE rings **88** with furan derivative **89** via an *ortho*-quinone methide (4+2) cycloaddition. This disconnection also removed three stereocentres that would need to be set in relation to each other, and to the distant stereocenters of the AB rings. Disconnection across the B ring with a Prins cyclisation would address the challenge of the seven-membered C ring. Finally, indanol core **90** would be synthesised by attaching the necessary functionality via furanyl organometallic addition and alkylation using an allylic electrophile derived from a simpler precursor **91**. The proposed transformations would in principle assemble the carbocyclic framework of rubriflordilactone A. Establishing the correct stereochemistry at seven stereocentres, however, would either be left to chance or extensive optimisation.

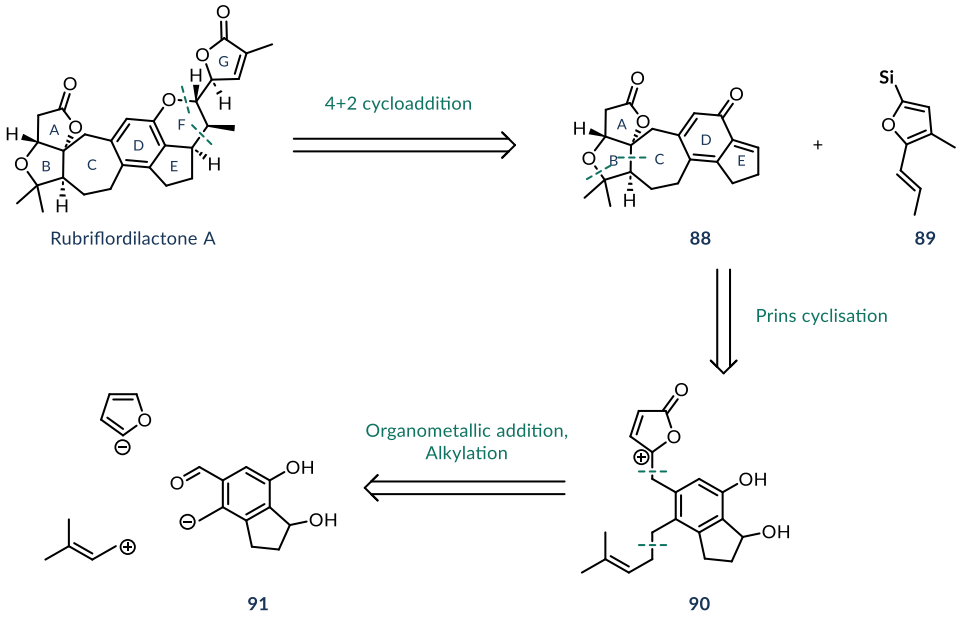


Figure 14. Chen's retrosynthesis of rubriflordilactone A

1.9.2 Forward synthesis

Starting from commercially available bromocresol **92** (Figure 15), acylation using acryloyl chloride via Fries rearrangement, followed by Nazarov cyclisation delivered indanone **93**. After cyanation, the phenol was protected as methoxymethyl ether **94**. Treatment of **94** with DIBAL partially reduced the nitrile to aldehyde, and at the same time reduced the ketone to an alcohol, which was protected as a silyl ether in the same step. Aldehyde **95** was *ortho*-lithiated by deprotonation of a temporary adduct formed by addition of the lithium salt of *N,N,N'*-trimethylethylenediamine[62] to the starting aldehyde, and alkylated using isopentenyl chloride. The aldehyde was revealed upon workup and reduced to the corresponding alcohol **96** in the following step. To attach the furan ring, this alcohol **96** was converted to a bromide under Corey-Kim conditions (without a base),[63] which was used as an electrophile in a reaction with 2-furanyllithium. Singlet oxygen oxidation of furan **97** resulted initially in endoperoxide formation, followed by *in situ* fragmentation to a lactone-hemiacetal. In the following step, this lactone-hemiacetal was converted to methyl acetal **98** via activation with acetic anhydride and treatment with methanol. Silyl deprotection, followed by oxidation of the resulting alcohol prepared indanone **99** for the first key step. The methyl acetal in **99** was activated by boron

trifluoride to give an oxocarbenium ion, which participated in the desired Prins cyclisation to form **100**. Boron trifluoride cleaved the methoxymethyl ether in the same step, and the authors found that sacrificial isobutene was required to scavenge the released formaldehyde. Product **100** was formed with low diastereoselectivity (2:1), slightly favouring the desired isomer. To close the B ring, this product **100** was reprotected as a MOM ether, then subjected to Mukaiyama hydration under Studer's conditions[64] with immediate oxa-Michael cyclisation. A final deprotection gave the ABCDE rings **101**.

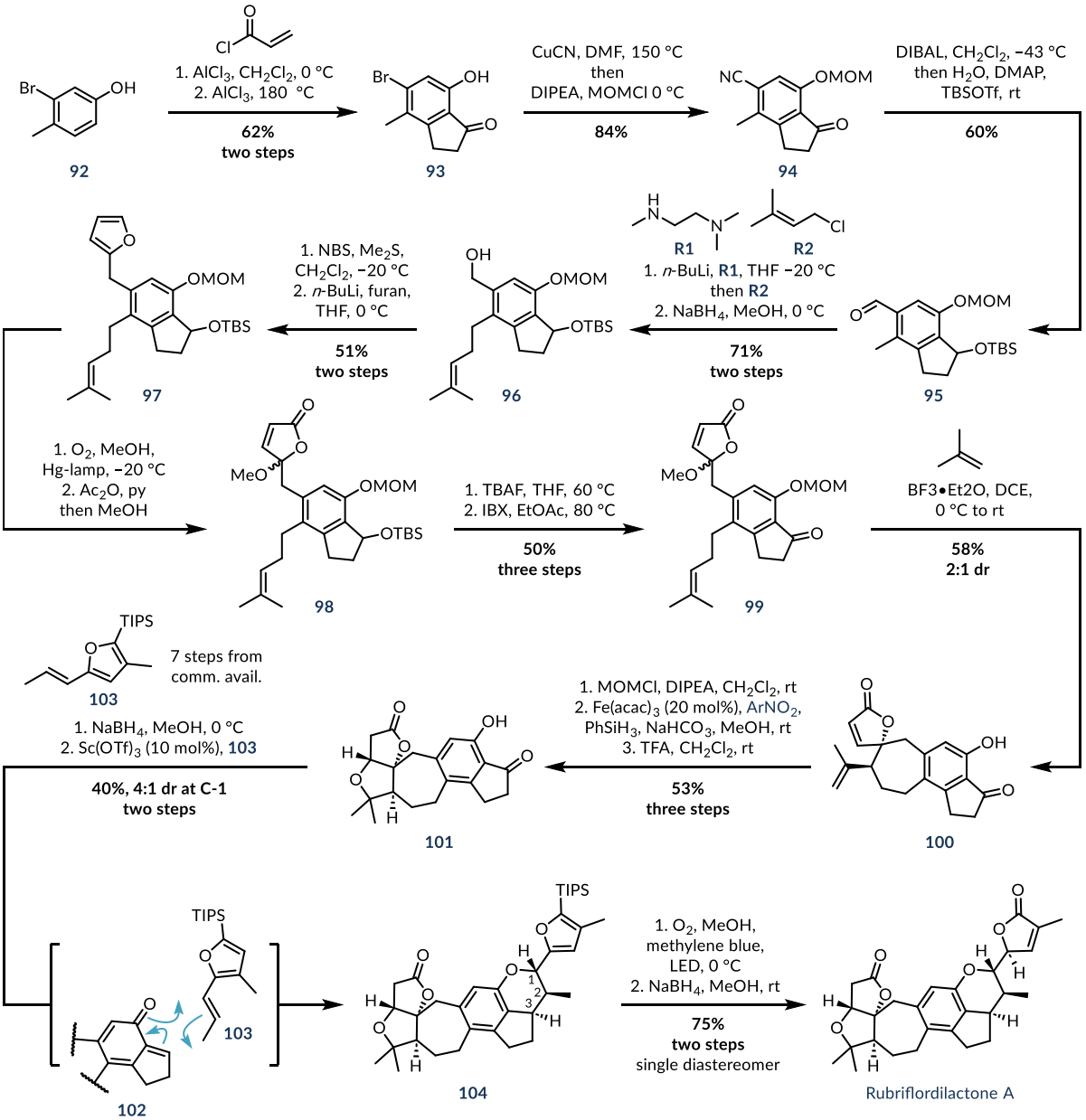


Figure 15. Chen's racemic synthesis of rubriflordilactone A

In the key step of the synthesis, after indanone **101** reduction to a phenol-alcohol, scandium-catalysed formation of *ortho*-quinone methide **102** set up a (4+2) cycloaddition with olefin **103**. This produced **104** as a mixture of diastereomers at C-1. If the cycloaddition was concerted, the relative stereochemistry at C-1, C-2 and C-3 in **104** would be controlled by either *exo* or *endo* transition states ('C1-up, C2-up, C3-down' for *exo* or 'C1-down, C2-down, C3-down' for *endo*). Since the *exo* transition state gives the desired product, the authors undertook extensive screening on a model system to identify an *exo*-favouring catalyst. The cycloaddition was, in fact, not concerted but stepwise, which resulted in a mixture of isomers at C-1. Initial bond formation between C3 and C2 could have also occurred via an open transition with the same outcome. In their computational modelling, however, the authors studied only closed transition states. Furthermore, in respect to quinone methide **102**, olefin **103** could approach from either the top or bottom face. The authors reported exclusive formation of the desired diastereomer resulting from the bottom face approach. This was evidenced based on isolation of only one product (apart from the C-1 epimer) that, when converted to rubriflordilactone A, matched the analytical data (^{1}H NMR, ^{13}C NMR and HRMS) with the literature. Given that sets of stereocentres in AB rings and EF rings could be sufficiently apart not to influence each other in NMR, the undesired diastereomer from top-face approach could have exactly the same shifts as the desired one, making the two diastereomers indistinguishable by the provided analytical data. In other words, a mixture of diastereomers would have the same proton and carbon shifts as either of the diastereomers alone. This confusion could have been avoided if the authors purposely made a diastereomeric mixture and separated and characterised each diastereomer, however, no such experiment was reported. Even if a single diastereomer had indeed been formed, the evidence provided would likely not have been sufficient to justify such a claim. Finally, singlet oxygen oxidation followed by *in situ* endoperoxide fragmentation and hemiacetal reduction completed this rubriflordilactone A synthesis in 26 steps (19 LLS) and 0.3% overall yield.

Chen's racemic synthesis of rubriflordilactone A started from the central benzene ring and gradually built the peripheral rings from it. The key transformations involved Prins cyclisation to form the seven-membered C ring and formal 4+2 cycloaddition via an *ortho*-quinone methide intermediate to build the right-hand side of the molecule. The synthesis features multiple uses of highly toxic chemicals such as MOMCl and CuCN, and 7 steps involving protecting group manipulation. It might come as a surprise that, despite Chen's synthesis being racemic, it has a similar number of steps to Li's asymmetric synthesis, but with an overall yield significantly lower than both Li's and Anderson's previous syntheses. However, if the goal had been to synthesise rubriflordilactone A as a mixture of eight or more isomers, then this synthesis could be considered suitable.

1.10 A. Li's synthesis of rubriflordilactone B (2016)

1.10.1 Overview of the strategy

Li's strategy for rubriflordilactone B[42] was similar to their previous strategy for rubriflordilactone A (Section 1.7.1). With 6π-electrocyclisation-oxidation in mind, the central benzene D ring was disconnected to tetraene **105** (Figure 16). This compound **105** would be made from the previously prepared ABC rings **45**, and a new building block, the EFG rings fragment **106**. To synthesise **106**, a Horner-Wadsworth-Emmons reaction between phosphonate **107** and aldehyde equivalent **108** was proposed to introduce the butenolide G ring, although stereocontrol at this stage remained uncertain.

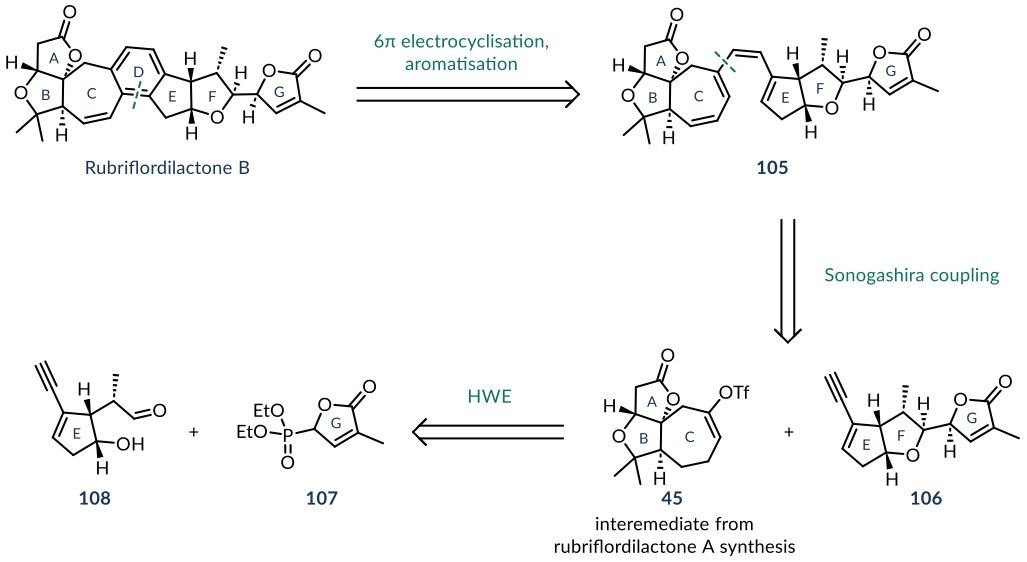


Figure 16. Li's retrosynthesis of rubriflordilactone B

1.10.2 Synthesis of the EFG fragment

The forward synthesis began with the preparation of enone **110** (Figure 17), a compound known in the literature,[65] in five steps from cyclopentadiene. Iodination, followed by Luche reduction gave alcohol **111** with excellent diastereoselectivity, as hydride delivery occurred opposite to the bulky OTBS group. After Sonogashira coupling, allylic alcohol **112** was subjected to a Johnson-Claisen rearrangement, similar to the one employed in their rubriflordilactone A synthesis (Section 1.7.3). This time, however, a much lower diastereselectivity (3:1 vs 8:1) was observed, which was ultimately of no consequence as the diastereomeric mixture **113** was deprotected with spontaneous lactonisation, and subjected to deprotonation-kinetic protonation sequence to generate lactone **115** as a single diastereomer. Reduction of this lactone **115** to lactol **116** prepared the substrate for a Horner-Wadsworth-Emmons reaction, where an aldehyde was revealed from lactol **116** and reacted with a phosphonate reagent, followed by spontaneous oxa-Michael cyclisation to form the target EFG rings system **117** as mixture of diastereomers at C-1. The stereochemistry at C-2 was set at the oxa-Michael cyclisation stage, with the butenolide ring positioned on the convex face of the forming ring. The stereochemistry at C-1, however, could not be controlled in this transformation.

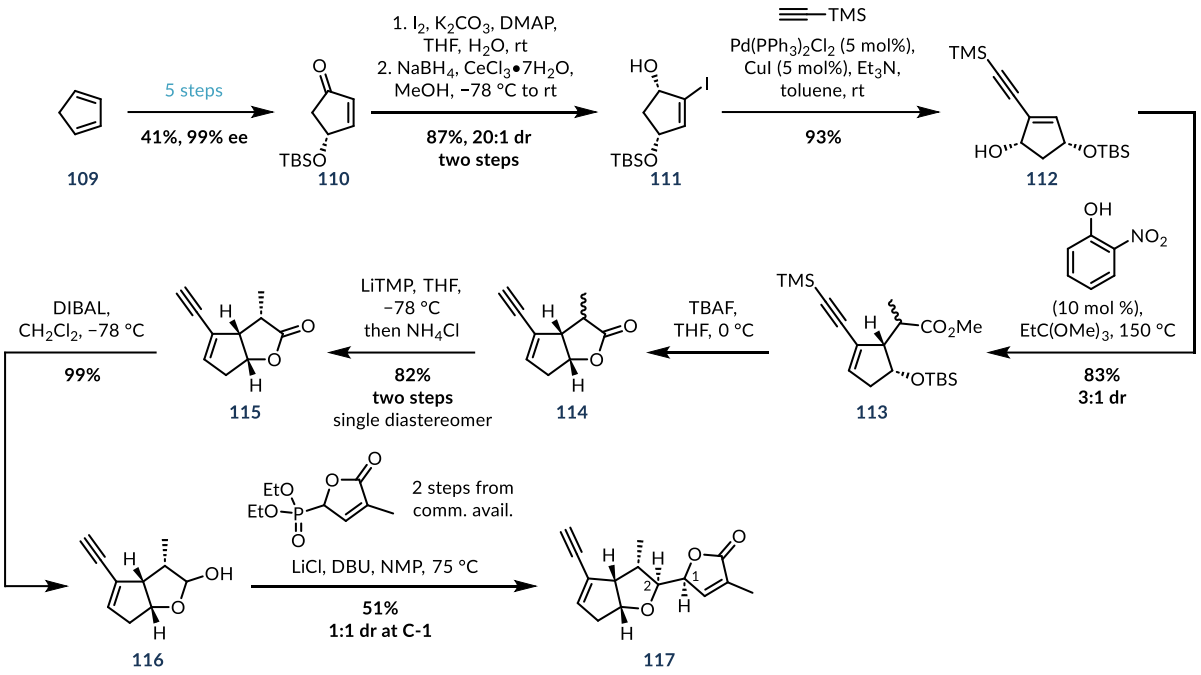


Figure 17. Synthesis of the EFG fragment

1.10.3 Completion of the synthesis

To complete their rubriflordilactone B synthesis, the ABC rings intermediate **45** (Figure 18) from the previous rubriflordilactone A synthesis was converted to a suitable intermediate for fragment unification, by introduction of an additional double bond. Radical bromination of **45** gave an inconsequential mixture of diastereomeric bromides **118**. Nucleophilic substitution with an *in situ* generated selenide, followed by oxidation and spontaneous selenoxide elimination, generated the required fragment **119**. This was merged with the EFG rings **117** using Sonogashira coupling. The idea behind the Sonogashira coupling was to use alkyne **120** as a precursor to a *cis*-alkene required for 6π-electrocyclisation, while relying on a robust reaction to join the fragments, and avoiding Stille coupling and issues with polyene isomerisation. In the event, partial hydrogenation of alkyne **120** proved troublesome, and an alternative solution involving platinum-cataylsed alkyne hydrosilation was found to be effective, giving a mixture of regioisomeric vinylsilanes **121**. An alkyloxysilane was used as it provided a good balance between reactivity and stability. The vinylsilane mixture **121** was heated to effect 6π-electrocyclisation, followed by DDQ oxidation to aromatise the hexadiene

ring to benzene. Finally, fluoride-mediated cleavage of the silyl group completed the first synthesis of rubriflordilactone B in 35 steps (21 LLS) and 1.4% overall yield.

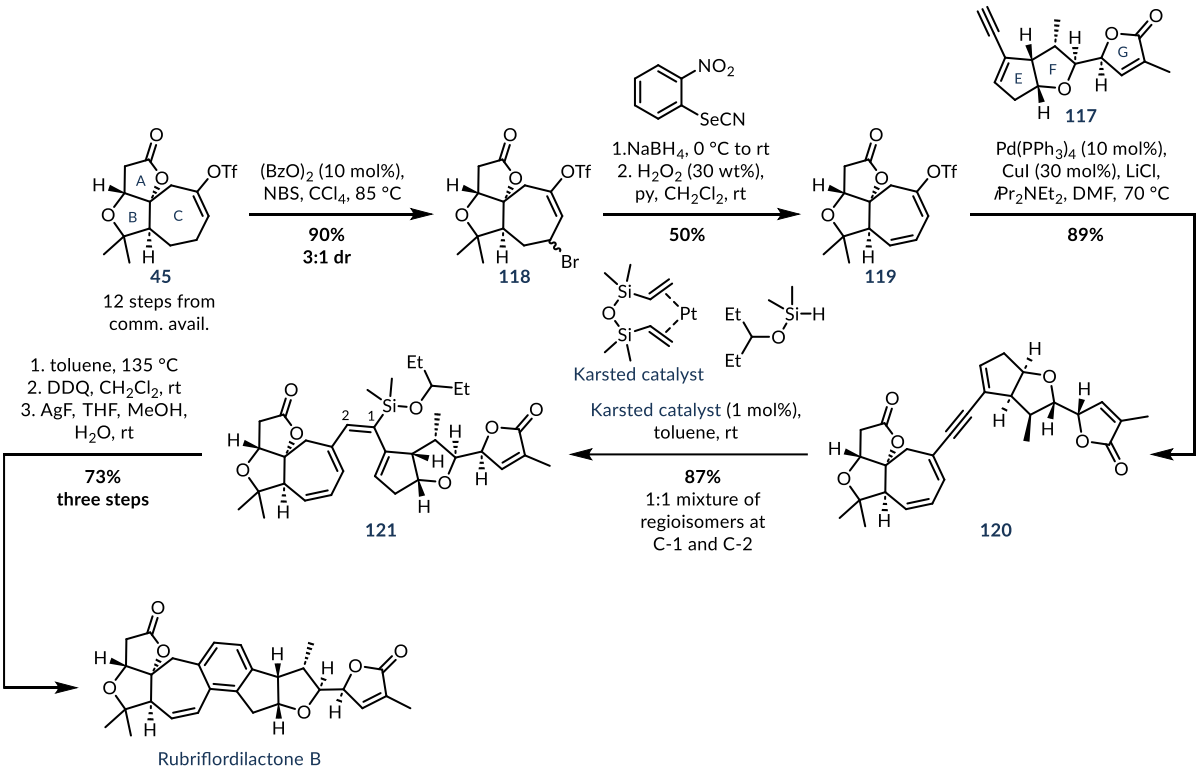


Figure 18. Completion of the rubriflordilactone B synthesis

A strategy relying on a convergent approach and central benzene ring synthesis via 6π-electrocyclisation-oxidation proved successful for rubriflordilactone B, just as it was for rubriflordilactone A. Postponing the unification of the fragments to the latest possible stage allowed for an efficient endgame, however, inefficiencies in the syntheses of the complex fragments were ultimately responsible for the high step count. Additionally, toxic selenium reagents and intermediates could likely have been avoided by using an alternative method for bromide elimination.

1.11 E. Anderson's synthesis of rubriflordilactone B (2019)

1.11.1 Overview of the strategy

The Anderson group's approach to rubriflordilactone B[43, 66] employed the same strategy as their previous synthesis of rubriflordilactone A: construction of the central benzene D ring via

(2+2+2) cyclotrimerisation, enabling a convergent synthesis from the AB rings and FG rings fragments (Figure 19). The AB rings fragment had previously been used in the synthesis of rubriflordilactone A. The FG fragment bears significant complexity, mainly due to its 5 contiguous sterecentres. In contrast to their rubriflordilactone A synthesis, the butenolide G ring would be introduced before fragment unification. Although this increased the complexity of the FG fragment, it would significantly simplify the endgame, reduce the length of longest linear sequence, and improve overall yield. However, no clear strategy for setting the butenolide stereochemistry was devised.

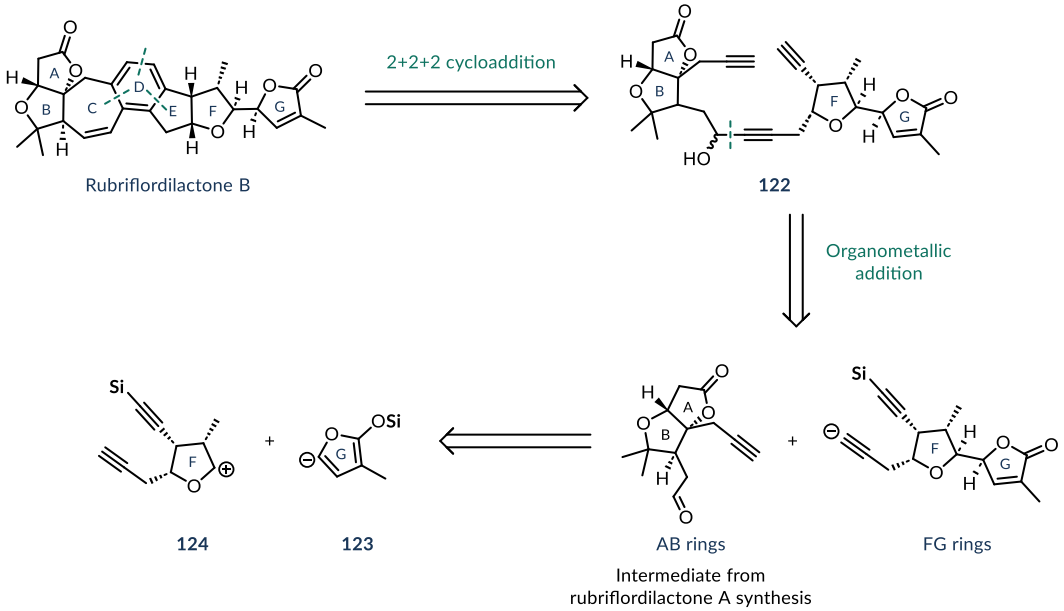


Figure 19. Anderson's retrosynthesis of rubriflordilactone B

1.11.2 Synthesis of the FG fragment

To tackle the challenge of five contiguous stereocentres in this molecule, an Ireland-Claisen rearrangement was planned to control two key stereocentres, with initial steps setting the stage for this transformation. Starting from commercially available diol **125** (Figure 20), monoprotection and Parikh-Doering oxidation gave aldehyde **126**. The first stereocentre was introduced via quinine derivative-catalysed (2+2) cycloaddition between aldehyde **126** and ketene derived from acetyl chloride. Although the enantioselectivity was not very high, this had no effect on the overall synthesis enantioselectivity because lactone **127** was merged with a

highly enantiopure alcohol in the next step. Combining two enantioenriched compounds gives a more enantioenriched product compared to either starting material. This comes at the expense of diastereoselectivity, with ester **128** produced as a 4:1 mixture of diastereomers at C-1, which is a consequence of only moderate enantioselectivity of the (2+2) cycloaddition step.

Ester **128**, as mixture of diastereomers at C-1, was subjected to dianionic Ireland-Claisen rearrangement to give an acid which was subsequently converted into ester **129** as a mixture of diastereomers at C-1. The Claisen rearrangement step proceeded via a chair-like transition state with the C-2 methyl group responsible for the stereochemical outcome, being positioned equatorially in the transition state. The C-1 stereochemistry did not influence the rearrangement. The hydroxy group at C-1 was designed to control enolate geometry through metal coordination, ensuring the hydroxy and carbonyl were on the same side of the enolate double bond.

Ester **129** was then reduced to a primary alcohol, which was protected as a silyl ether **130**. A two-step oxidative cleavage of the double bond in **130** produced an aldehyde/hemiacetal which was converted into a methyl acetal, followed by primary silyl ether deprotection to give tetrahydrofuran **131**. To install the first alkyne, the alcohol in **131** was oxidised to an aldehyde, and Stork-Zhao olefination took place, with telescoped iodide elimination and alkyne protection to give **132**. To install the second alkyne from PMB protected alcohol **132**, a four-step sequence was conducted: PMB deprotection, alcohol to aldehyde oxidation and Corey-Fuchs reaction, resulting in diyne-acetal **133**. Before the butenolide ring could be introduced, the methyl acetal **133** was activated as an acetate, and the alkyne was converted to an alkynyl iodide. Finally, Lewis acid-mediated vinylogous Mukaiyama aldol produced the desired FG rings as a 1:1 mixture of separable diastereomers at C-1.

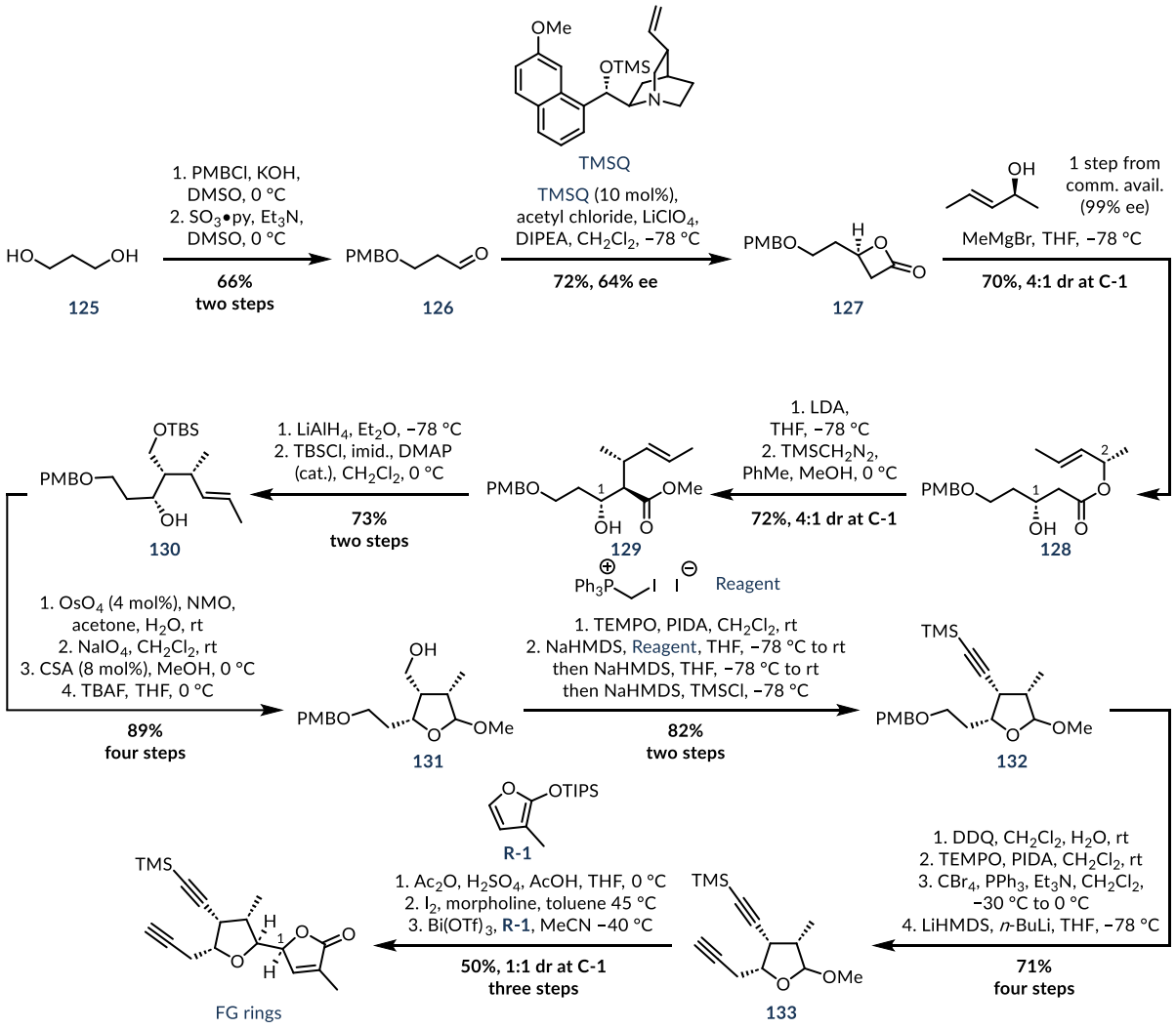


Figure 20. Synthesis of the FG rings

Even without control of the butenolide stereocentre, the FG rings synthesis took 22 steps (21 LLS), with 11 steps involving non-strategic redox and protecting group manipulations. The extent of functional group manipulations in this synthesis is best illustrated by following the fate of the lactone **127** carbonyl, which was first converted to an ester, then an acid, then an ester again, then a primary alcohol, protected, deprotected, oxidised to an aldehyde, and finally transformed into an alkyne.

1.11.3 Completion of the synthesis

The AB rings and FG rings were merged using a Nozaki-Hiyama-Kishi coupling (Figure 21). Silyl deprotection revealed triyne **134**, which underwent (2+2+2) cyclotrimerisation with

Wilkinson's catalyst to form the central CDE rings. Finally, dehydration of the benzylic alcohol completed the synthesis of rubriflordilactone B in 42 steps (25 LLS) and 0.6% overall yield.

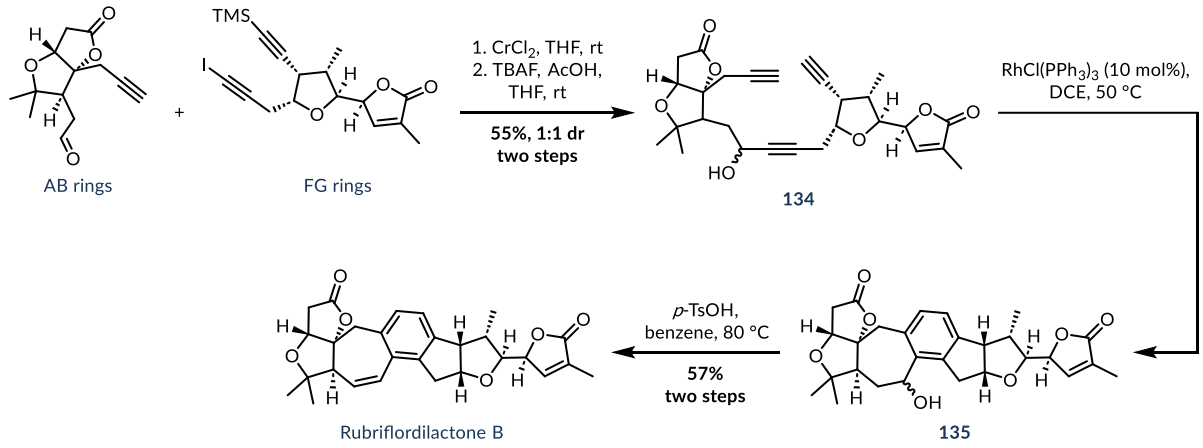


Figure 21. Completion of the synthesis

Anderson's rubriflordilactone B synthesis features a highly convergent approach, with the key (2+2+2) alkyne cyclotrimerization reaction efficiently forming the central three rings. However inefficiencies in fragment syntheses, especially the FG rings, resulted in a high overall step count. With the fragment syntheses addressed, however, this strategy could potentially become practical / usable.

1.12 A. Hoveyda's synthesis of the AB rings (2020)

The Hoveyda group developed an enantioselective multi-component ketone synthesis involving addition of allylcopper species to nitriles.[38] Recognising the importance of the AB rings for *Schisandra* triterpene synthesis, they aimed to apply this reaction to achieve an efficient synthesis of this fragment.

To synthesise a suitable substrate for their key reaction, alcohol **136** was subjected to Crabbe reaction (Figure 22), followed by alcohol protection to give allene **137**. This allene **137** underwent borylation-cupration to form an allylcopper species that reacted with allylnitrile to give an iminium that was hydrolysed to ketone **138**. Use of a Josiphos ligand ensured high enantioselectivity of this transformation. Double single electron reduction of chloropropane

reagent, followed by transmetallation to cerium and addition to ketone **138** produced tertiary alcohol **139** in high diastereoselectivity. The stereochemical outcome is consistent with the Felkin-Anh model, with the vinylboronic ester group positioned perpendicular to the carbonyl. The reaction was quenched with sodium perborate to oxidise vinylboronate functionality to a ketone. One-step acetal deprotection and oxidation with lactonization formed the first of the two rings in the AB rings fragment. Methylmagnesium bromide addition to the ketone gave tertiary alcohol **140**. To close the second ring of the AB rings, Mukaiyama dehydrogenation of lactone **140** introduced a double bond, enabling the tertiary alcohol to cyclise and form a tetrahydrofuran ring in **141**. To complete the synthesis, the alkene in **141** had to be converted into an alkyne. This was achieved via ozonolysis, followed by Seyferth–Gilbert homologation. Finally, silyl deprotection and alcohol oxidation completed the synthesis of the AB rings in 12 steps (11 LLS) and 15% overall yield.

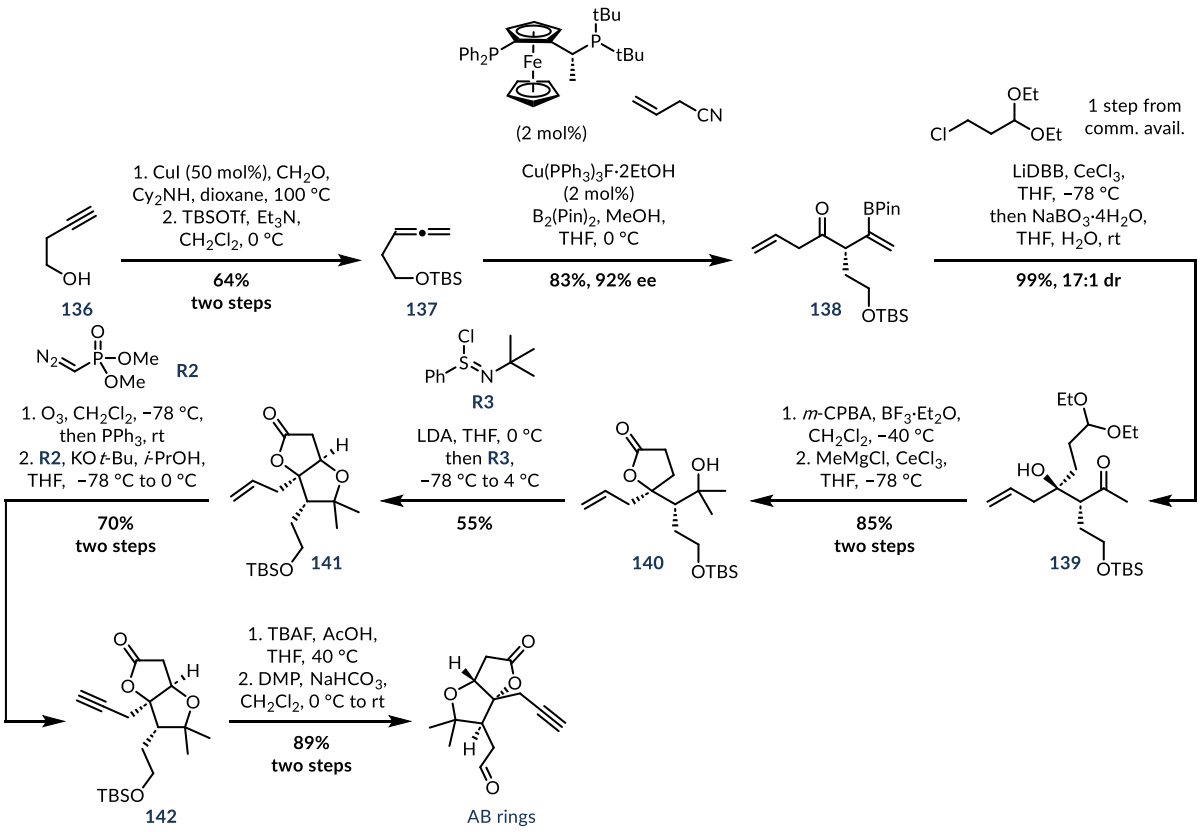


Figure 22. Hoveyda's synthesis of the AB rings

Hoveyda's synthesis of the AB rings presents an improvement compared to the previous synthesis of the same fragment by Anderson (12 vs 16 steps). The core carbon framework was assembled with the correct stereochemistry within several steps. Further functional group manipulations, however, contributed to high step count. Despite looking relatively appealing, this synthesis involved several operationally complex steps, which bring a higher chance of reproducibility issues. In our hands, we found the key enantioselective step to be batch dependent, while the following organometallic addition step was completely irreproducible. Furthermore, high cost of the Josiphos ligand would be prohibitive for large-scale adoption of this route.

1.13 Our approach to the *Schisandra* triterpenes

The overarching aim of this work is to develop a strategy that could enable an efficient, scalable and sustainable collective synthesis of triterpenes from the *Schisandraceae* family. To achieve this, we identified the ABCD rings fragment as a common precursor to three different types of Schisandra triterpenes (Figure 23). The CD rings of this fragment would be synthesised in a single cascade cyclisation event from the AB rings derivative. This cascade cyclisation would need to be developed using a model system, before applied to the *Schisandra* triterpene synthesis.

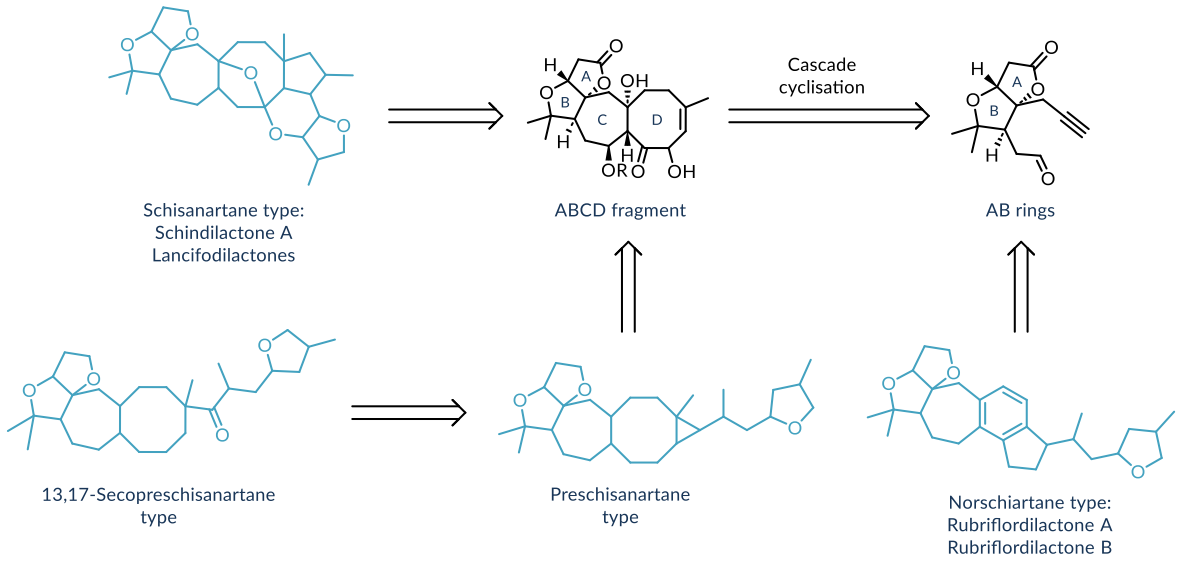


Figure 23. Our approach to the *Schisandra* triterpenes

The AB rings would serve as a key intermediate and branching point, allowing synthesis of either the ABCD fragment or the norshiartane type, which includes rubriflordilactones A and B (Figure 23). Previous syntheses of the AB rings by Anderson and Hoveyda suffered from high step count, excessive chromatography and poor scalability, along with limited reproducibility in the case of Hoveyda's synthesis. We set to develop a new synthesis of the AB rings that would align with our goals of efficient, sustainable and scalable synthesis. From the AB rings, we would pursue synthesis of lancifodilactone I (and further family members by single-step interconversions), rubriflordilactones A and/or B, also in line with the stated goals.

To summarise, our aim towards the efficient synthesis of *Schisandra* triterpenes can be divided into four stages:

1. Synthesis of the AB rings
2. Development of the cascade cyclisation and application to lancifodilactone I synthesis
3. Synthesis of rubriflordilactone B
4. Synthesis of rubriflordilactone A

The following chapters describe our efforts towards achieving these goals.

Chapter 2: Cyclisation cascade toward lancifodilactone I

2.1 Carbopalladation, Suzuki coupling and electrocyclisation cascade

The objective in this chapter was to develop an efficient collective synthesis of the *Schisandra* triterpenes. Lancifodilactone I (Figure 24), a previously unconquered target, was identified as a common precursor to other natural products in this family. We envisioned that the key 7,8-fused ring core of lancifodilactone I could be synthesized via a palladium catalysed cascade cyclisation reaction. Bromoene-ynamide **144** would react with Pd^0 via oxidative addition, followed by *syn*-carbopalladation (**145**), Suzuki coupling (with a suitable dienyl boronic acid) to give **146**, and 8π-electrocyclisation to deliver the 7,8-fused system **143** in one step. We proposed that an electron-donating ynamide functionality in **144** would enhance the nucleophilicity of the resulting enamide in **143** for further functionalisation, while the bulkiness of the ynamide nitrogen substituent should prevent *cis-trans* isomerisation of the intermediate vinyl palladium species **145** that has been observed with less bulky substituents by our group, and others.[67, 68]

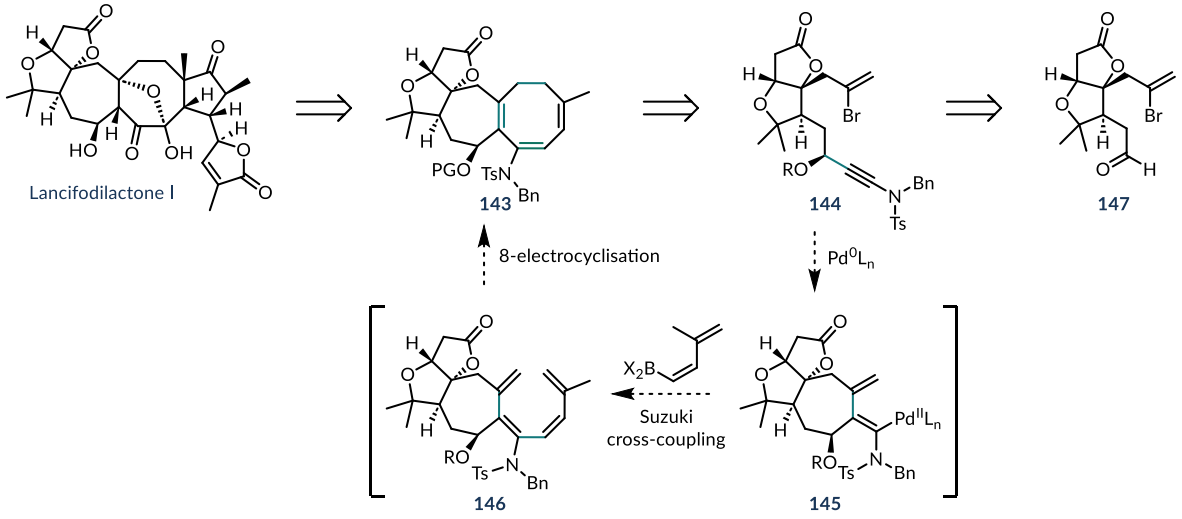


Figure 24. Retrosynthetic strategy towards lancifodilactone I.

Bromoenyne carbopalladation, coupling and electrocyclization sequences are generally well-established.[69] This reactivity was first explored by Negishi[70] in 1992. An example of the desired cascade was reported by Suffert[71] in 2001 (Figure 25a). A 4-*exo-dig* carbopalladation, followed

by Stille coupling and 6π-electrocyclisation delivered **150**. This was later extended to cascades incorporating 8π-electrocyclisation[72] (Figure 25b) and 5-*exo-dig* carbopalladation[73] (Figure 25c).

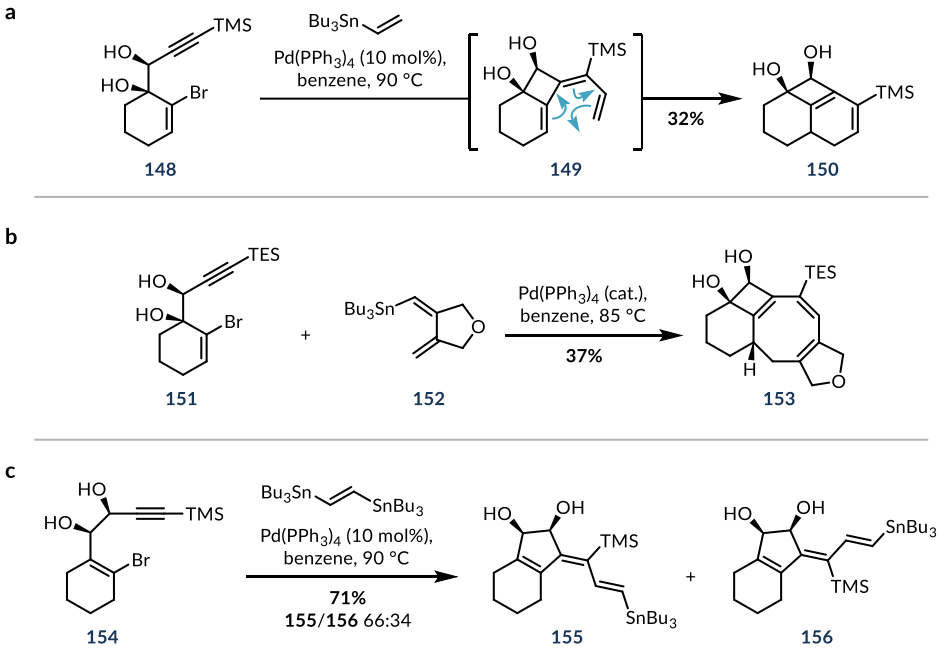


Figure 25. Previous work by Suffert on carbopalladation, coupling and electrocyclisation cascades

Previous work from the Anderson group[27, 74] showed that this type of cascade can be used to synthesize 7,8-fused ring systems (Figure 26a). However, we wanted to avoid the use of a toxic organotin coupling partner as employed in that work by switching to an untested dienyl Suzuki coupling / 8π strategy. The Anderson group have also shown that ynamides can undergo intramolecular carbopalladation cascades in a carbopalladation, Suzuki, 6π sequence in which the ynamide nitrogen atom is located 'inside' the tethering ring, affording tetrahydroindoline products[75] (Figure 26b).

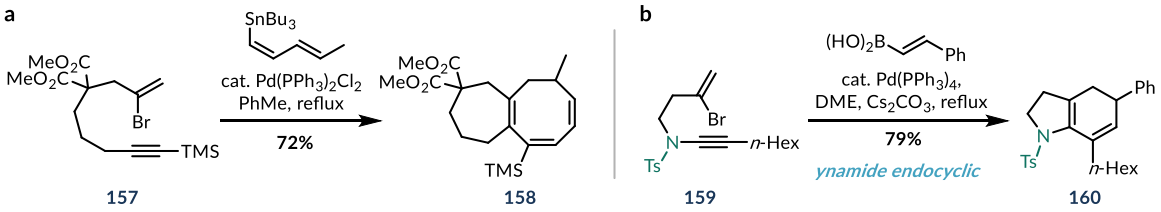


Figure 26. Synthesis of 7,8-fused systems via alkyne carbopalladation, Stille coupling, 8π-electrocyclisation tandem sequence, and synthesis of 5,6-fused systems via ynamide carboplladation, Suzuki coupling, 6π-eletrocyclisation sequence

For our synthesis, the nitrogen atom must be positioned at the alkyne terminus, rather than internally, which is an unprecedented tactic. At the outset, several questions therefore had to be answered (Figure 27):

1. Can carbopalladation, Suzuki, 6π cascades proceed with the ynamide nitrogen atom position exocyclic to the forming ring, and how does this alkyne polarity reversal affect reactivity (**161**→**162**)?

2. Can the bromoenynamide-Suzuki cascade be extended to the synthesis of 8-membered rings **163**?

3. Can the resulting 8-membered ring enamides undergo further selective functionalisation towards the carbocyclic core of lancifodilactone I (**164**)?

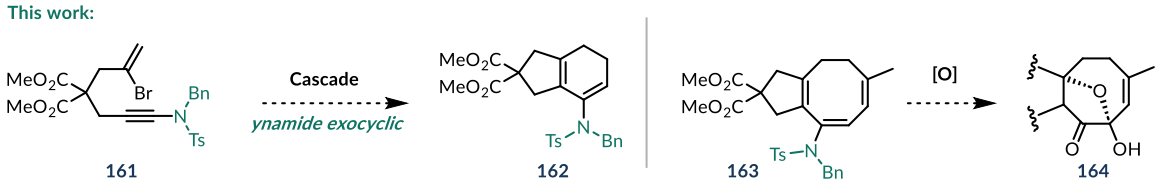


Figure 27. Proposed synthesis of 5,6- or 5,8-fused ring systems with external nitrogen position, and subsequent selective oxidations

2.2 Synthesis of 5,6-fused systems

To investigate the first question, bromoenynamide **161** was synthesized in four steps from dimethyl malonate **165** (Figure 28). Malonate deprotonation by sodium hydride, followed by allylation with 2,3-dibromopropene, gave the monoallylated product. Further deprotonation by sodium hydride and treatment with excess propargyl bromide gave bromoenyne **166**. Silver catalysed alkyne bromination[76], followed by chemoselective copper catalysed ynamide formation (using the conditions developed by Hsung et al.[77]), gave the desired bromoenynamide **167** in excellent yield.

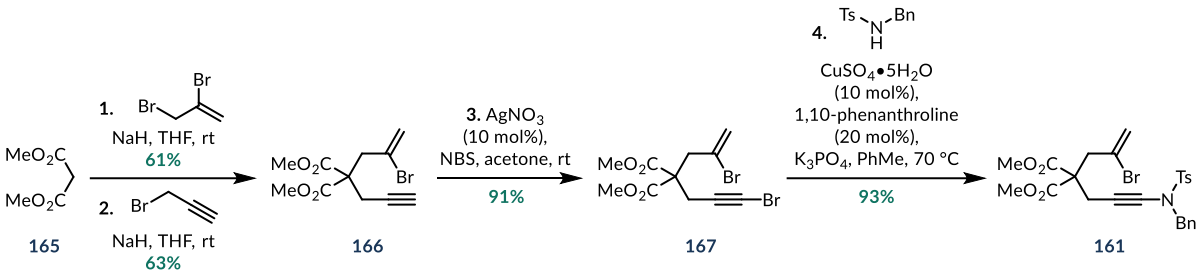
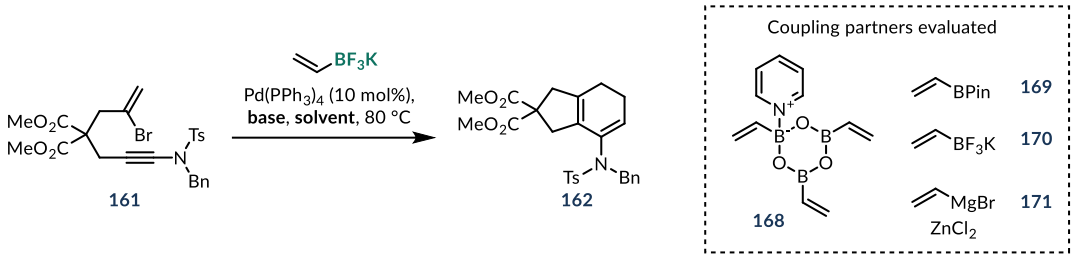


Figure 28. Synthesis of bromoynamide **11**

The carbopalladation, Suzuki, 6π cascade was investigated with three vinylboronic acid derivatives **168**–**170**, and a vinylzinc species **171** as coupling partners. Only the potassium vinyltrifluoroborate salt **170** was effective (Table 1), with other partners resulting in degradation or no reaction observed. Further optimisation (Table 1) led to the identification of tetrakis(triphenylphosphine)palladium(0) and potassium carbonate in THF/water 10:1 at 80 °C as optimal conditions to deliver the desired product **162** in 89% isolated yield.

Table 1. Optimisation of the carbopalladation/Suzuki coupling/6π-electrocyclisation cascade



Solvent	Base		
	K_2CO_3 (aq)	Cs_2CO_3 (s)	LiOH (aq)
Toluene	0 (100)	0 (24)	38 (80)
THF	100 (100)	7 (100)	25 (66)
Dioxane	88 (100)	34 (100)	27 (73)
THF/H_2O (10:1)	**89** [a]	–	–

Yield (%) and conversion (%, indicated in parentheses) for the reaction of **161** with potassium vinyltrifluoroborate salt **170**, determined by HPLC analysis after 10 h at 80 °C. [a] Isolated yield. Aq – aqueous solution, s – solid.

These results demonstrate that the position of the nitrogen atom on the alkyne (internal vs. external), and therefore the alkyne polarisation, does not strongly influence the efficiency of carbopalladation and subsequent Suzuki coupling, with both types of ynamide undergoing the desired cascade in excellent yields.[75]

2.3 Synthesis of 5,8-fused systems

To address the second question of extending the cascade to the formation of 5,8-fused systems from bromoenynamides, a dienylboronic acid equivalent **173** was required (Figure 29). After examination of several different routes, this simple but synthetically challenging fragment was synthesized from 2-methyl-3-butyn-2-ol **172** in two steps. Dehydration[78], followed by rhodium catalysed *trans*-hydroboration developed by Miyaura[79], gave the desired boronate ester **173** as a mixture of geometric isomers. It was possible to obtain the pure *Z* isomer by preparative HPLC. It is important to note that the stereochemical purity of the diene coupling partner **173** is crucial to the success of the planned cascade: any *E* isomer present in the mixture would preclude an 8π-electrocyclisation, therefore leading to side product formation and yield deterioration. Subjection of this dienyl pinacolboronic ester to the previously optimised conditions afforded the 5,8-fused product **163** in an excellent yield of 96% (Figure 29).

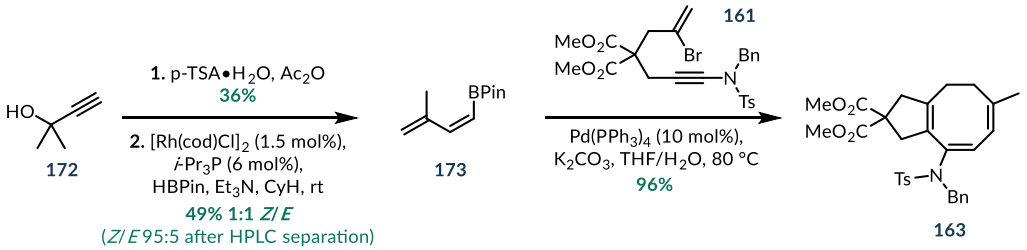


Figure 29. Synthesis of (*Z*)-3-methylbutadienyl boronate ester **173** and application of the optimized cascade to synthesis of 5,8-fused system **163**

2.4 Selective Functionalisation of 5,6- and 5,8-Fused Ring Systems

To investigate selective oxidations of the 5,6- and 5,8-fused ring scaffolds, hydrolysis of enamide **162** to the corresponding ketone **174** was attempted. Subjection of **162** to a range of strongly or weakly acidic conditions resulted in either no reaction, or decomposition of the starting material (Figure 30a). Attempts to cleave the sulfonamide under common reductive conditions (Mg, MeOH; Na, naphthalene, DME; SmI_2, pyrrolidine, THF/water) also led to either no reaction, or decomposition of the starting material. On the other hand, *m*-CPBA-mediated epoxidation of **162** selectively epoxidised the tetrasubstituted (non-enamide) alkene giving epoxide **176**. Upjohn dihydroxylation of **162** gave a mixture of products, with the major product

being **175**. Equivalent transformations of 5,8-fused ring enamide **163** (Figure 30b) with potassium osmate/NMO or *m*-CPBA resulted in the selective oxidation of the trisubstituted alkene to produce diol **177** or epoxide **178**, respectively. Oxidation of the enamide double bond was not observed.

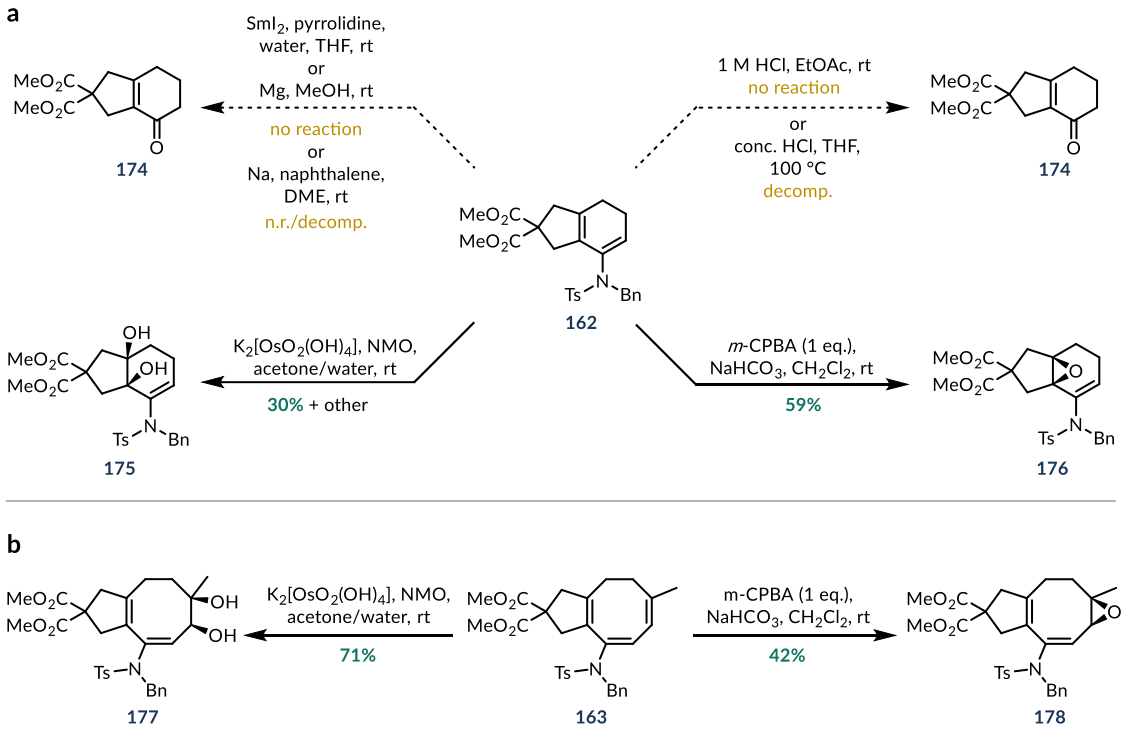


Figure 30. (**a**) Oxidations of the 5,6-fused ring system; (**b**) Oxidations of the 5,8-fused ring system

These results contradict our expectation that electron donating capabilities of a sulfonamide group, through conjugation of the enamide nitrogen lone pair with its alkene, would make the enamide more nucleophilic and therefore reactive towards oxidation. The results are likely a consequence of the reduced conjugation of the nitrogen lone pair with the double bond due to steric congestion in **162** and **163.** The lone pair could be positioned orthogonally or near orthogonally to the alkene π system. With the resonance electron-donating effect removed, the inductive electron-withdrawing effect of the sulfonamide group makes the 'enamide' actually an electron poor olefin, and therefore less reactive towards oxidation.

2.5 Attempted synthesis of 7,6- and 7,8-fused ring systems

To test if the developed cascade could be used in the synthesis of the 7,8- and 7,6- systems found in *Schisandra* triterpenes, model bromoenynamide **183** was synthesized in four steps from dimethyl malonate (Figure 31). Monoallylated malonate derivative **181** was first subjected to conjugate addition to acrolein, giving aldehyde **182**. Meanwhile, benzyl tosyl amine **179** was converted to dichloroenamide **180**, which served as a precursor to a lithiated ynamide.[80] Treatment of aldehyde **182** with the lithiated ynamide generated from **180** gave a secondary alcohol, which was protected as a *tert*-butyldimethylsilyl ether **183**.

Unfortunately, under the previously developed conditions using potassium vinyltrifluoroborate, bromoenynamide **183** was converted to a mixture of the 'direct' coupling product **185**, and side product **187,** which derives from a formal 4-*endo-trig* Heck-type cyclisation[67] from a vinylpalladium intermediate **186**. Examination of different bases (Cs_2CO_3, Na_2CO_3) for a reaction of bromoenynamide **183** with a previously used diene boronate ester resulted in complex mixtures of unidentifiable products (not shown). These results suggest that the vinylpalladium species **184** arising from oxidative addition undergoes direct Suzuki coupling at a comparable rate to carbopalladation, and that once carbopalladation has occurred, the resulting dienylpalladium intermediate **186** undergoes intramolecular Heck-type cyclisation to form side product **187** much faster than the desired Suzuki coupling. To prevent side product formation, it was required to increase the rate of both carbopalladation step and Suzuki coupling, such that carbopalladation rate exceeds Suzuki coupling rate, which in turn exceeds intramolecular Heck rate.

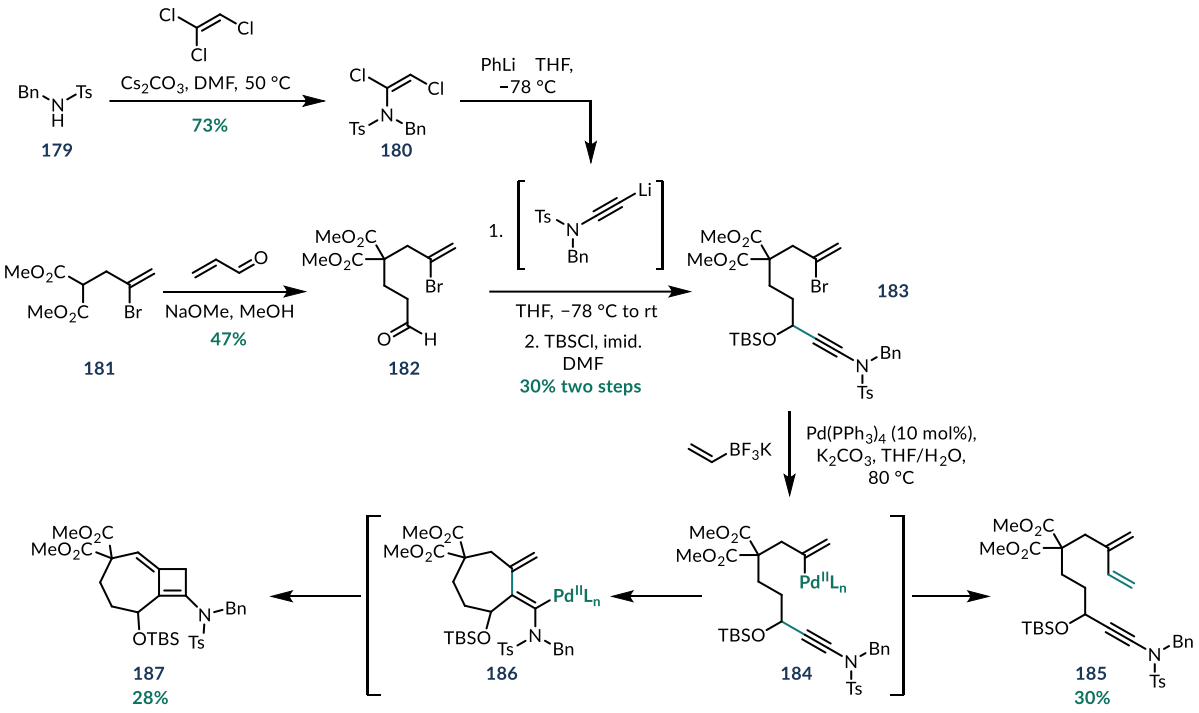


Figure 31. Application of the cascade to the synthesis of 7,6-fused system

2.6 Attempted application of the cascade towards the ABCD rings of Schisandra triterpenes

The cyclisation cascade substrate **189** was synthesized from a known aldehyde **147** used in previous synthetic studies in the Anderson group.[33] Addition of the lithiated ynamide derived from **180** to aldehyde **147** gave propargyl alcohol **189**. Unfortunately, with only milligram quantities of **189** in hand, attempts to apply the developed carbopalladation, Suzuki coupling, 8π-electrocyclisation cascade resulted only in the formation of complex mixtures of unidentifiable products.

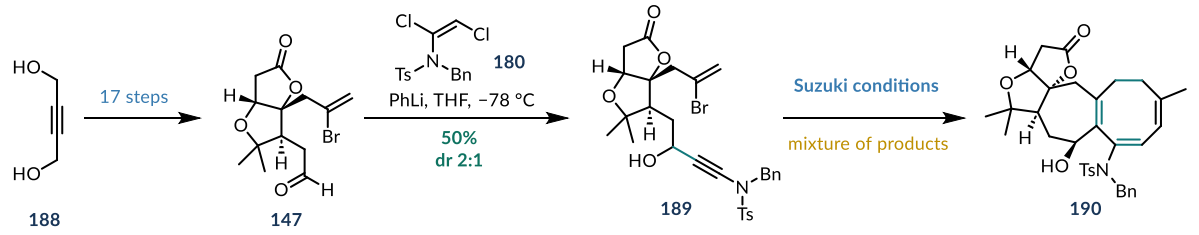


Figure 32. Application of the cascade to the 'real' substrate 39

2.7 Conclusion

A tandem carbopalladation, Suzuki coupling and 6π- or 8π-electrocyclisation reaction of bromoenynamides in which the ynamide nitrogen is exocyclic to the forming ring was explored in the context of synthesis of terpenes from the *Schisandraceae* family. It was shown that this tactic can be applied to the synthesis of 5,6- and 5,8-fused bicyclic ring systems in high yields. A route to a versatile dienylboronic ester building block was also developed. The reactivity of the resulting enamides was explored, and it was found that reactivity patterns differ to those observed with ynamides. Synthesis of 7,5- and 7,8-fused ring systems using the developed cascade was tested. However, the greater difficulty of 7-membered ring closure and propensity to form 7,4-fused ring byproducts hindered the application of this cascade. Nevertheless, for smaller ring tethers, the tandem carbopalladation, Suzuki coupling and 6/8π electrocyclisation was shown to be a highly efficient tactic, allowing a rapid increase in molecular complexity, and with a novel positioning of the ynamide nitrogen group. This process may therefore enable future applications in the synthesis of other classes of polycyclic natural products. In light of the challenges of this synthetic route, attention in this project turned to the synthesis of the main fragments in the overall strategy for the construction of the *Schisandra* triterpenes in line with the goals of efficient, scalable and sustainable chemistry, while avoiding previously developed impractical and lengthy synthetic sequences.

Chapter 3: Synthesis of the *Schisandra* AB ring system

3.1 Introduction

The successful and efficient synthesis of the AB rings is crucial for a unified synthesis of the Schisandra triterpenes. This fragment was previously synthesized by Anderson[81] (16 steps, 15% yield) and Hoveyda[82] (12 steps, 14% yield) groups. While Anderson's route suffers from a poor step count, Hoveyda's route, although slightly shorter, suffers from limited reproducibility and scalability, and despite significant efforts could not be productively progressed in this work.

3.2 C-H activation strategy

A new retrosynthetic analysis was considered (Figure 33), which relies on a highly simplifying disconnection of the quaternary stereocentre in **191** to a methylene group in **193**. To achieve this, a carefully designed substrate would be needed for a selective, non-directed C-H oxidation. Based on the guidelines published by White,[83] we predicted that a combination of electronic and steric effects would favour oxidation of the 'green' methylene group. By accessing the ketone oxidation state, we anticipated that we could then add an allenylmetal reagent to introduce the alkyne sidechain, and simultaneously cause lactonization to form **191**. Substrate **193** could in turn be constructed by another C-H disconnection via carbene insertion into the alpha C-H bond of **195**, a compound for which the synthesis has been reported in 3 steps from (-)-α-pinene.[84]

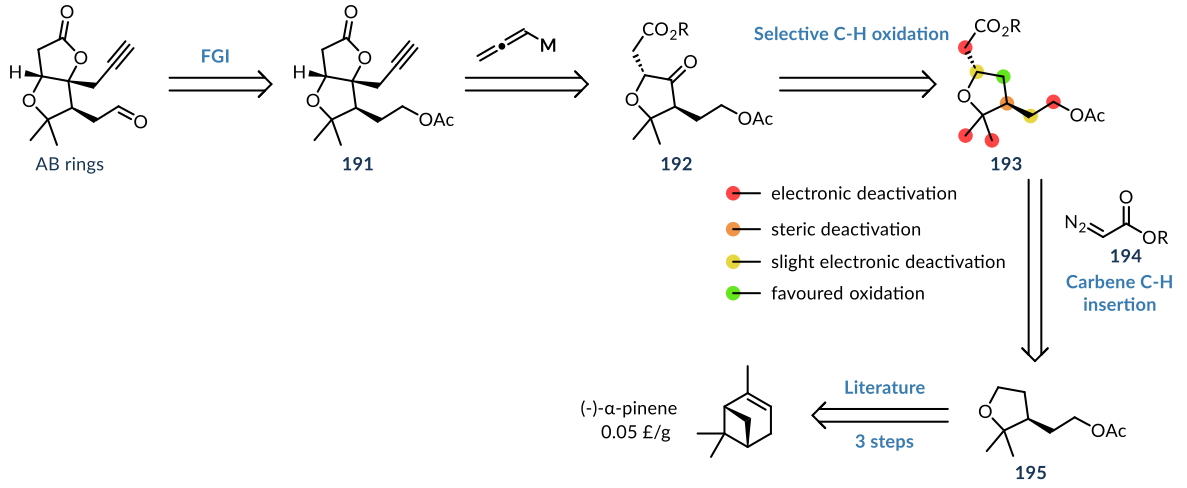


Figure 33. Retrosynthesis of AB rings using two C-H activation steps

We started by following the literature-described preparation of **195** (Figure 34) via ozonolysis of α-pinene[84], followed by an acid-induced rearrangement[84] and Baeyer-Villiger oxidation.[85] In the course of the preparation, we noticed and separated a side product **198**, which likely resulted from overoxidation during the ozonolysis stage. Compound **195** was subjected to a carbene insertion of ethyl diazoacetate using rhodium(II) acetate. Under different concentrations, rate of additions and catalyst loadings, we were unable to detect the desired product **193**. Instead, dimerisation of diazoacetate occurred exclusively, indicating that C-H insertion was too slow to compete with this process.

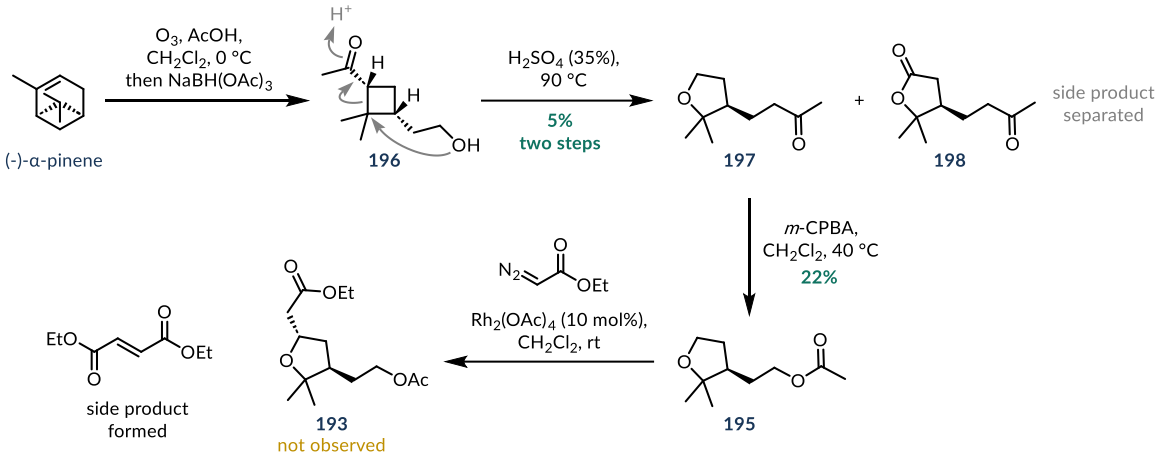


Figure 34. Tetrahydrofuran substrate synthesis and carbene insertion

To overcome the challenge of C-H carbene insertion, we recognised that we could take advantage of the side product **198** that had been unexpectedly observed during the

preparation of **195** (Figure 34). Thus, we targeted the preparation of **198** as the major product, and aimed to further explore its reactivity towards the AB rings (Figure 35). As such, oxidative cleavage of α-pinene,[86] followed by acid-promoted rearrangement gave ketone **198**. Baeyer-Villiger oxidation using m-CPBA was sluggish, and we used pertrifluoroacetic acid prepared from trifluoroacetic anhydride and hydrogen peroxide to obtain acetate **200**. We found that the challenging selective reduction of lactone **200** to a lactol in the presence of an ester could be effectively achieved by using a dilute solution of DIBAL at -90 °C, under which conditions the acetate group remained untouched. Fortunately, we were able to acetylate this lactol in the same step to give tentatively assigned **201** (^{1}H and ^{13}C NMR). A Mukaiyama aldol with a silyl ketene acetal produced tentatively assigned ester **202** as a 1:1 mixture of diastereomers (^{1}H and ^{13}C NMR). With ester **202** in hand, several protocols for C-H oxidation were examined: TFDO[87] led to a mixture of products, while decatungstate[88] showed no reactivity. Reaction using the Fe(PDP)[89] catalyst selectively delivered **200** in 40% yield, presumably by α-oxygen C-H oxidation and subsequent retro-aldol.

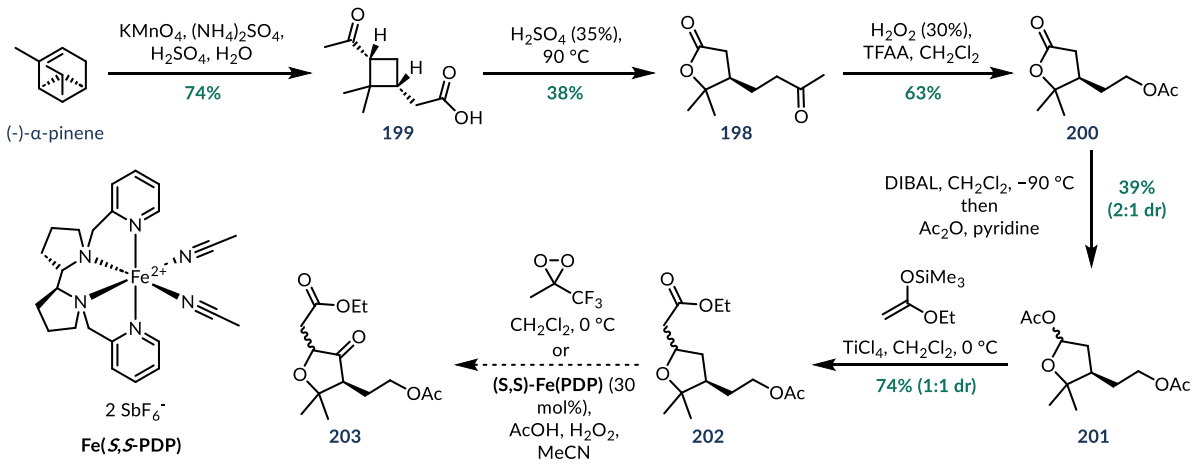


Figure 35. Synthesis of the AB rings

While other methods[90-93] for C–H oxidation remained untested, we decided to shift our approach due to concerns about the challenge of carbene insertion, and the lack of stereochemical influence of the present stereocentre in **201** in the aldol step (mandating a catalytic asymmetric Mukaiyama aldol to potentially solve this issue), as well as the inherent

substrate bias for the 'wrong' C-H bond and lack of commercial availability of other reagents for C-H oxidation.

3.3 Cyclobutane opening strategy

We came to the realisation that an appropriate cyclobutane opening/rearrangement (similar to the one observed in the preparation of **197**) could efficiently yield a tetrahydrofuran ring and subsequently the desired framework of the AB fragment, while at the same time deriving from a feedstock terpene source. This was the basis for the new approach (Figure 36).

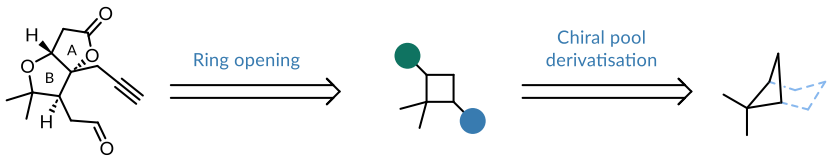


Figure 36. AB rings retrosynthesis using cyclobutane opening and chiral pool strategy

Starting from (–)-verbenone (Figure 37), addition of allenylmagnesium bromide produced alcohol **204** with complete stereoselectivity. The bicyclic framework in verbenone set efficiently what would become the adjacent quaternary and tertiary stereocentres in the AB rings. Ozonolysis, followed by Still-Gennari olefination[94] delivered ketone **206**. This ketone was reduced to alcohol **207** (with 4:1 dr), which was tentatively assigned, where the configuration of the major diastereomer of the alcohol remained uncertain.

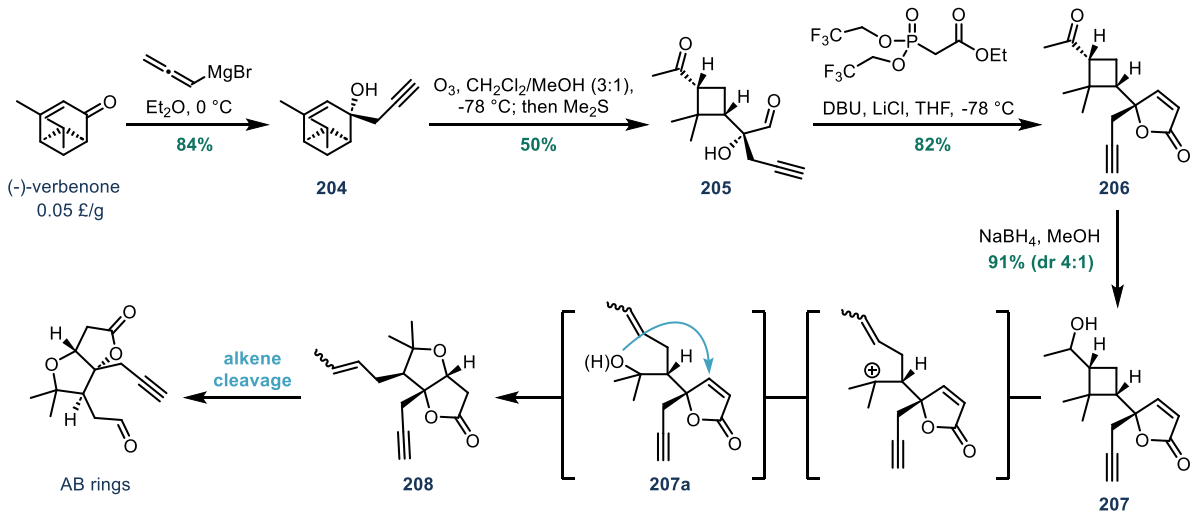


Figure 37. Forward synthesis of the AB rings

Cyclobutane ring-opening from alcohol **207** was investigated under various acidic conditions. The idea behind this fragmentation was to generate a tertiary carbocation that would be captured by an oxygen nucleophile. At the same time, the resulting alkene in **208** would be converted into an aldehyde by ozonolysis, completing the AB rings synthesis.

Treatment of **207** (Figure 38) with a range of acids (HCl, H_2SO_4, *p*-TSA, TfOH, $HClO_4$, HI) either at rt or heating resulted in no reaction or decomposition. When **207** (single diastereomer) was treated with iron(III) triflate, a ring expansion took place to form a product which was tentatively assigned as cyclopentane **209** (single diastereomer, Figure 38). Interestingly, the migration took place from a less substituted carbon, which stands in contrast to the general pattern of migration of the most cation-stabilising group. We reasoned that stereoelectronic and conformation effects were responsible for this outcome, although our understanding was limited as the alcohol stereochemistry of the starting material remained uncertain. Although cyclopentane **209** was not desired, this led us to test this type of ring expansion to form a tetrahydrofuran ring instead.

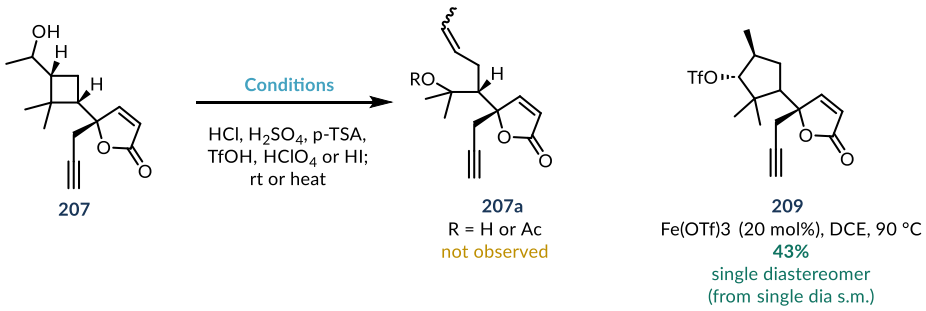


Figure 38. Studies of cyclobutane ring opening

3.4 Ring expansion rearrangement strategy

To explore a cyclobutane to tetrahydrofuran ring expansion, ketone **206** was synthesised in the same way as described in the previous section (Figure 39). Baeyer-Villiger oxidation of this ketone produced an acetate, which was solvolysed *in situ* to form alcohol **210**, with retention of configuration at the alcohol position. In the key step of the synthesis, a hypervalent iodine-

mediated ring expansion[95] delivered acetal **211**. To our knowledge, this was the first time this ring expansion has been used in targeted synthesis.

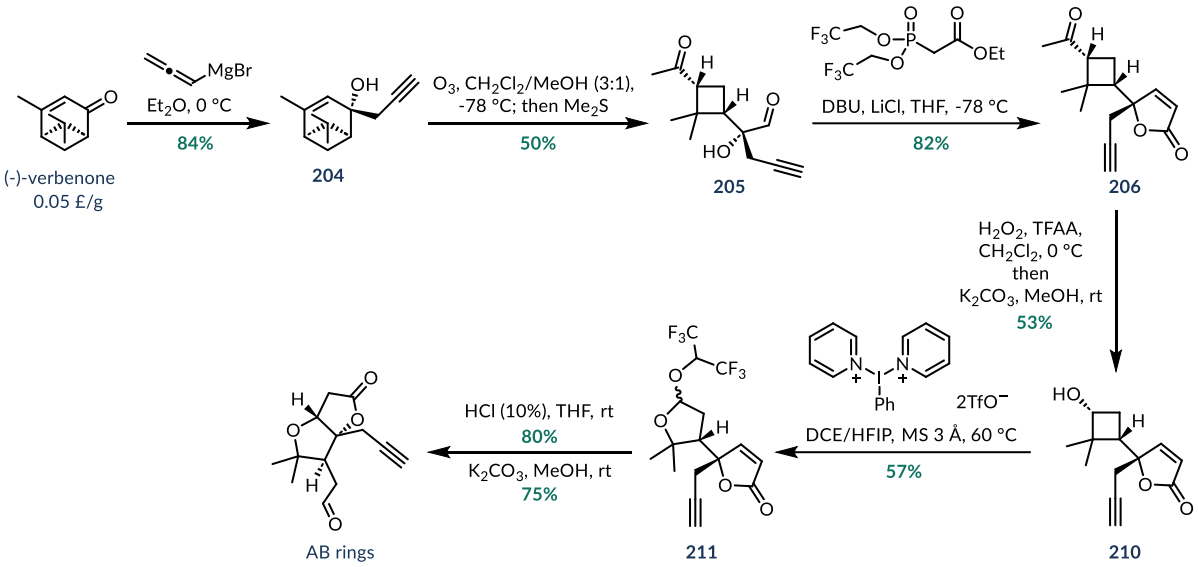


Figure 39. Successful forward synthesis of the AB rings

This reaction mechanism can be viewed as an oxygen variant of Beckmann rearrangement (Figure 40). Initially, the substrate displaces a pyridine group at the iodine(III) atom. The bulky *gem*-dimethyl group pushes the iodonium fragment away, aligning the migrating C-C bond and the breaking C-I bond in an antiperiplanar fashion. The *gem*-dimethyl group migrates to the electrophilic oxygen centre, with iodobenzene acting as a leaving group. A ring expansion takes place, resulting in the formation of a tetrahydrofuran oxocarbeninum ion. This ion then gets trapped by a molecule of solvent.

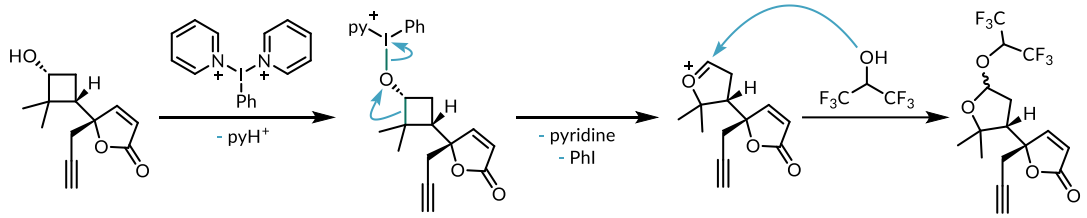


Figure 40. Ring expansion mechanism

Acetal **211** (Figure 39) contains atoms at the oxidation states found in the target AB rings. Following acetal hydrolysis (HCl, aq.) and treatment with potassium carbonate, the acetal carbon becomes the aldehyde in the AB rings, while the tertiary alcohol undergoes conjugate addition to the enoate, forming the tetrahydrofuran ring of the AB rings. Stereochemistry of

204, **205**, **206**, **210** and **211** was thus confirmed by the successful synthesis of the final compound that matched the literature data. These events completed the synthesis of the AB rings fragment in 7 steps.

3.5 Final route to the AB rings

After establishing a route towards the AB rings, further improvements were pursued in line with the goals of efficient and sustainable synthesis. The yields of the crude reaction mixtures presented in this section were determined either by quantitative NMR or HPLC assay.

In the first step, the addition of the allenyl Grignard reagent was improved to almost quantitative yield when 1.05 equivalent of the previously titrated allenyl Grignard was used on a gram scale. This resulted in clean formation of product **204** (Figure 43) as a single diastereomer, which was taken directly to the next step.

In the second, ozonolysis step, we tried to increase the yield. Employing recently developed ozonolysis conditions in an acetone-water mixture[96] eliminated the necessity for a reducing agent, however, the yield decreased to 35%. We also tested a novel photochemical alternative to ozonolysis developed by Leonori[97] using nitroarenes, however, it resulted in no reaction. Finally, ozonolysis yield was improved by using pure methanol as a solvent, and by taking the crude aldehyde directly to the next step. This avoided chromatography, and also the use of chlorinated solvents previously required.

In the third step, several sustainable alternatives to Still-Gennari reagents were examined, with the idea of using Knoevenagel chemistry with subsequent lactonization and decarboxylation to form the butanolide ring (Figure 41). However, none of the tested alternatives resulted in formation of the desired product **206**. Eventually, it turned out that Still-Gennari reaction worked well even when the crude aldehyde contained impurities from ozonolysis step. Furthermore, we found that recrystallising the crude product from isopropanol resulted in a highly pure olefination product, with impurities remaining dissolved in the solution (Figure 43).

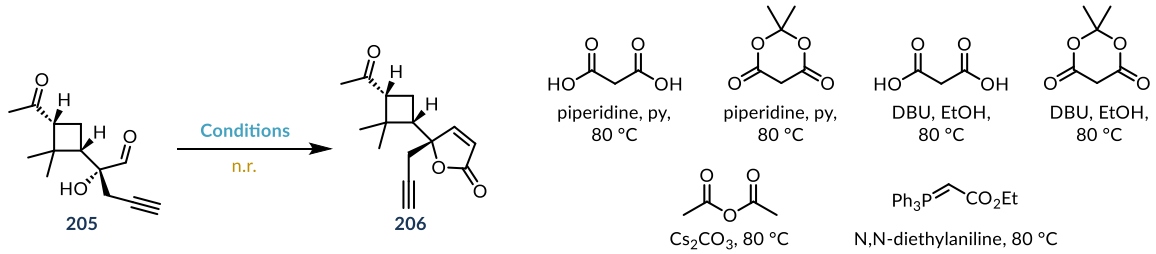


Figure 41. Attempted sustainable Still-Gennari alternatives

In the fourth, Baeyer-Villiger step, we tried to eliminate the necessity for dichloromethane as solvent by performing the reaction neat. The reaction worked, albeit in lower yield (30%). The crude product was pure and was taken forward without purification.

In the fifth step, we tested different hypervalent iodine reagents, solvents, temperatures and reaction times (Figure 42). We found that PIDA in HFIP at 60 °C cleanly effected the desired rearrangement in 51% yield, eliminating the need for chlorinated solvent and the commercially unavailable iodine(III) reagent we had used previously. Furthermore, we found that evaporation and treatment of the reaction mixture with diethyl ether precipitated reagent-related impurities. These were filtered to give the desired product, contaminated with small amounts of PIDA. This was taken forward without purification.

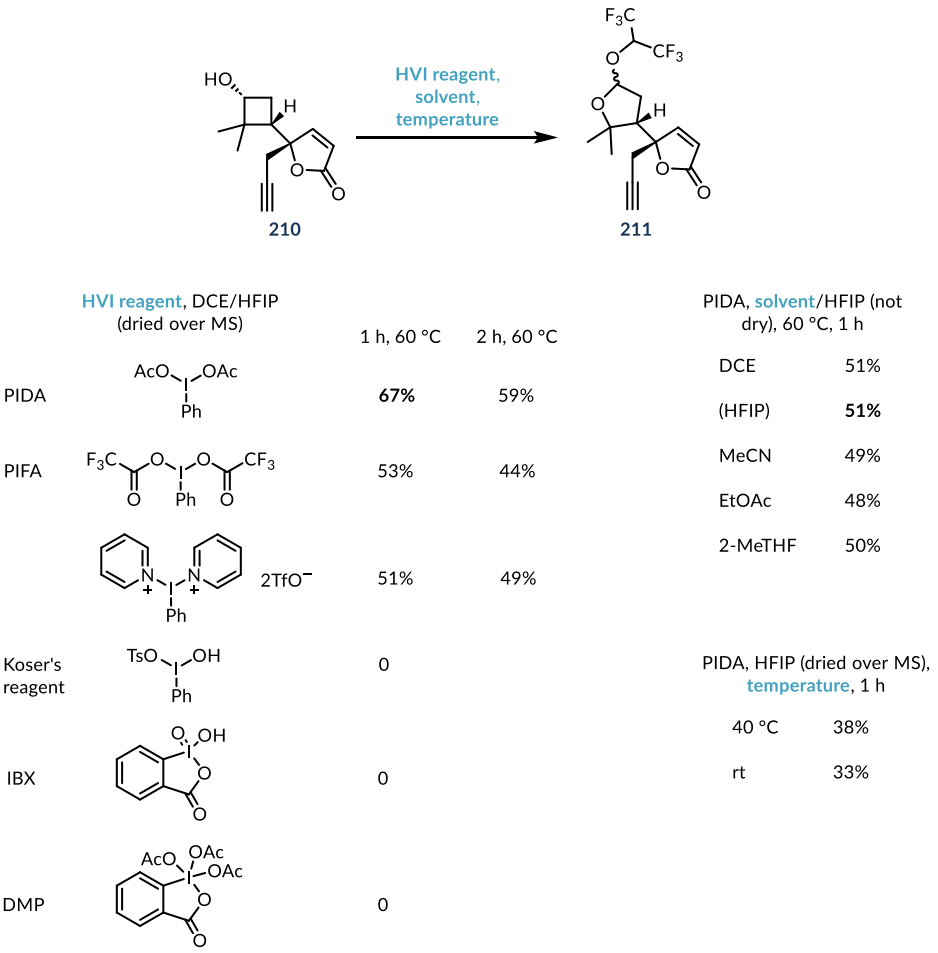


Figure 42. Studies of hypervalent iodine-mediated ring expansion. Conversion was always complete. Yields were determined by HPLC using pure product calibration.

Both the sixth and seventh steps (acetal hydrolysis and oxa-Michael addition) were clean reactions, not requiring purification in between. Fortunately, the solid state of the final product enabled its purification by recrystallisation (Figure 43).

The improvements described in this section led to an efficient, sustainable and scalable synthesis of the AB rings in just 7 steps and 17% yield (over the previous 16 steps), from inexpensive, commercially available starting material, without the need for any chromatographic separation (Figure 43). In addition, we demonstrated that chlorinated solvents could be removed to make the synthetic route less health and environmentally hazardous.

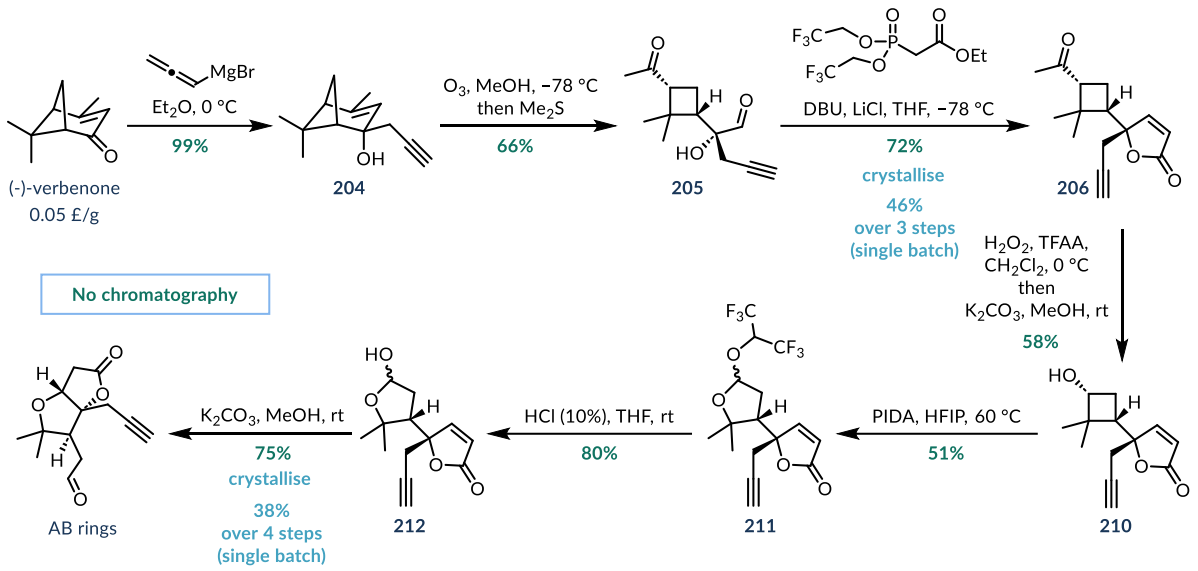


Figure 43. Final route to the AB rings

3.6 Comparative analysis of different routes to the AB rings

The AB rings synthesis was compared to previous syntheses by Anderson[81] and Hoveyda.[82] Synthetic efficiency was assessed by comparing the total number of steps, the number of chromatographic separations, and the overall yield for each synthetic route. Process-mass-intensity (PMI) was calculated to compare the amount of waste generated, and global warming potential (CO_2 kg-equivalent), of each route.[15] Process-mass-intensity (PMI) is defined as a ratio of mass of all input materials (substrates, reagents and solvents, including workup and purification) to the mass of the pure product. A lower PMI value is indicative of a more sustainable and efficient process, as it suggests that less waste is produced per mass unit of product.

Initially, PMI was calculated for every step in each synthetic route (Figure 44). Then, the individual step PMIs were summed to give an estimate of the whole process PMI (PMI_{tot}). The sum of individual step PMIs does not precisely equate to the overall process PMI. Given that steps in a multi-step synthesis are reported on different scales, and that direct calculation of the overall process PMI is not applicable, the sum of individual step PMI was used as an estimate for the overall process PMI. Finally, the average PMI per step (PMI_{avg}) was calculated to compare waste generated in each route, independent of the total number of steps.

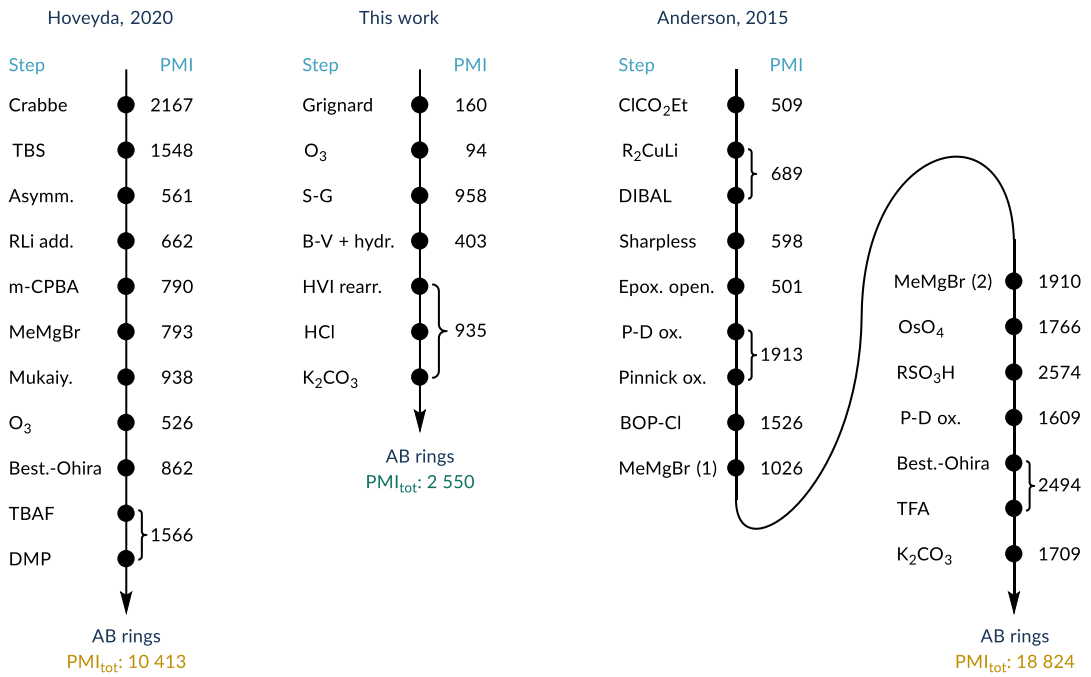


Figure 44. Process-mass-intensity analysis of three different routes to the AB rings

The AB rings synthesis presented in this work demonstrated superior performance across all evaluated metrics (Table 2). Notably, the number of chromatographic separations has been reduced from 13 and 10 in prior works to zero in the current synthesis. This synthesis also features an improved step count and lower average PMI, indicating greater operational efficiency for each step. These improvements have together resulted in a more sustainable synthesis, with waste and carbon emissions reduced by 86% and 75% when compared to the previous Anderson and Hoveyda syntheses, respectively.

Table 2. Comparative analysis of different routes to the AB rings

	No. of steps	No. of chromatography	Yield	PMI (tot)	PMI (avg)
Anderson, 2015	16	13	15%	18 824	1 176
Hoveyda, 2020	12	10	5-14%	10 413	947
This work, 2022	**7**	**0**	**17%**	**2 550**	**364**

3.7 Conclusion

The AB rings synthesis was investigated through C-H activation, ring fragmentation and ring expansion strategies. A successful synthesis was eventually achieved combining a chiral pool

approach with a cyclobutane ring expansion rearrangement, and all stereochemistry introduced using substrate stereocontrol. Further optimisation led to a synthesis without the need for any chromatographic separation, and only two crystallisation steps, while avoiding toxic and environmentally hazardous chemicals. The number of steps, number of chromatographic separations, yield and process-mass-intensity has been significantly improved, with waste and carbon emissions reduced by 86% and 75% compared to the previous AB rings syntheses. Having a robust, scalable and reliable route to the AB rings allowed us to move to the next stage of rubriflordilactone synthesis.

Chapter 4: FG rings synthesis

4.1 Introduction and retrosynthesis

Having secured a route to the AB rings, we turned our attention to the FG rings in the context of rubriflordilactone B synthesis. This fragment was previously synthesised by Anderson[43] (22 steps), where alkynes were substituted with iodide and TMS substituents to allow further functionalisation. Our goal was to differentiate the alkynes without recourse to protecting groups, and to match the efficiency and step count to the AB rings synthesis described in the previous chapter. If completed in 7 steps, this would enable a synthesis of rubriflordilactone B in 10 steps (LLS).

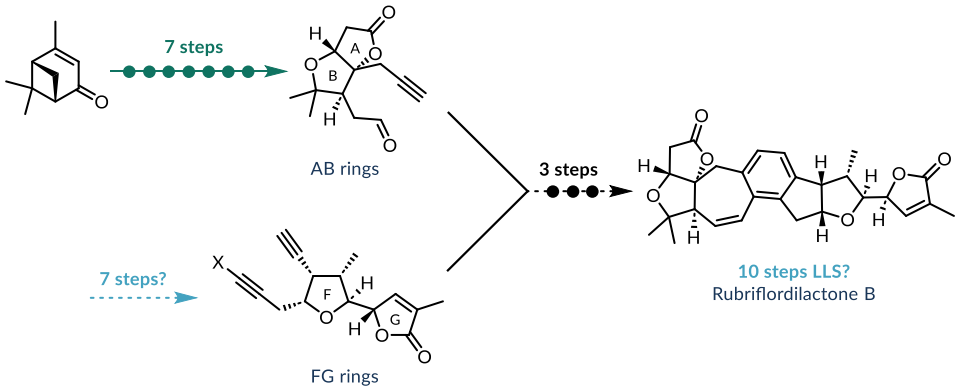


Figure 45. Synthetic plan for rubriflordilactone B

The two alkynes would need to be introduced sequentially (Figure 46) from an aldehyde and leaving group attached to a stereochemically complex tetrahydrofuran **214**. Considering the challenges in controlling stereochemistry within five-membered rings, and recognising that **214** contains a retron for pinacol rearrangement, we planned to employ a ring contraction strategy. This would convert a six-membered ring, whose stereochemistry is better controlled by its chair conformation, into the desired stereochemically-challenging tetrahydrofuran. With four ring substituents placed equatorially, the most stable chair conformer **215** would lead to the desired stereochemical outcome of the pinacol rearrangement, with the migrating group and breaking bond in antiperiplanar orientation.

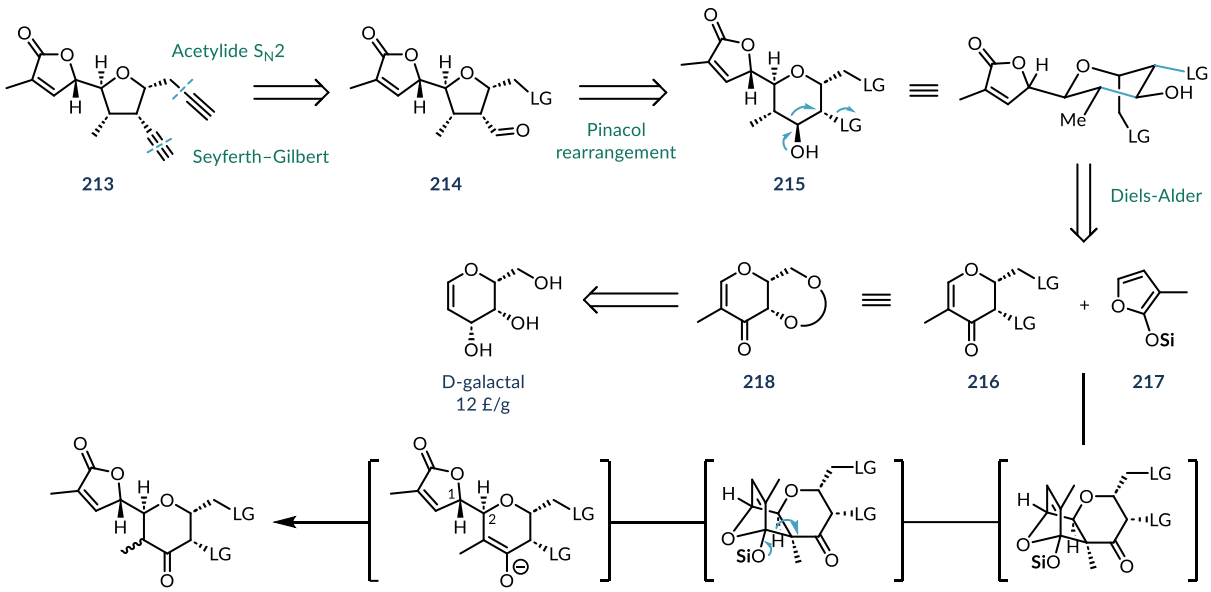


Figure 46. Retrosynthesis of FG rings

An *endo* Diels-Alder cycloaddition between **216** and siloxyfuran **217**, followed by retro-aldol cleavage would ensure the desired stereochemistry at the butenolide-tetrahydropyran junction (C1 and C2). Concurrently, we recognised that **216** could be derived from a carbohydrate chiral pool starting material D-galactal.

4.2 Diels-Alder or Mukaiyama-Michael strategies

In the forward synthesis, we employed a known procedure[98] to selectively oxidise the allylic secondary alcohol of D-galactal via Pd-catalysed transfer hydrogenation (Figure 47). Faced with difficulties in reproducing the literature procedure, we developed simple, solvent-free conditions using neat vinyl acetate and palladium catalyst. Using commercial palladium(II) acetate resulted in ~50% conversion and precipitation of black palladium residue. When this residue was used as the catalyst, the reaction worked even in presence of air and moisture. This black palladium residue (adsorbed on the round-bottomed flask) was reused multiple times.

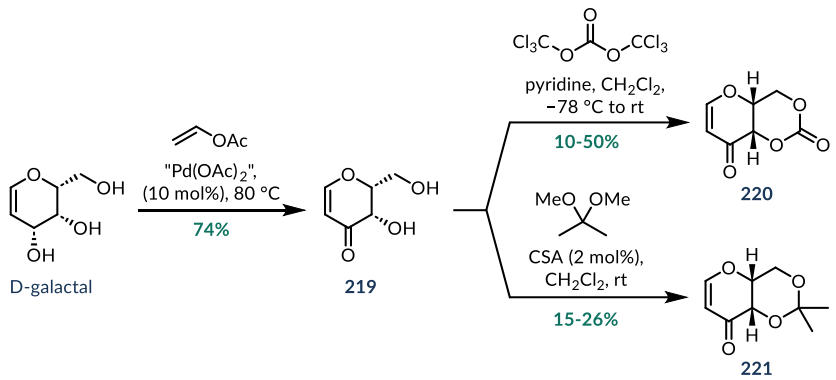


Figure 47. Synthesis of acetonide and cyclic carbonate

Moving forward, formation of cyclic carbonate **220** (Figure 47) transformed the alcohols into leaving groups. At the same, this established a concave/convex shape which would be responsible for the facial selectivity of the subsequent step. Isolation of the carbonate proved challenging, leading us to also synthesise acetonide **221**, although in low yield due to unidentified side reactions. Nevertheless, with enough material in hand, the Diels-Alder and/or Mukaiyama-Michael reactivity was explored with different nucleophiles under thermal (toluene, 60 °C or 120 °C), anionic (LDA, −78 °C) and Lewis acid (BF_3, Et_2O, −78 °C) conditions with carbonate **220** (Figure 48a) and acetonide **221** (Figure 48b).

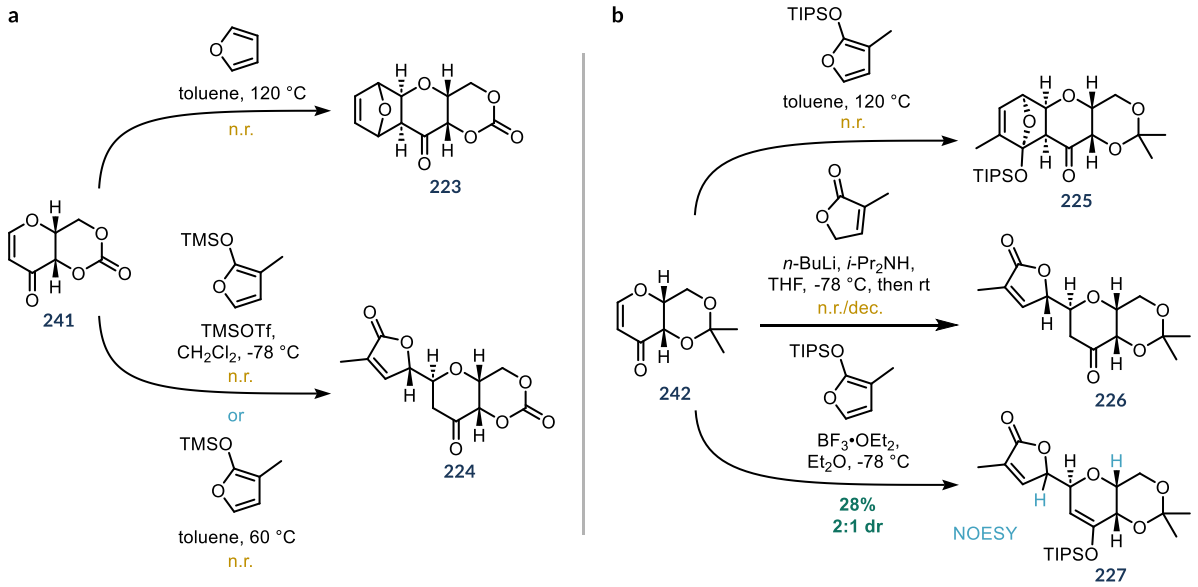


Figure 48. (**a**) Attempts at butanolide introduction with cyclic carbonate **220**; (**b**) Attempts at butanolide introduction with with acetonide **221**

Initial progress was made with acetonide **221** and TIPS-siloxyfuran under Lewis acid conditions, resulting in transfer of TIPS from siloxyfuran to the product, forming TIPS enol ether **227** (Figure

48b). Before exploring this reactivity further, we addressed the low yielding syntheses of **220** and **221** by using a different acetal.

Starting from D-galactal, benzylidene acetal **228** (Figure 50a) was synthesised in good yield, as a single diastereomer. The preferred diastereomer benefits from maximising O-C-C-O gauche orientations (anomeric effect), while minimising 1,3-diaxial interactions (Figure 49).

To understand this preference, we optimised geometry and calculated each diastereomer's free energy at 298 K at b3lyp/6-31g level of theory (Figure 49). The preferred diastereomer was calculated to be only 0.6 kcal/mol more stable. To demonstrate the extent of anomeric effect involved in stabilisation of the preferred isomer, we calculated natural bond orbital delocalisation energies for one of the O-C-C-O fragments in each isomer. When hyperconjugation from all bonds is taken into account, the gauche O-C-C-O conformation provides more delocalisation (15.6 vs 13.4 kcal/mol for this particular fragment), which contributes to the overall stability of the isomer. In addition, 1,3-diaxial interactions are minimised in the preferred isomer because axial substituents clash less with oxygen electron pairs than with C–H bonds. In 1,3-dioxane systems, if a substituent has to be axial, it is preferred to be in position 5, facing oxygen electron pairs, rather than 2,4 or 6, where it would face hydrogens. An extreme example of this is found in the preferred conformer of *cis*-5-(*tert*-butyl)-2-methyl-1,3-dioxane.

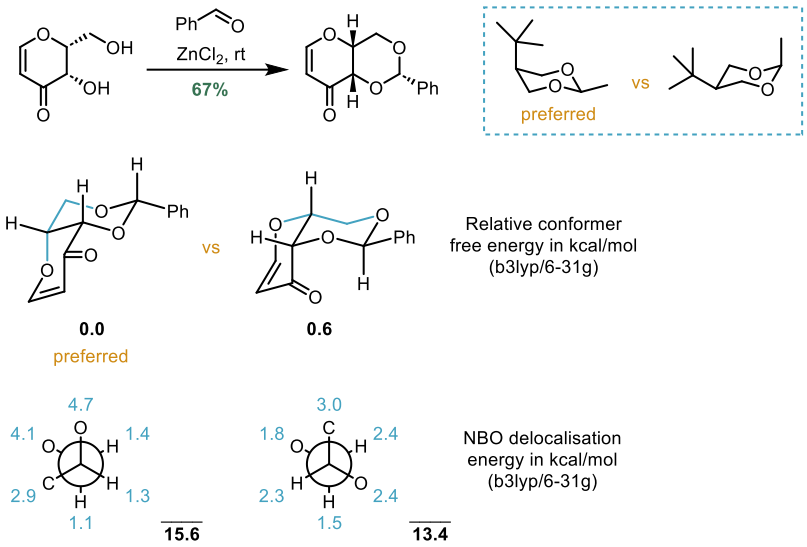


Figure 49. Understanding the origin of diastereoselectivity in benzylidene acetal formation

The above-described steric and stereoelectronic effects resulted in an effectively locked *cis*-decalin type system, which was exploited by leveraging the unique reactivity of vinyloguous esters. Treatment of **228** (Figure 50a) with TIPSOTf presumably resulted in formation of an oxonium ion (Figure 50c), which was captured by siloxyfuran exclusively from the top face, consistent with the Fürst-Plattner rule, and also attack on the less-hindered convex face of the *cis*-fused ring system. A remarkable 10:1 diastereoselectivity was observed at the butenolide stereocentre C1. The resulting silyl enol ether **229** was perfectly positioned for a subsequent axial methylation from the desired bottom face. Ketone **230** was also synthesised as an alternative substrate for methylation by treatment of **229** with TBAF.

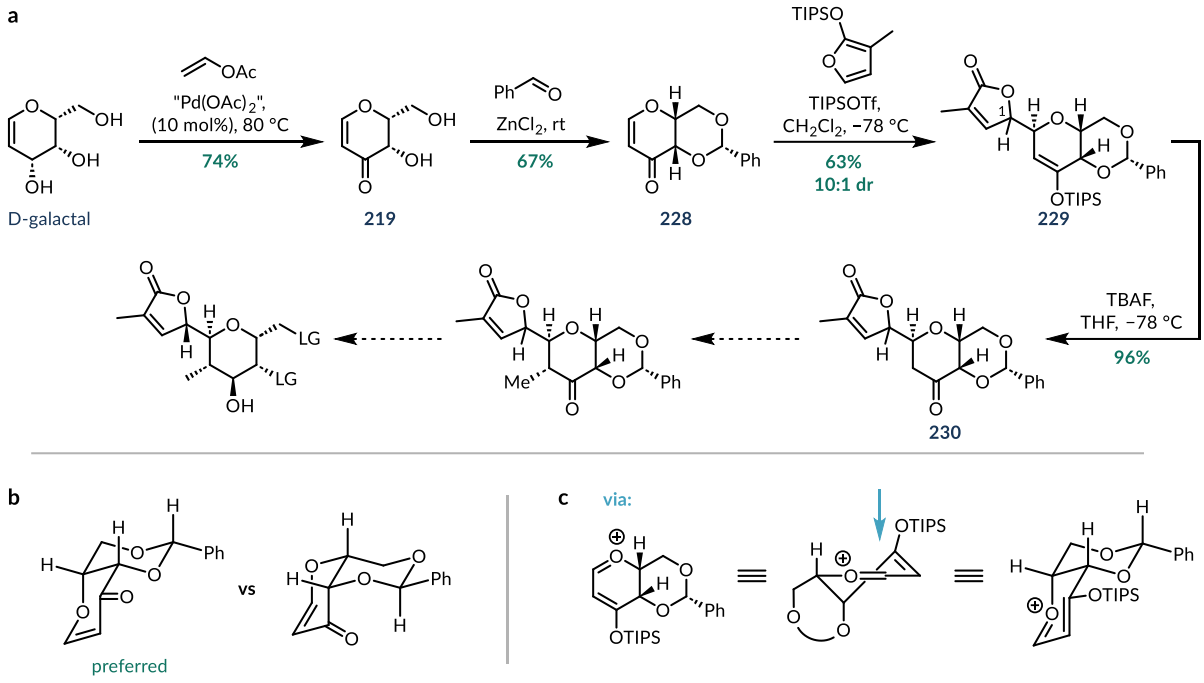


Figure 50. (**a**) Synthesis of FG rings; (**b**) Conformational preference for benzylidene acetal; (**c**) Stereochemistry of siloxyfuran addition to oxonium ion

Although **229** was obtained with high diastereoselectivity, the exact configuration of the butenolide stereocentre C1 remained uncertain. All other stereocentres were unambiguously determined by 2D ^{1}H–^{1}H NOESY (Figure 51). This technique was ineffective for the butenolide stereocentre (yellow) due to free rotation of the bond joining the two rings.

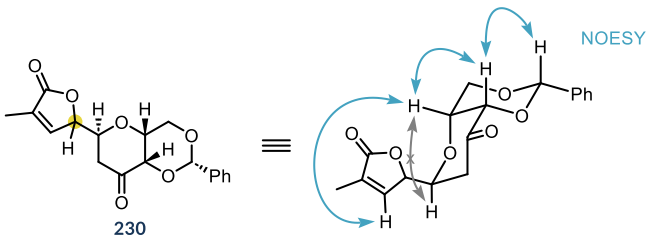


Figure 51. Stereochemical assignment of ketone **230**

4.3 Methylation tactics

4.3.1 From ketone

With the silyl enol ether **229** and ketone **230** in hand, we addressed the critical methylation, again hoping to take advantage of substrate stereocontrol. Surprisingly, deprotonation of ketone **230** with a strong amide base (Figure 52) resulted in immediate decomposition. The comparable acidity of the ketone and butenolide protons, together with the molecule's

predisposition for β-elimination (via the highlighted bonds), complicated the direct deprotonation-alkylation approach.

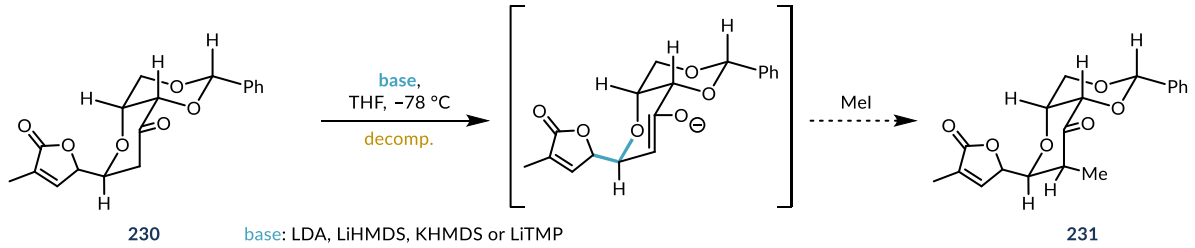


Figure 52. Ketone alkylation via enolate intermediate

To avoid enolate generation, a less direct α-methylenation using the Eschenmoser salt, followed by hydrogenation was tested, although with no success (Figure 53).

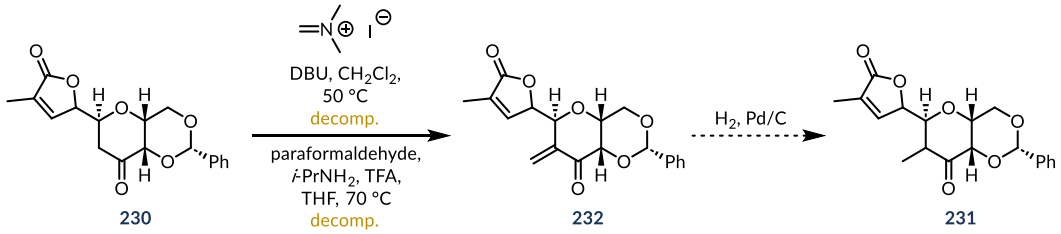


Figure 53. Ketone α-methylenation followed by hydrogenation

Interestingly, when treated with DMF·DMA in an attempt at alpha-formylation (Figure 54), an unexpected rearranged product **233** was formed. The X-ray structure of **233** confirmed the configuration of all stereocentres except for the butenolide stereocentre, which had been unfortunately converted into a trigonal carbon in the course of the reaction.

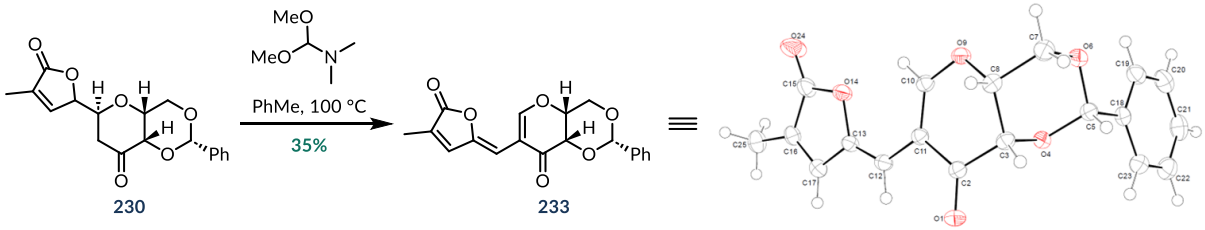


Figure 54. Ketone reaction with DMF·DMA and crystal structure of the product

4.3.2 From silyl enol ether: Silver-mediated alkylation

Application of silver-mediated alkylation conditions, as reported for TMS enol ethers,[99] to TIPS enol ether **229** resulted in no reaction (Figure 55).

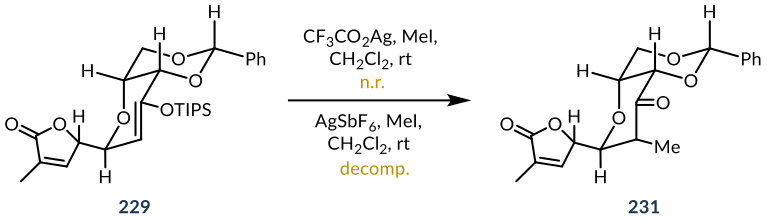
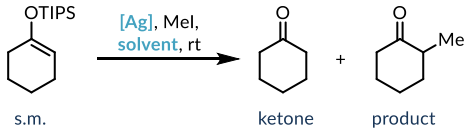


Figure 55. Silver-mediated alkylation of TIPS enol ether

Concerned with lower reactivity of TIPS enol ethers compared to TMS enol ethers, we tested multiple silver salts and solvents on a simple TIPS enol ether (Table 3). Only silver triflate was effective, with the best result obtained in dichloromethane, giving 76% yield based on a GC-MS analysis with a calibrated internal standard. Applying the same procedure to TIPS enol ether **229**, however, resulted in no reaction. We reasoned that steric hindrance further decreased the reactivity of **229** compared to a simple TIPS enol ether.

Table 3. Screening of silver salts and solvents for silver-mediated alkylation



	$AgOC(O)CF_3$	AgOTf	Ag_2O	AgF
acetone	77:23:0	0:1:0	1:0:0	1:0:0
CH_2Cl_2	71:29:0	0:19:81 **76%**	1:0:0	1:0:0
PhH	90:10:0	0:61:39 **38%**	1:0:0	1:0:0

Reported as GC area ratio s.m. : ketone : product. % – yield based on internal standard (decane), calibrated against the product. Solution of silyl enol ether and MeI in solvent added to a vial with silver salt under nitrogen, stirred rt, 1.5 h. Aliquot analysed by GC-MS.

4.3.3 From silyl enol ether: Fluoride-mediated

Using commercial TBAF, either as solid or solution, for the reaction of TIPS enol ether **229** with MeI only led to desilylated ketone **230** (Figure 56). Given TBAF's inherent water content, it is likley that the enolate formed in the reaction was immediately protonated.

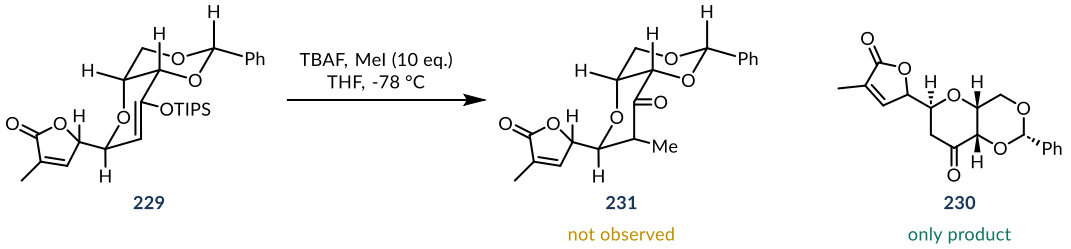


Figure 56. Fluoride-mediated TIPS enol ether alkylation

Because TBAF's thermal instability prevented drying at high temperature, we turned to BTAF, a more thermally stable analogue that can be effectively dried[100] (Figure 57a). Following the literature conditions[100] for a known substrate resulted in a product with a 4:6 methylation/desilylation ratio (Figure 57b). Since at least some methylation occurred, we tested this reaction on a previously unexplored simple TIPS enol ether (Figure 57c). An encouraging result with a 1:1 methylation/desilylation ratio was obtained. Under identical conditions, TIPS enol ether **229** (Figure 57d), however, produced only ketone. Faced again with the reduced reactivity of **229** compared to a simple TIPS enol ether, we explored more reactive methyl electrophiles (Meerwein's salt, MeOTf), unfortunately with no success (Figure 57e).

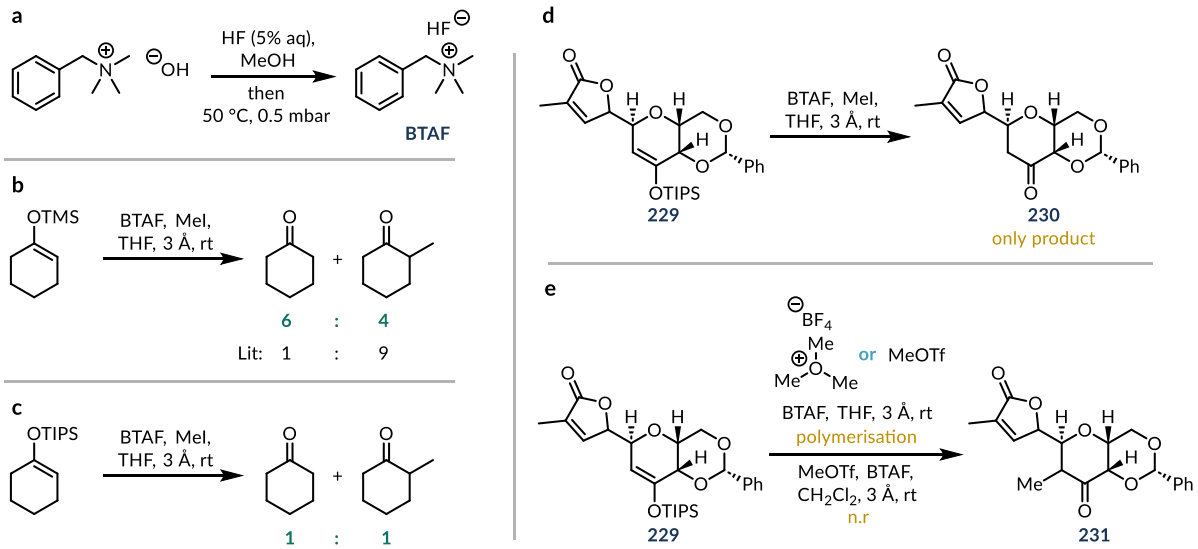


Figure 57. (**a**) BTAF preparation; (**b**) Alkylation of a TMS enol ether; (**c**) Alkylation of a TIPS enol ether; (**d**) Alkylation of the 'real' TIPS enol ether; (**e**) Alkylation with more reactive methyl electrophiles

The encountered challenges prompted us to investigate previously unreported "anhydrous" fluoride sources in combination with methyl iodide in hope to generate and alkylate a reactive naked enolate. TBAF with reduced water content[101] (*in situ* dried at 40 °C at 0.5 mbar

overnight), triethylamine trihydrofluoride and diethylaminosulfur trifluoride were examined (Figure 58), with only TBAF being somewhat effective. Finally, we tried to design a mild silyl enol ether alkylation using methanol as a source of methyl group. Methanol activation with aminosulfinium salts (e.g. XtalFluor-E) would release fluoride, which would generate a naked enolate (Nu). This enolate would act as a nucleophile, attacking species **235** and releasing stable fluorosulfinamide **236**. However, our attempts to make this reaction work with XtalFluor-E and DAST were unsuccessful.

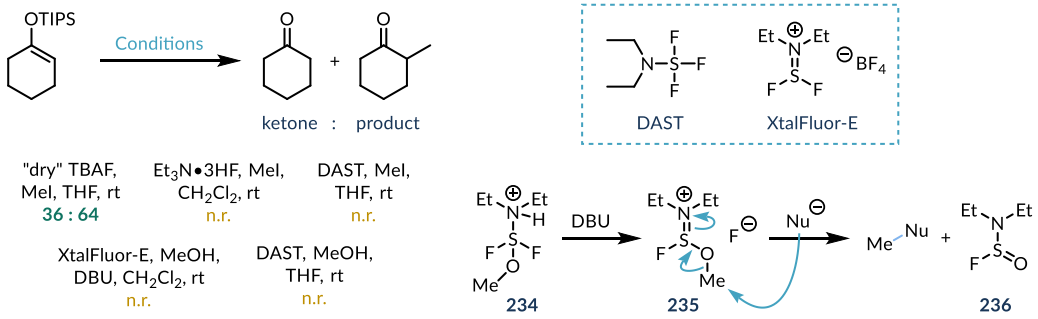


Figure 58. Exploration of previously not reported silyl enol ether alkylation conditions

Concerned with the lack of reactivity of TIPS enol ether **230**, we returned to the siloxyfuran addition and tested different silyl triflate reagents with a goal of making a more reactive TMS or TES enol ether (Figure 59). Under identical conditions, TMSOTf led to a complex mixture of products, TESOTf produced traces of the desired product **238**, accompanied with significant decomposition, while only TIPSOTf efficiently produced the desired silyl enol **229** ether with high diastereoselectivity. We believe that the stability of the TIPS enol ether was mainly responsible for such high yield in otherwise difficult reaction.

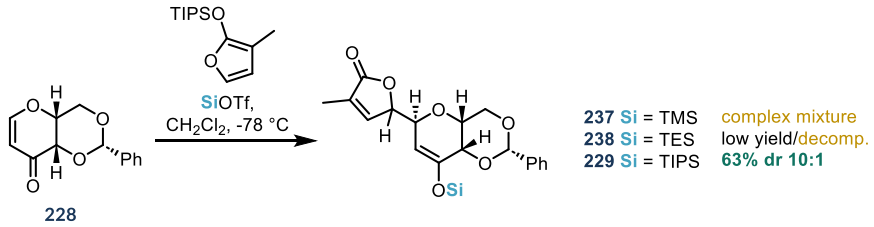


Figure 59. Siloxyfuran addition using different silyl triflate reagents

4.3.4 From silyl enol ether: Miscellaneous

Unable to directly introduce a methyl group, we explored several two-step tactics to address this challenge. Initially, we attempted bromination of TIPS enol ether to obtain a bromo ketone, which could potentially be converted into the desired methyl ketone (Figure 60a). Unfortunately, exposure of **229** to NBS resulted in immediate decomposition. Silyl enol ether cyclopropanation, followed by cyclopropane cleavage sequence was subsequently explored (Figure 60b). However, **229** was unreactive under Simmons-Smith conditions.[102] Lewis acid-promoted silyl enol ether alkylation was also explored. Since methyl halides are unsuitable for this reaction, chloromethyl phenyl sulfide was chosen as an electrophile because of sulfur's ability to stabilise adjacent carbocations, and its likely ease of removal in a subsequent step (Figure 60c). Treating **229** and chloromethyl phenyl sulfide with different Lewis acids, however, resulted in either no reaction or decomposition.

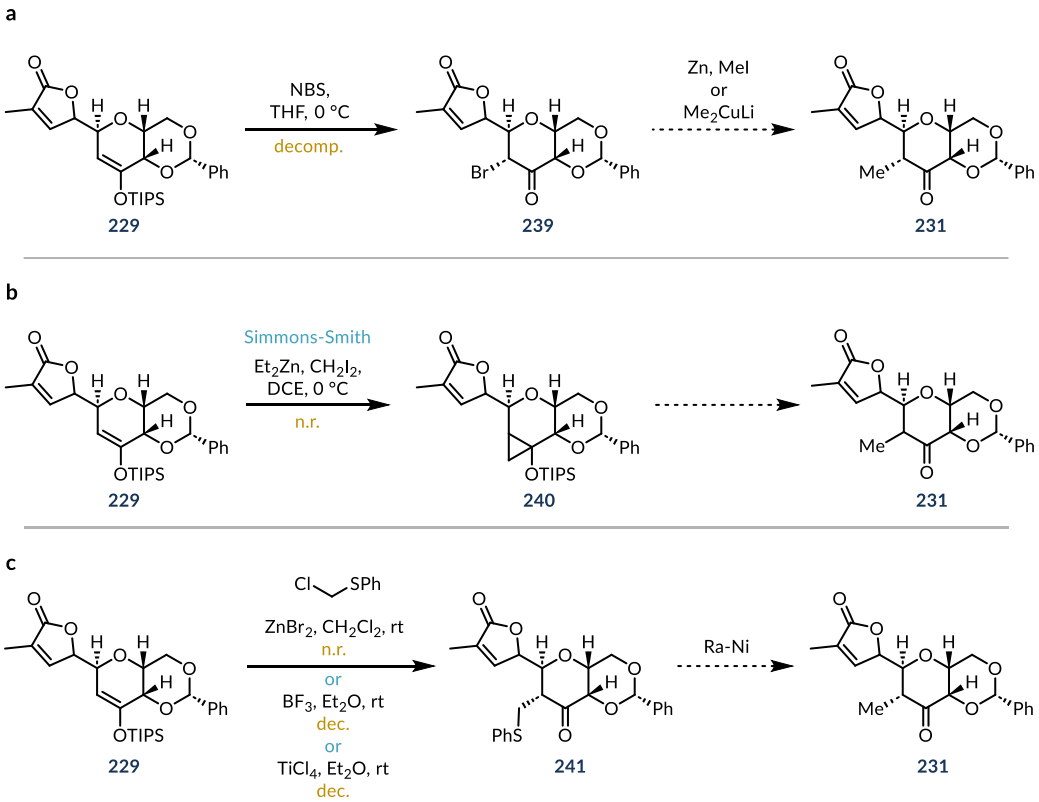


Figure 60. (**a**) Bromination followed by alkylation; (**b**) Cyclopropanation followed by cyclopropane cleavage; (**c**) Chloromethyl phenyl sulfide-based alkylation

With a goal of functionalising TIPS enol ether **229** in the α-position with *any* substitutent, it was subjected to Rubbottom oxidation conditions (Figure 61a), however the unexpected product **242** was obtained. It is proposed that after the initial epoxide formation, acid induced epoxide opening gives an TIPS oxocarbenium ion. *m*-Chlorobenozate captures this ion, where acyl transfer can take place, followed by extrusion of a silanol. Pleasingly, epoxide **243** was obtained cleanly and almost quantitatively using freshly prepared dimethyl dioxirane (Figure 61b). We also found that buffering *m*-CPBA with sodium bicarbonate delivered **243**, without subsequent epoxide opening. Unfortunately, efforts to transform epoxide **243** into products with a reactive functionality at the ketone α-position resulted in either no reaction or decomposition.

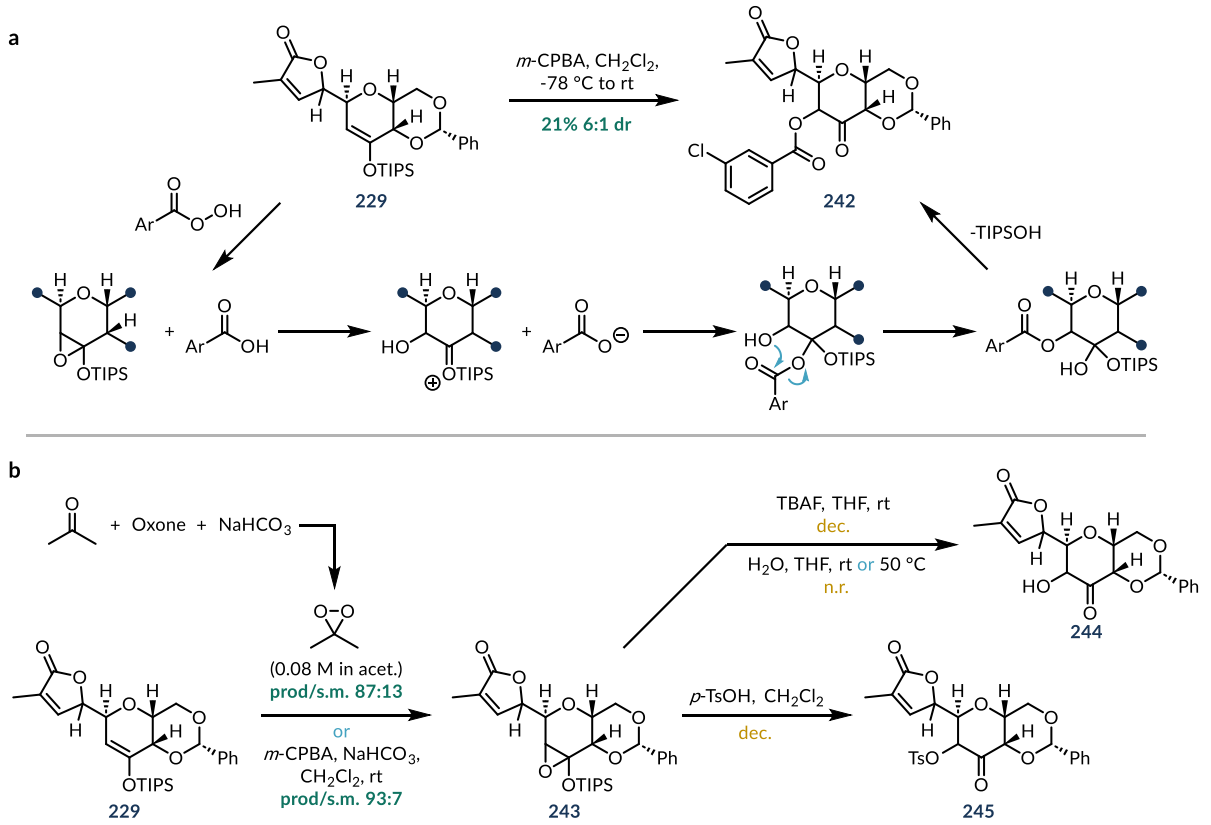


Figure 61. (**a**) Unexpected product from Rubbottom oxidation; (**b**) Synthesis and derivatisation of epoxide **243**

Finally, an approach based on methyl radical addition to a silyl enol ether was explored. Applying conditions described for trifluoromethyl iodide and a TES enol ether[103] (Figure 62a) to methyl iodide and our TIPS enol ether resulted in no reaction. Concerned with the mismatch

in radical philicity, we tested reagents **R1**-**R5** capable of generating a more electrophilic methyl radical, suitable for reaction with an electron-rich olefin (Figure 62b). Employing conditions that generate alkyl radicals via halogen abstraction by the supersilyl radical,[104] reagents **R1**-**R5** were tested with and without nickel catalyst. Although some conversion occurred, no desired products were obtained.

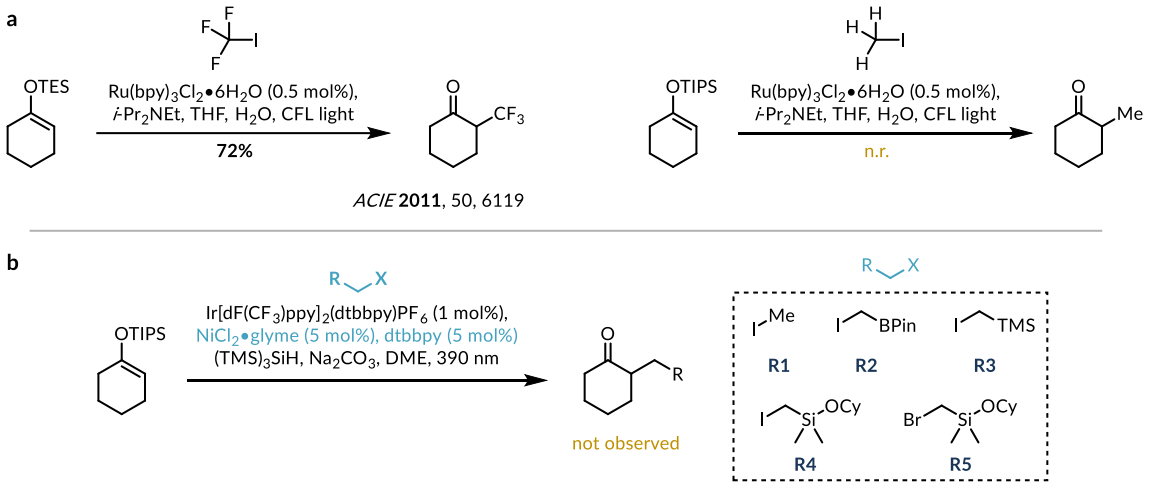


Figure 62. (**a**) Light-mediated radical silyl enol ether alkylation; (**b**) Light- and supersilane-mediated radical silyl enol ether alkylation

4.4 Methylation at earlier stage

We identified an elegant literature procedure[105] that could give a methylated intermediate directly from a carbohydrate-based commercially available starting material (Figure 63). This reaction proceeds via an *n*-BuLi induced dioxolane fragmentation, resulting in enolate formation, which subsequently undergoes alkylation.

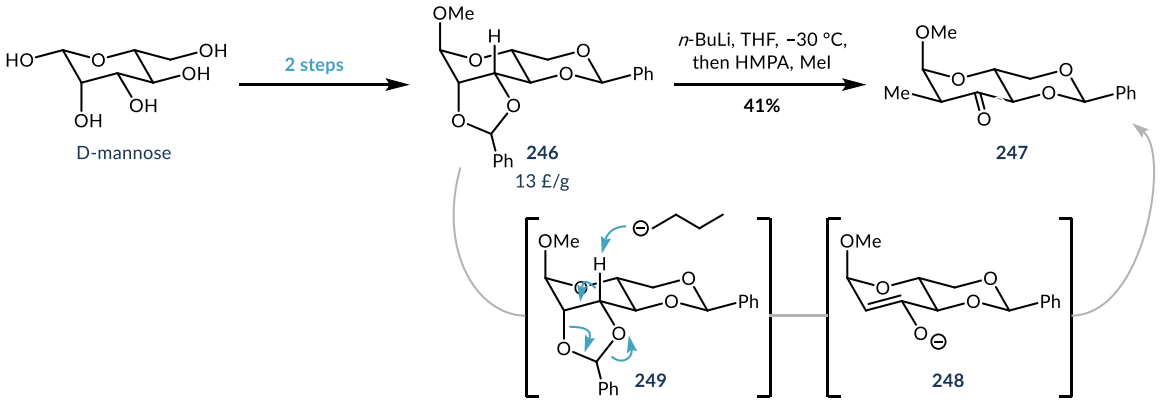


Figure 63. Early-stage methylation via dioxolane fragmentation

In our hands and to our delight, using DMPU instead of highly toxic HMPA, and further modifying the original procedure, **247** was obtained as a single diastereomer (Figure 64). Interestingly, the methyl group was positioned equatorial. The original report does not provide an explanation for this outcome. It seems likely that the initially formed axial α-methyl ketone undergoes equilibration to a more stable equatorial α-methyl ketone via an enolate intermediate. Observation of a minor doubly alkylated product supports this suggestion. Next, we focused on methanol elimination with the aim of using our previously developed TIPSOTf-mediated siloxyfuran addition to vinyloguous ester **250** (Figure 64). With both the leaving group and the adjacent proton axial, it was anticipated that **247** would be ideally situated to undergo this type of elimination. Different basic conditions were tested, however, either no reaction or decomposition occurred. Under acidic conditions, interestingly, the benzylidene acetal was cleaved preferentially over the methyl acetal.

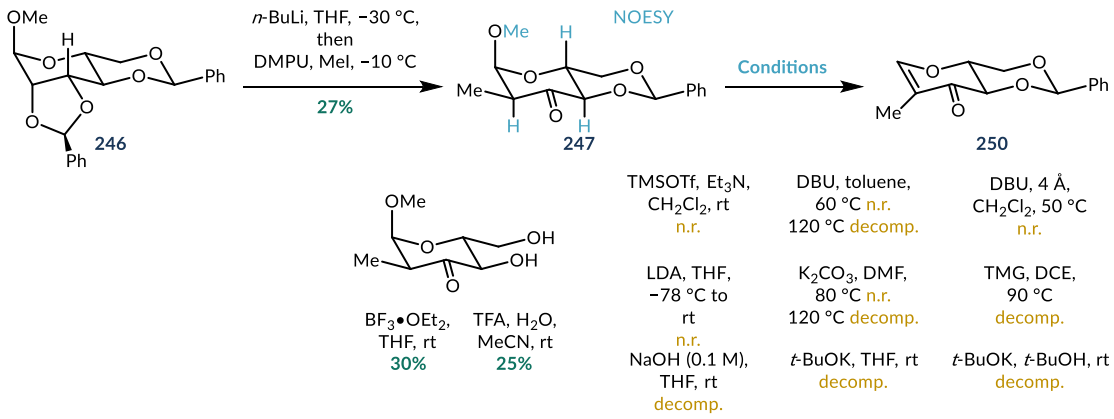


Figure 64. β-Elimination under acidic and basic conditions

We reasoned that removing a dioxane ring in **247** would allow us to explore acidic conditions for the desired methanol elimination. At the same time, we wanted to convert the dioxane ring into functional groups required for the reminder of the synthesis. To accomplish this, we aimed to exploit a convenient single-step conversion of benzylidene acetal into a double leaving group upon cleavage[106] (Figure 65a). However, applying the literature conditions[106] where carbon tetrachloride was replaced or radical initiator added were unsuccessful (Figure 65b).

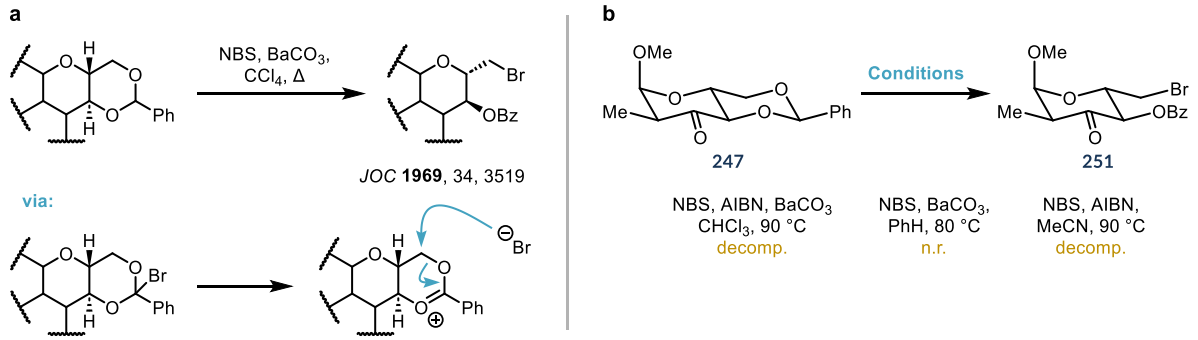


Figure 65. Benzylidene acetal cleavage

4.5 Conclusion

A ring contraction strategy via pinacol rearrangement was explored in the context of a concise synthesis of the FG rings of rubriflordilactone B. An unexpected new reactivity pathway of vinyloguous esters was discovered,[107] and subsequently exploited to introduce a butenolide ring with excellent diastereoselectivity. In addition, this reaction formed a silyl enol ether that should have been well positioned for the subsequent methylation step. However, this silyl enol ether and its derived ketone proved surprisingly difficult to methylate. An alternative route, where the methyl group had been introduced at an earlier stage, encountered challenges with methanol β-elimination, despite a favourable stereoelectronic arrangement. After these attempts, it became clear that we needed to rethink our approach to rubriflordilactone B.

Chapter 5: Towards rubriflordilactone B synthesis

5.1 Introduction and retrosynthesis

We decided to transition our approach towards a second generation rubriflordilactone B synthesis by merging the AB rings with a smaller fragment (Figure 66) instead of the complete FG rings. This would first construct the ABCDE rings from the AB rings, leaving the installation of the FG rings for a final stage. Given the concise synthesis of the AB rings, this approach could also lead to an efficient (if more linear) rubriflordilactone B synthesis.

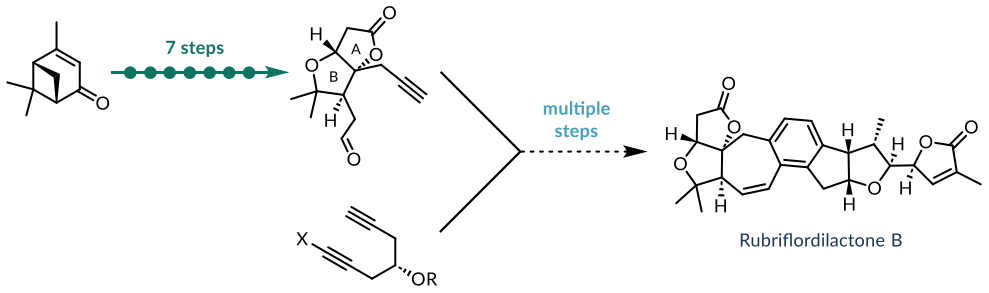


Figure 66. New strategy for rubriflordilactone B synthesis

5.2 Synthesis of ABCDE rings of rubriflordilactone B

To determine the most effective fragment that could enable subsequent FG ring construction, we started with known symmetrical alcohol **252** (Figure 67). This allowed us to explore the reactivity of advanced intermediates in the synthesis. The advantage of using a symmetric alcohol was that it temporarily avoided the issues of alkyne differentiation. However, functionalisation of one of the two alkynes in **252** would create a stereocentre at C1 in **253** without ability to control this stereochemistry.

To synthesise alcohol **252** (Figure 67), a double addition of allenylmagnesium bromide to ethyl formate was performed, as described in the literature.[108] Treatment of **252** with 2 equivalents of *n*-BuLi, followed by addition of the AB rings aldehyde, resulted in a complex mixture and low yield of the desired product **253**. We reasoned that the alkoxide generated in this process (on the diyne) may complicate the reaction. To address this, we protected the alcohol as a TBS ether

254. Treatment of **254** with one equivalent of *n*-BuLi, followed by addition to the AB rings aldehyde resulted in the clean formation of the desired triyne **255**.

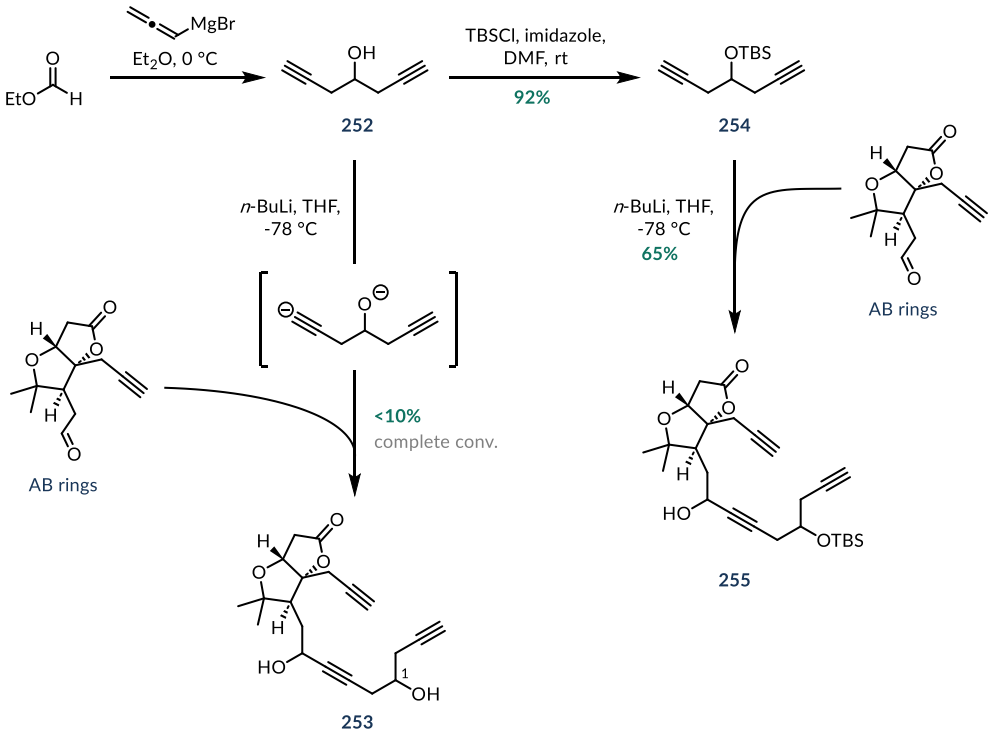


Figure 67. Union of the AB rings with a smaller diyne fragment

Cyclotrimerisation of this triyne was conducted under conditions similar to those reported in the previous Anderson group synthesis[43] (Figure 68). A high catalyst loading of Wilkinson's catalyst was used because the reaction was conducted only on a several milligram scale. Treatment with *p*-toluenesulfonic acid cleaved the silyl protecting group and selectively dehydrated only the benzylic alcohol. Though this dehydration was desired, it was not initially expected to occur simultaneously with deprotection. With alcohol **257** in hand, we moved to the next phase of constructing the FG rings via radical cyclisation.

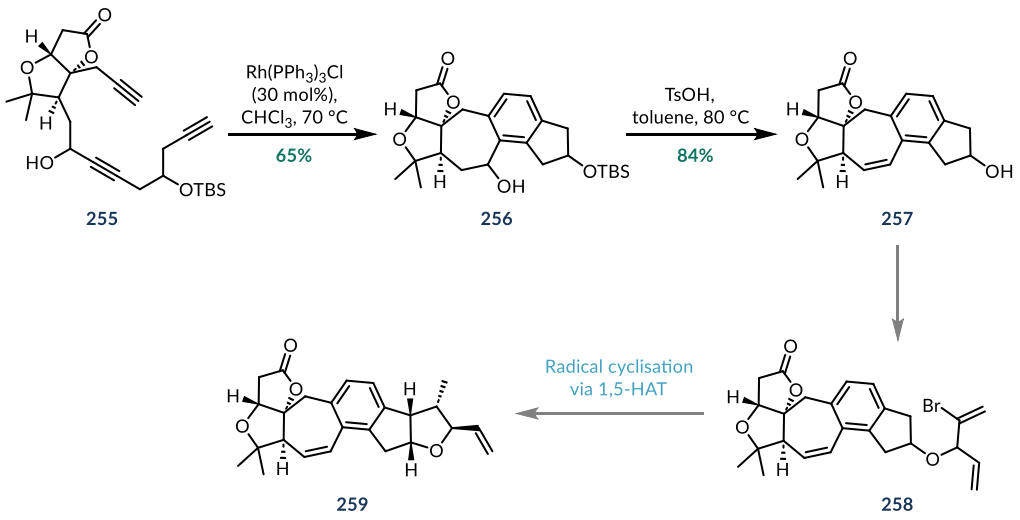


Figure 68. Formation of the ABCDE rings of rubriflordilactone B

The cyclisation that was planned to form the F ring was designed based on observations by Xie[36] during their study towards rubriflordilactone B, when they attempted to employ a radical-polar crossover methodology developed by Nicewicz[109] (Figure 69). In this reaction, indene is oxidised to a radical cation intermediate **int-1** by the excited form of a photocatalyst. This intermediate **int-1** is captured by an alcohol to give benzylic radical intermediate **int-2**, which cyclises onto one of the alkenes to form a tetrohydrofuran ring. A notable aspect of this cyclisation is its high degree of diastereoselectivity, favouring the formation of the desired isomer **260**. However, in the context of rubriflordilactone B synthesis, where the starting indene is chiral, this reaction is likely to be challenging in terms of controlling the facial selectivity of the indene double bond, and therefore could not be used to construct the F ring.

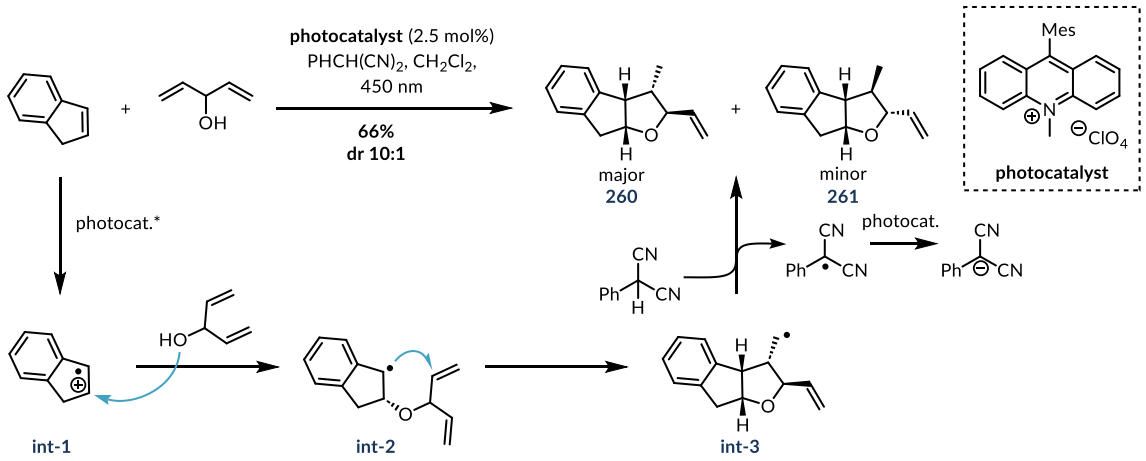


Figure 69. Literature precedent for radical cyclisation to form the F ring of rubriflordilactone B

Based on these observations, we proposed a radical cyclisation from intermediate **262** (Figure 70) to form the F ring, where the desired diastereomer formation would be consistent with the Houk-Beckwith model.[110] In the proposed cyclisation, homolytic cleavage of the vinyl bromide **262** would produce a vinyl radical **263**. This radical would undergo 1,5-HAT to generate a more stable benzylic radical **264**. While two sites of HAT are possible, we proposed that reaction would occur at the less-hindered benzylic carbon atom. At this point, the two vinyl groups would become equivalent, and could both react with the benzylic radical, leading to different stereochemical outcomes. The desired 1,5-*cis* and 1,4-*trans* outcome would result from an envelope-like transition state, where a non-reacting vinyl group is placed equatorially.

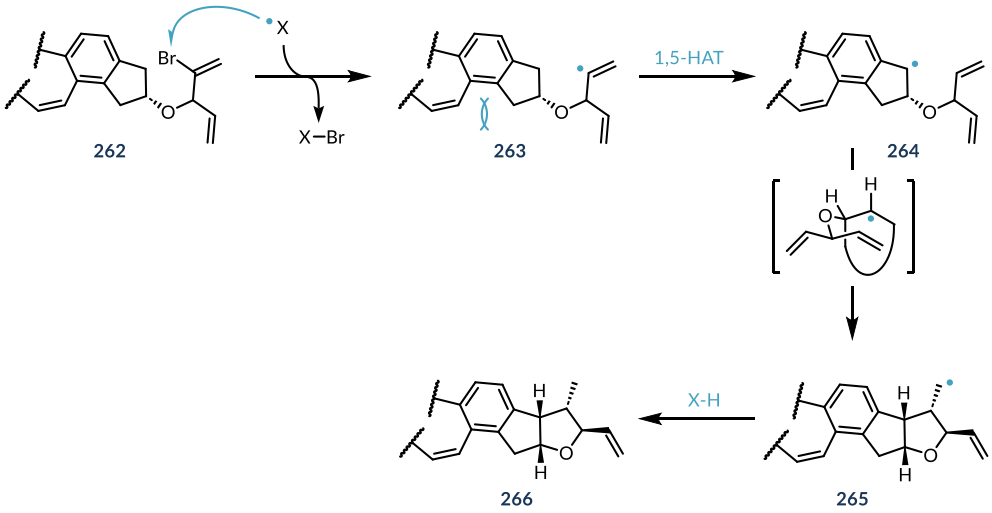


Figure 70. Proposed radical cyclisation via 1,5-HAT to form the F ring of rubriflordilactone B

5.3 Radical cyclisation via 1,5-HAT

Radical cyclisation via 1,5-HAT was studied on a model system **269** (Figure 71). Alkylation of 2-indanol with 2,3-dibromopropene resulted in formation of the desired model **269**, along with side product **268**, which presumably arose from bromide elimination by 2-indanol alkoxide.

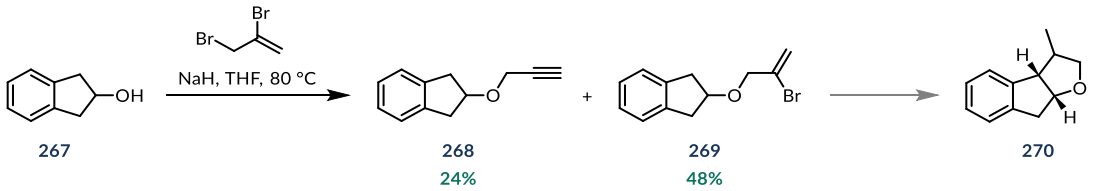
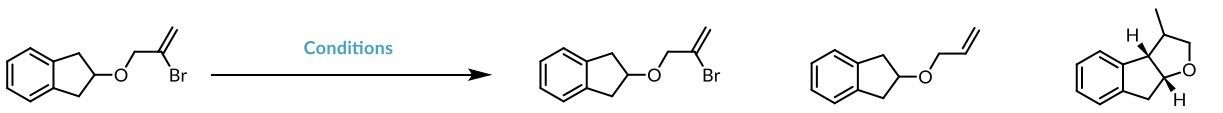


Figure 71. Synthesis of model substrate for radical cyclisation

With the model substrate in hand, we tested the radical cyclisation. Organotin chemistry was deliberately avoided because of high toxicity of organotin compounds. Instead, tris(trimethylsilyl)silane (supersilane) was employed as a hydrogen atom source. We first examined different solvents (toluene, cyclohexane, acetonitrile, *tert*-butanol) with AIBN as radical initiator. A promising result was obtained with acetonitrile, although other solvents gave similar results (Figure 72, entry 1). We observed formation of the desired product in 20% yield, demonstrating that the proposed radical cyclisation with 1,5-HAT can indeed take place. Formation of a diastereomeric mixture was understandable in this model since it lacks the additional vinyl group that would enforce stereochemistry via the chair-like transition state proposed earlier. However, protodehalogenation occurred predominantly via premature hydrogen atom transfer from supersilane to the vinyl radical.

To supress protodehalogenation and enhance the desired product yield, we tried running the reaction with higher or lower AIBN loading (entries 2,3), lower substrate concentration (entry 4), and slow addition of supersilane and AIBN to the solution of starting material in MeCN (entry 5), however without significant improvement.



		s.m.	dehal.	270: desired (1:1 dr)
1	$(TMS)_3SiH$, AIBN (0.4 eq.), MeCN (50 mM), 90 °C	0%	34%	20%
2	$(TMS)_3SiH$ (2 eq), AIBN (1.0 eq.), MeCN (50 mM), 100 °C, 2 h	0%	52%	**21%**
3	$(TMS)_3SiH$ (2 eq), AIBN (0.1 eq.), MeCN (50 mM), 100 °C, 2 h	35%	52%	15%
4	$(TMS)_3SiH$ (2 eq), AIBN (0.1 eq.), MeCN (10 mM), 100 °C, o/n	61%	5%	3%
5	$(TMS)_3SiH$ (2 eq), AIBN (0.5 eq.), slow add to s.m. toluene (25 mM), 80 °C, 4 h	83%	17%	0%

Figure 72. Study of the radical cyclisation under radical initiator conditions

We then tested different silanes as hydrogen atom donors (Figure 73, entry 1). It turned out that the Si-H bond in other silanes appeared to be too strong to participate in HAT, as no reaction occurred in all cases.

Samarium(II) iodide is known to initiate radical cyclisations via single electron reduction from vinyl bromides.[111] However, in our case, no reaction was observed (entry 2). Photoredox activation of vinyl halides has been reported only for iodides,[112] but reduction of aryl bromides using highly reducing acridinium photocatalyst has also been reported.[113] Employing the highly reducing acridinium and thioxanthone catalysts in the case of vinyl bromide **269** resulted in no reaction (entry 3), likely due to the lower reduction potential of vinyl bromides compared to vinyl iodides. We attempted to synthesise vinyl iodide substrate **271** (entry 4) by 2-indanol alkylation with 3-bromo-2-iodopropene, which had to be prepared in two steps from commercially available material. In the alkylation event, only side product **268** was formed via iodide elimination, which in the case of iodide, a better leaving group than bromide, had become a dominant reaction pathway.

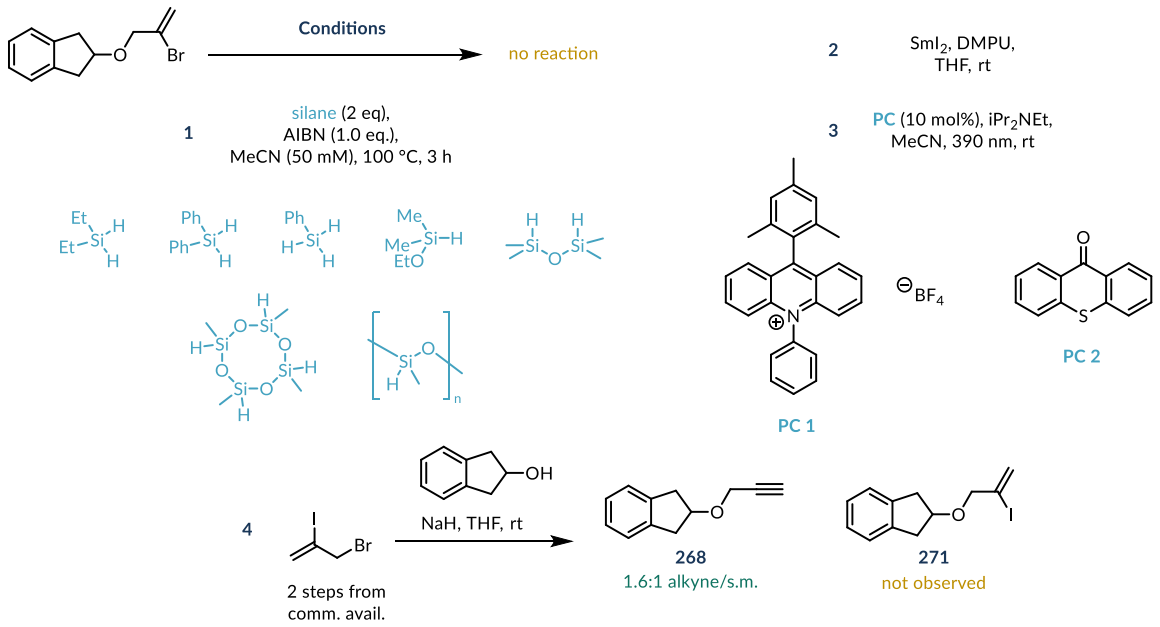


Figure 73. Further radical cyclisation study

5.5 Conclusion

In efforts towards rubriflordilactone B synthesis, a smaller fragment was joined with the AB ring aldehyde, followed by construction of the central CDE rings via [2+2+2] cyclotrimerisation and selective dehydration to afford an advanced ABCDE intermediate. A radical cyclisation via 1,5-HAT that would form the F ring was tested on a model system. A promising result was initially obtained, demonstrating the viability of this cyclisation, however improving the yield of the desired product proved challenging. At the same time, initial progress towards rubriflordilactone A indicated a higher chance of its successful synthesis, which is the subject of the following chapter.

Chapter 6: Synthesis of the diyne fragment and rubriflordilactone A

6.1 Introduction and retrosynthesis of the diyne fragment

Rubriflordilactone A (Figure 74) was previously synthesised by merging the AB rings with the diyne fragment in 38 overall steps.[40] With the goal of developing a more efficient synthesis of rubriflordilactone A, we initially tackled the diyne fragment synthesis. Despite its apparent simplicity, this fragment has previously proved challenging and was synthesised by Anderson in 14 steps.[40, 114]

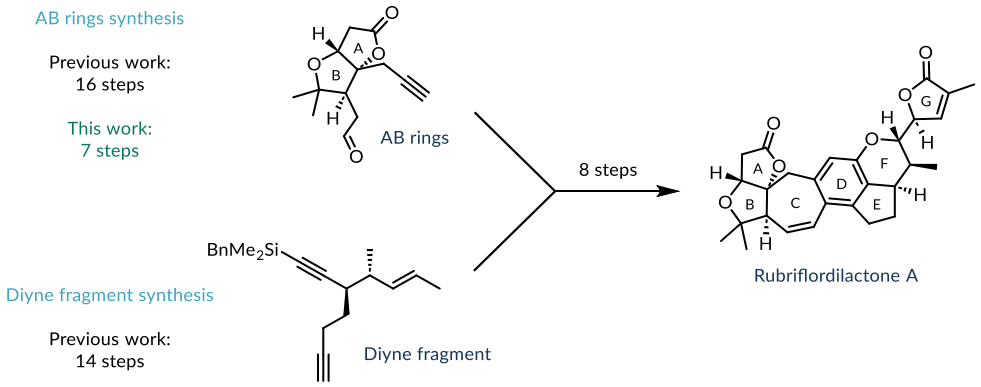


Figure 74. Overview of the rubriflordilactone A synthesis

The key synthetic challenges of the diyne fragment revolve around its two contiguous tertiary carbon stereocentres, one of which is directly attached to an alkyne. One of the alkynes bears a benzyldimethylsilyl group, which plays an important role in later stage Tamao-Fleming oxidation. However, at this stage it precludes the use of other silyl groups in the synthesis because it would be difficult to selectively deprotect another silyl group in the presence of the benzyldimethylsilyl group.

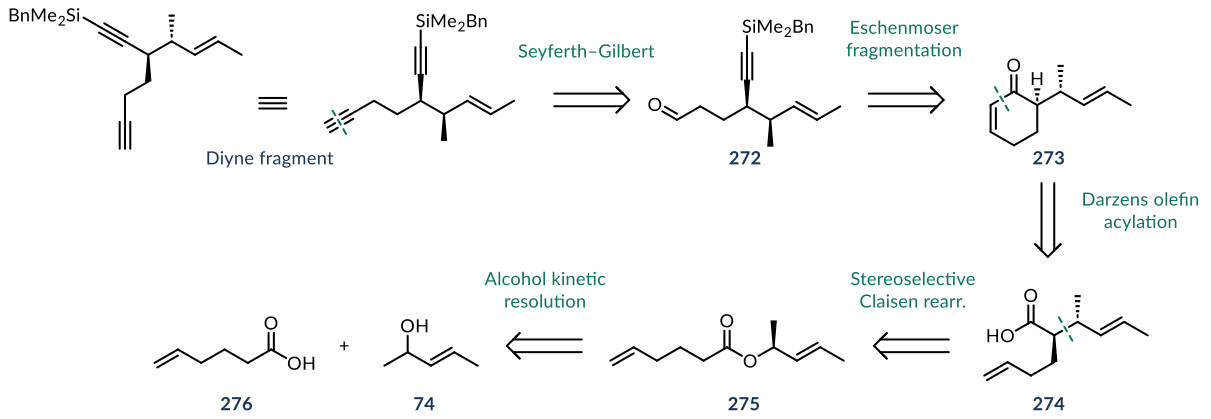


Figure 75. Retrosynthesis of the diyne fragment

A desirable synthetic strategy would differentiate the two alkynes by introducing them sequentially, while concurrently addressing the problem of the contiguous tertiary stereocentres. To achieve this, we disconnected the unsubstituted alkyne via Seyferth–Gilbert homologation.[115] The resulting enynal **272** features an aldehyde and ketone in a 1,5-relationship, making it a perfect retron for Eschenmoser-Tanabe fragmentation[116] from cyclohexenone **273**. The most direct way to synthesise cyclohexenone **273** would be to attach the acyclic side chain to cyclohexanone. Though this could be a feasible strategy for a racemic synthesis of **273**, there was no existing enantioselective method that would allow for the control of both stereocenters. Instead, we opted for somewhat unusual, but precedented Darzens acylation[117] (Figure 76a) to construct a cyclohexene ring from a carboxylic acid.

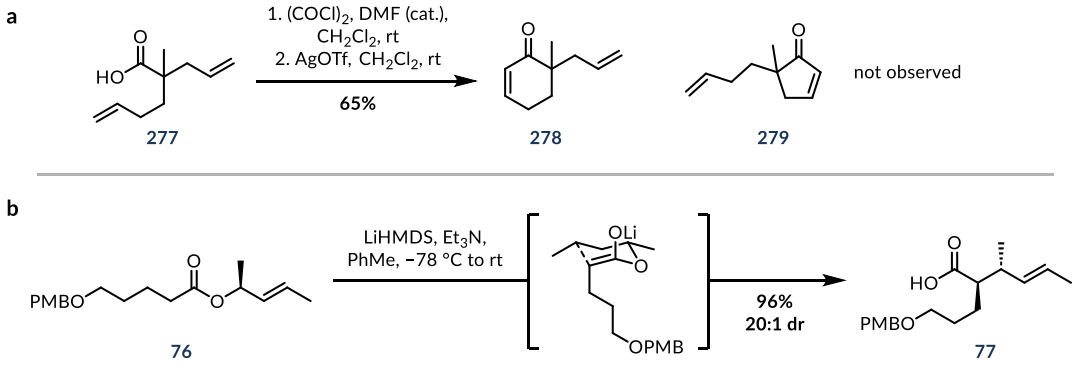


Figure 76. (**a**) Literature example of Darzens acylation on a similar substrate; (**b**) Literature example of stereoselective Ireland-Claisen rearrangement on a similar substrate

Disconnection to carboxylic acid **274** (Figure 75) allowed us to utilise a diastereoselective Ireland-Claisen rearrangement of ester **275**, a reaction that is well-precedented on a similar

substrate[40] (Figure 76b). This reaction would transform a single alcohol stereocentre into two contiguous all carbon tertiary stereocentres. Alcohol **74** (Figure 75) is known in the literature[60] and is obtained via enzymatic kinetic resolution of the commercially available racemic alcohol.

6.2 Darzens acylation strategy

To explore the Darzens acylation strategy, we started from commercially available alcohol **74** (Figure 77). This alcohol could also be prepared from crotonaldehyde by methyl Grignard addition. The following steps were explored with racemic alcohol **74**. Ester formation mediated by EDC·HCl delivered ester **275**. Deprotonation of ester **275** with LiHMDS at −78 °C, followed by warming to room temperature, effected Ireland-Claisen rearrangement with high diastereoselectivity. The configuration of two setereocentres in **274** was assigned by analogy to the close literature example (Figure 81b).[40]

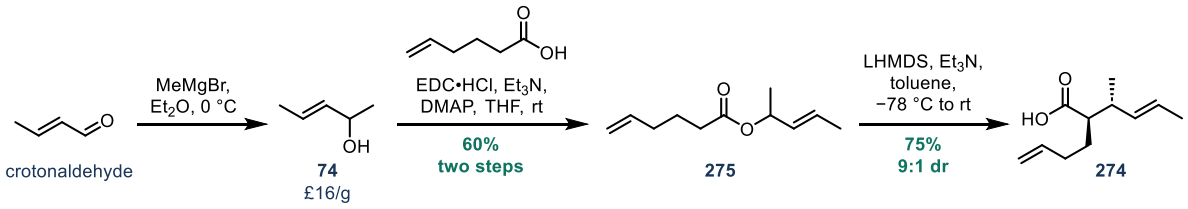


Figure 77. Darzens acylation strategy forward synthesis

With acid **274** in hand (Figure 78a), we tested the ring closure via intramolecular olefin acylation. Converting acid **274** into acid chloride **280**, followed by treatment with a range of Lewis acids resulted in either decomposition or no reaction. Next, we tested *in situ* carboxylic acid activation of via a mixed anhydride. Treatment of acid **274** with triflic anhydride resulted in complex mixture formation. Following the literature protocol using trifluoroacetic anhydride,[118] treatment of acid **274** with trifluoroacetic anhydride (Figure 78b) led to full conversion as monitored by GC-MS and yielded low quantities of ketone which structure was tentatively assigned as **281**.

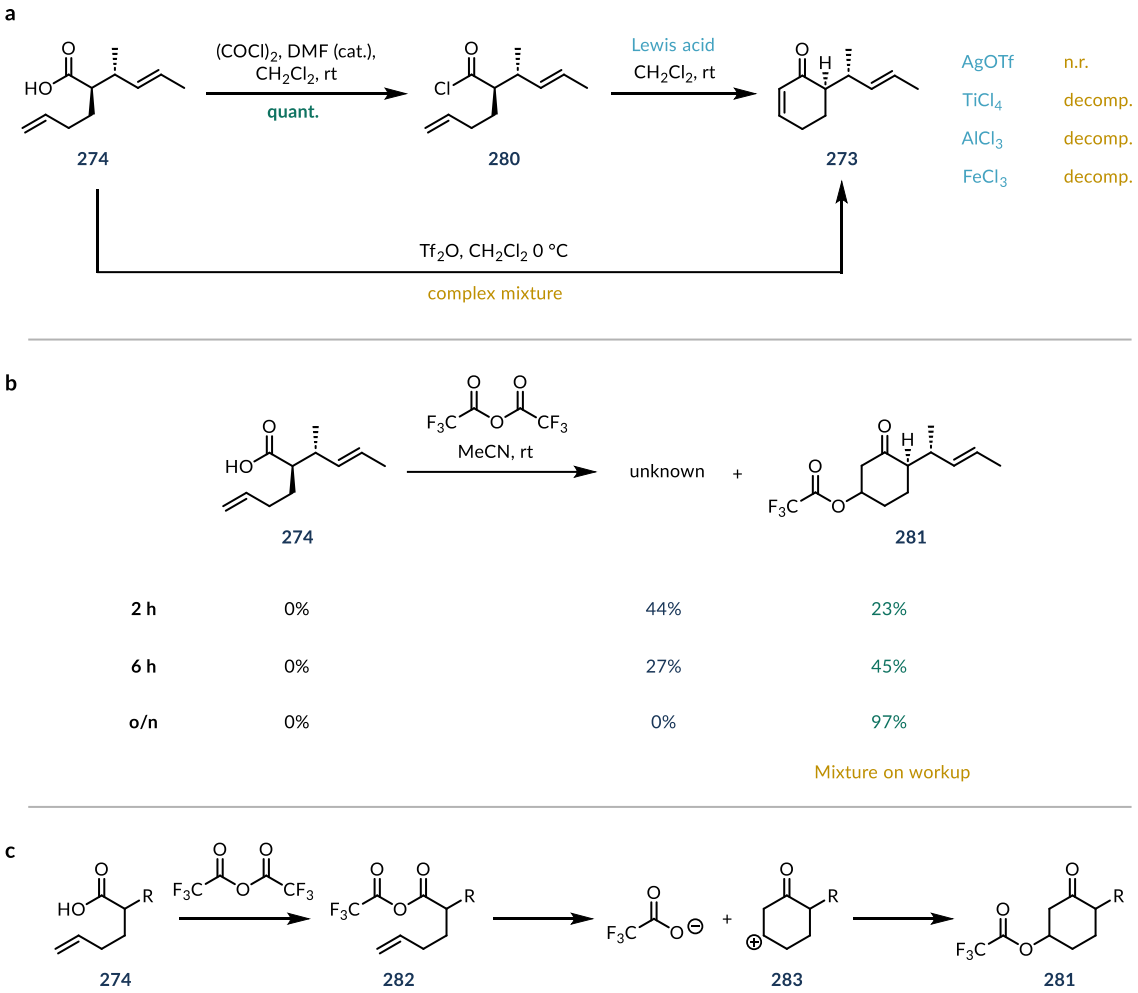


Figure 78. (**a**) Darzens acylation via acyl chloride; (**b**) Direct activation of carboxylic acid with trifluoroacetic anhydride; (**c**) Mechanism of reaction of carboxylic acid with trifluoroacetic anhydride

We noticed initial formation of an unknown intermediate, the concentration of which gradually diminished as the final product formed in high yield. Upon workup, however, a mixture of products was obtained. Although the reaction itself proceeded successfully, we were unable to isolate the desired product from the reaction mixture, presumably due to instability of **281**. Ketone **281** likely arose from the capture of carbocation **283** by trifluoroacetate anion (Figure 78c).

Intramolecular olefin acylation could proceed better by making the olefin more nucleophilic. To achieve this, vinyl silane **285** (Figure 79) was synthesised via rhodium-catalysed hydrosilation[119] from the corresponding alkyne **284**. Transforming acid **285** into its acid chloride **286**, followed by treatment with a Lewis acid ($TiCl_4$ or $AlCl_3$), resulted in decomposition of the starting acid

chloride. Direct activation of carboxylic acid **285** with trifluoroacetic anhydride gave no reaction.

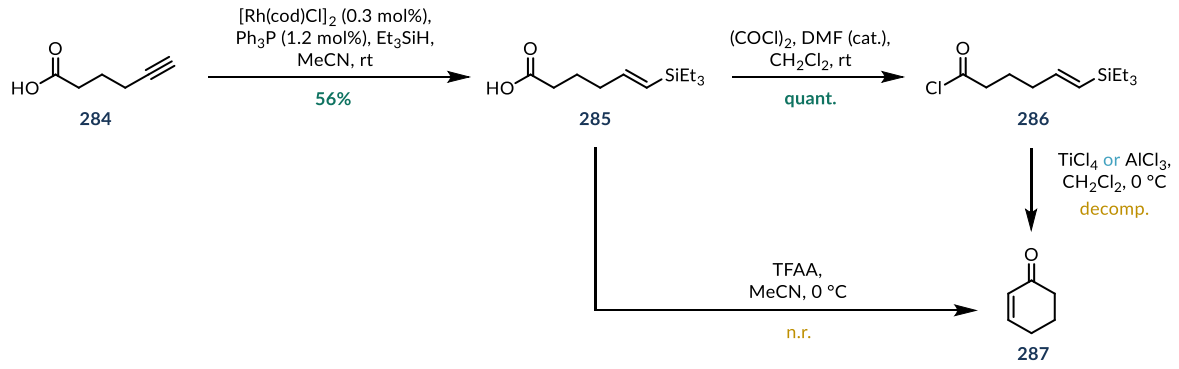


Figure 79. Alkyne hydrosilation and vinyl silane acylation

Faced with challenges with intramolecular olefin acylation, we decided to rethink our approach with a goal of pursuing a more direct diyne fragment synthesis.

6.3 Carboxylic acid to alkyne strategy

An ideal strategy for the diyne fragment synthesis would involve a direct conversion of carboxylic acid **274** into alkyne **288** (Figure 80). Importantly, the stereochemistry of the carbon atom attached to carboxylic acid had to be preserved. Although a transformation that could achieve this in a single step has not been described, we embarked on solving this challenge.

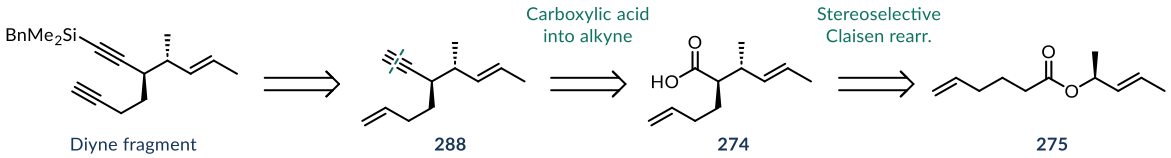


Figure 80. Carboxylic acid to alkyne retrosynthetic strategy

During this work, a report by Liu and co-workers[120] demonstrated the conversion of methyl esters **289** into alkynes **292** (Figure 81) using pre-formed solid lithiated bis[(pinacolato)boryl]methane **290** and the purposely developed triflating reagent **291**.

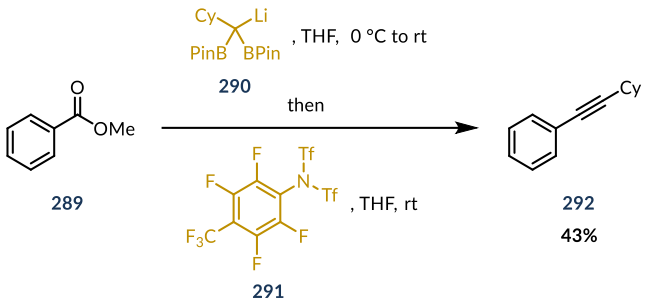


Figure 81. Literature reported conversion of ester into alkyne

Given the practical complexities of the reported procedure and the non-commercial availability of the required reagents, we modified the literature reagents while relying on the same reaction procedure (Figure 82). Deprotonation of bis[(pinacolato)boryl]methane by LiTMP generated lithiated derivative **293**. Nucleophilic addition of this organolithium **293** to methyl *p*-methoxybenzoate resulted in the formation of ketone **294**, which immediately isomerised to boron enolate **295**. Triflation of the boron enolate **295** with Comins' reagent gave vinyl triflate **296**, which underwent elimination to alkyne **297** upon warming to room temperature. Conducted in the described manner, we obtained the desired alkyne **297** in 37% yield and ketone **299** in 43% yield. Ketone **299** resulted from premature protodeborylation of intermediates **294** or **295**.

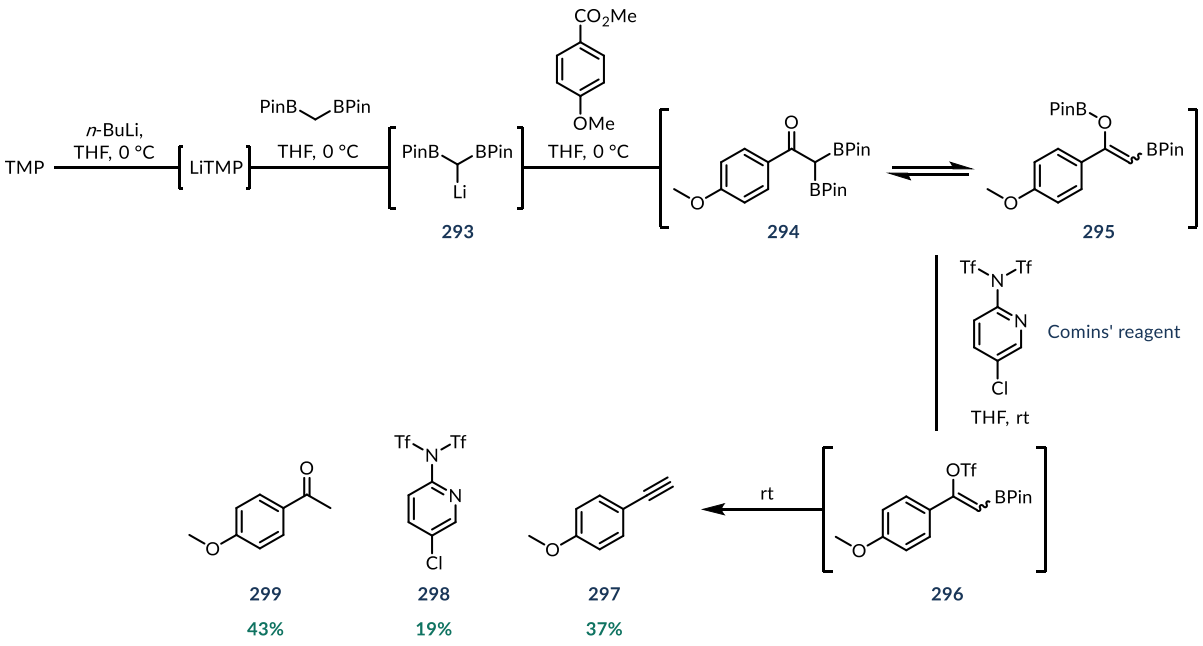


Figure 82. Modification of the literature protocol for ester to alkyne homologation

6.3 Alternative carboxylic acid to alkyne approach

With the promising results of ester-to-alkyne homologation, we applied this transformation to the diyne fragment synthesis. Ester **300** (Figure 83) was prepared from carboxylic acid **274** via silver(I) oxide-mediated alkylation in 46% yield. We found that ester **300** could be prepared in significantly higher yield (96%) by formation of the acid chloride, followed by *in situ* methanol quenching. When the described ester to alkyne homologation[120] was tested on ester **300**, a mixture of ketone **301** and starting material was obtained, with no traces of the desired alkyne **288**.

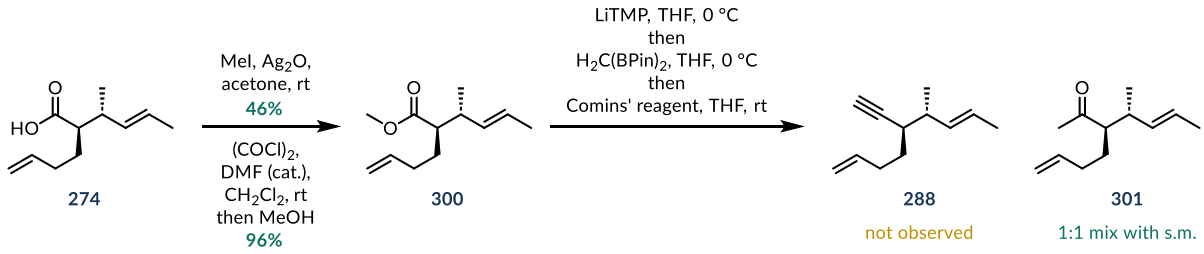


Figure 83. Application of ester to alkyne homologation to the diyne fragment synthesis

Inspired by the tactic of vinyl triflate or other leaving group elimination from a ketone intermediate, we explored an alternative way to achieve a conceptually similar transformation. To pursue this goal, methyl ketone **301** was synthesised by treating carboxylic acid **274** with excess methyllithium (Figure 84a). Next, we tested a ketone dehydration method originally developed by Negishi[121] and described in *Organic Syntheses.*[122] Kinetic deprotonation of methyl ketone **301** with LDA followed by trapping of the resulting enolate with diethyl chlorophosphate generated vinyl phosphate **302**. When this solution was added to a solution of LDA, phosphate elimination took place to deliver alkyne **288** in 40% yield over two steps from carboxylic acid **274**. Alkyne **288** was subsequently silylated using LDA and benzyldimethylsilyl chloride to give **303**. This sequence of steps enabled us to transform a carboxylic acid into an appropriately substituted alkyne in three steps.

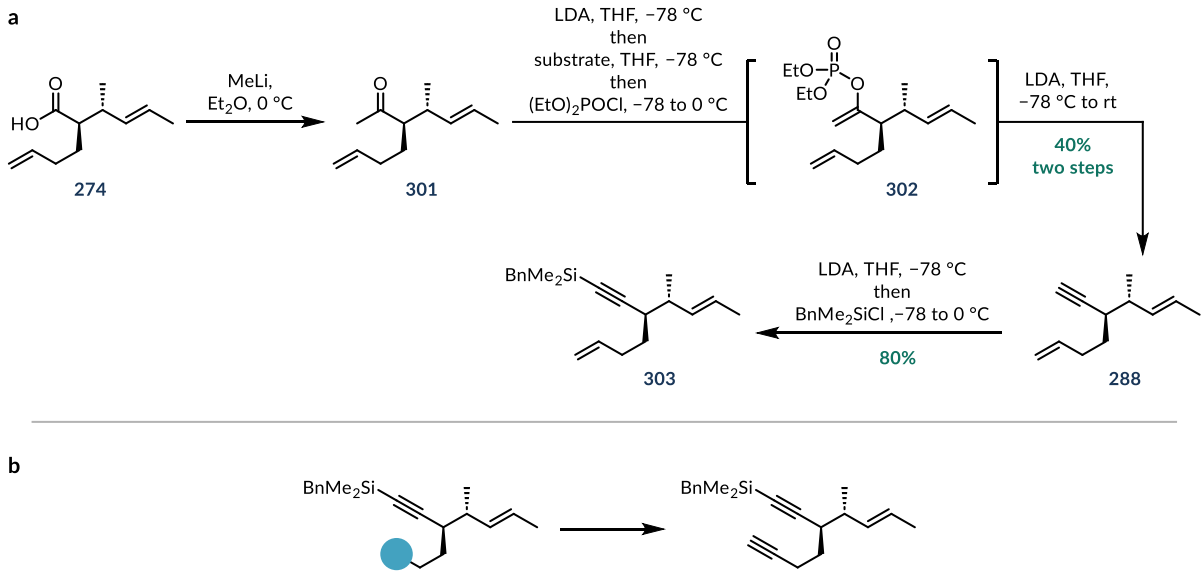


Figure 84. (**a**) Synthesis of silylacetylene from carboxylic acid via methyl ketone intermediate; (**b**) Need for a suitable terminal alkyne equivalent

Having successfully introduced the first alkyne with the correct stereochemistry, we focused on introducing the second, terminal alkyne. To achieve this goal, it was necessary to find an alkyne equivalent that can reveal an alkyne or acetylide at an appropriate point in the synthesis (Figure 84b), while remaining intact until the first alkyne is silylated. If an intermediate with two terminal (free) alkynes formed, selective silylation of only one of them would be highly improbable.

6.4 Masked alkyne equivalents

6.4.1 Bromoalkyne

We first explored a bromoalkyne as a terminal alkyne equivalent that could, at the desired point in synthesis, reveal an acetylide nucleophile by halogen-lithium exchange (Figure 85).

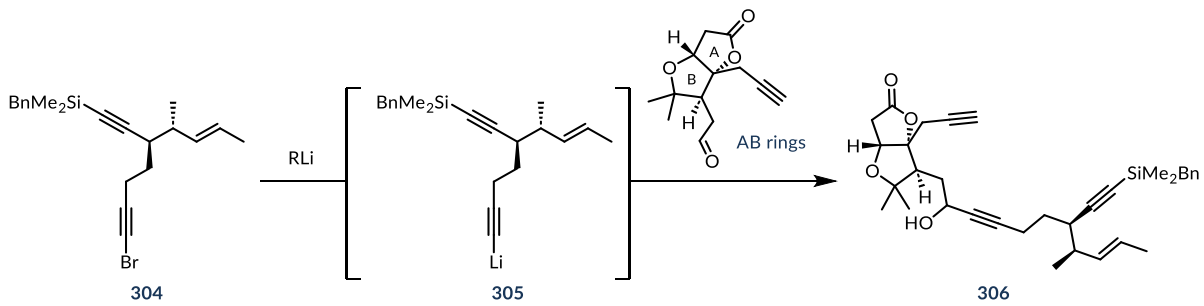


Figure 85. Bromoacetylene as a masked acetylide in the context of rubriflordilactone A synthesis

The forward synthesis started from crotonaldehyde (Figure 86). Addition of methylmagnesium bromide, followed by ester formation with 5-hexynoic acid delivered ester **307** in 69% yield over two steps. Ireland-Claisen rearrangement necessitated an additional equivalent of base to deprotonate the alkyne proton to give acid **308** with excellent diastereoselectivity (9:1). Treatment of acid **308** with excess methyllithium produced ketone **309**, however the yield and conversion were significantly lower compared to the substrate with an alkene in place of the alkyne (27% vs quantitative). The observed difference in reactivity could likely be attributed to the low solubility of the dianion of **308**, as evidenced by persistent precipitation throughout the reaction. We tried conducting the same reaction in the presence of TMEDA to decomplex organolithium aggregates.[123] This indeed prevented precipitation, but only traces of the desired product were formed. To increase the yield of the transformation of the carboxylic acid into the methyl ketone, we eventually employed a Weinreb amide, as will be discussed later.

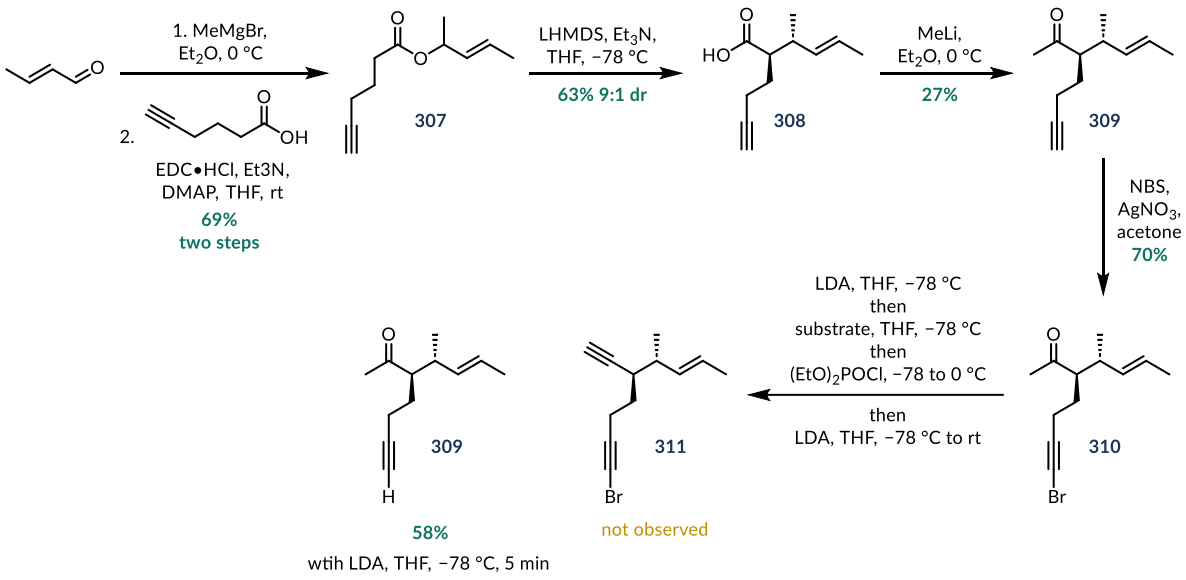


Figure 86. Bromoacetylene synthesis

With ketone **309** in hand (Figure 86), bromoacetylene **310** was synthesised by silver-catalysed bromination[76] which proceeds via a silver acetylide intermediate. Next, we employed the previously described conditions involving diethyl chlorophosphite for ketone dehydration to obtain alkyne **311**. However, when ketone **310** was exposed to LDA, rapid debromination took place to produce ketone **309**. In this unexpected outcome, bromoacetylene **310** likely serves

as an electrophilic bromine source, while LDA functions as a nucleophile in an *N*-bromination event. This leaves behind an acetylide that is ultimately protonated to form ketone **309**. Even if the ketone dehydration from this intermediate **309** had proceeded well, loss of the bromine atom at this stage would have resulted in the formation of two terminal alkynes, which would be difficult to differentiate. To circumvent this issue, we aimed to identify a stronger carbon–halogen bond and employ a milder base.

6.4.2 Chloroacetylene

We anticipated that substituting the bromine atom with chlorine, and use of a milder base such as LiHMDS, would help preserve the chloroacetylene intact, while successfully achieve the desired ketone dehydration. To achieve this, chloroacetylene **312** was synthesised by silver-catalysed chlorination using *N*-chlorosuccinimide as an electrophilic chlorine source (Figure 87).

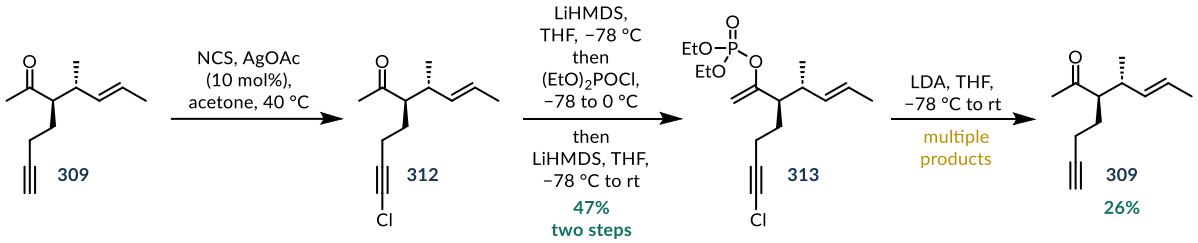


Figure 87. Chloroacetylene synthesis

Treatment of ketone **312** with LiHMDS indeed resulted in ketone deprotonation while preserving the chloroacetylene functionality. Trapping the enolate with diethyl chlorophosphate formed vinyl phosphate **313** with complete conversion as monitored by TLC. Treatment of the reaction mixture with additional LiHMDS, however, did not result in phosphate elimination and alkyne formation. As a result, vinyl phosphate **313** was isolated after chromatographic purification in 47% yield over two steps (partial hydrolysis of vinyl phosphate occurred during chromatography). To achieve the desired phosphate elimination, purified vinyl phosphate **313** was treated with LDA, however this resulted in a complex mixture of products from which we were only able to recover protodechlorinated ketone **309** in 26% yield. These results indicate that the reduced basicity of LiHMDS, compared to LDA, tolerated the

chloroacetylene functionality. However, LiHMDS was not a strong enough base to effect vinyl phosphate elimination.

As an alternative to the vinyl phosphate, we explored ketone dehydration via an *in situ* formed vinyl triflate intermediate and excess base. To this end, different combinations of amide bases and triflating reagents were tested (Figure 88). Use of LiHMDS with Comins' reagent resulted in no reaction, with recovery of the starting material. Use of LiHMDS with triflic anhydride or KHMDS with phenyl triflimide resulted in decomposition after the addition of the triflating reagent.

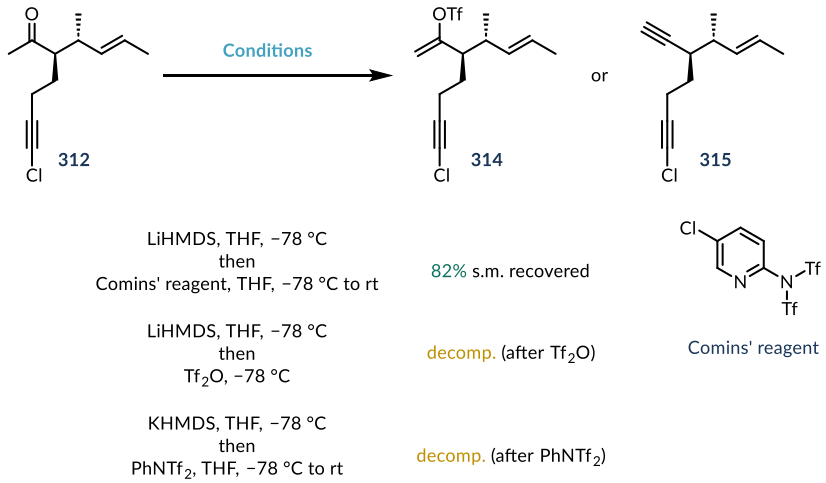


Figure 88. Ketone dehydration via vinyl triflate intermediate

Unable to achieve ketone dehydration with a chloroacetylene substrate, we set out to find a better alternative that could unmask the terminal alkyne functionality at the appropriate stage of the synthesis.

6.4.3 Germylacetylene

After an extensive literature search, we discovered a report[124] demonstrating a strategy for alkyne protection/deprotection that is orthogonal to silicon-based protecting groups. More specifically, when a substrate contains both germanium- and silicon-bearing alkynes, either the germyl or silyl group could be cleaved under different conditions (Figure 89). According to this report, treatment of substrate **316** with potassium fluoride in THF resulted in selective

trimethylsilyl cleavage while the trimethylgermanium motif remained intact. Alternatively, treatment of the same substrate with catalytic copper(I) bromide in THF/MeOH resulted in selective trimethylgermyl cleavage while the TMS group remained intact. Similar outcomes were observed with substrates **319** and **322**. We sought to apply this strategy to our diyne fragment synthesis.

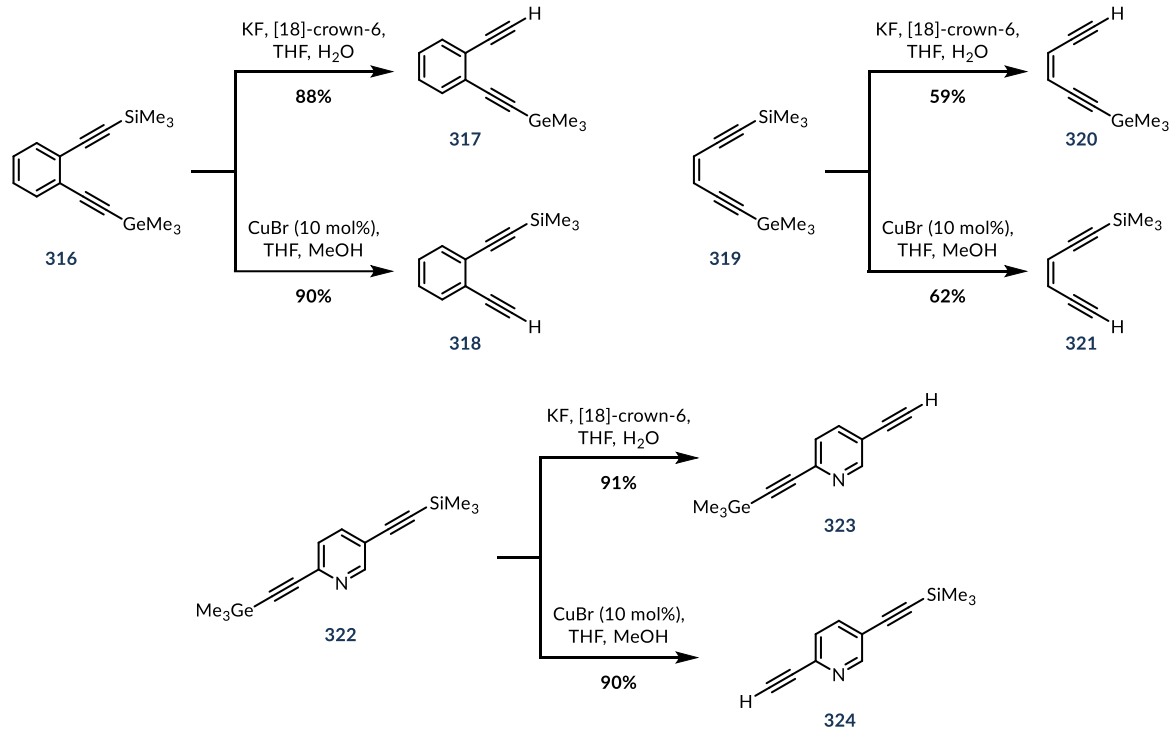


Figure 89. Literature reports of orthogonal alkynylsilane and alkynylgermane cleavage

Before incorporating germanium into our synthesis, we had to address the low-yielding conversion of the carboxylic acid into the methyl ketone. Starting from carboxylic acid **308** (Figure 90), instead of direct addition of methyl lithium, we first formed Weinreb amide **325** via EDC-mediated amide coupling. Addition of methyl magnesium bromide to Weinreb amide **325** cleanly afforded ketone **309** in excellent overall yield from carboxylic acid **308**, representing a significant improvement from the previous 27% yield. Silver-catalysed germylation[125] of ketone **309** using commercially available chlorotrimethylgermane formed alkynylgermylated ketone **326** in 91% yield over two steps from Weinreb amide **325**.

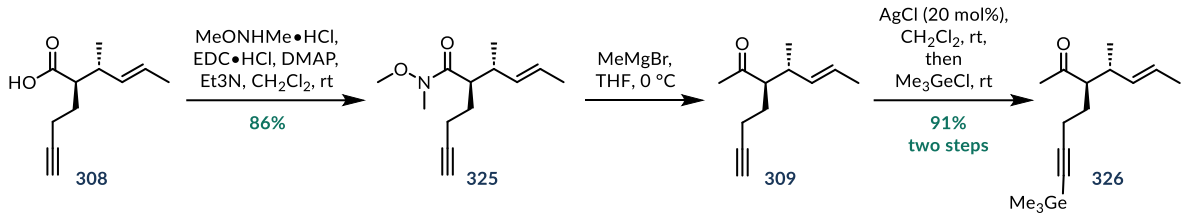


Figure 90. Synthesis of germylated methyl ketone

With ketone **326** in hand, we tested the previously described one-pot ketone dehydration via vinyl phosphate intermediate (Figure 91). Although the trimethylgermyl group remained unchanged when exposed to LDA, applying the previously used conditions for ketone dehydration to **326** initially resulted in formation of vinyl phosphate, as monitored by TLC. However, upon subsequent treatment with LDA, decomposition was observed. Attempts to synthesise alkyne **327** via either vinyl triflate or vinyl chloride intermediates were also unsuccessful.

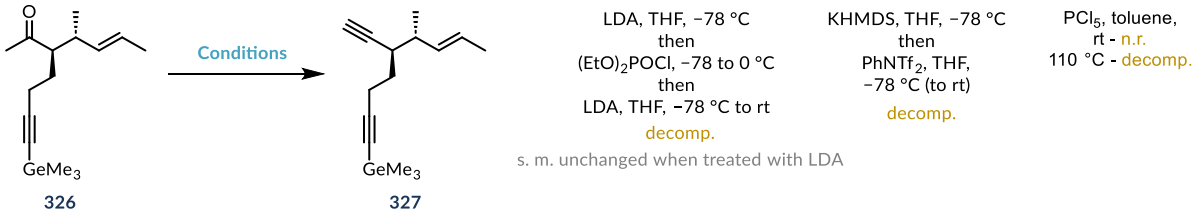


Figure 91. Ketone dehydration to alkyne via vinyl triflate or vinyl chloride intermediates

Unable to achieve the one-pot conversion of methyl ketone into an alkyne, we turned to a two-step approach, with a plan to later merge these two steps into a single telescoped step. Reaction of ketone **326** with LiHMDS and diethyl chlorophosphate gave vinyl phosphate **328** (Figure 92), which was isolated and purified in 71% yield. It has been reported that vinyl phosphates could undergo elimination when treated with *tert*-butyl lithium.[126] In the context of the subsequent phosphate elimination, a trimethylgermyl substituted alkyne holds an advantage over halogen-substituted alkynes, as it can tolerate both organolithium and organomagnesium reagents, although at this stage, there were no literature examples to support this. In the event, treatment of vinyl phosphate **328** with *tert*-butyl lithium immediately resulted in phosphate elimination to give the desired alkyne **327**. Subsequent silylation using LDA and benzyldimethylsilyl

chloride afforded **329**. In the final step, the trimethylgermanium group was selectively cleaved in the presence of the silane using catalytic copper(I) bromide in methanol/THF in excellent yield, completing the synthesis of the diyne fragment.

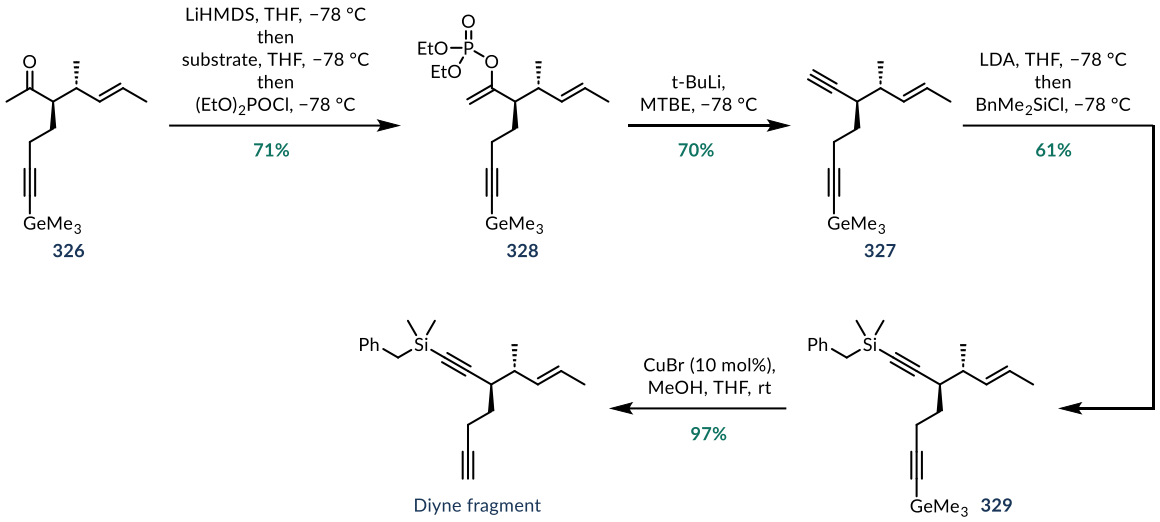


Figure 92. Successful synthesis of the diyne fragment

After establishing a successful route to the diyne fragment, we sought to improve this route in line with our goals of efficient, sustainable and scalable synthesis.

6.5 Improvement of the diyne fragment synthesis

6.5.1 Overview of the initial diyne fragment synthesis

The initial route to the diyne fragment consisted of 9 steps for the racemic synthesis and 10 steps for the enantioselective synthesis (Figure 93). Our goal was to reduce the step count, remove chromatographic separations, and avoid hazardous reagents. To achieve these goals, we identified several improvement areas. First, enzymatic kinetic resolution (step 1) to form alcohol **75** required chromatographic separation, which suffered from losses due to product volatility. Second, conversion of carboxylic acid **308** into methyl ketone **309** required a two-step procedure (steps 4 and 5) because the free alkyne complicated direct methylation using methyllithium. Introducing the germanium group at an earlier stage could potentially solve this problem. Third, given that phosphate elimination from vinyl phosphate **328** generated an acetylide as the final intermediate before work up (step 8), this acetylide intermediate could

potentially be used in a telescoped silylation to produce silylacetylene **329** in one step from vinyl phosphate **328**. Fourth, we wanted to avoid the use of *tert*-butyl lithium for phosphate elimination and eventually develop a one-pot procedure for converting ketone **326** into diyne **329**.

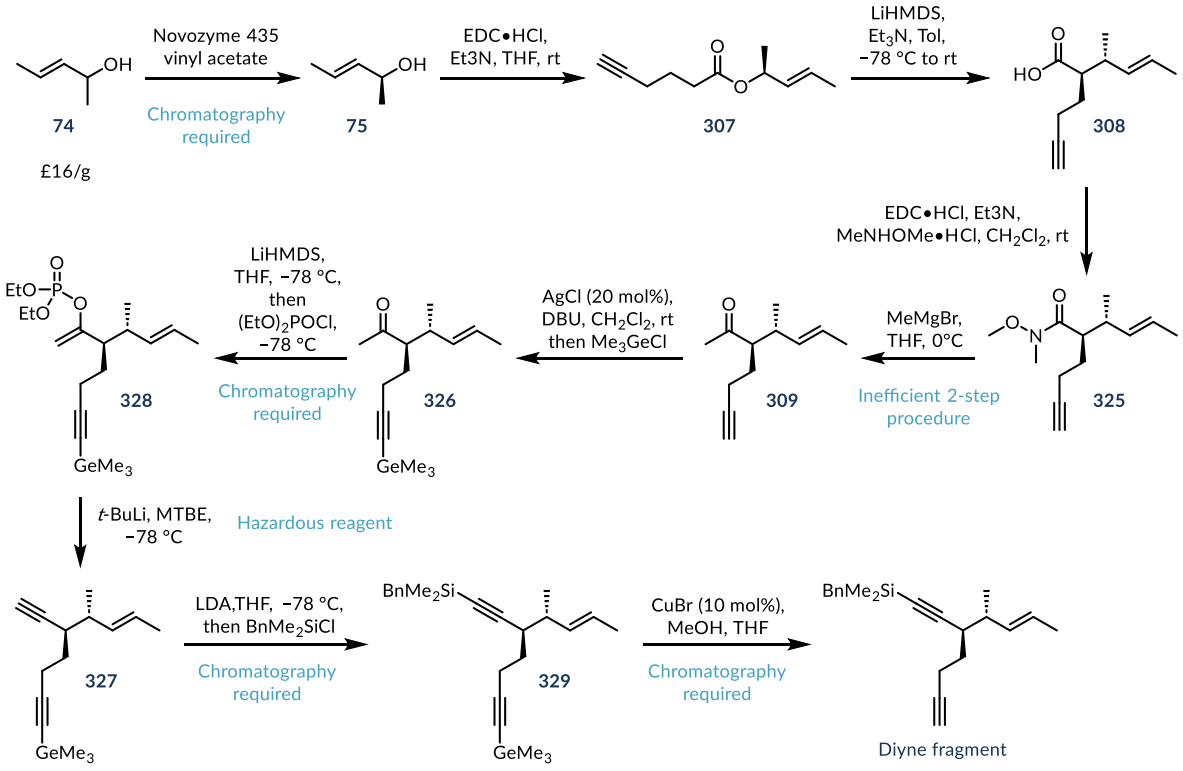


Figure 93. Overview of the initial diyne fragment synthesis

6.5.2 Enzymatic kinetic resolution via alcohol acylation

The enantioselective preparation of alcohol **75** via enzymatic kinetic resolution has been reported in the literature[60] (Figure 94a). The procedure necessitates chromatography to separate the desired alcohol **75** from the unwanted acetylated product **330**. In this case, use of chromatography is especially disadvantageous due to the volatility of alcohol **75**. In this way, alcohol **75** could only be obtained as a solution in ether or ethyl acetate, with significant losses on evaporation.

We wanted to avoid chromatography and instead distil alcohol **75** (bp 124 °C) directly from the reaction mixture after removing the enzyme. However, the presence of excess vinyl acetate (bp

72 °C) and undesired acetate product **330** (bp 139 °C) in the reaction mixture greatly complicated this distillation due to close similarities in boiling points. Our solution to this issue was to use a long-chain acyl donor instead of vinyl acetate (Figure 94b). From a reaction mixture containing pentane, desired alcohol **75**, vinyl laurate (high bp) and undesired laurate product **331** (high bp), we were able to distil pure alcohol **75** at 50-60 °C at 30 mbar, in a modest 22% yield. Surprisingly, alcohol **75** normally distilled at 124 °C at atmospheric pressure, however, from this particular mixture, we were unable to distill anything at atmospheric pressure, therefore reduced pressure was used. We were pleased to see that, similar to vinyl acetate, the enzymatic kinetic resolution with vinyl laurate proceeded with excellent enantioselectivity. The reaction with vinyl laurate was complete in 1 h compared to vinyl acetate which required 3 h. Furthermore, in the original procedure, this kinetic resolution was conducted with molecular sieves and dry pentane under nitrogen atmosphere. We found that this reaction works equally well without molecular sieves, with ordinary (non-dried) pentane and open to air. Absolute stereochemistry of **75** was assigned by analogy to the literature example where vinyl acetate was used as acyl donor.

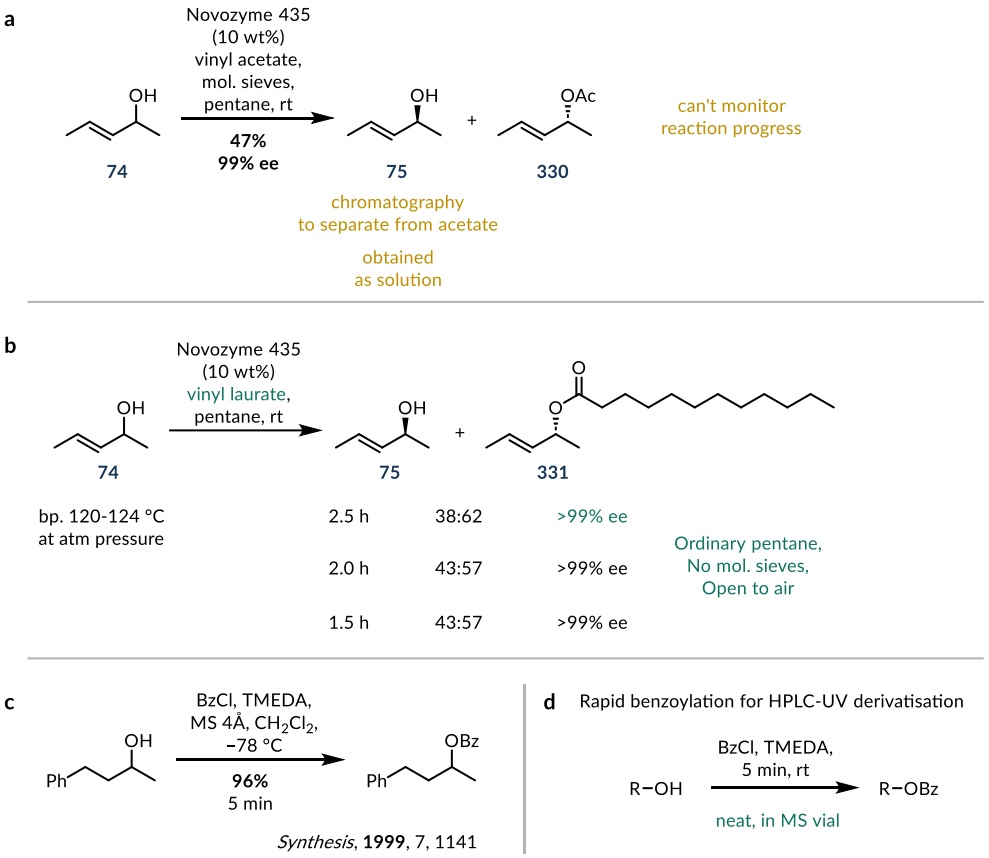


Figure 94. (**a**) Literature reported enzymatic kinetic resolution; (**b**) Modified enzymatic kinetic resolution to avoid chromatography; (**c**) Literature reported rapid benzoylation; (**d**) Rapid benzoylation for HPLC-UV derivatisation

It proved difficult to quantitatively monitor the progress and enantiomeric excess of this kinetic resolution via HPLC equipped with only a UV-Vis detector, as the products did not absorb UV light. In the previous Anderson synthesis,[40] monitoring was achieved via benzoylation of alcohol **75** to produce a benzoate, after which enantiomeric excess could be determined by a UV detector. To analyse a reaction this way, it took a separate reaction (3 h) in addition to two chromatographic separations to determine the enantiomeric excess of the kinetic resolution. We found this unacceptably inefficient.

Inspired by the rapid benzoylation conditions discovered by Sano[127] (Figure 94c), we developed a simple and fast derivatisation protocol suitable for converting alcohols into the corresponding benzoates for HPLC-UV analysis (Figure 94d). Taking an aliquot of the reaction mixture and letting it stand with neat TMEDA and benzoyl chloride in a vial for 5 min, followed by addition

of hexane and microfiltration, afforded a sample suitable for HPLC-UV analysis. This protocol could be used generally when alcohol derivatisation for a UV detector is required.

6.5.3 Early-stage germylation

As described earlier, conversion of an alkyne-bearing carboxylic acid into a methyl ketone was achieved either in one step with methyllithium or two steps via a Weinreb amide. We recalled that the carboxylic acid without a terminal alkyne reacted smoothly with methyllithium to give the corresponding ketone in high yield. Our plan was to protect the alkyne-bearing carboxylic acid with the trimethylgermyl group prior to methyllithium addition, with a goal of synthesising the desired germylated ketone in one step and good yield. At this stage, it was uncertain whether the trimethylgermyl group would remain intact on treatment with methyllithium, particularly given that its silicon counterpart, the trimethylsilyl group, typically undergoes rapid cleavage under same conditions.

Unfortunately, attempting the previously used silver-mediated germylation conditions[125] with acid **308** resulted in no reaction (Figure 95a). The carboxylic acid functionality was incompatible with this chemistry even when excess DBU was used. Binding of the carboxylate anion to the silver(I) ion possibly prevented formation of the active catalyst species.

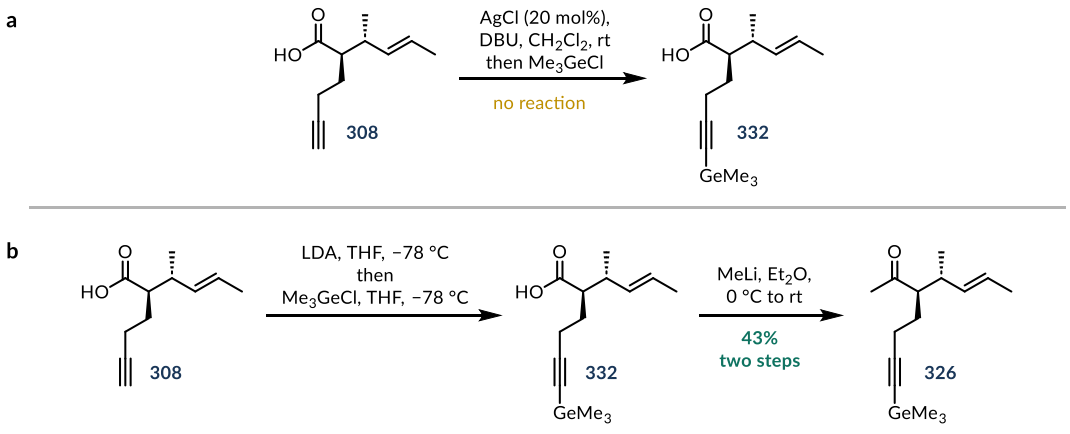


Figure 95. (**a**) Attempted silver-mediated alkyne germylation in the presence of the carboxylic acid; (**b**) LDA-mediated alkyne germylation via double deprotonation

In an alternative procedure, not precedented in the literature, acid-alkyne **308** was doubly deprotonated, followed by addition of one equivalent of trimethylgermyl chloride to give acid-

germylacetylene **332** (Figure 95b). Subsequent reaction with methyl lithium produced the desired ketone **326** in 43% yield over two steps. We were pleased to find that the trimethylgermyl group remained intact, demonstrating greater resistance to organometallic reagents compared to the trimethylsilyl group.

6.5.4 Telescoped phosphate elimination and alkyne silylation

Phosphate elimination and alkyne silylation were initially performed as separate steps to simplify the reactions when working with unfamiliar substrates and products. However, given that lithium acetylide was generated in the first step, the reaction could potentially be quenched with chlorosilane to form the silylated product immediately. Indeed, treatment of vinyl phosphate **328** with *tert*-butyllithium (Figure 96), followed by addition of benzylchlorodimethysilane, formed silylacetylene **329** in 81% yield. We found it was important to add no more than 1.1 equivalent of silyl chloride to prevent formation of silane-related impurities that were inseparable from the product.

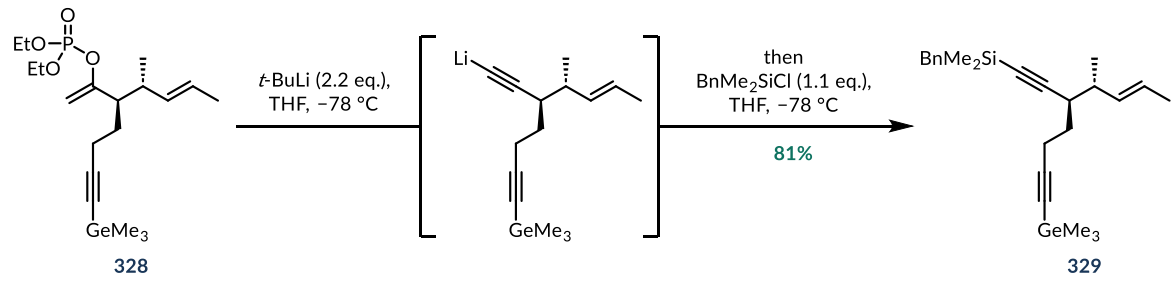


Figure 96. Telescoped phosphate elimination and alkyne silylation

6.5.5 Alternative to organolithium-induced phosphate elimination

Driven by our goals of efficient, sustainable and scalable synthesis, we also aimed to avoid the need for *tert*-butyllithium because of its hazardous nature. We hoped to enhance the efficiency of the elimination step by using a more electron deficient phosphate, which would serve as a better leaving group. To explore this idea, we synthesised trifluoroethyl phosphate derivative **335** (Figure 97). Starting from phosphite **333**, a literature reported radical chlorination[128] using sulfuryl chloride gave the required bis(trifluoroethyl) chlorophosphate reagent **334**.

Deprotonation of ketone **326** and treatment with bis(trifluoroethyl) chlorophosphate **334** gave the corresponding bis(trifluoroethyl) vinyl phosphate **335**.

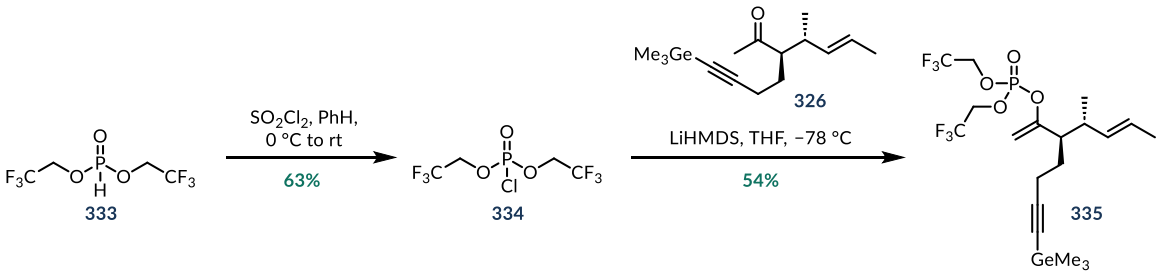
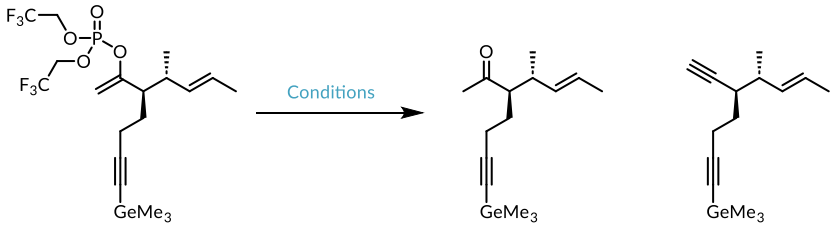


Figure 97. Synthesis of bis(trifluoroethyl) vinyl phosphate substrate

We tested different organolithium and amide bases (Figure 98) to achieve phosphate elimination. Employing *n*-BuLi resulted in exclusive formation of ketone **326**. This was likely a result of the direct attack of *n*-BuLi on the phosphorous atom, with the organolithium acting as a nucleophile instead of a base. Employing *sec*-BuLi produced a mixture of ketone **326** and the desired alkyne **327**, favouring the ketone. The increased steric hindrance around the carbon-lithium bond in *sec*-BuLi presumably reduced the nucleophilicity of the reagent, resulting in partial alkyne formation. Amide bases (LDA and LiHMDS) gave exclusively ketone **326**, presumably via *N*-attack on the phosphorus atom. Even the hindered LiTMP resulted in exclusive ketone formation.



	326 ketone		327 alkyne
n-BuLi, THF, −78 °C	1	:	0
sec-BuLi, THF, −78 °C	7	:	3
LDA, THF, −78 °C	1	:	0
LiHMDS, THF, −78 °C	1	:	0
LiTMP, THF, −78 °C	1	:	0

Figure 98. Elimination of vinyl phosphate with different bases

Although these experiments did not result in synthetic route improvements, they increased our understanding of the interplay between nucleophilicity and basicity of organolithium and amide reagents in this type of elimination.

6.6 Final route to the diyne fragment

6.6.1 Overview of the final route

Enzymatic kinetic resolution of racemic alcohol **74** gave alcohol **75** (Figure 99) after chromatographic separation from the corresponding acetate. Use of vinyl laurate instead of vinyl acetate enabled product separation via distillation instead of chromatography. Coupling of the alcohol with 5-hexynoic acid produced ester **307**, which was taken without purification to the next step. Ireland-Claisen rearrangement of ester **307** delivered acid **308**, which was obtained pure and with high diastereoselectivity after an acid/base wash workup.

From this point, the synthesis could be continued in two ways. The first involves Weinreb ketone synthesis, followed by silver-mediated germylation to form ketone **326**. The second involves germylation of acid **308** using LDA, followed by methyllithium addition to convert the germylated acid into ketone **326**. While the second route has a lower step count, we found the

first approach via Weinreb ketone synthesis to be more practical, higher yielding and requiring no chromatographic purification.

Deprotonation of methyl ketone **326** using LiHMDS and treatment with diethyl chlorophosphate gave vinyl phosphate **328** in 71% yield after chromatography. One-pot phosphate elimination and alkyne silylation produced diyne **329** in 81% yield after chromatography. Finally, selective copper(I)-catalysed cleavage of germyl in presence of silyl group delivered the target diyne fragment in 97% yield, completing the synthesis of this fragment in 9 steps and 10% overall yield. The same fragment could also be synthesised in 8 steps and 6% overall yield if germanium is introduced at the carboxylic acid stage.

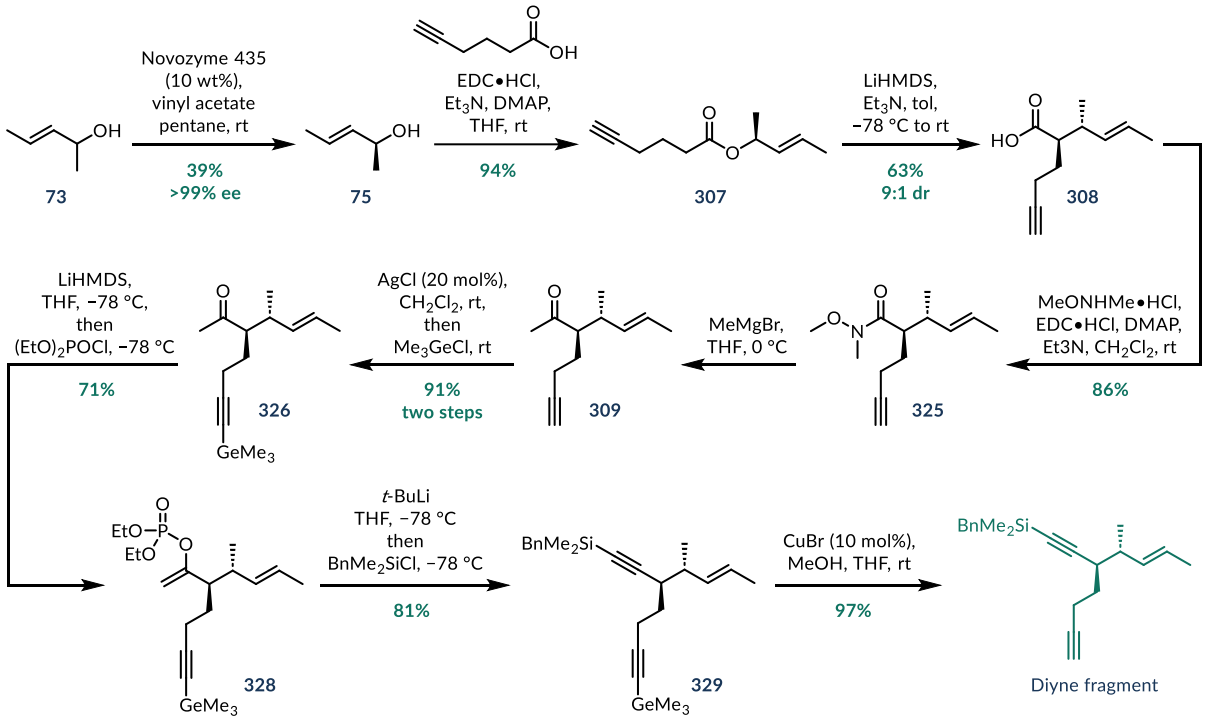


Figure 99. Final route to the diyne fragment

6.6.2 Comparative analysis of different routes to the diyne fragment

The diyne fragment synthesis was compared to the previous synthesis by Anderson.[40] Synthetic efficiency was assessed by comparing the total number of steps, the number of chromatographic separations, and the overall yield for each synthetic route. Process-mass-

intensity (PMI) was calculated to compare the amount of waste generated, and global warming potential (CO_2 kg-equivalent), of each route.[15]

PMI was calculated for every step in each synthetic route (Figure 100). The whole process PMI (PMI_{tot}) was estimated by summing the individual step PMIs. Finally, the average PMI per step (PMI_{avg}) was calculated to compare the waste generated in each route, independent of the total number of steps.

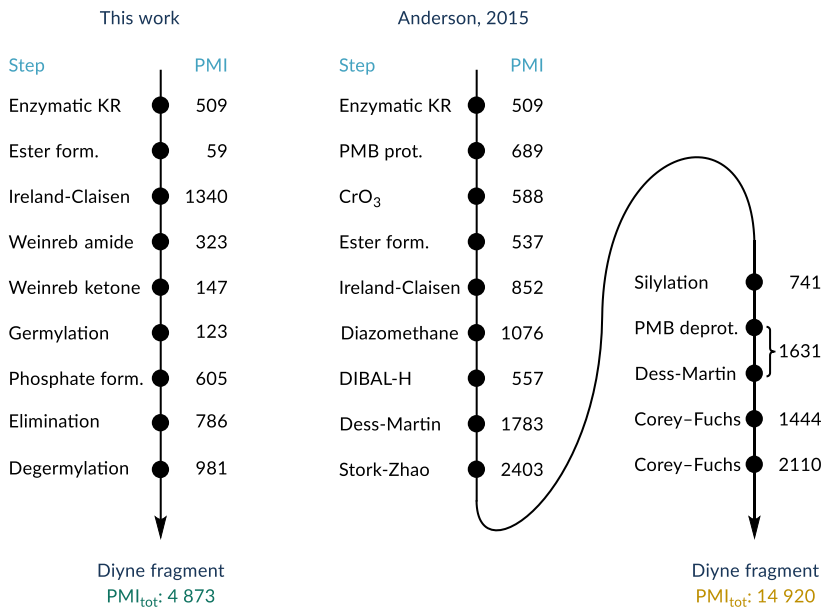


Figure 100. Comparative analysis of process mass intensity of each step in two different diyne fragment syntheses

Comparison of two different syntheses of the diyne fragment is summarised in Table 4. This work features a lower step count (9 vs 14), and significantly lower number of chromatographic steps (4 vs 13) than the previously reported synthesis. The overall yields are similar. The previous synthesis requires five low-temperature steps (−78 °C) compared to only three in this work. This work avoided use of highly toxic chemicals such as chromium(VI) oxide and diazomethane (which is also explosive) that were used in the previous synthesis, however it unfortunately required highly flammable *tert*-butyllithium to achieve phosphate elimination.

Table 4. Comparative analysis of different routes to the AB rings

	No. of steps	No. of chromatography	Yield	PMI (tot)	PMI (avg)
Anderson, 2015	14	13	12%	18 824	1 176
This work, 2022	**9**	**4**	**10%**	**4 873**	**541**

Lower step count, lower number of chromatographic separation and lower average PMI in this work indicate higher operational efficiency of each step. These have together resulted in a more sustainable synthesis (PMI_{tot} 4873 vs 14920), with waste and carbon emissions reduced by 67% compared to the previous diyne fragment synthesis.

6.7 Conclusion

Synthesis of the diyne fragment in the context of rubriflordilactone A synthesis was explored. Darzens acylation, followed by Eschenmoser fragmentation strategy was explored first. Difficulties encountered in the intramolecular olefin acylation step led us to explore alternative methods for converting carboxylic acids directly into alkynes. After examination of a promising modern method, we identified an approach involving dehydration of a methyl ketone via a vinyl phosphate intermediate. Having solved the carboxylic acid to alkyne challenge, we turned our efforts to identify the most suitable masked free alkyne or masked acetylide. Bromo- and chloroalkynes were tested with different bases, but both resulted in protodehalogenation to varying extents. Finally, we found a trimethylgermyl group effective, which enabled us to complete the initial diyne fragment synthesis. We sought to improve the initial diyne fragment synthesis by removing chromatography, improving the enzymatic kinetic resolution of the starting alcohol, lowering the step count by early-stage germanium introduction, telescoping phosphate elimination with alkyne silylation and finding alternatives to hazardous reagents. With some of these goals achieved, we developed the final diyne fragment synthesis in 9 steps and 10% overall yield, requiring only 4 chromatographic separations. Higher operational

efficiency of each step and a lower overall step count compared to the previously published route resulted in a more sustainable synthesis, with waste and carbon emissions reduced by 67% compared to the previous synthesis.

With successful and efficient diyne synthesis, we also achieved a second generation rubriflordilactone A synthesis in 24 total steps (17 LLS), which presents a significant improvement over the previous 38 steps (24 LLS) by Anderson[40] and 34 steps (20 LLS) by Li.[39]

Chapter 7: Experimental

7.1 Experimental considerations

All reactions were performed open to air and without precautions to exclude air/moisture unless specified otherwise. Reagents and solvents were purchased from commercial sources and used without further purification unless specified otherwise. NMR spectra were recorded on Bruker AVIII HD 400, NEO 400, AVIII HD 500 and AVII 500 spectrometers. Chemical shifts (δ) are quoted in parts per million (ppm). ^{1}H and ^{13}C NMR spectra are referenced to residual protons in chloroform-d (δ_H = 7.26, δ_C = 77.16) and acetone-d_6 (δ_H = 2.05, δ_C = 28.95). Peak multiplicities are defined as s (singlet), d (doublet), t (triplet), q (quartet), qu (quintet), m (multiplet) and br (broad). Coupling constants (J) are reported to the nearest 0.1 Hz. High-resolution mass spectra (HRMS) were recorded on a Thermo Scientific exactive mass spectrometer (Waters Equity autosampler and pump) for electrospray ionisation (ESI). Flash chromatography refers to normal phase column chromatography on silica gel (Merck Si 60, 0.040–0.063 mm) under a positive pressure of nitrogen.

7.2 Process-mass-intensity calculations

Process-mass-intensity for each step was calculated by summing the total mass of input that included, reagents, catalysts, substrates, reaction solvent, workup solvent and chromatography solvent and dividing by the mass of the desired product. The following assumptions were used if information was not explicitly written in the experimental procedure:

1. Workup: usage of organic solvent was estimated to be 5× the volume of the reaction mixture. Water volume was estimated to be 30% of that organic solvent volume.

2. Chromatography: 600 mL of chromatography solvent per 1 g of the product was used for large scale. When a reaction was reported on ≤200 mg scale, 150 mL of chromatography solvent per 100 mg of the product was estimated.[129]

7.3 Computational details

Density functional theory calculations were performed with Gaussian 16 software, revision A.03, using Oxford Advanced Research Computing (ARC) facility. Geometries were optimised using b3lyp functional with 6-31g basis set. Vibrational frequencies and free energy were calculated at 298.15 K. Natural bond orbital analysis was performed with Gaussian NBO version 3.1.

228-preferred conformer input:

```
******************************************
 Gaussian 16:  ES64L-G16RevA.03 25-Dec-2016
               16-Sep-2022
******************************************
 %mem=8000MB
 %nprocshared=16
 Will use up to   16 processors via shared memory.
 ----------------------------------------------------
 # opt freq b3lyp/6-31g pop=nbo geom=connectivity
 ----------------------------------------------------
 1/18=20,19=15,26=3,38=1,57=2/1,3;
 2/9=110,12=2,17=6,18=5,40=1/2;
 3/5=1,6=6,11=2,25=1,30=1,71=1,74=-5/1,2,3;
 4//1;
 5/5=2,38=5/2;
 6/7=2,8=2,9=2,10=2,28=1,40=1/1,7;
 7//1,2,3,16;
 1/18=20,19=15,26=3/3(2);
 2/9=110/2;
 99//99;
 2/9=110/2;
 3/5=1,6=6,11=2,25=1,30=1,71=1,74=-5/1,2,3;
 4/5=5,16=3,69=1/1;
 5/5=2,38=5/2;
 7//1,2,3,16;
 1/18=20,19=15,26=3/3(-5);
 2/9=110/2;
 6/7=2,8=2,9=2,10=2,19=2,28=1,40=1/1,7;
 99/9=1/99;
 ------------------
 Title Card Required
 ------------------
 Symbolic Z-matrix:
 Charge =  0 Multiplicity = 1
 C
 C                1    B1
 H                1    B2       2    A1
```

H	2	B3	1	A2	3	D1	0
C	1	B4	2	A3	4	D2	0
H	5	B5	1	A4	2	D3	0
H	5	B6	1	A5	2	D4	0
C	5	B7	1	A6	2	D5	0
H	8	B8	5	A7	1	D6	0
C	8	B9	5	A8	1	D7	0
C	10	B10	8	A9	5	D8	0
C	10	B11	8	A10	5	D9	0
C	11	B12	10	A11	8	D10	0
H	11	B13	10	A12	8	D11	0
C	12	B14	10	A13	8	D12	0
H	12	B15	10	A14	8	D13	0
C	15	B16	12	A15	10	D14	0
H	13	B17	11	A16	10	D15	0
H	15	B18	12	A17	10	D16	0
H	17	B19	15	A18	12	D17	0
O	8	B20	5	A19	1	D18	0
O	8	B21	5	A20	1	D19	0
O	1	B22	5	A21	22	D20	0
C	23	B23	1	A22	5	D21	0
C	24	B24	23	A23	1	D22	0
H	25	B25	24	A24	23	D23	0
H	24	B26	23	A25	1	D24	0
C	24	B27	23	A26	1	D25	0
O	28	B28	24	A27	23	D26	0

Variables:

B1	1.52949
B2	1.12871
B3	1.12874
B4	1.52133
B5	1.12144
B6	1.12252
B7	2.50193
B8	1.12182
B9	1.54
B10	1.39516
B11	1.39483
B12	1.39471
B13	1.09966
B14	1.39514
B15	1.0996
B16	1.39483
B17	1.09968
B18	1.09976
B19	1.09968
B20	1.51427
B21	1.51407
B22	1.52099
B23	2.49742
B24	1.51415
B25	1.07

B26	1.07
B27	1.5142
B28	1.2584
A1	107.22992
A2	107.22939
A3	110.80364
A4	109.2388
A5	108.567
A6	91.0381
A7	93.26746
A8	143.83548
A9	119.99722
A10	120.00432
A11	120.00863
A12	119.98077
A13	120.00002
A14	120.008
A15	120.0047
A16	120.01279
A17	119.98395
A18	120.02486
A19	89.96025
A20	34.29318
A21	111.49799
A22	90.38571
A23	34.44603
A24	124.44495
A25	136.75197
A26	90.13352
A27	123.11683
D1	-52.4051
D2	64.85963
D3	174.15602
D4	-68.9114
D5	25.04922
D6	-107.43621
D7	126.59488
D8	146.93359
D9	-33.07168
D10	-179.97293
D11	-0.05203
D12	-179.97984
D13	-0.00555
D14	-0.03761
D15	179.96185
D16	179.97501
D17	-179.95633
D18	2.1323
D19	131.93554
D20	-73.33651
D21	152.13061
D22	129.04739

D23	180.
D24	-146.48494
D25	-0.91391
D26	153.76667

228-preferred conformer optimised geometry:

Standard orientation:

Center Number	Atomic Number	Atomic Type	Coordinates (Angstroms) X	Y	Z
1	6	0	-2.169509	-1.007269	-0.603729
2	6	0	-1.714638	0.443740	-0.791868
3	1	0	-3.138018	-1.158133	-1.100197
4	1	0	-1.751545	0.706761	-1.857919
5	6	0	-1.136533	-1.988325	-1.142425
6	1	0	-1.352237	-3.001430	-0.803117
7	1	0	-1.152632	-1.958962	-2.242811
8	6	0	0.593922	-0.313994	-0.908825
9	1	0	0.573377	-0.128911	-1.995919
10	6	0	1.949113	-0.068912	-0.320100
11	6	0	2.859838	0.762262	-0.985963
12	6	0	2.296812	-0.633554	0.915851
13	6	0	4.112762	1.027918	-0.423766
14	1	0	2.588541	1.203651	-1.940819
15	6	0	3.550029	-0.370219	1.475126
16	1	0	1.587770	-1.280659	1.417848
17	6	0	4.459239	0.461095	0.807904
18	1	0	4.813835	1.672086	-0.944574
19	1	0	3.817853	-0.811286	2.429975
20	1	0	5.431814	0.664466	1.245098
21	8	0	-0.350432	0.608344	-0.280047
22	8	0	0.200510	-1.680867	-0.653048
23	8	0	-2.371746	-1.342683	0.821675
24	6	0	-3.057951	0.931699	1.275207
25	6	0	-2.888566	-0.364216	1.628829
26	1	0	-3.155708	-0.767565	2.597797
27	1	0	-3.523074	1.626774	1.962016
28	6	0	-2.577480	1.432187	-0.000143
29	8	0	-2.778607	2.585049	-0.429075

228-unpreferred conformer input:

```
******************************************
 Gaussian 16:  ES64L-G16RevA.03 25-Dec-2016
               16-Sep-2022
******************************************
 %mem=8000MB
```

```
%nprocshared=16
Will use up to   16 processors via shared memory.
-----------------------------------------------
# opt freq b3lyp/6-31g pop=nbo geom=connectivity
-----------------------------------------------
1/18=20,19=15,26=3,38=1,57=2/1,3;
2/9=110,12=2,17=6,18=5,40=1/2;
3/5=1,6=6,11=2,25=1,30=1,71=1,74=-5/1,2,3;
4//1;
5/5=2,38=5/2;
6/7=2,8=2,9=2,10=2,28=1,40=1/1,7;
7//1,2,3,16;
1/18=20,19=15,26=3/3(2);
2/9=110/2;
99//99;
2/9=110/2;
3/5=1,6=6,11=2,25=1,30=1,71=1,74=-5/1,2,3;
4/5=5,16=3,69=1/1;
5/5=2,38=5/2;
7//1,2,3,16;
1/18=20,19=15,26=3/3(-5);
2/9=110/2;
6/7=2,8=2,9=2,10=2,19=2,28=1,40=1/1,7;
99/9=1/99;
-------------------
Title Card Required
-------------------
Symbolic Z-matrix:
Charge =  0 Multiplicity = 1
C
C                  1    B1
C                  2    B2       1    A1
C                  3    B3       2    A2       1    D1       0
H                  1    B4       2    A3       3    D2       0
H                  2    B5       1    A4       4    D3       0
H                  2    B6       1    A5       4    D4       0
H                  3    B7       2    A6       1    D5       0
H                  4    B8       3    A7       2    D6       0
O                  3    B9       2    A8       1    D7       0
O                  1    B10      2    A9       3    D8       0
O                  1    B11     11   A10       4    D9       0
C                  4    B12      3    A11      2    D10      0
C                 13    B13      4    A12      3    D11      0
C                 14    B14     13    A13      4    D12      0
O                 13    B15      4    A14      3    D13      0
C                  1    B16     12    A15      2    D14      0
C                 17    B17      1    A16     12    D15      0
C                 17    B18      1    A17     12    D16      0
C                 18    B19     17    A18      1    D17      0
H                 18    B20     17    A19      1    D18      0
C                 19    B21     17    A20      1    D19      0
H                 19    B22     17    A21      1    D20      0
```

C	22	B23	19	A22	17	D21	0
H	20	B24	18	A23	17	D22	0
H	22	B25	19	A24	17	D23	0
H	24	B26	22	A25	19	D24	0
H	15	B27	14	A26	13	D25	0
H	14	B28	13	A27	4	D26	0

Variables:

B1	2.49742
B2	1.52099
B3	1.52944
B4	1.12189
B5	1.12153
B6	1.12139
B7	1.12871
B8	1.12871
B9	1.52136
B10	1.5142
B11	1.51415
B12	1.52099
B13	1.51424
B14	1.51415
B15	1.2584
B16	1.54
B17	1.39516
B18	1.39483
B19	1.39471
B20	1.09966
B21	1.39514
B22	1.0996
B23	1.39483
B24	1.09968
B25	1.09976
B26	1.09968
B27	0.9416
B28	0.9416
A1	90.38571
A2	112.00652
A3	93.29844
A4	92.94625
A5	143.95252
A6	107.36736
A7	107.2261
A8	111.49586
A9	90.13352
A10	111.42037
A11	112.00652
A12	111.21384
A13	111.1101
A14	124.71459
A15	109.57243
A16	119.99722
A17	120.00432

A18	120.00863
A19	119.98077
A20	120.00002
A21	120.008
A22	120.0047
A23	120.01279
A24	119.98395
A25	120.02486
A26	124.44935
A27	124.60784
D1	-27.31773
D2	110.59438
D3	-92.59799
D4	141.91236
D5	90.13881
D6	169.94011
D7	-152.13191
D8	0.91391
D9	53.91274
D10	-72.51884
D11	-55.42913
D12	56.41422
D13	124.44501
D14	-176.55405
D15	-107.77619
D16	72.21853
D17	-179.97293
D18	-0.05203
D19	-179.97984
D20	-0.00555
D21	-0.03761
D22	179.96185
D23	179.97501
D24	-179.95633
D25	124.51149
D26	-123.51729

228-unpreferred conformer optimised geometry:

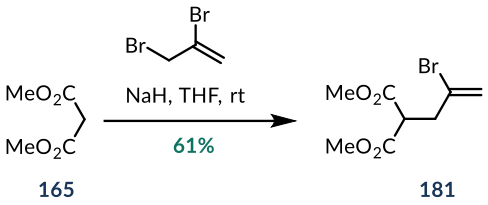
Standard orientation:

Center Number	Atomic Number	Atomic Type	Coordinates (Angstroms) X	Y	Z
1	6	0	0.510421	-0.163704	0.284244
2	6	0	-1.335497	-1.686277	0.528534
3	6	0	-2.016006	-1.037947	-0.686369
4	6	0	-1.550579	0.421713	-0.868359
5	1	0	0.140647	0.373621	1.169701
6	1	0	-1.673533	-1.215154	1.462632
7	1	0	-1.542650	-2.755244	0.569528
8	1	0	-1.794871	-1.612512	-1.585323

9	1	0	-1.854864	0.793468	-1.853237
10	8	0	-3.484441	-1.141614	-0.520251
11	8	0	-0.099530	0.448066	-0.895867
12	8	0	0.110099	-1.550502	0.387497
13	6	0	-2.169044	1.355967	0.188813
14	6	0	-3.546991	1.036185	0.539200
15	6	0	-4.119010	-0.129593	0.158275
16	8	0	-1.545838	2.333990	0.645788
17	6	0	2.002012	-0.058015	0.143177
18	6	0	2.564059	1.197559	-0.137786
19	6	0	2.832756	-1.173332	0.309911
20	6	0	3.949983	1.332966	-0.252402
21	1	0	1.911671	2.053236	-0.274118
22	6	0	4.220653	-1.032557	0.194934
23	1	0	2.388490	-2.137228	0.524191
24	6	0	4.781711	0.217983	-0.085809
25	1	0	4.379958	2.305033	-0.472132
26	1	0	4.861032	-1.899691	0.323075
27	1	0	5.858514	0.324545	-0.173911
28	1	0	-5.150196	-0.392770	0.359444
29	1	0	-4.113324	1.757492	1.114636

7.4 Procedures and characterisation from Chapter 2

181: Dimethyl 2-(2-bromoallyl)malonate



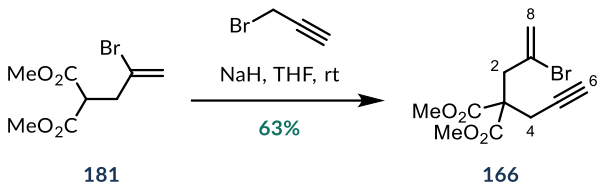
165 181

To a stirred suspension of pentane-washed NaH (1.09 g pre-wash weight, 27.2 mmol, 1.2 eq., 60% in oil) in dry THF (68 mL) at room temperature under N_2 was slowly added dimethyl malonate (2.61 mL, 22.7 mmol, 1.0 eq.), and the mixture was stirred for 30 min. 2,3-Dibromopropene (2.22 mL, 22.7 mmol, 1.0 eq. neat) was slowly added and the reaction mixture was stirred overnight. Diethyl ether and NH_4Cl (sat., aq.) were added. The organic layer was separated, washed with brine, dried over $MgSO_4$ and concentrated. The product was distilled under reduced pressure (0.5 mbar) and three fractions were collected. The first fraction (45 °C) contained unreacted dimethyl malonate, the second (65–90 °C) contained pure monoallylated product and the third fraction (100–110 °C) contained mostly diallylated product (these products were very hard to separate by chromatography). The desired product was thus obtained (3.49 g, 13.9 mmol, 61%) as a colourless liquid.

^{1}H NMR (400 MHz, $CDCl_3$) δ 5.69 (s, $1H_{CH2\text{-}alkene}$), 5.47 (s, $1H_{CH2\text{-}alkene}$), 3.82 (t, J = 7.5 Hz, $1H_{CH}$), 3.75 (s, $6H_{OMe}$), 3.02 (d, J = 7.5 Hz, $2H_{CH2\text{-}aliphatic}$).

Data in agreement with the literature values.[130]

166: Dimethyl 2-(2-bromoallyl)-2-(prop-2-yn-1-yl)malonate



181 166

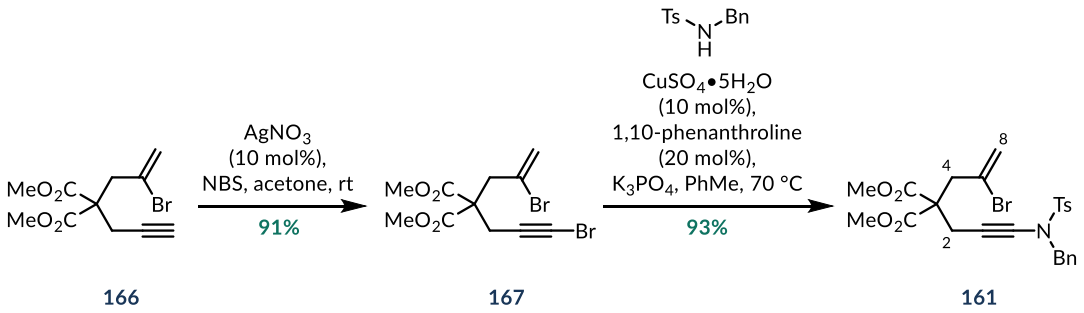
To a stirred suspension of pentane-washed NaH (162 mg pre-wash weight, 4.04 mmol, 1.5 eq., 60% in oil) in dry THF (12 mL) at room temperature under N_2 was slowly added malonate **181** (676 mg, 2.69 mmol, 1.0 eq.), and the mixture was stirred for 30 min. Propargyl bromide (160 µL, 5.38 mmol, 2.0 eq., 80% wt. in toluene) was slowly added and the reaction mixture was stirred overnight. Diethyl ether and NH_4Cl (sat., aq.) were added and the organic layer was separated, washed with brine, dried over $MgSO_4$ and concentrated. Purification via flash chromatography (pentane/EtOAc 9:1) afforded the product (490 mg, 1.69 mmol, 63%) as a colourless oil.

^{1}H NMR (400 MHz, $CDCl_3$) δ 5.84 (br s, $1H_8$), 5.63 (d, J = 1.6 Hz, $1H_8$), 3.77 (s, $6H_{OMe}$), 3.31 (br s, $2H_2$), 2.93 (d, J = 2.7 Hz, $2H_4$), 2.05 (t, J = 2.7 Hz, $1H_6$).

Data in agreement with the literature values.[131]

161: Dimethyl 2-(3-((*N*-benzyl-4-methylphenyl)sulfonamido)prop-2-yn-1-yl)-2-(2-bromoallyl)-malonate

167: Dimethyl 2-(2-bromoallyl)-2-(3-bromoprop-2-yn-1-yl)malonate



To a stirred solution of alkyne **166** (50 mg, 0.17 mmol, 1.0 eq.) in acetone (0.34 mL) at room temperature was added $AgNO_3$ (2.9 mg, 10 mol%). After stirring for 5 min, *N*-bromosuccinimide (34 mg, 0.19 mmol, 1.1 eq.) was added and the resulting mixture was stirred for a further 4 h at rt. The reaction mixture was concentrated, then pentane was added, and the suspension was filtered through cotton wool to remove the white precipitate. The resulting solution was concentrated to obtain the corresponding bromoalkyne (58 mg, 0.16 mmol), which was of sufficient purity to be used without further purification. Note 1: Because of similar R_f values of reactant and product, the reaction was monitored by NMR aliquot (conversion of singlet at 5.84 to 5.80 ppm). Note 2: If acetone is not evaporated completely before trituration with pentane, some succinimide will dissolve and contaminate the product. Note 3: The product was used immediately in the next step due to its tendency to decompose on storage.

To a mixture of *N*-tosylbenzylamine (245 mg, 0.938 mmol, 1.0 eq.), K_3PO_4 (398 mg, 1.88 mmol, 2.0 eq.), $CuSO_4$ (23 mg, 0.094 mmol, 0.1 eq.) and 1,10-phenanthroline (34 mg, 0.187 mmol, 0.2 eq.) in a vial was added a solution of bromoalkyne (380 mg, 1.03 mmol, 1.1 eq.) in toluene (1 mL). The vial was sealed and heated in an oil bath at 75 °C for 4 days. The reaction mixture was cooled to room temperature, diluted with EtOAc, filtered through Celite and concentrated. The

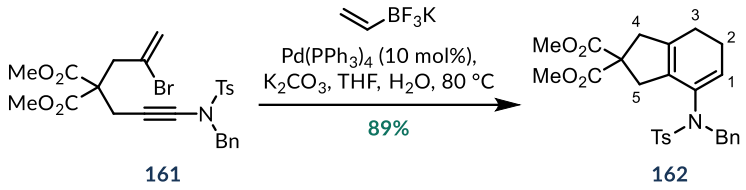
product was purified via flash chromatography (pentane/EtOAc 7:3) to afford the product (481 mg, 0.877 mmol, 93%) as a pale green gel.

^{1}H NMR (400 MHz, $CDCl_3$) δ 7.73 (d, *J* = 8.0 Hz, $2H_{Ts}$), 7.33 (d, *J* = 8.0 Hz, $2H_{Ts}$), 7.30 – 7.27 (m, $3H_{Bn}$), 7.25 – 7.21 (m, $2H_{Bn}$), 5.45 (s, $2H_8$), 4.41 (s, $2H_{Bn}$), 3.67 (s, $6H_{OMe}$), 3.07 (s, $2H_2$), 2.91 (s, $2H_4$), 2.45 (s, $3H_{Ts}$).

^{13}C NMR (101 MHz, $CDCl_3$) δ 169.8, 144.9, 135.1, 134.8, 130.1, 128.9, 128.9, 128.6, 127.9, 126.3, 123.2, 76.9, 65.6, 56.5, 55.6, 53.8, 53.3, 43.1, 22.0.

HRMS (ESI) calc. for $C_{25}H_{27}{}^{79}BrNO_6S$ $[M+H]^+$ 548.0737, found 548.0734.

162: Dimethyl 7-((*N*-benzyl-4-methylphenyl)sulfonamido)-1,3,4,5-tetrahydro-2H-indene-2,2-dicarboxylate



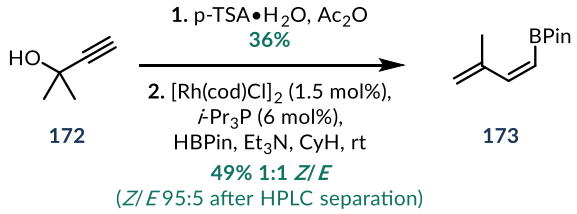
A vial loaded with potassium vinyltrifluoroborate (3.7 mg, 0.027 mmol, 1.5 eq.) was taken into the glovebox, and a solution of bromoynamide **161** (10.0 mg, 0.018 mmol, 1.0 eq. in 100 µL) and $Pd(PPh_3)_4$ (2.1 mg, 0.002 mmol, 10 mol%) in degassed THF (300 µL) were added. The vial was sealed, removed from the glovebox, and then a degassed solution of K_2CO_3 in water (7.6 mg, 0.055 mmol, 3.0 eq. in 50 µL) was quickly added under an inverted cone of nitrogen. The mixture was heated at 80 °C for 10 h. The mixture was cooled to room temperature and directly purified via flash chromatography (pentane/EtOAc 7:3) to afford the solid product (8.0 mg, 0.016 mmol, 89%).

^{1}H NMR (400 MHz, acetone-d_6) δ 7.74 (d, *J* = 8.1 Hz, $2H_{Ts}$), 7.44 (d, *J* = 8.1 Hz, $2H_{Ts}$), 7.36 – 7.15 (m, $5H_{Bn}$), 5.20 (t, *J* = 4.6 Hz, $1H_1$), 4.46 (s, $2H_{Bn}$), 3.66 (s, $6H_{Me}$), 2.91 (s, $2H_5$), 2.87 (s, $2H_4$), 2.46 (s, $3H_{Ts}$), 2.22 – 2.13 (m, $2H_2$), 2.04 – 1.99 (m, $2H_3$).

^{13}C NMR (101 MHz, $CDCl_3$) δ 172.4, 143.5, 136.2, 136.1, 136.0, 134.8, 131.3, 129.5, 129.3, 128.4, 128.0, 127.8, 125.1, 54.7, 52.9, 43.6, 39.8, 29.8, 23.7, 22.5, 21.7.

HRMS (ESI) calc. for $C_{27}H_{29}NO_6SNa$ $[M+Na]^+$ 518.1608, found 548.1609.

173: (*Z*)-4,4,5,5-Tetramethyl-2-(3-methylbuta-1,3-dien-1-yl)-1,3,2-dioxaborolane



A protocol for *trans*-selective alkyne hydroboration developed by Miyaura and co-workers[79] was applied. To a flame dried Schlenk flask was added anhydrous cyclohexane (27 mL, 0.25 M). The flask was taken into the glovebox and $[Rh(cod)Cl]_2$ (66

mg, 0.13 mmol, 1.5 mol%) and *i*-Pr_3P (86 mg, 0.54 mmol, 6.0 mol%) were added. The flask capped with a septum and removed from the glovebox, then Et_3N (6.26 mL, 44.9 mmol, 5.0 eq.) and HBPin (1.15 g, 8.99 mmol, 1.0 eq.) were added and the mixture was stirred at room temperature for 30 min. 2-Methyl-1-buten-3-yne** (0.71 g, 10.8 mmol, 1.2 eq.) was added and the mixture was stirred for 3–4 h at room temperature (it could be also left overnight). The reaction was quenched by addition of MeOH (~10 mL) and evaporated (150 mbar, 30 °C). Purification via flash chromatography (pentane/EtOAc 98:2) afforded yellow oily product (850 mg, 5.29 mmol, 49%) as a ~1:1 *Z*/*E* mixture that was separated by reversed phase HPLC (Gemini-NX C18 5 µm, 21×150 mm, H_2O/MeCN 20:80, 9 mL/min, 6.6 min *Z*-isomer, 7.0 min *E*-isomer) to afford pure *Z* isomer.

^{1}H NMR (500 MHz, $CDCl_3$) δ 6.73 (d, *J* = 14.9 Hz, $1H_{CH\text{-}alkene}$), 5.36 (d, *J* = 14.9 Hz, $1H_{CH\text{-}alkene}$), 5.07–5.04 (m, $2H_{CH2\text{-}alkene}$), 1.96 (s, $3H_{Me}$), 1.29 (s, $12H_{BPin}$).

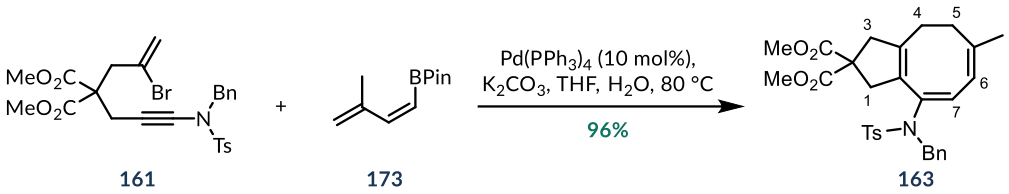
^{13}C NMR (126 MHz, $CDCl_3$) δ 148.6, 144.0, 119.2, 83.7, 24.9, 20.5. The alkene carbon atom bonded to boron was not observed due to quadrupolar relaxation.

HRMS (EI) calc. for $C_{11}H_{19}{}^{10}BO_2$ $[M]^{+\cdot}$ 193.1509, found 193.1521.

E isomer **^{1}H NMR** (400 MHz, $CDCl_3$) δ 7.11 (d, *J* = 18.2 Hz, 1H), 5.56 (d, *J* = 18.2 Hz, 1H), 5.16 (s, 2H), 1.85 (s, 3H), 1.29 (s, 12H).

**2-Methyl-1-buten-3-yne (b.p. 35 °C) could be synthesized from 2-methylbut-3-yn-2-ol according to a literature procedure,[132] or purchased directly from a commercial source.

163: Dimethyl (6*Z*,8*E*)-9-((N-benzyl-4-methylphenyl)sulfonamido)-6-methyl-1,3,4,5-tetrahydro-2*H*-cyclopenta[8]annulene-2,2-dicarboxylate



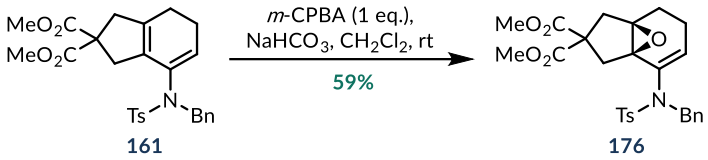
To a vial loaded with bromoynamide (34 mg, 0.062 mmol, 1.0 eq.) and (*Z*)-boronate ester (18 mg, 0.093 mmol, 1.5 eq.) was added dry and degassed THF (1.3 mL, 50 mM), degassed K_2CO_3 solution in water (0.13 mL, 19 mg/mL, 0.19 mmol, 3.0 eq.) and $Pd(PPh_3)_4$ (7.2 mg, 0.006 mmol, 10 mol%). The mixture was further degassed by bubbling N_2, then sealed and heated overnight at 80 °C. After cooling to rt, water and EtOAc were added, and the organic layer was separated and washed with brine, dried over $MgSO_4$ and concentrated. Purification via flash chromatography (pentane/EtOAc 7:3) afforded the cyclised clear oil product (32 mg, 0.060 mmol, 96%).

^{1}H NMR (400 MHz, $CDCl_3$) δ 7.76 (d, *J* = 8.3 Hz, $2H_{Ts}$), 7.37 – 7.13 (m, $7H_{Ts+Bn}$), 5.77 (dd, *J* = 5.1, 1.5 Hz, $1H_6$), 5.51 (d, *J* = 5.1 Hz, $1H_7$), 4.55 (s, $2H_{Bn}$), 3.71 (s, $6H_{OMe}$), 2.91 (s, $2H_{1/3}$), 2.61 (s, $2H_{1/3}$), 2.44 (s, $3H_{Ts}$), 2.02 – 1.96 (m, $2H_{4/5}$), 1.84 – 1.78 (m, $2H_{4/5}$), 1.65 (s, $3H_{Me}$).

^{13}C NMR (101 MHz, $CDCl_3$) δ 172.4, 143.4, 143.2, 143.0, 137.8, 136.7, 131.7, 129.6, 129.2, 128.6, 128.5, 128.3, 127.8, 127.6, 120.1, 56.9, 52.9, 52.7, 46.0, 43.4, 30.5, 27.8, 25.4, 21.7.

HRMS (ESI) calc. for $C_{30}H_{34}NO_6S$ $[M+H]^+$ 536.2100, found 536.2101.

176: Dimethyl (3a*R,7a*R**)-7-((*N*-benzyl-4-methylphenyl)sulfonamido)-4,5-dihydro-1*H*-3a,7a-epoxyindene-2,2(3*H*)-dicarboxylate**



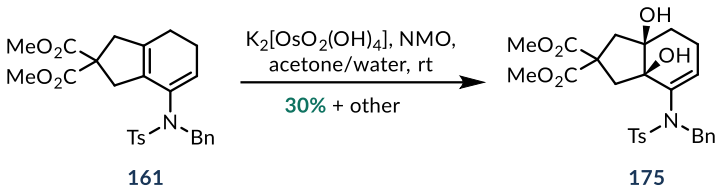
To a solution of diene (10.0 mg, 0.020 mmol) in CH_2Cl_2 (0.40 mL) was added $NaHCO_3$ (2.0 mg, 0.024 mmol, 1.2 eq.) and *m*-CPBA (70%, 5.5 mg, 0.022 mmol, 1.1 eq.) and the mixture was stirred for 30 min at rt. The colour turned from red to yellow upon addition of *m*-CPBA. The reaction was diluted with CH_2Cl_2, and the organic layer was washed with aqueous $NaHCO_3$, $Na_2S_2O_3$ and brine, dried ($MgSO_4$) and concentrated. Purification via flash chromatography (pentane/EtOAc 7:3 to 1:1) afforded 6.1 mg (0.012 mmol, 59%) of the epoxide product as colourless droplets on the vial wall.

^{1}H NMR (400 MHz, $CDCl_3$) δ 7.70 (d, *J* = 8.3 Hz, $1H_{Ts}$), 7.35 – 7.21 (m, $2H_{Ts}$+$5H_{Bn}$), 5.29 (t, *J* = 4.9 Hz, $1H_{olefin}$), 4.65 (d, *J* = 13.5 Hz, $1H_{Bn}$), 4.26 (d, *J* = 13.5 Hz, $1H_{Bn}$), 3.70 (s, $3H_{OMe}$), 3.66 (s, $3H_{OMe}$), 3.02 (d, *J* = 14.2 Hz, $1H_{CH2}$), 2.96 (d, *J* = 14.2 Hz, $1H_{CH2}$), 2.44 (s, $3H_{Ts}$), 2.19 – 1.96 (m, $5H_{CH2}$), 1.48 (dt, *J* = 14.0, 9.1 Hz, $1H_{CH2}$).

^{13}C NMR (126 MHz, $CDCl_3$) δ 171.4, 171.3, 143.8, 135.8, 135.6, 134.8, 131.1, 129.8, 129.6, 128.5, 128.1, 128.1, 68.8, 63.5, 56.6, 55.2, 53.1, 53.0, 38.9, 36.3, 22.1, 21.9, 21.7.

HRMS (ESI) calc. for $C_{27}H_{29}NO_7SNa$ $[M+Na]^+$ 534.1557, found 534.1550.

175: Dimethyl (3a*R,7a*R**)-7-((*N*-benzyl-4-methylphenyl)sulfonamido)-3a,7a-dihydroxy-1,3,3a,4,5,7a-hexahydro-2*H*-indene-2,2-dicarboxylate**



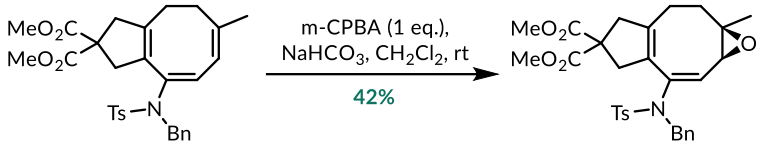
To a solution of diene (10.0 mg, 0.020 mmol) in acetone (0.30 mL) was added NMO·H_2O (6.2 mg, 0.040 mmol, 2.0 eq.) and solution of $K_2OsO_2(OH)_4$ (0.7 mg, 0.002 mmol, 10 mol%) in water (0.10 mL). The reaction mixture was stirred for 4 h at room temperature. Aqueous $Na_2S_2O_3$ and EtOAc were added, and the organic layer was washed with sat. $NaHCO_3$, brine, dried ($MgSO_4$) and concentrated. Purification via flash chromatography (pentane/EtOAc 1:1) afforded the diol product (3.2 mg, 0.006 mmol, 30%) as colourless droplets on the vial wall.

^{1}H NMR (400 MHz, $CDCl_3$) δ 7.69 (d, *J* = 8.3 Hz, 1H_{Ts}), 7.33 – 7.19 (m, 2H_{Ts}+5H_{Bn}), 5.27 (dd, *J* = 5.0, 3.0 Hz, 1H_{olefin}), 4.57 (d, *J* = 14.1 Hz, 1H_{Bn}), 4.41 (d, *J* = 14.1 Hz, 1H_{Bn}), 3.74 (s, 3H_{OMe}), 3.63 (s, 3H_{OMe}), 2.64 (d, *J* = 14.4 Hz, 1$H_{CH2\text{-}a}$), 2.50 – 2.44 (m, 1$H_{CH2\text{-}b}$), 2.44 (s, 3H_{Ts}), 2.31 – 2.19 (m, 1$H_{CH2\text{-}a}$+1$H_{CH2\text{-}c}$), 2.06 – 1.97 (m, 1$H_{CH2\text{-}b}$) 1.95 – 1.86 (m, 1$H_{CH2\text{-}c}$), 1.82 – 1.74 (m, 1$H_{CH2\text{-}d}$), 1.72 – 1.60 (m, 1$H_{CH2\text{-}d}$).

^{13}C NMR (126 MHz, $CDCl_3$) δ 172.8, 144.2, 137.5, 135.7, 135.4, 134.1, 129.9, 129.6, 128.6, 128.6, 128.3, 79.5, 56.7, 55.7, 53.2, 53.1, 44.6, 44.5, 30.5, 22.7, 21.7.

HRMS (ESI) calc. for $C_{27}H_{31}NO_8SNa$ $[M+Na]^+$ 552.1663, found 552.1659.

178: Dimethyl (1a*R,8a*S**,*E*)-7-((*N*-benzyl-4-methylphenyl)sulfonamido)-1a-methyl-1a,2,3,4,6,8a-hexahydro-5*H*-cyclopenta[5,6]cycloocta[1,2-*b*]oxirene-5,5-dicarboxylate**



163 178

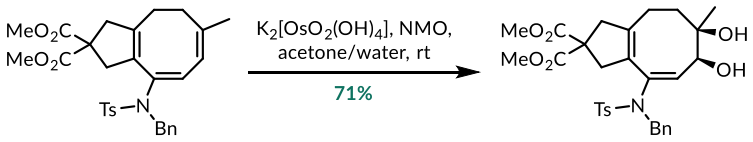
To a solution of triene (20 mg, 0.037 mmol) in CH_2Cl_2 (0.5 mL) was added $NaHCO_3$ (5 mg, 0.056 mmol, 1.5 eq.) and *m*-CPBA (70%, 10 mg, 0.041 mmol, 1.1 eq.). The mixture was stirred overnight at rt, diluted with CH_2Cl_2, and washed with aqueous $Na_2S_2O_3$ (aq., sat.), $NaHCO_3$ (aq., sat.), and brine, dried ($MgSO_4$) and concentrated. Purification via flash chromatography (pentane/EtOAc 7:3) afforded the epoxide product (8.7 mg, 0.016 mmol, 42%) as colourless droplets on the vial wall.

^{1}H NMR (400 MHz, $CDCl_3$) δ 7.76 (d, *J* = 8.2 Hz, $2H_{Ts}$), 7.32 (d, *J* = 8.2 Hz, $2H_{Ts}$), 7.25 – 7.18 (m, $3H_{Bn}$), 7.14 – 7.07 (m, $2H_{Bn}$), 5.54 (s, $1H_{olefin}$), 4.86 (d, *J* = 15.0 Hz, $1H_{Bn}$), 4.18 (d, *J* = 15.0 Hz, $1H_{Bn}$), 3.76 (s, $3H_{OMe}$), 3.70 (s, $3H_{OMe}$), 3.24 (s, $1H_{epoxide}$), 2.98 – 2.84 (m, $2H_{CH2\text{-}a}$), 2.81 (d, *J* = 16.0 Hz, $1H_{CH2\text{-}b}$), 2.56 (d, *J* = 16.0 Hz, $1H_{CH2\text{-}b}$), 2.45 (s, $3H_{Ts}$), 1.89 – 1.84 (m, $2H_{CH2\text{-}c}$), 1.49 (dt, *J* = 13.8, 4.4 Hz, $1H_{CH2\text{-}d}$), 1.13 (s, $3H_{Me}$), 1.06 – 0.96 (m, $1H_{CH2\text{-}d}$).

^{13}C NMR (101 MHz, $CDCl_3$) δ 172.3, 172.1, 143.9, 137.6, 136.3, 129.8, 128.7, 128.5, 127.9, 127.8, 127.7, 124.8, 61.0, 59.9, 57.2, 53.1, 53.0, 51.8, 47.2, 43.8, 29.8, 27.3, 21.7.

HRMS (ESI) calc. for $C_{30}H_{34}NO_7S$ $[M+H]^+$ 552.2050, found 552.2052.

177: Dimethyl (6*R,7*S**,*E*)-9-((*N*-benzyl-4-methylphenyl)sulfonamido)-6,7-dihydroxy-6-methyl-1,3,4,5,6,7-hexahydro-2*H*-cyclopenta[8]annulene-2,2-dicarboxylate**



163 177

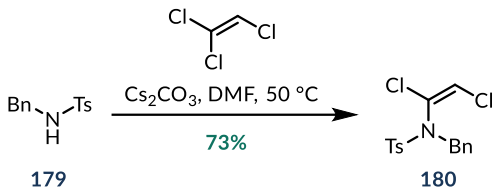
To a solution of triene (10.0 mg, 0.019 mmol) in acetone (0.30 mL) was added NMO·H_2O (3.4 mg, 0.040 mmol, 2.0 eq.) and a solution of $K_2OsO_2(OH)_4$ (0.7 mg, 0.002 mmol, 10 mol%) in water (0.10 mL). The reaction mixture was stirred at rt, 3 h. Aqueous $Na_2S_2O_3$ and EtOAc were added, and the organic layer was washed with sat. $NaHCO_3$, brine, dried ($MgSO_4$) and concentrated. Purification via flash chromatography (pentane/EtOAc 1:1) afforded the diol product (7.5 mg, 0.013 mmol, 71%) as colourless droplets on the vial wall.

^{1}H NMR (400 MHz, $CDCl_3$) δ 7.77 (d, *J* = 8.2 Hz, 1H_{Ts}), 7.35 – 7.14 (m, 2H_{Ts}+5H_{Bn}), 5.41 (d, *J* = 7.6 Hz, 1H_{olefin}), 4.95 (d, *J* = 14.4 Hz, 1H_{Bn}), 4.15 (d, *J* = 14.4 Hz, 1H_{Bn}), 3.93 (d, *J* = 7.6 Hz, 1$H_{CH\text{-}OH}$), 3.75 (s, 3H_{OMe}), 3.67 (s, 3H_{OMe}), 3.01 – 2.91 (m, 1$H_{CH2\text{-}a}$+1$H_{CH2\text{-}b}$), 2.76 (d, *J* = 17.1 Hz, 1$H_{CH2\text{-}a}$), 2.44 (s, 3H_{Ts}), 2.39 – 2.31 (m, 1$H_{CH2\text{-}b}$), 2.07 – 1.90 (m, 2$H_{CH2\text{-}c}$), 1.25 – 1.20 (m, 2$H_{CH2\text{-}d}$), 1.19 (s, 3H_{Me}).

^{13}C NMR (126 MHz, $CDCl_3$) δ 172.8, 144.2, 137.5, 135.7, 135.4, 134.1, 129.9, 129.6, 128.6, 128.6, 128.3, 79.5, 56.7, 55.7, 53.2, 53.1, 44.6, 44.5, 30.5, 22.7, 21.7.

HRMS (ESI) calc. for $C_{27}H_{31}NO_8SNa$ $[M+Na]^+$ 552.1663, found 552.1659.

180: (*E*)-*N*-Benzyl-*N*-(1,2-dichlorovinyl)-4-methylbenzenesulfonamide



179 180

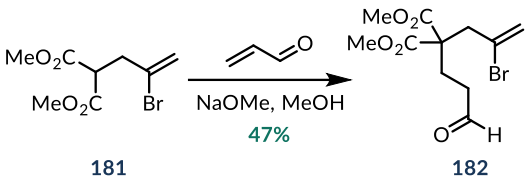
Prepared according to a literature procedure.[80] To a stirred suspension of *N*-tosylbenzylamine (1.50 g, 5.74 mmol, 1.0 eq.) and powdered Cs_2CO_3 (2.81 g, 8.61 mmol, 1.5 eq.) in DMF (4.3 mL), at 50 °C was added trichloroethylene (0.57 mL, 6.31 mmol, 1.1 eq.) dropwise over 10 min. The resulting mixture was stirred at 50 °C for 1–2 h. The mixture was cooled to room temperature, then partitioned between EtOAc and H_2O. The organic layer was separated and further washed with water (×2) and brine. The organic layer was then dried ($MgSO_4$), filtered and concentrated. Recrystallisation from EtOAc (10–20 mL) afforded the enamide product (1.50 g, 4.20 mmol, 73%) as white crystals.

^{1}H NMR (400 MHz, $CDCl_3$) δ 7.86 (d, *J* = 8.3 Hz, $2H_{Ts}$), 7.36 (d, *J* = 8.3 Hz, $2H_{Ts}$), 7.34 – 7.27 (m, $5H_{Bn}$), 6.27 (s, 1H), 5.08 – 3.69 (very br s, $2H_{Bn}$) 2.47 (s, $3H_{Ts}$).

^{13}C NMR (101 MHz, $CDCl_3$) δ 144.7, 135.2, 133.4, 129.8, 129.4, 128.5, 128.5, 128.4, 121.7, 77.2, 51.8, 21.7.

Data in agreement with the literature values.[80]

182: Dimethyl 2-(2-bromoallyl)-2-(3-oxopropyl)malonate



181 182

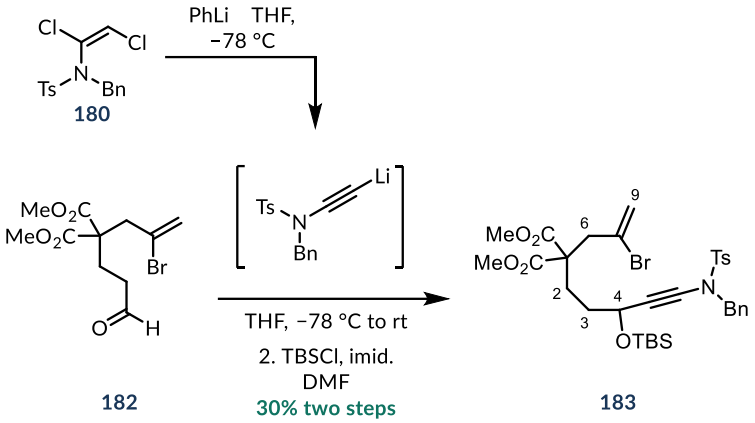
A modified literature protocol for acrolein conjugate addition was applied.[133] To a mixture of acrolein (120 µL, 1.78 mmol, 1.0 eq.) and bromoallyl malonate (448 mg, 1.78 mmol, 1.0 eq.) in MeOH (5.2 mL) at room temperature was slowly added NaOMe (25% wt solution in MeOH, 82 µL, 0.36 mmol, 0.2 eq.). The resulting mixture was stirred for 4 h, then the solvent was evaporated under reduced pressure. The residue was dissolved in Et_2O and washed with water, brine, dried over $MgSO_4$, filtered and concentrated under reduced pressure. The residue was purified via flash column chromatography (pentane/EtOAc 7:3) to give the desired product (259 mg, 0.84 mmol, 47%) as a viscous liquid.

^{1}H NMR (400 MHz, $CDCl_3$) δ 9.73 (t, *J* = 1.3 Hz, 1H), 5.67 (dt, *J* = 1.8, 0.9 Hz, 1H), 5.60 (d, *J* = 1.8 Hz, 1H), 3.74 (s, 6H), 3.18 (d, *J* = 0.9 Hz, 2H), 2.52–2.46 (m, 2H), 2.37–2.27 (m, 2H).

^{13}C NMR (101 MHz, $CDCl_3$) δ 200.3, 170.5, 126.6, 122.3, 56.3, 52.8, 44.0, 39.1, 24.4.

Data in agreement with the literature values.[133]

183: Dimethyl 2-(5-((*N*-benzyl-4-methylphenyl)sulfonamido)-3-((*tert*-butyldimethylsilyl)oxy)-pent-4-yn-1-yl)-2-(2-bromoallyl)malonate



Synthesized according to the protocol for ynamide synthesis developed by Anderson et al.[80] To an oven dried, argon flushed flask was added 1,2-dichloroenamide (116 mg, 0.33 mmol, 2.5 eq.) and anhydrous THF (1.1 mL), and the mixture was cooled to −78 °C whilst stirring. A solution of phenyllithium (1.9 M solution in dibutyl ether, 0.34 mL, 5.0 eq.) was then added dropwise, and the mixture was left to stir at −78 °C for 15 min. After complete conversion to the lithiated ynamide (as confirmed by TLC consumption of the dichloroenamide), a solution of the aldehyde (40 mg, 0.13 mmol, 1.0 eq.) in anhydrous THF (0.6 mL) was added at −78 °C and the mixture was stirred for 1 h. The reaction was quenched with NH_4Cl (at −78 °C, sat., aq.), then warmed to room temperature and extracted with Et_2O. The organic extract was washed with brine, dried ($MgSO_4$) and concentrated. The crude product was used directly in the next step.

To a stirred solution of the crude alcohol in DMF (1 mL) at room temperature was added imidazole (14 mg, 0.19 mmol, 1.5 eq.) and TBSCl (20 mg, 0.13 mmol, 1.0 eq.), and the mixture was stirred for 1 h until complete (as monitored by TLC). Water and Et_2O were added, then the organic layer was separated and washed with brine, dried ($MgSO_4$) and concentrated. Since the ynamide impurity (resulting from protonation of excess lithiated ynamide from previous step) has a similar R_f value to the product, it was removed by washing the crude product with pentane several times (until the yellow colour faded). A solid, white impurity that is not soluble in

pentane remains as a precipitate. The pentane washes were concentrated, and the residue was purified via flash chromatography (pentane/EtOAc 85:15) to afforded the desired product (28 mg, 0.04 mmol, 30% over two steps) as an oil.

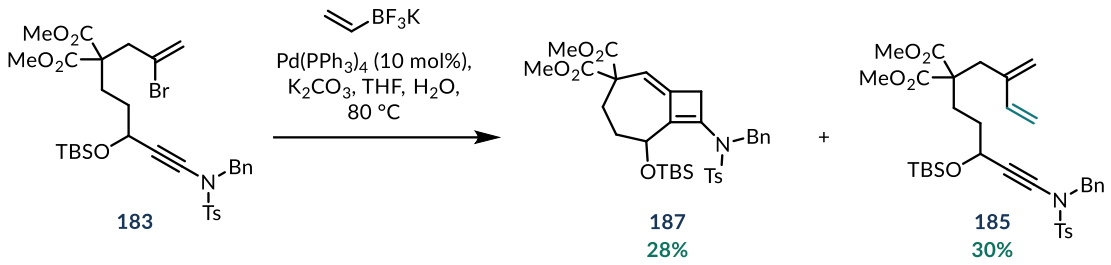
^{1}H NMR (400 MHz, d_6-acetone) δ 7.84 (d, *J* = 8.3 Hz, 2H), 7.49 (d, *J* = 8.3 Hz, 2H), 7.40–7.24 (m, 5H), 5.81–5.69 (m, 1H), 5.56 (d, *J* = 1. Hz, 1H), 4.54 (s, 1H), 4.52 (s, 1H), 4.50–4.46 (m, 1H), 3.72 (s, 3H), 3.71 (s, 3H), 3.13 (s, 2H), 2.48 (s, 3H), 2.15–2.09 (m, 2H), 1.54–1.42 (m, 2H), 0.83 (s, 9H), 0.01 (s, 3H), −0.04 (s, 3H).

^{13}C NMR (101 MHz, d_6-acetone) δ 170.4, 144.9, 135.1, 134.9, 130.0, 128.7, 128.5, 128.2, 127.7, 126.9, 122.1, 78.2, 72.0, 62.5, 56.4, 55.4, 52.1, 52.1, 42.9, 33.3, 27.2, 25.3, 20.7, 17.8, −5.3, −5.9.

HRMS (ESI) calc. for $C_{33}H_{44}{}^{79}BrNO_7SSiNa$ $[M+Na]^+$ 728.1683, found 728.1679.

187: Dimethyl 8-((*N*-benzyl-4-methylphenyl)sulfonamido)-6-((*tert*-butyldimethylslyl)-oxy)bicyclo[5.2.0]nona-1,7-diene-3,3-dicarboxylate

185: Dimethyl 2-(5-((*N*-benzyl-4-methylphenyl)sulfonamido)-3-((*tert*-butyldimethylsilyl)oxy)pent-4-yn-1-yl)-2-(2-methylenebut-3-en-1-yl)malonate

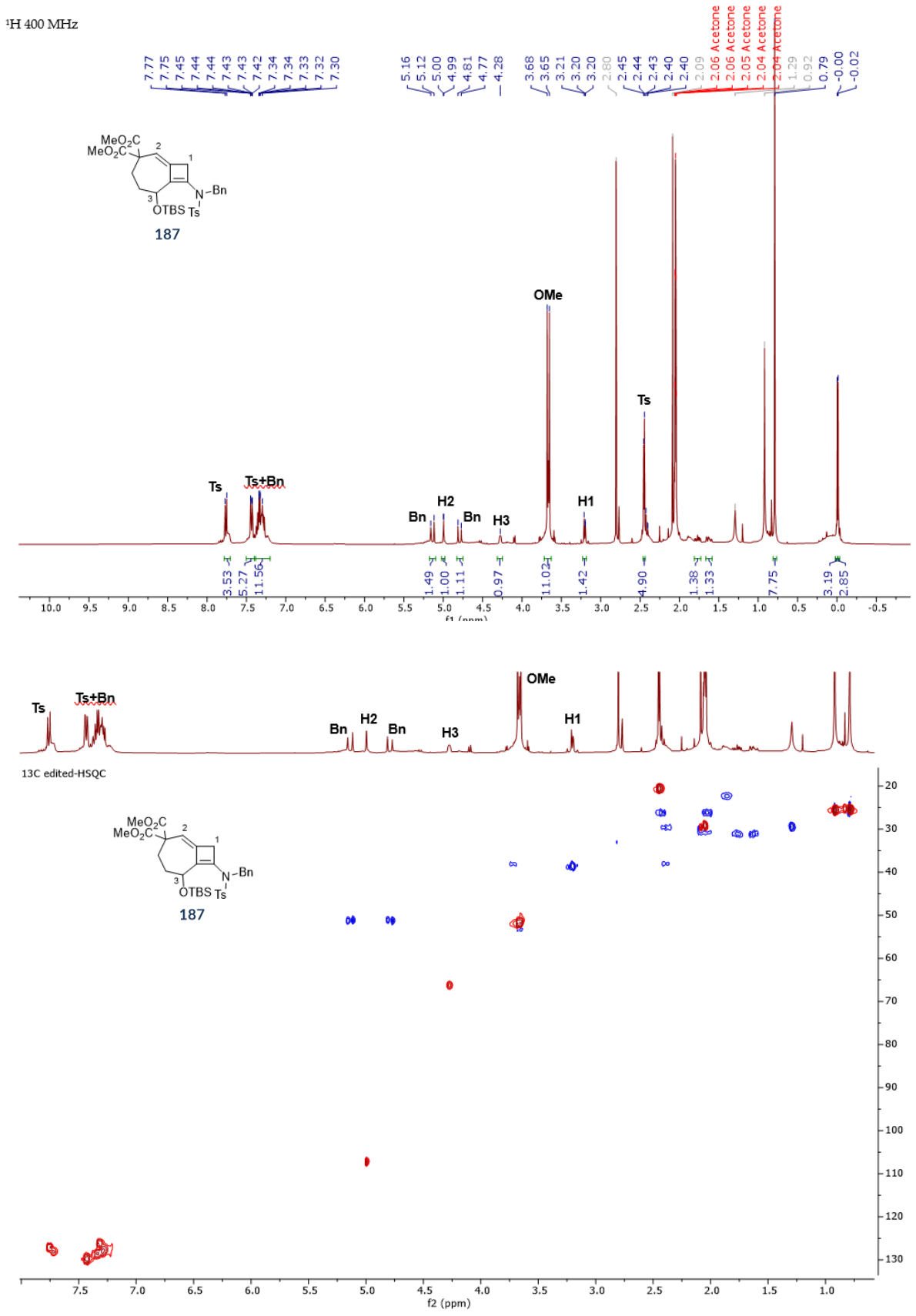


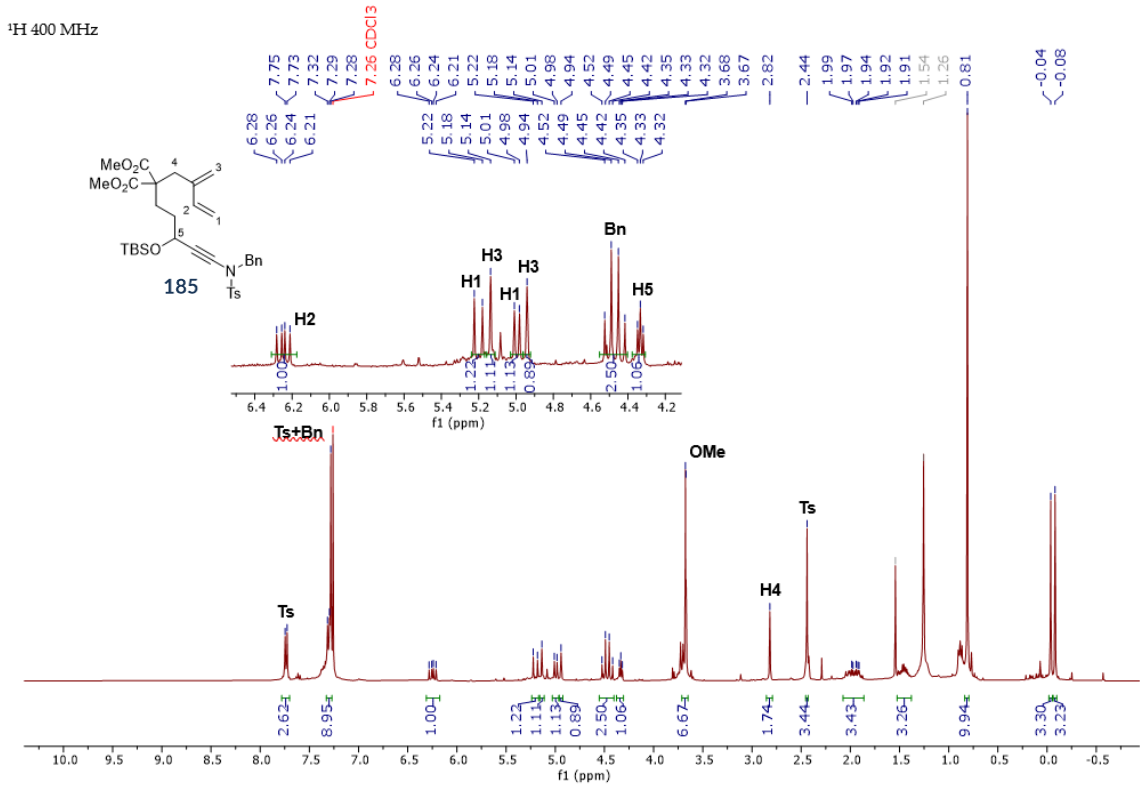
To a vial loaded with bromoynamide (11 mg, 0.016 mmol, 1.0 eq.) and potassium vinyltrifluoroborate 20 (3.1 mg, 0.023 mmol, 1.5 eq.) was added dry and degassed THF (0.40 mL), degassed K_2CO_3 solution in water (6.4 mg in 40 µL water, 0.047 mmol, 3.0 eq.) and $Pd(PPh_3)_4$ (1.8 mg, 0.002 mmol, 10 mol%). The mixture was further degassed by bubbling N_2, then sealed and heated overnight at 80 °C. After cooling to rt, water and EtOAc were added, the organic layer was separated and washed with brine, dried over $MgSO_4$ and concentrated. Purification via flash chromatography (pentane/EtOAc 7:3) afforded **187** (2.8 mg, 0.005 mmol, 28%) and **185** (3.1 mg, 0.005 mmol, 30%), both as colourless droplets on the vial wall.

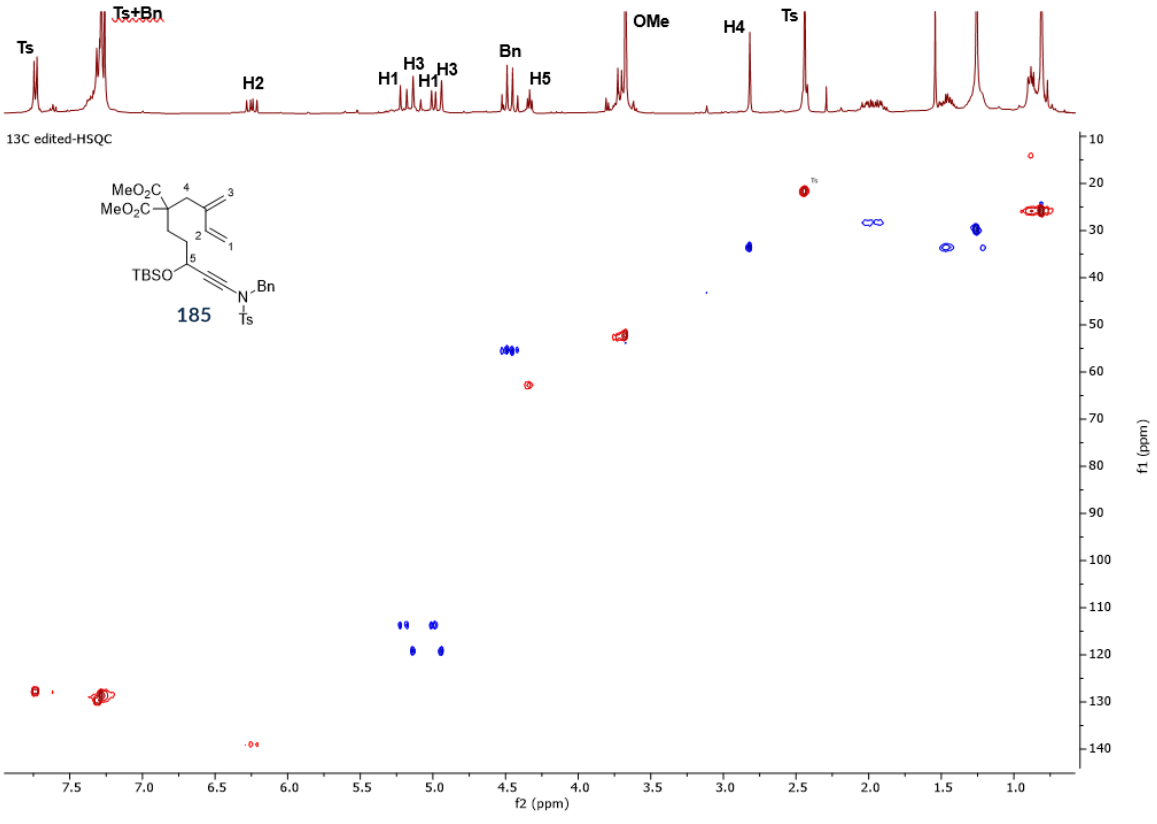
187: ^{1}H NMR (400 MHz, Acetone) δ 7.76 (d, *J* = 8.4 Hz, 2H), 7.52–7.38 (m, 2H), 7.40–7.24 (m, 5H), 5.14 (d, *J* = 16.8 Hz, 1H), 5.00 (s, 1H), 4.79 (d, *J* = 16.8 Hz, 1H), 4.28 (br s, 1H), 3.68 (s, 3H), 3.65 (s, 3H), 3.23–3.18 (m, 2H), 2.44 (s, 3H), 2.44–2.40 (m, 1H), 2.08–2.02 (m, 1H), 1.82–1.71 (m, 1H), 1.68–1.58 (m, 1H), 0.79 (s, 9H), −0.00 (s, 3H), −0.02 (s, 3H).

185: ^{1}H NMR (400 MHz, $CDCl_3$) δ 7.74 (d, *J* = 8.3 Hz, 2H), 7.34–7.27 (m, 5H+2H), 6.25 (dd, *J* = 17.5, 10.9 Hz, 1H), 5.20 (d, *J* = 17.5 Hz, 1H), 5.14 (s, 1H), 5.00 (d, *J* = 10.9 Hz, 1H), 4.94 (s, 1H), 4.51 (d, *J* = 14.0 Hz, 1H), 4.43 (d, *J* = 14.0 Hz, 1H), 4.33 (t, *J* = 6.1 Hz, 1H), 3.68 (s, 3H), 3.67 (s, 3H), 2.82 (s, 2H), 2.44 (s, 3H), 2.07–1.85 (m, 2H), 1.54–1.39 (m, 2H), 0.81 (s, 9H), −0.04 (s, 3H), −0.08 (s, 3H).

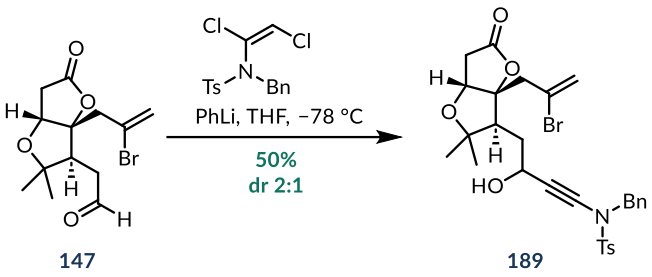
Detailed structural assignment is provided below:




¹H 400 MHz
MeO2C
MeO2C
TBSO
N
Bn
Ts
185
H2
H1
H3
H3
H1
H5
Bn
Ts+Bn
Ts
OMe
H4
Ts
f1 (ppm)


Ts+Bn
Ts
H2
H1
H3
H1
H3
Bn
H5
OMe
H4
Ts
13C edited-HSQC
MeO2C
MeO2C
TBSO
N
Bn
Ts
185
f2 (ppm)
f1 (ppm)

189: N-Benzyl-N-(4-((3*S*,3a*R*,6a*R*)-3a-(2-bromoallyl)-2,2-dimethyl-5-oxohexahydrofuro[3,2-*b*]furan-3-yl)-3-hydroxybut-1-yn-1-yl)-4-methylbenzenesulfonamide



147 189

To an oven dried, argon flushed flask was added 1,2-dichloroenamide (18 mg, 0.051 mmol, 3.0 eq.) and anhydrous THF (0.5 mL), and the mixture was cooled to −78 °C. A solution of phenyllithium (1.9 M solution in dibutyl ether, 25 µL, 2.8 eq.) was then added dropwise, and the mixture was left to stir at −78 °C for 15 min. After almost complete conversion to the lithiated ynamide (the 1,2-dichloroenamide is in excess, so a small amount remains), the aldehyde (5.4 mg, 0.017 mmol) in anhydrous THF (0.5 mL) was added at −78 °C and stirred for 1 h. The reaction was quenched by the addition of NH_4Cl (at −78 °C, sat., aq.), then warmed to room temperature and extracted with Et_2O. The organic extract was washed with brine, dried ($MgSO_4$) and concentrated. The product was purified via flash chromatography to afford 5.1 mg (0.008 mmol, 50%) of oily product as a 2:1 mixture of diastereomeric alcohols.

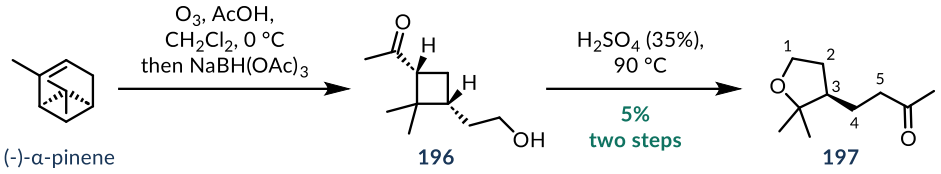
^{1}H NMR (500 MHz, $CDCl_3$) δ 7.78 – 7.74 (m, $2H_{Ts}$), 7.39 – 7.25 (m, $2H_{Ts}$+$5H_{Bn}$), 5.77 – 5.63 (m, $2H_{CH2\text{-}olefin}$), 4.83 – 4.79 (m, $1H_{CH\text{-}OH}$), 4.58 – 4.54 (m, $1H_{CH\text{-}bridgehead}$), 4.51 – 4.43 (m, $2H_{CH2\text{-}a}$), 3.37 – 3.25 (m, $1H_{CH2\text{-}allyl}$), 2.93 – 2.82 (m, $1H_{CH2\text{-}b}$), 2.71 – 2.59 (m, $1H_{CH2\text{-}b}$), 2.59 – 2.52 (m, $1H_{CH2\text{-}allyl}$), 2.46 (s, $3H_{Ts}$), 2.29 (dd, *J* = 9.6, 3.9 Hz, $1H_{CH}$), 1.94 (d, *J* = 5.6 Hz, $1H_{CH\text{-}OH}$), 1.74 – 1.67 (m, $1H_{CH2\text{-}c}$), 1.46 – 1.38 (m, $1H_{CH2\text{-}c}$), 1.13 (s, $3H_{Me}$), 1.02 (s, $3H_{Me}$).

HRMS (ESI) calc. for $C_{29}H_{33}{}^{79}BrNO_6S$ $[M+H]^+$ 602.1207, found 602.1207.

7.5 Procedures and characterisation from Chapter 3

197: (*R*)-4-(2,2-dimethyltetrahydrofuran-3-yl)butan-2-one

196: 1-((1*R*,3*R*)-3-(2-hydroxyethyl)-2,2-dimethylcyclobutyl)ethan-1-one



This is not a preparative procedure. The title compound was prepared by following the literature procedure.[84] A solution of (−)-α-pinene (1.95 g, 14.3 mmol) and glacial acetic acid (1.64 mL, 28.6 mmol, 2.0 eq.) in CH_2Cl_2 (40 mL) was stirred at 0 °C and ozone was bubbled for 1 h. The reaction mixture was purged with nitrogen and diluted with CH_2Cl_2 (20 mL). TLC analysis showed complete consumption of starting material. This solution was cannulated into the solution of $NaHB(OAc)_3$ (14 g, 66 mmol, 4.6 eq.) in CH_2Cl_2 (120 mL) at 0 °C and stirred for 3 h at rt. 1 M NaOH was added carefully, and the organic layer was separated, washed with sat. NH_4Cl, brine, dried ($MgSO_4$) and concentrated.

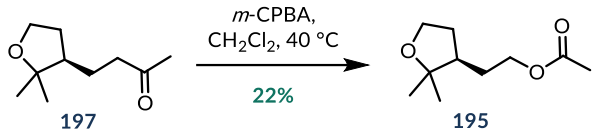
To this was added aq. H_2SO_4 (35%, 19 mL, 6.0 eq.) and the mixture was heated at 92 °C for 50 min. Solid Na_2CO_3 was added carefully until the acid was neutralised. Et_2O was added, and the organic layer was separated, washed with brine, dried ($MgSO_4$) and concentrated. The desired product was difficult to separate and only pure fractions were taken (pent/EA 9:1 to 1:1) to afford 109 mg (5%) of yellow oil. In addition, traces of compound **198** were also isolated and characterised separately, as described in the procedure when obtained as the main product.

^{1}H NMR (500 MHz, $CDCl_3$) δ 3.83 (td, *J* = 8.3, 3.1 Hz, $1H_{CH2\text{-}1}$), 3.74 (m, $1H_{CH2\text{-}1}$), 2.56 – 2.38 (m, $2H_{CH2\text{-}5}$), 2.15 (s, $3H_{Me\text{-}ketone}$), 2.11 – 2.01 (m, $1H_{CH2\text{-}2}$), 1.75 – 1.64 (m, $1H_{CH2\text{-}4}$+$1H_{CH\text{-}3}$), 1.64 – 1.53 (m, $1H_{CH2\text{-}2}$), 1.48 – 1.35 (m, $1H_{CH2\text{-}4}$), 1.23 (s, $3H_{Me}$), 1.01 (s, $3H_{Me}$).

^{13}C NMR (126 MHz, $CDCl_3$) δ 208.6, 81.7, 64.9, 48.2, 43.1, 31.9, 30.1, 27.6, 24.4, 22.0.

Data in agreement with the literature values.[84]

195: (*S*)-2-(2,2-dimethyltetrahydrofuran-3-yl)ethyl acetate



To a solution of ketone (109 mg, 0.64 mmol) in CH_2Cl_2 (1.4 mL) was added m-CPBA (77 mg, 0.49 mmol, 0.7 eq.) and the mixture was refluxed for 92 h. During this time, after each day, an additional portion of m-CPBA (44 mg, 0.26 mmol, 0.4 eq.) was added. As the reaction showed no further progress by TLC analysis, Et_2O was added, and the organic layer was separated, washed with sat. $NaHCO_3$, aq. $Na_2S_2O_3$, brine, dried ($MgSO_4$) and concentrated. Purification by flash chromatography (pent/EtOAc 8:2) afforded 26 mg (22%) of oily product and 30 mg (28%) of the recovered starting material.

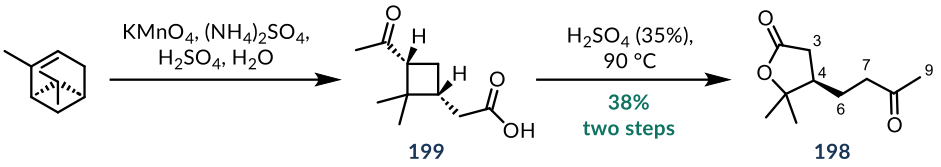
^{1}H NMR (500 MHz, $CDCl_3$) δ 4.15 – 4.04 (m, 2H), 3.83 (td, *J* = 8.6, 3.2 Hz, 1H), 3.75 (dd, *J* = 16.1, 8.6 Hz, 1H), 2.14 – 2.07 (m, 1H), 2.04 (s, 3H), 1.83 – 1.70 (m, 2H), 1.69 – 1.59 (m, 1H), 1.52 – 1.44 (m, 1H), 1.23 (s, 3H), 0.99 (s, 3H).

^{13}C NMR (126 MHz, $CDCl_3$) δ 171.2, 81.6, 65.0, 63.9, 45.4, 31.9, 29.6, 27.5, 22.1, 21.1.

Data in agreement with the literature values.[85]

198: (*R*)-5,5-Dimethyl-4-(3-oxobutyl)dihydrofuran-2(3*H*)-one

199: 2-((1*R*,3*R*)-3-Acetyl-2,2-dimethylcyclobutyl)acetic acid



Following a literature procedure,[86] to a two neck round bottom flask equipped with thermometer was placed crushed ice (110 g), powdered potassium permanganate (12 g, 0.73 mmol, 2.0 eq.), ammonium sulfate (2.4 g, 0.18 mmol, 0.5 eq.) and water (7 mL). With vigorous stirring, (−)-α-pinene (5.8 g, 5.8 mL, 0.37 mmol; 97% ee) was added. The reaction temperature was kept below 15 °C by cooling with an ice bath. After complete change of the pink colour to brown (4 h), the mixture was acidified with sulfuric acid solution (4.5 mL conc. H_2SO_4 in 8.6 mL water) and sodium bisulfite (10 g) was added while keeping the temperature below 15 °C. The brown precipitate of manganese dioxide dissolves. Mixture was extracted with ether (×3-4), washed with brine, dried ($MgSO_4$) and concentrated to give 4.99 g of solid product.

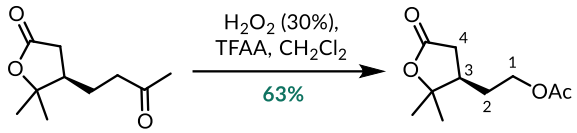
To a crude product from previous step was added 35% solution of H_2SO_4 in water (25 mL) and vigorously stirred at 92 °C for 1-2 h. After cooling, the mixture was neutralized with solid Na_2CO_3 and extracted with ether. Organic layer was washed with brine, dried ($MgSO_4$), concentrated and purified by flash chromatography (pentane/EtOAc 7:3 to 1:1) to afford 1.88 g (38%) of brown solid.

^{1}H NMR (400 MHz, $CDCl_3$) δ 2.64 – 2.53 (m, $1H_3$), 2.51 – 2.37 (m, $2H_7$), 2.34 – 2.22 (m, $1H_3$), 2.22 – 2.18 (m, $1H_4$), 2.16 (s, $3H_9$), 1.86 – 1.74 (m, $1H_6$), 1.61 – 1.47 (m, $1H_6$), 1.44 (s, $3H_{Me}$), 1.26 (s, $3H_{Me}$).

^{13}C NMR (101 MHz, $CDCl_3$) δ 207.3, 175.3, 86.7, 45.3, 41.9, 34.9, 30.2, 27.5, 23.3, 22.0.

Data in agreement with the literature values.[86]

200: (*R*)-2-(2,2-Dimethyl-5-oxotetrahydrofuran-3-yl)ethyl acetate



198 200

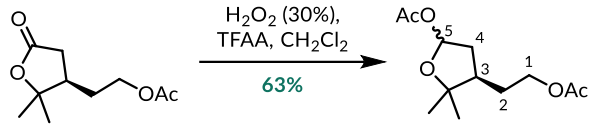
To H_2O_2 (30% aq., 12.3 mL, 120 mmol, 37 eq.) in CH_2Cl_2 (76 mL) at 0 °C was added TFAA (70 mL, 490 mmol, 150 eq.) dropwise through separatory funnel. After TFAA addition was done, substrate (600 mg, 3.3 mmol) in CH_2Cl_2 (51 mL) was added dropwise at 0 °C (although no noticeable exotherm), and mixture was stirred overnight at rt. The mixture was neutralized with solid Na_2CO_3 and extracted with ether. Organic layer was washed with brine, dried ($MgSO_4$), concentrated and purified by flash chromatography (pentane/EtOAc 1:1) to afford 408 mg (63%) of oily product.

^{1}H NMR (400 MHz, $CDCl_3$) δ 4.08 (td, *J* = 6.3, 1.8 Hz, $2H_1$), 2.66 (d, *J* = 9.2 Hz, $1H_4$), 2.40 – 2.24 (m, $1H_3$+$1H_4$), 2.05 (s, $1H_{Ac}$), 1.89 – 1.76 (m, $1H_2$), 1.69 – 1.57 (m, $1H_2$), 1.44 (s, $3H_{Me}$), 1.25 (s, $3H_{Me}$).

^{13}C NMR (101 MHz, $CDCl_3$) δ 175.3, 170.9, 86.4, 62.9, 43.1, 35.0, 28.8, 27.4, 22.0, 20.9.

Data in agreement with the literature values.[134]

201: 2-((3*R*)-5-Acetoxy-2,2-dimethyltetrahydrofuran-3-yl)ethyl acetate



200 201

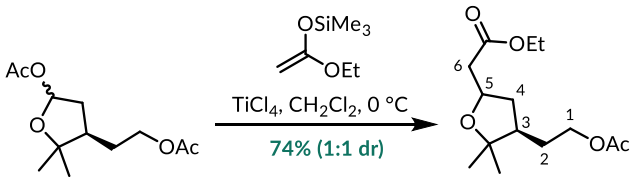
To a solution of substrate (100 mg, 0.50 mmol) in dry CH_2Cl_2 (12 mL) is added solution of DIBAL in CH_2Cl_2 (0.25 M, 5.0 mL, 1.25 mmol, 2.5 eq.) over 2 h at < −90 °C. After DIBAL addition is completed, only traces of starting material are visible on TLC. At the same temperature, pyridine (2.0 mL, 25 mmol, 50 eq.) and Ac_2O (1.4 mL, 15 mmol, 30 eq.) are added and the reaction mixture is left to warm to rt and stirred overnight. Several drops of MeOH are added and mixture concentrated to minimum volume (~2 mL) and purified twice by flash chromatography (pentane/EtOAc 7:3) to afford 48 mg (39%, dr 2:1) as clear oil.

Major: **^{1}H NMR** (400 MHz, $CDCl_3$) δ 6.31 – 6.12 (m, $1H_5$), 4.15 – 4.08 (m, $2H_1$), 2.20 – 2.13 (m, $1H_4$+$1H_3$), 2.07 (s, $3H_{Ac}$), 2.04 (s, $3H_{Ac}$), 1.98 – 1.85 (m, $1H_4$), 1.82 – 1.73 (m, $1H_2$), 1.57 – 1.52 (m, $1H_2$), 1.36 (s, $3H_{Me}$), 1.06 (s, $3H_{Me}$).

Minor: **^{1}H NMR** (400 MHz, $CDCl_3$) δ 6.31 – 6.12 (m, $1H_5$), 4.15 – 4.07 (m, $2H_1$), 2.59 – 2.58 (m, $1H_4$), 2.06 (s, $3H_{Ac}$), 2.04 (s, $3H_{Ac}$), 1.98 – 1.85 (m, $1H_3$), 1.82 – 1.73 (m, $1H_4$+$1H_2$), 1.57 – 1.52 (m, $1H_2$), 1.29 (s, $3H_{Me}$), 1.18 (s, $3H_{Me}$).

^{13}C NMR (101 MHz, $CDCl_3$) δ 171.1, 170.7, 97.7, 97.4, 85.6, 84.9, 63.7, 63.5, 45.2, 42.5, 38.4, 38.3, 29.3, 29.2, 28.9, 27.7, 23.4, 22.9, 21.6, 21.6, 21.1, 21.1.

202: Ethyl 2-((4*R*)-4-(2-acetoxyethyl)-5,5-dimethyltetrahydrofuran-2-yl)acetate



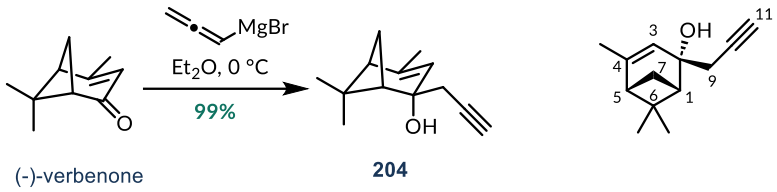
201 202

To a solution of substrate (47 mg, 0.19 mmol) in dry CH_2Cl_2 (5.0 mL) under nitrogen atmosphere at 0 °C was added $TiCl_4$ (two drops, solution changes colour to yellow upon addition of $TiCl_4$) and the mixture was stirred at 0 °C for 1-2 h. $NaHCO_3$ solution was added, and the mixture was extracted with ether, washed with brine, dried ($MgSO_4$) and concentrated. Purification by flash chromatography (pentane/EtOAc 7:3) afforded 41 mg (77%, dr ~1:1) of clear oil.

^{1}H NMR (400 MHz, $CDCl_3$) δ 4.45 – 4.33 (m, 0.5$H_{I,5}$), 4.31 – 4.24 (m, 0.5$H_{II,5}$), 4.18 – 3.98 (m, 2H_1+2H_{Et}), 2.69 – 2.52 (m, 1H_6), 2.47 – 2.33 (m, 1H_6), 2.31 – 2.21 (m, 0.25$H_{II,4}$), 2.05 (s, 3H_{Ac}), 2.02 – 1.80 (m, 1$H_{I,4}$+1H_3), 1.79 – 1.65 (m, 1H_2), 1.57 – 1.36 (m, 1H_2), 1.24 (s, 3H_{Me}+3H_{Et}), 1.03 (s, 1.5$H_{I/II,Me}$), 1.01 (s, 1.5$H_{I/II,Me}$).

^{13}C NMR (101 MHz, $CDCl_3$) δ 171.36, 171.33, 171.15, 82.78, 82.33, 73.39, 72.14, 63.84, 63.77, 60.53, 60.50, 46.26, 44.47, 42.17, 41.99, 38.15, 36.88, 29.83, 29.49, 29.26, 28.26, 27.86, 24.49, 21.61, 21.10, 14.34.

204: (1*S*,2*S*,5*S*)-4,6,6-Trimethyl-2-(prop-2-yn-1-yl)bicyclo[3.1.1]hept-3-en-2-ol



Preparation of the Grignard reagent:[135] A two neck round bottom flask fitted with a condenser was charged with magnesium turnings (1.51 g, 62 mmol, 1.2 eq.), dry ether (25 mL) and $HgCl_2$ (64 mg, 0.45 mol%). The suspension was stirred for 30 min at ambient temperature before it was cooled to 0 °C. A small portion of a solution of propargyl bromide was added to initiate the reaction. Once initiated (20 min, 0 to 15 °C, becomes cloudy-white), the mixture was cooled to 0 °C and the remaining propargyl bromide (5.6 mL in total, 52 mmol, 80% soln. in toluene) was added dropwise over 30 min. After stirring for 1-2 h at 0 °C, the pale grey/green mixture was formed (1.69 M, titrated with I_2, LiCl in THF) and kept in an ice-bath and used directly throughout the day.

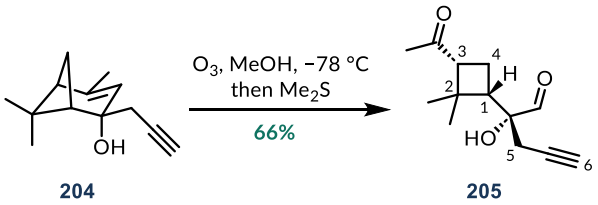
To a solution of (-)-verbenone (4.60 g, 31 mmol, 1.0 eq.) in dry Et_2O (160 mL) was added the Grignard reagent solution (1.69 M, 20 mL, 34 mmol, 1.1 eq.) dropwise at 0 °C over 30-45 min and stirred 15 min at the same temperature. The reaction was quenched with sat. NH_4Cl and extracted with Et_2O. Ether extract was washed with brine, dried ($MgSO_4$) and concentrated to afford 5.78 g (99%) of clean oily product.

^{1}H NMR (400 MHz, $CDCl_3$) δ 5.36 – 5.28 (m, $1H_3$) 2.54 – 2.40 (m, $2H_9$+$1H_7$), 2.28 (td, *J* = 5.9, 2.1 Hz, $1H_{1/5}$), 2.11 (s, $1H_{OH}$), 2.08 (t, *J* = 2.7 Hz, $1H_{11}$), 2.02 – 1.98 (m, $1H_{1/5}$), 1.74 (d, *J* = 1.6 Hz, $3H_{4\text{-}Me}$), 1.38 (s, $3H_{6\text{-}Me}$), 1.34 (d, *J* = 9.4 Hz, $1H_7$), 1.10 (s, $3H_{6\text{-}Me}$).

^{13}C NMR (101 MHz, $CDCl_3$) δ 147.9, 120.9, 80.8, 75.9, 71.2, 51.2, 48.2, 42.9, 35.8, 31.4, 27.3, 23.6, 22.8.

HRMS (ESI) calc. for $C_{13}H_{20}O$ $[M+H]^+$ 191.1430, found 191.1426.

205: (*R*)-2-((1*S*,3*R*)-3-Acetyl-2,2-dimethylcyclobutyl)-2-hydroxypent-4-ynal



204 205

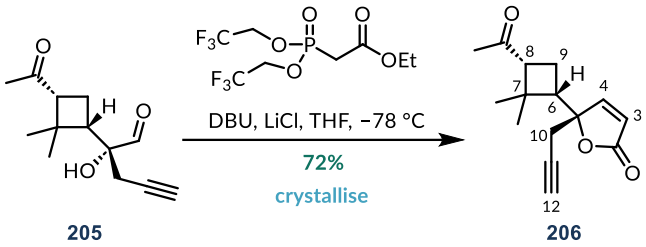
A solution of alkene (850 mg, 4.5 mmol) in MeOH (74 mL), with Sudan III added as an indicator, was cooled to -78 °C and ozone was bubbled until solution turned colourless (15 min). The mixture was purged with O_2 (10 min) and then with N_2 (10 min). Me_2S (1.2 mL, 16 mmol, 3.5 eq.) was added and the mixture left to warm to rt and stirred overnight. Evaporation of volatiles afforded a crude oily mixture containing 655 mg (66%) of the desired product as determined by quantitative NMR measurement with trimethoxybenzene as an internal standard.

^{1}H NMR (400 MHz, $CDCl_3$) δ 9.67 (d, *J* = 1.1 Hz, $1H_{CHO}$), 3.47 (d, *J* = 1.1 Hz, $1H_{OH}$), 2.81 (dd, *J* = 10.3, 7.3 Hz, $1H_3$), 2.62 (dd, *J* = 17.0, 2.7 Hz, $1H_5$), 2.54 – 2.43 (m, $1H_5$+$1H_1$), 2.41 – 2.27 (m, $1H_4$), 2.10 (t, *J* = 2.7 Hz, $1H_6$), 2.04 (s, $3H_{MeCO}$), 1.68 – 1.58 (m, $1H_4$), 1.45 (s, $3H_{Me}$), 1.01 (s, $3H_{Me}$).

^{13}C NMR (101 MHz, $CDCl_3$) δ 207.0, 201.8, 79.5, 77.8, 72.7, 54.0, 45.8, 45.1, 32.1, 30.5, 26.2, 18.8, 18.0.

HRMS (ESI) calc. for $C_{13}H_{20}O_3$ $[M+H]^+$ 223.1329, found 223.1324.

206: (*S*)-5-((1*S*,3*R*)-3-Acetyl-2,2-dimethylcyclobutyl)-5-(prop-2-yn-1-yl)furan-2(5H)-one



205 206

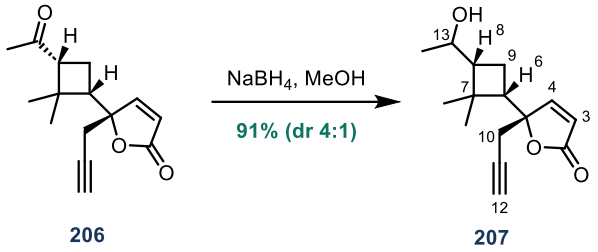
To a suspension of anhydrous lithium chloride (572 mg, 13.5 mmol, 2.7 eq.) in dry THF (90 mL) under a nitrogen atmosphere, ethyl [bis(2,2,2-trifluoroethoxy)phosphinyl]acetate (3.15 g, 9.5 mmol 1.5 eq.) was added and stirred for 15 min at rt. After cooling to 0 °C, DBU (2.03 mL, 13.5 mmol, 2.7 eq.) was added dropwise, and the mixture stirred at the same temperature for an additional 30 min. Next, the reaction mixture was cooled to -78 °C and a solution of aldehyde (1.10 g, 5.0 mmol, 1.0 eq.) in THF (30 mL) was added dropwise over 45 min. As soon as the addition was over, the reaction mixture was allowed to slowly warm to 0 °C (complete conversion occurs during this stage). The reaction was quenched with sat. NH_4Cl and extracted with ether. Ether layer was washed with brine, dried ($MgSO_4$) and concentrated. The product was purified by crystallisation from IPA/MTBE 8:2 (2.2 mL/g) to afford 875 mg (72%) of white solid. Alternatively, the product could be purified by flash chromatography (pentane/EtOAc 1:1).

^{1}H NMR (500 MHz, $CDCl_3$) δ 7.35 (d, *J* = 5.6 Hz, $1H_4$), 6.13 (d, *J* = 5.6 Hz, $1H_3$), 2.81 – 2.69 (m, $1H_8$+$1H_{10}$), 2.63 – 2.45 (m, $1H_6$+$1H_{10}$), 2.12 (t, *J* = 2.7 Hz, $1H_{12}$), 2.04 (s, $3H_{MeCO}$+$1H_9$), 1.55 (dt, *J* = 11.0, 7.6 Hz, $1H_9$), 1.47 (s, $3H_{Me}$), 1.07 (s, $3H_{Me}$).

^{13}C NMR (126 MHz, $CDCl_3$) δ 206.6, 172.0, 157.2, 122.3, 89.1, 77.6, 72.8, 53.5, 45.9, 44.8, 31.8, 30.4, 27.3, 18.6, 18.6.

HRMS (ESI) calc. for $C_{15}H_{20}O_3$ $[M+H]^+$ 247.1329, found 247.1326.

207: (5*S*)-5-((1*S*,3*R*)-3-(1-Hydroxyethyl)-2,2-dimethylcyclobutyl)-5-(prop-2-yn-1-yl)furan-2(5*H*)-one



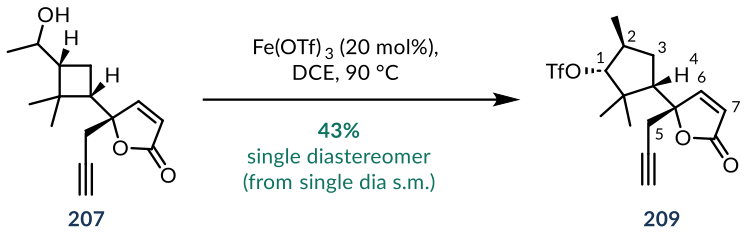
206 207

To a solution of ketone (9.2 mg, 0.037 mmol) in dry MeOH (1.5 mL) under N_2 at 0 °C was added $NaBH_4$ (5.7 mg, 0.150 mmol, 4.0 eq.) and stirred at rt for 10 min. Water and EtOAc were added and the organic layer was separated, washed with brine, dried ($MgSO_4$) and concentrated. Purification by flash chromatography (DCM/MeOH 97:3) afforded 8.4 mg (91%) of product as an inseparable 4:1 mixture of diastereomers. For easier characterisation, several fractions containing the pure major diastereomer were evaporated individually, and the reported NMR shifts correspond to this isomer.

^{1}H NMR (500 MHz, $CDCl_3$) δ 7.30 (d, *J* = 5.6 Hz, 1H_4), 6.09 (d, *J* = 5.6 Hz, 1H_3), 3.78 – 3.69 (m, 1H_{13}), 2.81 (dd, *J* = 16.7, 2.7 Hz, 1H_{10}), 2.58 (dd, *J* = 16.7, 2.7 Hz, 1H_{10}), 2.39 (dd, *J* = 11.4, 7.7 Hz, 1H_6), 2.10 (t, *J* = 2.7 Hz, 1H_{alkyne}), 1.69 (td, *J* = 10.3, 7.8 Hz, 1H_8), 1.52 (dt, *J* = 10.5, 7.8 Hz, 1H_9), 1.31 (s, 3H_{Me}), 1.27 (s, 3H_{Me}), 1.24 – 1.13 (m, 1H_9), 1.03 (d, *J* = 6.1 Hz, 3H_{Me}).

^{13}C NMR (126 MHz, $CDCl_3$) δ 172.5, 157.8, 121.8, 89.6, 77.9, 72.5, 68.9, 49.5, 44.6, 42.7, 32.9, 26.8, 21.4, 20.9, 17.9.

209: (1*R*,3*S*,5*S*)-2,2,5-Trimethyl-3-((*S*)-5-oxo-2-(prop-2-yn-1-yl)-2,5-dihydrofuran-2-yl)cyclopentyl trifluoromethanesulfonate



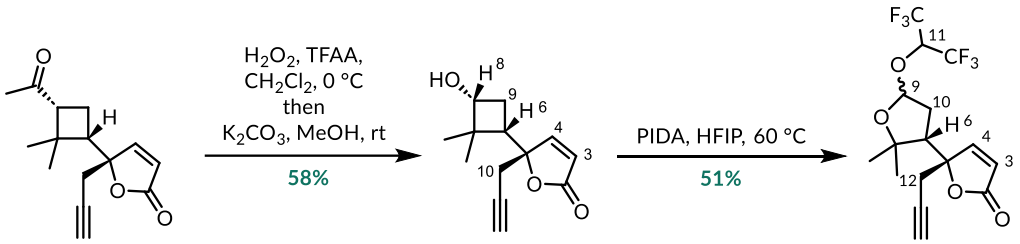
207 209

This is not a preparative procedure. To a solution of alcohol (15 mg, 0.060 mmol) and molecular sieves 3Å (36 mg) in dry CH_2Cl_2 (0.5 mL) under N_2 was quickly added $Fe(OTf)_3$ (6 mg, 0.012 mmol, 0.2 eq.) and the vial was capped and heated overnight at 90 °C. Water and EtOAc were added and the organic layer was separated, washed with brine, dried ($MgSO_4$) and concentrated. Purification by flash chromatography (DCM/MeOH 97:3) afforded 9.8 mg (43%) of the oily product as a single isomer and 2.1 mg of accompanying unidentified side product.

^{1}H NMR (500 MHz, $CDCl_3$) δ 7.42 (d, *J* = 5.6 Hz, $1H_6$), 6.12 (d, *J* = 5.6 Hz, $1H_7$), 3.07 (d, *J* = 9.8 Hz, $1H_1$), 2.90 (dd, *J* = 16.8, 2.7 Hz, $1H_5$), 2.65 (dd, *J* = 16.8, 2.7 Hz, $1H_5$), 2.25 (t, *J* = 10.0 Hz, $1H_4$), 2.12 (t, *J* = 2.7 Hz, $1H_{alkyne}$), 1.81 – 1.66 (m, $1H_2$), 1.59 – 1.53 (m, $1H_3$), 1.27 – 1.24 (m, $1H_3$), 1.20 (s, $3H_{Me}$), 1.06 (d, *J* = 6.6 Hz, $3H_{Me\text{-}2}$), 0.89 (s, $3H_{Me}$).

211: (5*S*)-5-((3*S*)-5-((1,1,1,3,3,3-Hexafluoropropan-2-yl)oxy)-2,2-dimethyltetrahydrofuran-3-yl)-5-(prop-2-yn-1-yl)furan-2(5*H*)-one

210: (*S*)-5-((1*S*,3*R*)-3-Hydroxy-2,2-dimethylcyclobutyl)-5-(prop-2-yn-1-yl)furan-2(5*H*)-one



206 210 211

A solution of H_2O_2 (30%, 0.27 mL, 2.68 mmol, 2.2 eq.) in CH_2Cl_2 (1.7 mL) was cooled to 0 °C and TFAA (1.51 mL, 10.7 mmol, 8.8 eq.) was added dropwise and stirred for 5-15 min at 0 °C. This order of addition prevents high ratio of local concentrations of TFAA to H_2O_2 that leads to formation of explosive trifluoroacetic peroxyanhydride. Excess TFAA consumes water from 30% hydrogen peroxide solution. Substrate (300 mg, 1.22 mmol) in CH_2Cl_2 (5.09 mL) was added fast dropwise at 0 °C and then stirred for 1.5 h at rt. Solid K_2CO_3 (ca. 3.5 g) was carefully added until pH was greater than 8. MeOH (4.8 mL) was added and the reaction mixture was stirred at rt overnight. Water and EtOAc were added, and the organic layer was washed with brine, dried ($MgSO_4$) and concentrated to give 154 mg (58%) of the desired product as white solid. The crude product was of sufficient purity and was taken to the next step without purification. The yield was determined by quantitative NMR measurement using trimethoxybenzene as an internal standard.

^{1}H NMR (500 MHz, $CDCl_3$) δ 7.31 (d, *J* = 5.6 Hz, $1H_4$), 6.10 (d, *J* = 5.6 Hz, $1H_3$), 3.71 (dd, *J* = 7.9, 7.7 Hz, $1H_8$), 2.81 (dd, *J* = 16.7, 2.7 Hz, $1H_{10}$), 2.58 (dd, *J* = 16.7, 2.7 Hz, $1H_{10}$), 2.16 – 2.08 (m, $1H_6$+$1H_{alkyne}$), 2.00 (dt, *J* = 11.0, 7.7 Hz, $1H_9$), 1.67 (d, *J* = 7.9 Hz, $1H_{OH}$), 1.49 (td, *J* = 11.0, 8.6 Hz, $1H_9$), 1.24 (s, $3H_{Me}$), 1.17 (s, $3H_{Me}$).

^{13}C NMR (126 MHz, $CDCl_3$) δ 172.3, 157.7, 121.9, 89.1, 77.8, 72.7, 71.5, 46.5, 40.4, 29.6, 29.5, 27.2, 16.1.

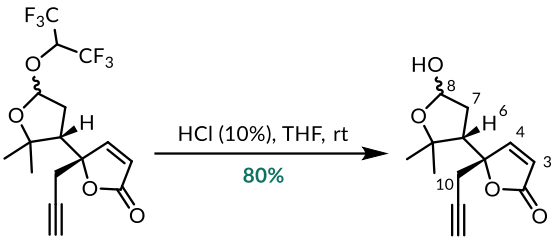
To a flask with the substrate (313 mg, 1.42 mmol) and PIDA (915 mg, 2.84 mmol, 2.0 eq.) was added HFIP (8.7 mL, dried over MS 4Å) under nitrogen atmosphere and the reaction mixture was heated at 70 °C for 1 h. The reaction mixture was evaporated to dryness. Excess reagent and impurities were precipitated by addition of Et_2O, and removed by filtration through cotton wool. The filtrate was concentrated to afford 281 mg (51%, dr ~1:1) of the desired product as white solid. The crude product contained only traces of PIDA-related impurities and was taken to the next step without purification. The yield was determined by quantitative NMR measurement using trimethoxybenzene as an internal standard.

^{1}H NMR (500 MHz, $CDCl_3$) δ 7.57 (d, J = 5.6 Hz, $1H_4$), 6.17 (d, J = 5.6 Hz, $1H_3$), 5.23 (d, J = 4.5 Hz, $1H_9$), 4.51 (hept, J = 6.1 Hz, $1H_{11}$), 2.95 – 2.85 (m, $1H_{12}$+$1H_6$), 2.61 (dd, J = 16.8, 2.7 Hz, $1H_{12}$), 2.20 (t, J = 2.7 Hz, $1H_{alkyne}$), 1.98 (td, J = 13.0, 4.6 Hz, $1H_{10}$), 1.89 (dd, J = 13.0, 6.4 Hz, $1H_{10}$), 1.54 (s, $3H_{Me}$), 1.29 (s, $3H_{Me}$).

^{13}C NMR (126 MHz, $CDCl_3$) δ 171.6, 159.1, 121.7 (q, $J_{C\text{-}F}$ = 276 Hz) 121.3, 101.2, 87.0, 85.9, 73.7, 47.5, 34.4, 30.7, 29.7, 27.7, 25.4. *C-11 is not visible due to the coupling with six fluorine atoms, causing it to be spread out and blend into the baseline noise.

HRMS (ESI) calc. for $C_{16}H_{16}F_6O_6Na$ $[M+Na]^+$ 409.0845, found 409.0844.

212: (5*S*)-5-((3*S*)-5-Hydroxy-2,2-dimethyltetrahydrofuran-3-yl)-5-(prop-2-yn-1-yl)furan-2(5*H*)-one



211 212

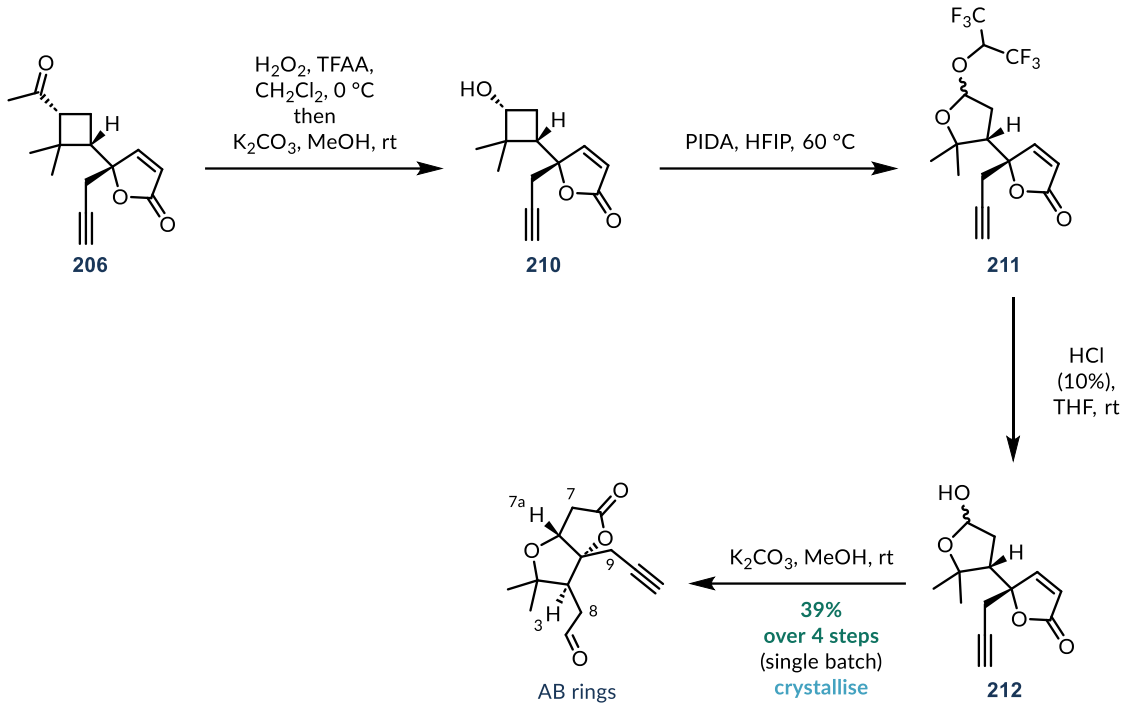
To the substrate (38 mg, 0.098 mmol) in THF (1.1 mL) was added HCl (6 M, 0.36 mL, 10 eq.) and the reaction mixture was stirred at rt overnight. Solid $NaHCO_3$ was carefully added to neutralise the reaction mixture. Water and EtOAc were added and the organic layer was washed with brine, dried ($MgSO_4$) and concentrated. The crude product was of sufficient purity to be taken to the next step without purification. For the purposes of characterisation, purification by flash chromatography (DCM/MeOH 96:4) afforded 19 mg (80%) of the desired oily product.

^{1}H NMR (500 MHz, $CDCl_3$) δ 7.54 (d, *J* = 5.7 Hz, $1H_3$), 6.15 (d, *J* = 5.6 Hz, $1H_4$), 5.38 (dd, *J* = 4.8, 2.4 Hz, $1H_8$), 2.99 (dd, *J* = 13.2, 6.5 Hz, $1H_6$), 2.94 (dd, *J* = 16.7, 2.7 Hz, $1H_{10}$), 2.62 (dd, *J* = 16.7, 2.7 Hz, $1H_{10}$), 2.17 (t, *J* = 2.8 Hz, $1H_{alkyne}$), 1.90 – 1.83 (m, $1H_7$), 1.73 (dd, *J* = 12.5, 6.5 Hz, $1H_7$), 1.43 (s, $3H_{Me}$), 1.35 (s, $3H_{Me}$).

^{13}C NMR (126 MHz, $CDCl_3$) δ 172.0, 159.3, 121.4, 95.2, 87.7, 83.7, 77.4, 73.6, 48.1, 35.3, 32.4, 28.0, 25.5.

HRMS (ESI) calc. for $C_{13}H_{13}O_4$ $[M+H]^+$ 237.1121, found 237.1121.

AB rings: 2-((3*S*,3a*R*,6a*R*)-2,2-Dimethyl-5-oxo-3a-(prop-2-yn-1-yl)hexahydrofuro[3,2-*b*]furan-3-yl)acetaldehyde



A solution of H_2O_2 (30% aq., 0.46 mL, 4.56 mmol, 2.2 eq.) in CH_2Cl_2 (2.9 mL) was cooled to 0 °C and TFAA (2.57 mL, 18.2 mmol, 8.8 eq.) was added dropwise and stirred for 5-15 min at 0 °C. Starting material (510 mg, 2.07 mmol) in CH_2Cl_2 (8.7 mL) was added fast dropwise at 0 °C and then stirred for 1.5 h at rt. Solid K_2CO_3 (ca. 6 g) was carefully added until pH was greater than 8. MeOH (8.1 mL) was added and the reaction mixture was stirred at rt overnight. Water and EtOAc were added, and the organic layer was washed with brine, dried ($MgSO_4$) and concentrated.

To a flask with the crude material from the previous step and PIDA (915 mg, 2.84 mmol, 2.0 eq.) was added HFIP (8.7 mL, dried over MS 4Å) under nitrogen atmosphere and the reaction mixture was heated at 70 °C for 1 h. The reaction mixture was evaporated to dryness. Excess reagent and impurities were precipitated by addition of Et_2O, and removed by filtration through cotton wool. The filtrate was concentrated.

To a solution of the crude material from the previous step in THF (13 mL) was added HCl (6 M, 4.8 mL, 10 eq.) and the reaction mixture was stirred at rt overnight. Solid $NaHCO_3$ was carefully

added to neutralise the reaction mixture. Water and EtOAc were added and the organic layer was washed with brine, dried ($MgSO_4$) and concentrated.

To a solution of the crude material from the previous step in MeOH (18 mL) was added K_2CO_3 (785 mg, 5.68 mmol, 4.0 eq.) and the reaction mixture was stirred 2 h at rt. Water and EtOAc were added and the organic layer was washed with brine, dried ($MgSO_4$) and concentrated. Recrystallisation of the crude product (hexane/EtOAc 8:2, 0.1 mL per mg) afforded 189 mg (39% over 4 steps) of purified AB rings as white solid.

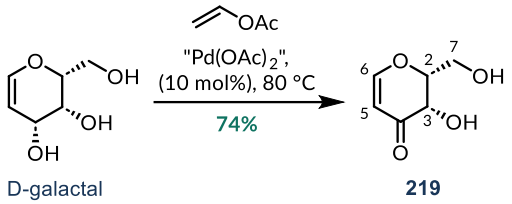
^{1}H NMR (400 MHz, $CDCl_3$) δ 9.78 (t, *J* = 2.1 Hz, $1H_{aldehyde}$), 4.51 (dd, *J* = 6.6, 0.9 Hz, $1H_{7a}$), 3.00 (dd, *J* = 18.7, 6.6 Hz, $1H_7$), 2.77 (dd, *J* = 9.1, 6.1 Hz, $1H_3$), 2.69 (dd, *J* = 18.6, 0.9 Hz, $1H_7$), 2.67 (dd, *J* = 17.0, 2.7 Hz, $1H_9$), 2.58 (ddd, *J* = 16.7, 9.1, 2.1 Hz, $1H_8$), 2.48 (dd, *J* = 17.0, 2.7 Hz, $1H_9$), 2.40 (ddd, *J* = 16.7, 6.1, 2.1 Hz, $1H_8$), 2.11 (t, *J* = 2.7 Hz, $1H_{alkyne}$), 1.34 (s, $3H_{Me}$), 1.11 (s, $3H_{Me}$).

^{13}C NMR (101 MHz, $CDCl_3$) δ 199.3, 175.0, 94.1, 83.1, 78.7, 77.4, 72.9, 52.7, 40.7, 37.3, 27.9, 25.5, 21.2.

Data in agreement with the literature values.[114]

7.6 Procedures and characterisation from Chapters 4 and 5

219: (*2R*,*3S*)-3-Hydroxy-2-(hydroxymethyl)-2,3-dihydro-4*H*-pyran-4-one



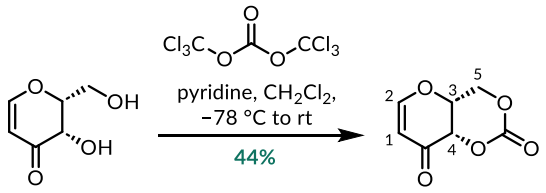
To a round bottom flask containing black palladium leftover from previous reaction run (where 92 mg $Pd(OAc)_2$ was used) was added, without exclusion of air, D-galactal (1.20 g, 8.21 mmol), vinyl acetate (48 mL) and commercial $Pd(OAc)_2$ (147 mg, 0.66 mmol, 8 mol%). Reaction was heated to 80 °C overnight and full conversion of starting material confirmed by GC-MS. The product peak accounted for 80% of the area, with traces of overhydrogenation product (double bond reduction) observed. When the reaction concentration is higher, significant amounts of this by-product form. The reaction mixture was evaporated and purified by flash chromatography (DCM/MeOH 92:8) to obtain 876 mg (74%) of white solid.

^{1}H NMR (400 MHz, CD_3OD) δ 7.53 (d, *J* = 6.0 Hz, $1H_6$), 5.39 (dd, *J* = 6.0, 1.2 Hz, $1H_5$), 4.46 – 4.38 (m, $1H_2$), 4.05 (dd, *J* = 3.4, 1.2 Hz, $1H_3$), 3.95 (dd, *J* = 12.0, 7.4 Hz, $1H_7$), 3.87 (dd, *J* = 12.0, 4.7 Hz, $1H_7$).

^{13}C NMR (101 MHz, CD_3OD) δ 194.08, 165.04, 105.31, 84.25, 70.07, 60.32, 49.00.

Data in agreement with the literature values.[98]

220: (4a*R*,8a*S*)-4a,8a-Dihydropyrano[3,2-*d*][1,3]dioxine-2,8(4*H*)-dione



219 220

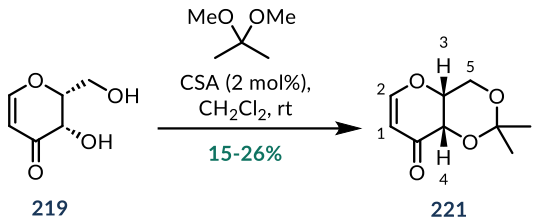
To a solution of diol (16.5 mg, 0.114 mmol) in anhydrous CH_2Cl_2 (0.7 mL) was added pyridine (55 µL, 0.687 mmol, 6.0 eq.) and the resulting solution was cooled to −78 °C. Solution of triphosgene (17.0 mg, 0.057 mmol, 0.5 eq.) in anhydrous CH_2Cl_2 (0.4 mL) was added dropwise and the reaction mixture was warmed to rt. Sat. aq. $CuSO_4$ and EtOAc were added and the organic layer was separated, washed with brine, dried ($MgSO_4$) and concentrated. Purification by flash chromatography (pent/EtOAc 1:4) afforded 8.6 mg (44%) of the pure product. Note: This product decomposes in contact with acid.

^{1}H NMR (500 MHz, $CDCl_3$) δ 7.49 (d, *J* = 6.2 Hz, $1H_2$), 5.63 (d, *J* = 6.2 Hz, $1H_1$), 4.88 – 4.65 (m, $1H_3$+$1H_4$+$2H_5$).

^{13}C NMR (126 MHz, $CDCl_3$) δ 181.4, 163.2, 145.6, 105.8, 75.0, 70.1, 69.5.

HRMS (ESI) calc. for $C_7H_8O_5$ $[M+H]^+$ 171.0288, found 171.0287.

221: (4a*R*,8a*S*)-2,2-Dimethyl-4a,8a-dihydropyrano[3,2-*d*][1,3]dioxin-8(4*H*)-one



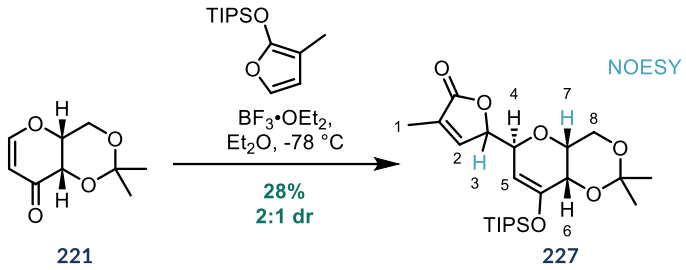
Not a preparative procedure. To a solution of diol (428 mg, 2.97 mmol) in anhydrous CH_2Cl_2 (15 mL) under N_2 atmosphere were added 2,2-dimethoxypropane (1.83 mL, 14.8 mmol, 5.0 eq.) and CSA (14 mg, 0.059 mmol, 0.02 eq.). The reaction mixture was stirred at rt overnight. Sat. aq. $NaHCO_3$ and EtOAc were added, and the organic layer was separated, washed with brine, dried ($MgSO_4$) and concentrated. Purification by flash chromatography (pent/EtOAc 1:1) afforded 69 mg (13%) of yellow oil.

^{1}H NMR (500 MHz, $CDCl_3$) δ 7.50 (d, *J* = 6.1 Hz, $1H_2$), 5.52 (dd, *J* = 6.2, 1.3 Hz, $1H_1$), 4.19 – 4.11 (m, $1H_3$+$1H_4$+$2H_5$), 1.54 (s, $3H_{Me}$), 1.46 (s, $3H_{Me}$).

^{13}C NMR (126 MHz, $CDCl_3$) δ 186.8, 164.3, 105.5, 99.3, 73.2, 69.1, 61.5, 29.2, 18.5.

HRMS (ESI) calc. for $C_9H_{14}O_4$ $[M+H]^+$ 185.0808, found 185.0806.

227: 5-((4a*R*,6*S*,8a*S*)-2,2-Dimethyl-8-((triisopropylsilyl)oxy)-4,4a,6,8a-tetrahydropyrano[3,2-*d*][1,3]dioxin-6-yl)-3-methylfuran-2(5*H*)-one



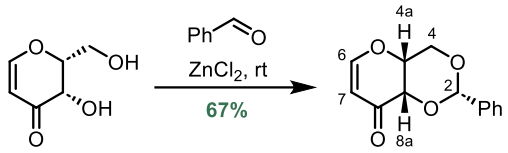
This is not a preparative procedure. To a vail with septum were added pyranodioxinone (10 mg, 0.054 mmol) and siloxyfuran (17 mg, 0.065 mmol, 1.2 eq.). Atmosphere was changed to N_2, and anhydrous Et_2O (0.6 mL) was added. The solution was cooled to −78 °C and one drop of $BF_3{\cdot}OEt_2$ was added. The reaction mixture was stirred for 2.5 h at −78 °C. Sat. aq. $NaHCO_3$ and EtOAc were added, the solution was warmed to rt and the organic layer was separated, passed through a Pasteur pipette with $MgSO_4$ and concentrated. Purification by flash chromatography (pent/EtOAc 7:3 to 1:1) afforded 6.6 mg (28%) of oily product as a diastereomeric mixture of silyl enol ethers.

^{1}H NMR (400 MHz, $CDCl_3$) δ 7.12 (t, *J* = 1.7 Hz, $1H_2$), 5.03 – 4.98 (m, $1H_3$), 4.88 (d, *J* = 3.5 Hz, $1H_5$), 4.47 (dd, *J* = 5.4, 3.5 Hz, $1H_4$), 4.14 (dd, *J* = 13.0, 3.2 Hz, $1H_8$), 4.03 (d, *J* = 2.0 Hz, $1H_6$), 3.93 (dd, *J* = 13.0, 2.2 Hz, $1H_8$), 3.90 – 3.87 (m, $1H_7$), 1.92 (t, *J* = 1.7 Hz, $3H_{Me\text{-}1}$), 1.46 (s, $3H_{Me}$), 1.42 (s, $3H_{Me}$), 1.10 – 1.03 (m, $21H_{TIPS}$).

^{13}C NMR (126 MHz, $CDCl_3$) δ 174.0, 149.9, 146.0, 131.3, 102.1, 99.1, 83.4, 73.8, 66.5, 65.7, 63.0, 28.7, 19.2, 18.0, 12.6, 10.8.

Assignment based on analogy with compound **229**.

228: (*2S,4aR,8aS*)-2-Phenyl-4a,8a-dihydropyrano[3,2-d][1,3]dioxin-8(4*H*)-one



219 228

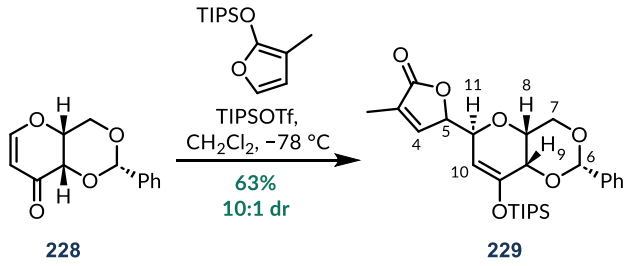
To a flask with diol (810 mg, 5.62 mmol) was quickly added commercial anhydrous $ZnCl_2$ (842 mg, 6.18 mmol, 1.1 eq.) and benzaldehyde directly from the commercial bottle (2.85 mL, 28.1 mmol, 5.0 eq.) and stirred at rt overnight. Water and EtOAc were added, and the organic layer was washed with brine, dried ($MgSO_4$) and concentrated. Purification by flash chromatography (pentane/EtOAc 1:1) afforded 870 mg (67%) of white-brownish solid.

^{1}H NMR (500 MHz, $CDCl_3$) δ 7.54 (d, *J* = 6.1 Hz, $1H_6$), 7.51 – 7.47 (m, $2H_{Ph}$), 7.38 – 7.34 (m, $3H_{Ph}$), 5.66 (s, $1H_2$), 5.55 (dd, *J* = 6.1, 1.2 Hz, $1H_7$), 4.56 (dd, *J* = 13.0, 1.6 Hz, $1H_4$), 4.28 – 4.24 (m, $1H_{4a}$+$1H_{8a}$), 4.20 (dd, *J* = 13.0, 1.2 Hz, $1H_4$).

^{13}C NMR (101 MHz, $CDCl_3$) δ 185.9, 164.4, 137.0, 133.8, 129.4, 128.6, 128.4, 126.3, 105.6, 100.9, 75.3, 73.4, 68.1.

HRMS (ESI) calc. for $C_{13}H_{13}O_4$ $[M+H]^+$ 233.0808, found 233.0801.

229: 3-Methyl-5-((*2S,4aR,6S,8aS*)-2-phenyl-8-((triisopropylsilyl)oxy)-4,4a,6,8a-tetrahydropyrano[3,2-d][1,3]dioxin-6-yl)furan-2(5*H*)-one



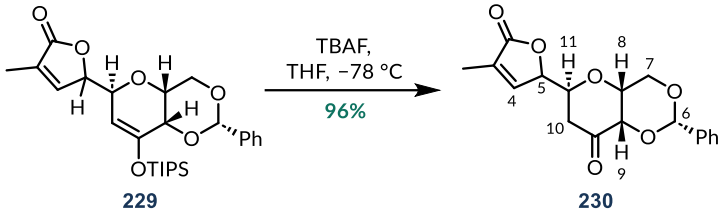
To a solution of pyranodioxinone (214 mg, 0.92 mmol) in anhydrous CH_2Cl_2 (10 mL) under N_2 atmosphere was added siloxyfuran (305 mg, 1.20 mmol, 1.3 eq.) via syringe and needle. The solution was cooled to -78 °C and TIPSOTf (275 µL, 1.01 mmol, 1.1 eq.) was added dropwise. After stirring for 30-40 min at -78 °C, the reaction mixture was quenched by addition of sat. aq. $NaHCO_3$ (at -78 °C), warmed to rt and extracted with Et_2O. Ether layer was washed with brine, dried ($MgSO_4$) and concentrated. Purification by flash chromatography (pentane/EtOAc 7:3) afforded 281 mg (63%, dr 10:1) of white foam.

^{1}H NMR (500 MHz, $CDCl_3$) δ 7.52 – 7.47 (m, $2H_{Ph}$), 7.38 – 7.27 (m, $3H_{Ph}$), 7.11 (t, *J* = 1.7 Hz, $1H_4$), 5.59 (s, $1H_6$), 5.10 – 5.06 (m, $1H_5$), 4.84 (d, *J* = 3.4 Hz, $1H_{10}$), 4.57 (dd, *J* = 4.9, 3.4 Hz, $1H_{11}$), 4.38 (d, *J* = 12.8 Hz, $1H_{7eq}$), 4.17 (dd, *J* = 12.8, 2.2 Hz, $1H_{7ax}$), 4.12 (d, *J* = 1.7 Hz, $1H_9$), 4.00 – 3.98 (m, $1H_8$), 1.93 (t, *J* = 1.8 Hz, $3H_{Me}$), 1.11 – 1.03 (m, $21H_{TIPS}$).

^{13}C NMR (126 MHz, $CDCl_3$) δ 174.0, 149.6, 145.8, 138.0, 131.4, 128.8, 128.1, 128.1, 126.2, 101.4, 100.6, 83.8, 73.9, 72.7, 70.0, 66.4, 18.0, 10.8.

HRMS (ESI) calc. for $C_{27}H_{39}O_6Si$ $[M+H]^+$ 487.2510, found 487.2489.

230: (*2S,4aR,6S,8aS*)-6-(4-Methyl-5-oxo-2,5-dihydrofuran-2-yl)-2-phenyltetrahydropyrano[3,2-*d*][1,3]dioxin-8(4*H*)-one



229 **230**

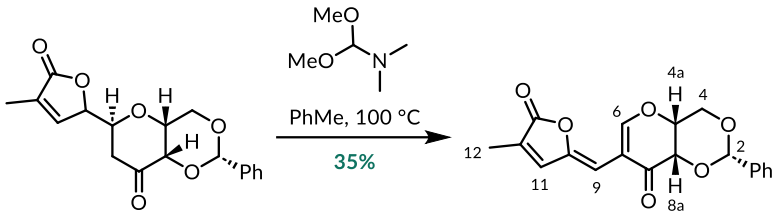
A solution of silyl enol ether (120 mg, 0.25 mmol) in anhydrous THF (2.4 mL), under N_2 atmosphere, was cooled to -78 °C and TBAF (1 M in THF, 296 µL, 0.30 mmol, 1.2 eq.) was added. After stirring 10 min at -78 °C, water and EtOAc were added and the mixture was warmed to rt. Organic layer was separated, washed with brine, dried ($MgSO_4$) and concentrated. Purification by flash chromatography (pentane/EtOAc 1:1) afforded 78 mg (96%, dr 10:1) of white foam.

^{1}H NMR (400 MHz, $CDCl_3$) δ 7.53 – 7.46 (m, $2H_{Ph}$), 7.42 – 7.31 (m, $3H_{Ph}$), 7.04 (dt, *J* = 2.0, 1.7 Hz, $1H_4$), 5.62 (s, $1H_6$), 5.16 (ddq, *J* = 4.0, 2.0, 1.7 Hz, $1H_5$), 4.70 (dt, *J* = 7.0, 4.0 Hz, $1H_{11}$), 4.42 (dd, *J* = 13.0, 1.5 Hz, $1H_{7eq}$), 4.35 (d, *J* = 1.8 Hz, $1H_9$), 4.22 (ddd, *J* = 2.1, 1.8, 1.5 Hz, $1H_8$), 4.15 (dd, *J* = 13.0, 2.1 Hz, $1H_{7ax}$), 2.99 (dd, *J* = 15.5, 7.0 Hz, $1H_{10eq}$), 2.26 (dd, *J* = 15.5, 4.0 Hz, $1H_{10ax}$), 1.96 (t, *J* = 1.7 Hz, $3H_{Me}$).

^{13}C NMR (101 MHz, $CDCl_3$) δ 199.8, 144.8, 137.2, 132.4, 129.4, 128.4, 126.2, 100.8, 83.7, 78.9, 77.4, 76.8, 74.9, 70.1, 68.2, 36.6, 11.0.

HRMS (ESI) calc. for $C_{18}H_{19}O_6$ $[M+H]^+$ 331.1176, found 331.1161.

233: (2*S*,4a*R*,8a*S*)-7-((*Z*)-(4-methyl-5-oxofuran-2(5*H*)-ylidene)methyl)-2-phenyl-4a,8a-dihydropyrano[3,2-*d*][1,3]dioxin-8(4*H*)-one



230 233

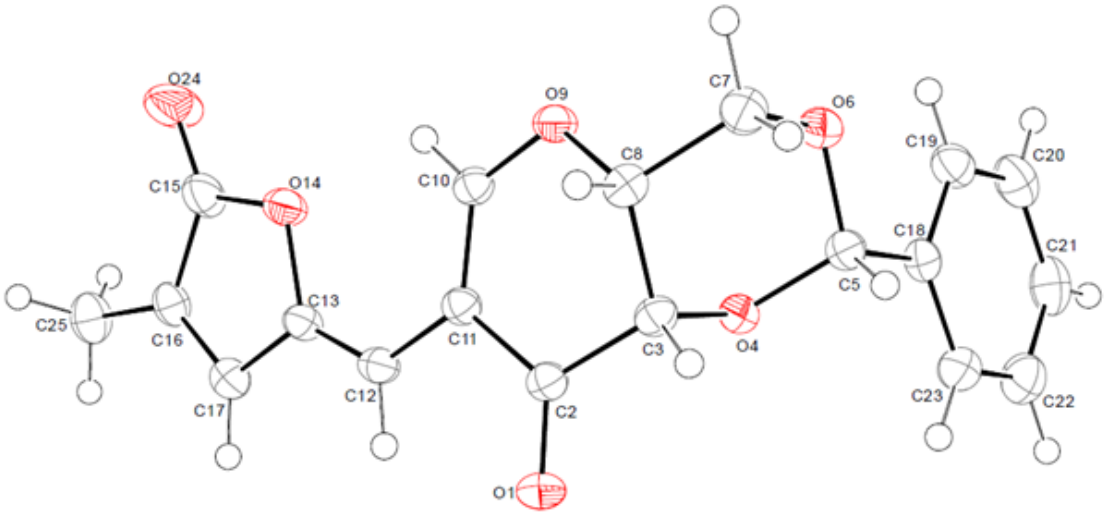
To a vial with ketone (30 mg, 0.09 mmol) was added toluene (0.92 mL) and DMF-DMA (103 µL, 0.77 mmol, 8.5 eq.). The vial was capped and heated at 110 °C for 1 h. Upon DMF-DMA addition, the reaction mixture colour turned yellow, but starting material remained unchanged (checked by TLC). When heated it turned dark orange. Water and EtOAc were added, and the organic layer was separated, washed with brine, dried ($MgSO_4$) and concentrated. Purification by flash chromatography afforded 11 mg (35%) of yellow to orange solid.

^{1}H NMR (400 MHz, $CDCl_3$) δ 8.59 (s, $1H_6$), 7.53 – 7.44 (m, $2H_{Ph}$), 7.41 – 7.31 (m, $3H_{Ph}$), 7.09 (q, *J* = 1.5 Hz, $1H_{11}$), 5.96 (s, $1H_9$), 5.67 (s, $1H_2$), 4.61 (dd, *J* = 13.1, 1.7 Hz, $1H_4$), 4.37 (d, *J* = 1.9 Hz, $1H_{8a}$), 4.36 – 4.34 (m, $1H_{4a}$), 4.26 – 4.18 (m, $1H_4$), 2.02 (d, *J* = 1.5 Hz, $3H_{Me}$).

^{13}C NMR (101 MHz, $CDCl_3$) δ 183.5, 170.9, 167.4, 146.8, 139.0, 136.8, 129.6, 128.6, 128.5, 126.3, 112.0, 101.0, 100.7, 74.7, 73.5, 68.0, 10.7.

HRMS (ESI) calc. for $C_{19}H_{17}O_6$ $[M+H]^+$ 341.1020, found 341.1018.

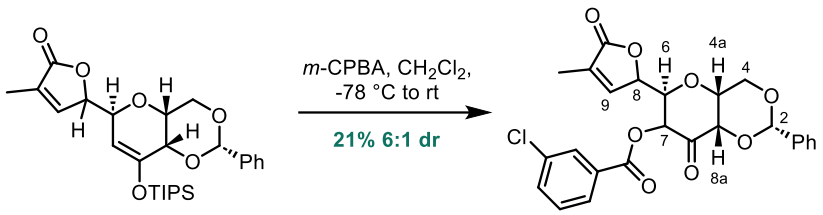
Crystal data



Empirical formula	C19 H16 O6
Formula weight	340.33
Temperature	150 K
Wavelength	1.54184 Å
Crystal system	Monoclinic
Space group	C 2
Unit cell dimensions	a = 11.7572(2) Å = 90°. b = 4.99590(10) Å = 97.6834(13)°. c = 27.8163(4) Å = 90°.
Volume	1619.20(5) Å3
Z	4
Density (calculated)	1.396 Mg/m3
Absorption coefficient	0.875 mm-1
F(000)	712
Crystal size	0.30 x 0.20 x 0.10 mm3
Theta range for data collection	4.813 to 76.274°.
Index ranges	-14<=h<=14, -6<=k<=6, -31<=l<=35
Reflections collected	18119
Independent reflections	3326 [R(int) = 0.025]
Completeness to theta = 74.748°	99.9 %
Absorption correction	Semi-empirical from equivalents

Max. and min. transmission	0.92 and 0.64
Refinement method	Full-matrix least-squares on F2
Data / restraints / parameters	3326 / 1 / 227
Goodness-of-fit on F2	1.0198
Final R indices [I>2sigma(I)]	R1 = 0.0284, wR2 = 0.0778
R indices (all data)	R1 = 0.0287, wR2 = 0.0781
Absolute structure parameter	-0.03(4)
Largest diff. peak and hole	0.08 and -0.06 e.Å-3

242: (2*S*,4a*R*,6*R*,8a*S*)-6-(4-Methyl-5-oxo-2,5-dihydrofuran-2-yl)-8-oxo-2-phenylhexahydropyrano[3,2-*d*][1,3]dioxin-7-yl 3-chlorobenzoate



229 242

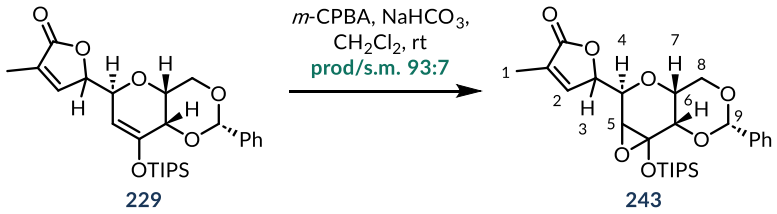
To a solution of TIPS enol ether (20 mg, 0.041 mmol) in CH_2Cl_2 (0.4 mL) at −78 °C was added m-CPBA (70%, 11 mg, 0.045 mmol, 1.1 eq.) as a solution in CH_2Cl_2 (0.2 mL), and the reaction mixture was warmed to rt. As no reaction was observed, additional m-CPBA was added (70%, 19 mg, 0.076 mmol, 1.9 eq.) and the reaction mixture was stirred overnight at rt. Aqueous solution of thiosulfate and bicarbonate was added, and the reaction mixture was extracted with EtOAc. Organic layer was dried over $MgSO_4$ and solvent removed under reduced pressure. Purification by flash chromatography (pentane/EtOAc 1:1) afforded 4.2 mg (21%) of the desired solid product as a 6:1 mixture of diastereomers at C-7.

^{1}H NMR (500 MHz, $CDCl_3$) δ 7.92 – 7.83 (m, 1H$_{m\text{-}CBA}$), 7.62 – 7.48 (m, 3H$_{m\text{-}CBA}$), 7.48 – 7.33 (m, 5H$_{Ph}$), 7.03 (t, *J* = 1.7 Hz, 1H$_9$), 6.20 (d, *J* = 7.0 Hz, 1H$_7$), 5.66 (s, 1H$_2$), 5.33 – 5.30 (m, 1H$_8$), 5.11 (dd, *J* = 7.0, 2.2 Hz, 1H$_6$), 4.70 (d, *J* = 1.7 Hz, 1H$_{8a}$), 4.45 (dd, *J* = 13.0, 1.5 Hz, 1H$_4$), 4.41 – 4.36 (m, 1H$_{4a}$), 4.25 (dd, *J* = 13.0, 2.1 Hz, 1H$_4$), 1.81 (t, *J* = 1.7 Hz, 3H$_{Me}$).

^{13}C NMR (126 MHz, $CDCl_3$) δ 193.8, 172.6, 163.7, 144.9, 136.9, 134.9, 134.0, 130.9, 130.4, 130.1, 129.9, 129.5, 128.5, 128.4, 126.2, 100.9, 82.8, 80.4, 76.6, 72.6, 69.5, 68.5, 10.9.

HRMS (ESI) calc. for $C_{25}H_{22}{}^{35}ClO_8$ $[M+H]^+$ 485.0998, found 485.0995.

243: 3-Methyl-5-((2*R*,3a*R*,6*S*,7a*S*)-6-phenyl-7b-((triisopropylsilyl)oxy)hexahydrooxireno[2',3':4,5]pyrano[3,2-*d*][1,3]dioxin-2-yl)furan-2(5*H*)-one



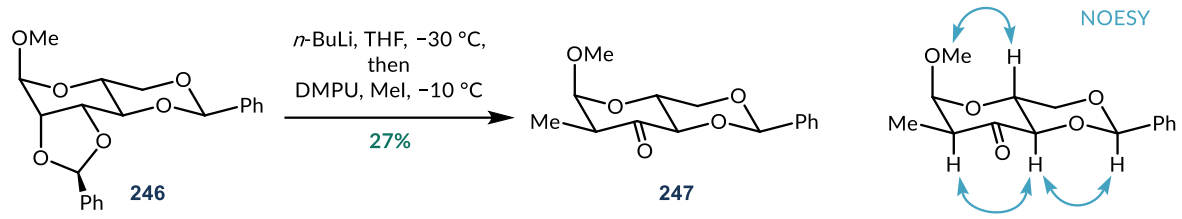
This is not a preparative procedure. To a mixture of silyl enol ether (20 mg, 0.041 mmol) and $NaHCO_3$ (8.6 mg, 0.100 mmol, 2.5 eq.) in CH_2Cl_2 (0.7 mL) was added m-CPBA (50%wt, 17 mg, 0.049 mmol, 1.2 eq.). The reaction mixture was stirred for 4 h at rt. The reaction was difficult to monitor by TLC, as both the starting material and the product had the same Rf. If worked up prematurely, the crude mixture could be resubmitted to the same conditions again to achieve full conversion. Aq. solution of $NaHCO_3/Na_2S_2O_3$ mixture and Et_2O were added. The organic layer was separated, dried ($MgSO_4$) and concentrated. The ratio of epoxide to silyl enol ether in the crude product was 93:7 as determined by NMR.

^{1}H NMR (500 MHz, $CDCl_3$) δ 7.54 – 7.49 (m, $2H_{Ph}$), 7.38 – 7.33 (m, $3H_{Ph}$), 7.18 – 7.17 (m, $1H_2$), 5.58 (s, $1H_9$), 5.03 (dt, J = 8.7, 1.8 Hz, $1H_3$), 4.28 – 4.26 (m, $1H_6$+$1H_8$), 4.09 (dd, J = 8.7, 2.7 Hz, $1H_4$), 4.03 (dd, J = 12.7, 1.8 Hz, $1H_8$), 3.72 (d, J = 2.7, $1H_5$), 3.65 – 3.63 (m, $1H_7$), 1.95 (t, J = 1.8 Hz, $3H_{Me}$), 1.07 – 1.04 (m, $21H_{TIPS}$).

^{13}C NMR (126 MHz, $CDCl_3$) δ 173.8, 147.6, 138.0, 130.8, 129.2, 128.3, 126.2, 101.3, 79.7, 77.6, 74.7, 72.3, 70.1, 65.4, 59.7, 17.9, 12.7, 10.8.

HRMS (ESI) calc. for $C_{27}H_{39}O_7Si$ $[M+H]^+$ 503.2460, found 503.2451.

247: (2*R*,4a*R*,6*S*,7*S*,8a*R*)-6-Methoxy-7-methyl-2-phenyltetrahydropyrano[3,2-*d*][1,3]dioxin-8(4*H*)-one



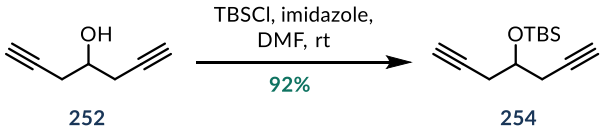
Starting material was commercially available, however, it could be prepared as a single diastereomer by following a literature procedure.[105] A solution of starting material (500 mg, 1.35 mmol) in anhydrous THF (23 mL) was cooled to −30 °C under nitrogen atmosphere and *n*-BuLi (1.4 M, 2.18 mL, 2.97 mmol, 2.2 eq.) was added dropwise. The reaction mixture was stirred 15 min at −30 °C. During this time, the starting material was completely consumed as monitored by TLC. Anhydrous DMPU (1.6 mL) and MeI (93 µL, 1.48 mmol, 1.1 eq.) were added and the reaction mixture was stirred at −10 °C for 24 h. After NH_4Cl (sat.) addition, the reaction mixture was extracted with Et_2O and the organic layer was washed with brine, dried ($MgSO_4$) and concentrated. Some amount of dialkylated side product was observed in the crude product. Purification by flash chromatography (pentane/EtOAc 75:25) afforded 96 mg (27%) of white solid.

^{1}H NMR (500 MHz, $CDCl_3$) δ 7.54 – 7.48 (m, $2H_{Ph}$), 7.37 – 7.34 (m, $3H_{Ph}$), 5.57 (s, $1H_2$), 4.96 (d, *J* = 4.2 Hz, $1H_6$), 4.37 (dd, *J* = 10.2, 4.7 Hz, $1H_4$), 4.29 (dd, *J* = 9.9, 1.4 Hz, $1H_{8a}$), 4.11 (td, *J* = 9.9, 4.7 Hz, $1H_{4a}$), 3.93 (t, *J* = 10.2 Hz, $1H_4$), 3.38 (s, $3H_{OMe}$), 2.91 – 2.83 (m, $1H_7$), 1.10 (d, *J* = 6.8 Hz, $3H_{Me}$).

^{13}C NMR (126 MHz, $CDCl_3$) δ 199.4, 136.8, 129.4, 128.4, 126.6, 104.7, 102.2, 83.2, 69.7, 65.9, 55.5, 48.9, 8.8.

Data in agreement with the literature values.[105]

254: *tert*-Butyl(hepta-1,6-diyn-4-yloxy)dimethylsilane



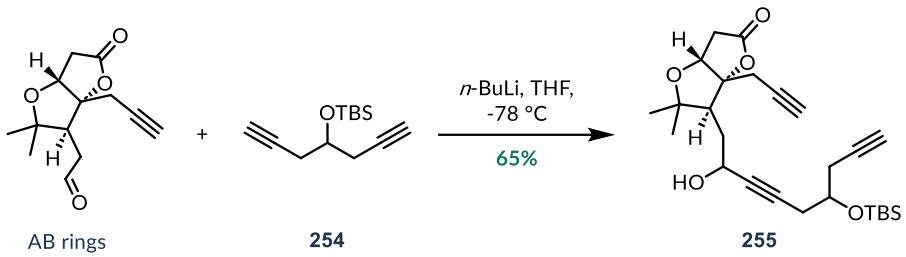
To a solution of starting material (50 mg, 0.46 mmol) prepared by the literature procedure[108] in anhydrous DMF (1.0 mL), imidazole (63 mg, 0.93 mmol, 2.0 eq.) and TBSCl (105 mg, 0.69 mmol, 1.5 eq.) were added under nitrogen atmosphere. The reaction mixture was stirred at rt for 4 h. Water was carefully added and the reaction mixture was extracted with Et_2O. The organic layer was washed with brine, passed through a Pasteur pipette with silica and concentrated. Purification by flash chromatography afforded 94 mg (92%) of oil.

^{1}H NMR (400 MHz, $CDCl_3$) δ 3.96 (qu, *J* = 5.9 Hz, $1H_{CH}$), 2.46 (qdd, *J* = 16.7, 5.9, 2.7 Hz, $5H_{CH2}$), 2.00 (t, *J* = 2.7 Hz, $2H_{alkyne}$), 0.90 (s, $9H_{TBS}$), 0.11 (s, $6H_{TBS}$).

^{13}C NMR (101 MHz, $CDCl_3$) δ 81.1, 77.4, 70.4, 69.8, 26.9, 25.9, -4.5.

Data in agreement with the literature values.[136]

255: (3a*R*,6*S*,6a*R*)-6-(6-((*tert*-Butyldimethylsilyl)oxy)-2-hydroxynona-3,8-diyn-1-yl)-5,5-dimethyl-6a-(prop-2-yn-1-yl)tetrahydrofuro[3,2-*b*]furan-2(3*H*)-one



AB rings **254** **255**

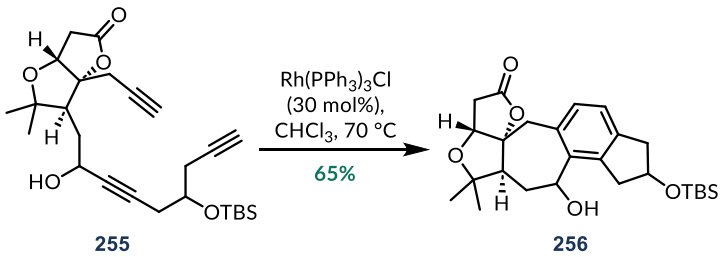
To a solution of alkyne (16 mg, 0.25 mmol, 4.0 eq.) in anhydrous THF (1.0 mL) was cooled to −78 °C under nitrogen atmosphere and *n*-BuLi (2.3 M, 113 µL, 0.25 mmol, 4.0 eq.) was added dropwise. After stirring for 10 min at −78 °C, aldehyde (15 mg, 0.064 mmol) in anhydrous THF (0.5 mL) was added dropwise and the reaction mixture was stirred for 10 min at −78 °C. The reaction was quenched with NH_4Cl (sat.) and warmed to rt and extracted with Et_2O. The organic layer was washed with brine, dried ($MgSO_4$) and concentrated. Purification by flash chromatography (pentane/EtOAc 7:3) afforded 19 mg (65%) of oil.

^{1}H NMR (400 MHz, $CDCl_3$) δ 4.54 – 4.46 (m, $1H_{CH}$+$1H_{CH}$), 3.99 – 3.88 (m, $1H_{CH}$), 3.11 – 2.95 (m, $1H_{CH2}$+$1H_{CH2}$), 2.76 – 2.62 (m, $1H_{CH2}$), 2.54 – 2.40 (m, $3H_{CH2}$+$1H_{CH}$), 2.07 (t, *J* = 2.6 Hz, $1H_{alkyne}$), 1.99 (t, *J* = 2.6 Hz, $1H_{alkyne}$), 1.87 – 1.75 (m, $1H_{CH2}$), 1.60 – 1.48 (m, $1H_{CH2}$), 1.33 (s, $3H_{Me}$), 1.07 (s, $3H_{Me}$), 0.89 (s, $9H_{TBS}$), 0.10 (s, $6H_{TBS}$).

^{13}C NMR (101 MHz, $CDCl_3$) δ 175.5, 94.8, 83.5, 82.1, 81.0, 78.8, 78.0, 77.4, 72.4, 70.6, 69.7, 61.1, 54.7, 37.7, 33.6, 27.7, 27.0, 26.9, 25.9, 20.6, 18.2, −4.5.

HRMS (ESI) calc. for $C_{26}H_{39}O_5Si$ $[M+H]^+$ 459.2561, found 459.2556.

256: (3a*R*,5a*S*,13a*R*)-9-((*tert*-Butyldimethylsilyl)oxy)-7-hydroxy-5,5-dimethyl-3,3a,5,5a,6,7,8,9,10,13-decahydro-2*H*-furo[3,2-*b*]indeno[4',5':5,6]cyclohepta[1,2-*c*]furan-2-one



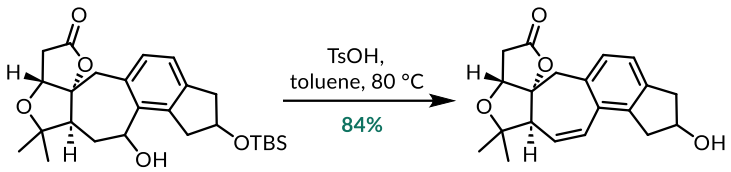
In a vial with triyne (9.4 mg, 0.021 mmol) and Wilkinson's catalyst (5.7 mg, 0.006 mmol, 30 mol%), atmosphere was changed to nitrogen and anhydrous $CHCl_3$ (2.0 mL) was added. The vial was capped and heated at 70 °C overnight. Volatiles were removed under reduced pressure. Purification by flash chromatography (pentane/EtOAc 1:2) afforded 6.1 mg (65%) of product as droplets on the vial wall.

^{1}H NMR (500 MHz, $CDCl_3$) δ 7.02 (dd, *J* = 15.9, 7.6 Hz, $1H_{Ar}$), 6.77 (t, *J* = 8.4 Hz, $1H_{Ar}$), 4.95 (m, $1H_{CH}$), 4.64 (qu, *J* = 6.9 Hz, $1H_{CH}$), 4.33 (dd, *J* = 8.6, 5.2 Hz, $1H_{CH}$), 3.61 (dd, *J* = 15.0, 8.7 Hz, $1H_{CH2\text{-}d}$), 3.41 (dd, *J* = 16.4, 6.6 Hz, $1H_{CH2\text{-}ab}$), 3.13 (td, *J* = 15.0, 6.7 Hz, $1H_{CH2\text{-}ab}$), 3.05 (dt, *J* = 15.0, 7.1 Hz, $1H_{CH2\text{-}ab}$), 2.89 – 2.78 (m, $1H_{CH2\text{-}ab}$+$1H_{CH2\text{-}c}$), 2.69 (dd, *J* = 18.3, 2.7 Hz, $1H_{CH2\text{-}c}$), 2.58 (dd, *J* = 15.0, 3.2 Hz, $1H_{CH2\text{-}d}$), 2.31 – 2.20 (m, $1H_{CH}$), 2.16 – 2.06 (m, $2H_{CH2\text{-}e}$), 1.36 (s, $3H_{Me}$), 1.21 (s, $3H_{Me}$), 0.91 (s, $9H_{TBS}$), 0.11 (s, $6H_{TBS}$).

^{13}C NMR (combined isomers, 126 MHz, $CDCl_3$) δ 174.9, 174.8, 171.3, 143.2, 142.7, 141.8, 141.5, 135.1, 134.8, 132.2, 130.8, 130.7, 130.6, 128.6, 124.8, 124.6, 98.9, 98.7, 84.8, 84.7, 79.5, 79.4, 74.0, 73.3, 71.8, 71.7, 60.5, 52.7, 52.1, 42.8, 42.4, 42.1, 42.0, 39.8, 39.6, 36.2, 36.1, 34.9, 34.5, 29.8, 29.2, 29.0, 26.1, 26.1, 22.6, 22.2, 21.2, 18.4, 18.4, 14.3, -4.5, -4.5, -4.6.

HRMS (ESI) calc. for $C_{26}H_{39}O_5Si$ $[M+H]^+$ 459.2561, found 459.2556.

257: (3a*R*,5a*S*,13a*R*)-9-Hydroxy-5,5-dimethyl-3,3a,5,5a,8,9,10,13-octahydro-2*H*-furo[3,2-*b*]indeno[4',5':5,6]cyclohepta[1,2-*c*]furan-2-one



256 257

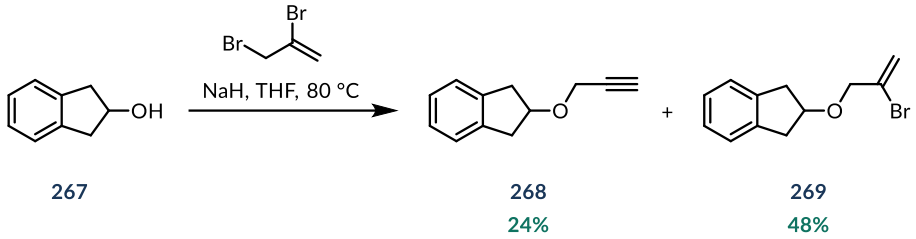
To a vial with starting material (6.0 mg, 0.013 mmol) in toluene (1.0 mL) was added *p*-TSA·H_2O (0.7 mg, 0.004 mmol, 30 mol%). The vial was capped and heated at 80 °C for 2 h. $NaHCO_3$ (sat.) and EtOAc were added and the organic layer was passed through a Pasteur pipette with $MgSO_4$ and concentrated. Purification by flash chromatography (DCM/MeOH 95:5) afforded 3.6 mg (84%) of the dehydrated-desilylated product as droplets on the vial wall.

^{1}H NMR (400 MHz, $CDCl_3$) δ 7.10 (d, *J* = 7.5 Hz, 1H_{Ar}), 6.96 (d, *J* = 7.5 Hz, 1H_{Ar}), 6.65 (dd, *J* = 12.1, 2.1 Hz, 1H_{alkene}), 5.83 (s br, 1H_{alkene}), 4.79 – 4.68 (m, 1H_{CH}), 4.32 (s br, 1H_{CH}), 3.28 – 3.08 (m, 2H_{CH2}), 2.97 – 2.83 (m, 3H_{CH2}+1H_{CH}), 2.72 (d, *J* = 18.7 Hz, 1H_{CH2}), 1.39 (s, 3H_{Me}), 0.87 (s br, 3H_{Me}).

^{13}C NMR (combined isomers, 126 MHz, $CDCl_3$) δ 174.8, 139.9, 139.8, 132.3, 132.2, 132.1, 132.1, 129.5, 129.5, 128.7, 128.6, 124.3, 73.0, 42.8, 41.4, 35.8, 29.9, 22.3.

HRMS (ESI) calc. for $C_{20}H_{23}O_4$ $[M+H]^+$ 327.1591, found 327.1588.

269: 2-((2-Bromoallyl)oxy)-2,3-dihydro-1*H*-indene



267 | 268 24% | 269 48%

To a solution of 2-indanol (150 mg, 1.12 mmol) in anhydrous THF (3.0 mL) under nitrogen atmosphere was added NaH (60% in oil, 89 mg, 2.24 mmol, 2.0 eq.) and the reaction mixture was stirred for 30 min at rt. Dibromopropene (447 mg, 2.24 mmol, 2.0 eq.) was added and the reaction mixture was refluxed overnight. Ether and water were added and the organic layer was washed with brine, dried ($MgSO_4$) and concentrated. Purification by flash chromatography (hexane/EtOAc 96:4) afforded 133 mg (48%, fraction 8-10) of the desired bromide **269** and 47 mg (24%, fraction 4-6) of the undesired alkyne **268**.

^{1}H NMR (400 MHz, $CDCl_3$) δ 7.24 – 7.20 (m, $2H_{Ar}$), 7.19 – 7.15 (m, $2H_{Ar}$), 5.94 – 5.92 (m, $1H_{alkene}$), 5.62 – 5.59 (m, $1H_{alkene}$), 4.45 (tt, *J* = 6.4, 4.5 Hz, $1H_{CH}$), 4.16 (s, $2H_{CH2\text{-}allylic}$), 3.19 (dd, *J* = 16.1, 6.4 Hz, $2H_{CH2\text{-}benzylic}$), 3.04 (dd, *J* = 16.1, 4.5 Hz, $2H_{CH2\text{-}benzylic}$).

^{13}C NMR (101 MHz, $CDCl_3$) δ 140.8, 129.8, 126.8, 124.8, 117.4, 80.3, 73.2, 39.4.

HRMS (ESI) calc. for $C_{12}H_{13}{}^{79}BrONa$ $[M+Na]^+$ 275.0042, found 275.0040.

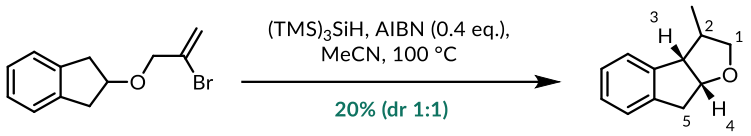
Undesired alkyne:

268: 2-(prop-2-yn-1-yloxy)-2,3-dihydro-1*H*-indene

^{1}H NMR (400 MHz, $CDCl_3$) δ 7.25 – 7.18 (m, $2H_{Ar}$), 7.19 – 7.13 (m, $2H_{Ar}$), 4.62 – 4.54 (m, $1H_{CH\text{-}O}$), 4.21 (dd, *J* = 2.4, 0.8 Hz, $2H_{CH2\text{-}allylic}$), 3.19 (dd, *J* = 16.1, 6.5 Hz, $2H_{CH2\text{-}indane}$), 3.02 (dd, *J* = 15.7, 4.7 Hz, $2H_{CH2\text{-}indane}$), 2.47 – 2.40 (m, $1H_{alkyne}$).

^{13}C NMR (101 MHz, $CDCl_3$) δ 140.7, 126.7, 124.8, 80.1, 79.7, 74.3, 56.3, 39.2.

270: (3a*S,8a*R**)-3-Methyl-3,3a,8,8a-tetrahydro-2*H*-indeno[2,1-*b*]furan**



269 270

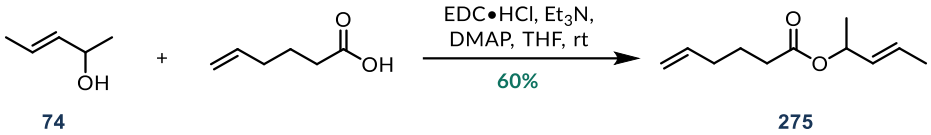
To a vial with bromoalkene (15.0 mg, 0.059 mmol), $(TMS)_3SiH$ (37 µL, 0.119 mmol, 2.0 eq.) and AIBN (3.9 mg, 0.024 mmol, 0.4 eq.) was added MeCN (1.2 mL), and the solvent was bubbled with N_2 for 5 min. The vial was capped and heated at 100 °C for 4 h. The reaction was analysed by taking a 40 µL aliquot to which an internal standard and EtOAc were added to 1.0 mL and analysed using GC-MS. The reaction mixture was concentrated and the crude product was purified by flash chromatography (Hex/EtOAc 96:4) to give 3.5 mg (34%) of dehalogenated product and 2.1 mg (20%) of cyclised product as droplets on the vial wall as an inseparable mixture of diastereomers (1:1).

^{1}H NMR (500 MHz, $CDCl_3$) δ 7.23 – 7.17 (m, $4H_{Ar}$), 4.98 (td, *J* = 6.9, 2.1 Hz, $1H_4$), 3.86 (dd, *J* = 8.3, 6.6 Hz, $1H_1$), 3.81 – 3.77 (m, $1H_3$), 3.26 – 3.11 (m, $1H_5$+$1H_1$), 3.04 (dd, *J* = 17.6, 2.1 Hz, $1H_5$), 2.66 – 2.55 (m, $1H_2$), 1.02 (d, *J* = 7.0 Hz, $3H_{Me}$).

^{13}C from HSQC NMR (126 MHz, $CDCl_3$) δ 127.0 (C_{Ar}), 126.4 (C_{Ar}), 124.8 (C_{Ar}), 124.4 (C_{Ar}), 83.7 (C_4), 73.6 (C_1), 53.4 (C_3), 40.4 (C_5), 37.9 (C_2), 13.1 (C_{Me})

7.7 Procedures and characterisation from Chapter 6

275: (*E*)-Pent-3-en-2-yl hex-5-enoate



74 275

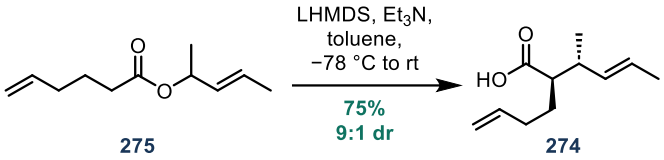
To a flask with crude alcohol (700 mg, 8.13 mmol) and acid (1.10 g, 9.75 mmol, 1.2 eq.) was added anhydrous THF (8.2 mL) under nitrogen atmosphere. EDC·HCl (2.34 g, 12.2 mmol, 1.5 eq.), Et_3N (2.3 mL, 16.3 mmol, 2.0 eq.) and DMAP (99 mg, 0.80 mmol, 10 mol%) were added at 0 °C and the mixture was stirred overnight at rt. Diluted HCl (1 M) and ether were added and the organic layer was washed with $NaHCO_3$ (sat.), brine, dried ($MgSO_4$) and concentrated. Purification by flash chromatography (hexane/EtOAc 96:4) afforded 899 mg (60% over two steps) of oil. The product should not be dried on high-vac due to its volatility.

^{1}H NMR (500 MHz, $CDCl_3$) δ 5.84 – 5.66 (m, $1H_{CH\text{-}int.alkene}$+$1H_{CH\text{-}term.alkene}$), 5.51 – 5.43 (m, $1H_{CH\text{-}int.alkene}$), 5.31 (p, *J* = 6.5 Hz, $1H_{CH\text{-}allylic}$), 5.06 – 4.94 (m, $2H_{CH2\text{-}alkene}$), 2.32 – 2.25 (m, $2H_{CH2}$), 2.13 – 2.04 (m, $2H_{CH2}$), 1.76 – 1.67 (m, $2H_{CH2}$+$3H_{Me}$), 1.28 (d, *J* = 6.4 Hz, $3H_{Me}$).

^{13}C NMR (126 MHz, $CDCl_3$) δ 173.0, 137.9, 131.0, 128.2, 115.4, 71.1, 34.1, 33.2, 24.3, 20.5, 17.8.

HRMS (ESI) calc. for $C_{11}H_{19}O_2$ $[M+H]^+$ 183.1380, found 183.1380.

274: (2*R,3*R**,*E*)-2-(But-3-en-1-yl)-3-methylhex-4-enoic acid**



A flask with HMDS (3.19 mL, 15.3 mmol, 3.1 eq.) and anhydrous toluene (112 mL) was cooled to −78 °C under nitrogen atmosphere. *n*-BuLi (2.3 M, 6.30 mL, 14.8 mmol, 3.0 eq.) was added dropwise and the mixture was stirred for 10 min at −78 °C. Anhydrous Et_3N (20 mL) was added fast dropwise, followed by slow addition of the substrate (899 mg, 4.93 mmol) in anhydrous toluene (17 mL) over 50 min. This slow addition prevents local excess of the starting ester in presence of its enolate, which results in an undesired Claisen condensation reaction. The reaction mixture was left to warm to rt over 5 h. The acid product was purified by an acid-base extraction procedure. First, $NaHCO_3$ and Et_2O were added and the water layer was separated and acidified with conc. HCl to pH ≤ 2. This was then extracted with Et_2O (×2) and the combined ether layers were dried ($MgSO_4$) and concentrated to obtain 672 mg (75%) of yellow oil.

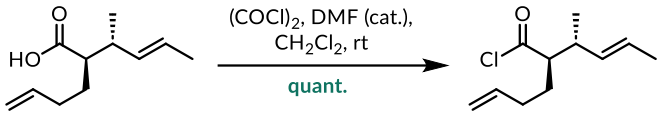
^{1}H NMR (400 MHz, $CDCl_3$) δ 5.77 (ddt, *J* = 16.9, 10.2, 6.5 Hz, $1H_{CH\text{-}term.alkene}$), 5.53 – 5.41 (m, $1H_{CH\text{-}int.alkene}$), 5.22 (ddd, *J* = 15.2, 8.7, 1.6 Hz, $1H_{CH\text{-}int.alkene}$), 5.07 – 4.92 (m, $2H_{CH2\text{-}alkene}$), 2.42 – 2.29 (m, $1H_{CH\text{-}allylic}$), 2.25 – 2.06 (m, $1H_{CH\text{-}α\text{-}carbonyl}$+$1H_{CH2}$), 2.05 – 1.94 (m, $1H_{CH2}$), 1.69 – 1.59 (m, $2H_{CH2}$+$3H_{Me}$), 1.03 (d, *J* = 6.7 Hz, $3H_{Me}$).

^{13}C NMR (101 MHz, $CDCl_3$) δ C(carboxylic acid), 138.0, 133.9, 126.1, 115.3, 51.1, 39.8, 31.9, 29.6, 19.3, 18.0.

HRMS (ESI) calc. for $C_{11}H_{17}O_2$ $[M-H]^-$ 181.1234, found 181.1229.

The stereochemistry of the double bond was assigned based on the chair-like transition state model of Claisen rearrangement and by analogy to a close literature example (Figure 76b).

280: (2*R,3*R**,*E*)-2-(But-3-en-1-yl)-3-methylhex-4-enoyl chloride**



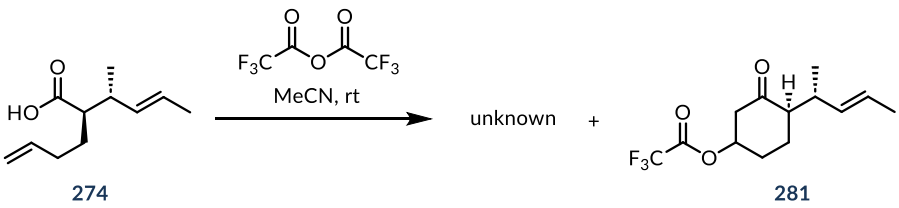
274 280

To a solution of acid (15 mg, 0.082 mmol) in dry CH_2Cl_2 (1.3 mL) under N_2 was added one drop of DMF. Oxalyl chloride (8 µL, 0.090 mmol, 1.1 eq.) was slowly added via microsyringe at rt, and the mixture was stirred for 1 h at rt. Solvent was evaporated, and the crude product was immediately used in the next step, after confirming complete conversion of acid to acyl chloride by ^{1}H NMR.

^{1}H NMR (400 MHz, $CDCl_3$) δ 5.74 (ddt, *J* = 17.0, 10.2, 6.6 Hz, $1H_{CH\text{-}term.alkene}$), 5.59 – 5.46 (m, $1H_{CH\text{-}int.alkene}$), 5.18 (ddd, *J* = 15.2, 8.6, 1.6 Hz, $1H_{CH\text{-}int.alkene}$), 5.08 – 4.96 (m, $2H_{CH2\text{-}term.alkene}$), 2.64 – 2.57 (m, $1H_{CH}$), 2.57 – 2.47 (m, $1H_{CH}$), 2.22 – 2.10 (m, $1H_{CH2}$), 2.07 – 1.93 (m, $1H_{CH2}$), 1.81 – 1.69 (m, $2H_{CH2}$), 1.67 (dd, *J* = 6.4, 1.6 Hz, $3H_{Me\text{-}alkene}$), 1.08 (d, *J* = 6.6 Hz, $3H_{Me\text{-}aliphatic}$).

Peaks were assigned by analogy to 274.

281: (4*R)-3-Oxo-4-((*R**,*E*)-pent-3-en-2-yl)cyclohexyl 2,2,2-trifluoroacetate**

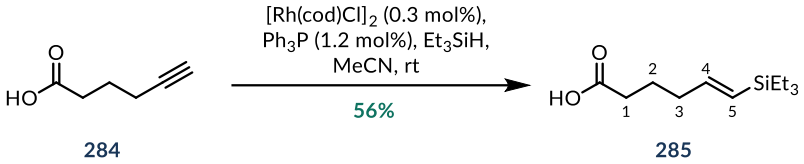


274 281

2 h	0%	44%	23%
6 h	0%	27%	45%
o/n	0%	0%	97%
			Mixture on workup

This is not a preparative procedure. To a septum sealed vial with acid (5.3 mg, 0.029 mmol) and anhydrous MeCN (1.4 mL) under N_2 and at 0 °C was dropwise added trifluoroacetic anhydride (8.2 µL, 0.058 mmol, 2.0 eq.). The reaction mixture was stirred at rt. During this time, aliquotes were taken at interval of 2, 6 and 16 h and analyzed by GC-MS using *n*-decane as an internal standard (2.8 µL, 0.015 mmol, 0.5 eq.). Two new peaks were observed, which were tentatively assigned to 281 based on the m/z ratio and an unknown intermediate. Sat. $NaHCO_3$ and ether were added and the organic layer was washed with brine, dried ($MgSO_4$) and concentrated. When this this crude product was analyzed by GC-MS, the peak corresponding to 281 was not present. Purification by flash chromatography (pent/EtOAc 95:5) gave a mixture of unidentifiable products.

285: (*E*)-6-(Triethylsilyl)hex-5-enoic acid



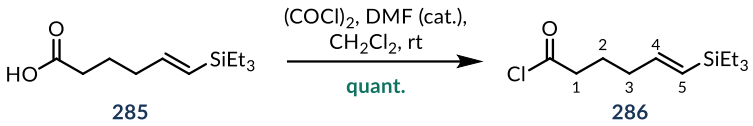
284 285

This is not a preparative procedure. To a solution of acid (100 mg, 0.89 mmol) in MeCN (1.4 mL) were added Et_3SiH (214 µL, 1.34 mmol, 1.5 eq.), $[Rh(cod)Cl]_2$ (1.3 mg, 0.003 mmol, 0.3 mol%) and PPh_3 (2.8 mg, 0.011 mmol, 1.2 mol%). The reaction mixture was stirred for 2 days at rt. Solvent was evaporated and the crude product was purified by flash chromatography (pent/EtOAc 75:25) to afford 114 mg (56%) of clear oil.

^{1}H NMR (400 MHz, $CDCl_3$) δ 5.99 (dt, *J* = 18.7, 6.3 Hz, $1H_4$), 5.59 (dt, *J* = 18.7, 1.5 Hz, $1H_5$), 2.35 (t, *J* = 7.6 Hz, $2H_{CH2\text{-}1}$), 2.23 – 2.09 (m, $2H_{CH2}$), 1.81 – 1.69 (m, $2H_{CH2}$), 0.92 (t, *J* = 7.8 Hz, $9H_{SiEt3}$), 0.54 (q, *J* = 7.8 Hz, $6H_{SiEt3}$).

HRMS (ESI) calc. for $C_{12}H_{22}O_2Si$ $[M-H]^-$ 227.1473, found 227.1468.

286: (*E*)-6-(Triethylsilyl)hex-5-enoyl chloride



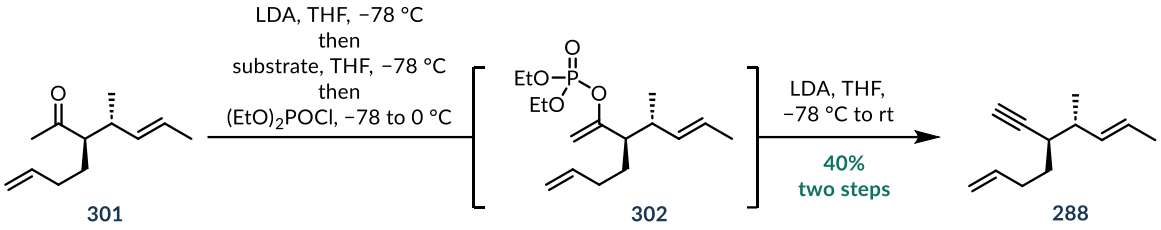
285 286

To a solution of acid (30 mg, 0.131 mmol) in dry CH_2Cl_2 (2.0 mL) under N_2 was added one drop of DMF. Oxalyl chloride (13 µL, 0.144 mmol, 1.1 eq.) was slowly added at rt, and the mixture was stirred until bubbles were no longer evolving (1 h). Solvent was evaporated, and the crude product was immediately used in the next step.

^{1}H NMR (400 MHz, $CDCl_3$) δ 5.95 (dt, *J* = 18.7, 6.3 Hz, $1H_4$), 5.61 (dt, *J* = 18.7, 1.5 Hz, $1H_5$), 2.88 (t, *J* = 7.3 Hz, $2H_{CH2\text{-}1}$), 2.24 – 2.16 (m, $2H_{CH2\text{-}3}$), 1.83 (p, *J* = 7.3 Hz, $2H_{CH2\text{-}2}$), 0.93 (t, *J* = 7.9 Hz, $9H_{SiEt3}$), 0.55 (q, *J* = 7.9 Hz, $6H_{SiEt3}$).

Peaks were assigned by analogy to 285.

288: (5*R,6*R**,*E*)-5-Ethynyl-6-methylnona-1,7-diene**

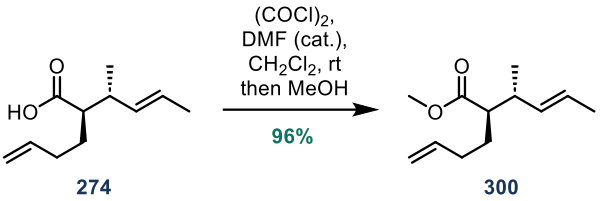


A solution of LDA [prepared by addition of *n*-BuLi (2.3 M, 159 µL, 0.37 mmol, 1.2 eq.) to a solution of i-Pr_2NH (56 µL, 0.40 mmol, 1.3 eq.) in anhydrous THF (0.5 mL) under N_2 at 0 °C, then stirred for 10 min] was cooled to −78 °C, and a solution of ketone (55 mg, 0.31 mmol, 1.0 eq.) in THF (0.5 mL) was added over 7 min and left to stir for 1 h at −78 °C. Chlorophosphate (49 µL, 0.34 mmol, 1.1 eq.) was added via microsyringe at −78 °C, and the reaction mixture stirred in ice-bath for 4 h. A separate solution of LDA was prepared by addition of *n*-BuLi (2.3 M, 305 µL, 0.70 mmol, 2.3 eq.) to a solution of i-Pr_2NH (108 µL, 0.76 mmol, 2.5 eq.) in anhydrous THF (0.7 mL) under N_2 at −78 °C, then stirred for 15 min. The reaction mixture containing the vinyl phosphate was added to the newly prepared LDA solution at −78 °C, and then left to warm to rt over 3.5 h. Sat. aq. NH_4Cl and Et_2O were added, and the organic layer was separated, washed with brine, dried ($MgSO_4$) and concentrated (without high-vac). Purification by flash chromatography (Hex/EtOAc 99:1) afforded 44 mg (40% over two steps from acid **274**) of colourless oil. The product was not dried on high-vac due to its volatility. Electrospray ionisation was unsuccessful for the analysis of this compound, likely due to the absence of ionisable functional groups.

^{1}H NMR (400 MHz, $CDCl_3$) δ 5.87 – 5.75 (m, $1H_{CH\text{-}term.alkene}$), 5.51 – 5.41 (m, $1H_{CH\text{-}int.alkene}$), 5.40 – 5.32 (m, $1H_{CH\text{-}int.alkene}$), 5.11 – 4.92 (m, $2H_{CH2\text{-}term.alkene}$), 2.36 – 2.22 (m, $1H_{CH}$+$1H_{CH2\text{-}a}$), 2.20 – 2.11 (m, $1H_{CH}$+$1H_{CH2\text{-}a}$), 2.07 (d, J = 2.4 Hz, $1H_{alkyne}$), 1.69 – 1.64 (m, $3H_{Me}$), 1.59 – 1.43 (m, $2H_{CH2\text{-}b}$), 1.08 (d, J = 6.7 Hz, $3H_{Me}$).

^{13}C NMR (101 MHz, $CDCl_3$) δ 138.4, 135.2, 124.9, 115.0, 86.3, 70.6, 40.7, 37.3, 32.1, 31.8, 18.1, 17.7.

300: Methyl (2*R,3*R**,*E*)-2-(But-3-en-1-yl)-3-methylhex-4-enoate**



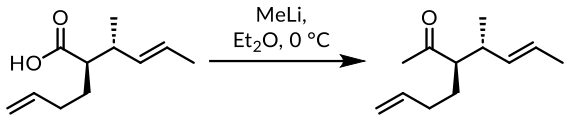
To a solution of the substrate (110 mg, 0.60 mmol) in anhydrous CH_2Cl_2 (9.1 mL) under nitrogen atmosphere was added oxalyl chloride (58 µL, 0.66 mmol, 1.1 eq.) via microsyringe. The mixture was stirred at rt until gas evolution ceased (1 h). Then, MeOH (244 µL, 6.04 mmol, 10 eq.) was added and the mixture was stirred for 15 min at rt. $NaHCO_3$ and Et_2O were added, and the organic later was passed through a Pasteur pipette with $MgSO_4$ and concentrated to give 113 mg (96%) of the pure oily product. The only side product, dimethyl oxalate (^{1}H NMR δ 3.91), was removed by drying the product on high-vac for a short period of time.

^{1}H NMR (400 MHz, $CDCl_3$) δ 5.74 (ddt, *J* = 16.9, 10.2, 6.7 Hz, $1H_{CH\text{-}term.alkene}$), 5.49 – 5.38 (m, $1H_{CH\text{-}int.alkene}$), 5.19 (ddd, *J* = 15.2, 8.6, 1.7 Hz, $1H_{CH\text{-}int.alkene}$), 5.07 – 4.90 (m, $2H_{CH2\text{-}alkene}$), 3.67 (s, $3H_{OMe}$), 2.35 – 2.24 (m, $1H_{CH}$), 2.22 – 2.09 (m, $1H_{CH}$), 2.08 – 1.85 (m, $2H_{CH2}$), 1.72 – 1.53 (m, $2H_{CH2}$+$3H_{Me}$), 0.94 (d, *J* = 6.7 Hz, $3H_{Me}$).

^{13}C NMR (101 MHz, $CDCl_3$) δ 176.2, 138.1, 134.3, 125.7, 115.1, 51.4, 51.3, 40.1, 32.0, 29.9, 19.3, 18.0.

HRMS (ESI) calc. for $C_{12}H_{21}O_2$ $[M+H]^+$ 197.1536, found 197.1535.

301: (3*R,4*R**,*E*)-3-(But-3-en-1-yl)-4-methylhept-5-en-2-one**



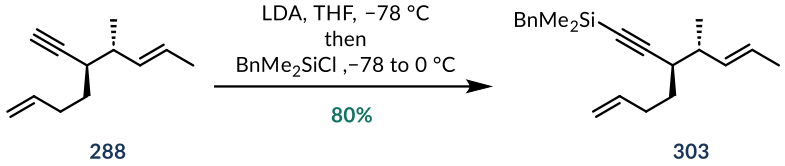
274 301

To a solution of acid (61 mg, 0.33 mmol) in anhydrous Et_2O (2.0 mL) under N_2 and at 0 °C was added MeLi (1.6 M, 411 µL, 0.67 mmol, 2.0 eq.) dropwise over 5 min. The reaction mixture was left in ice-bath for 30 min, and then stirred at rt for additional 30 min. The reaction mixture initially turned cloudy, but cleared after some time. The reaction was carefully quenched with sat. aq. NH_4Cl and Et_2O was added. The organic layer was separated, washed with brine, dried ($MgSO_4$) and concentrated without high-vac. The crude gel-like product was directly used in the next step.

^{1}H NMR (400 MHz, $CDCl_3$) δ 5.73 (ddt, *J* = 17.0, 10.3, 6.7 Hz, $1H_{CH\text{-}term.alkene}$), 5.50 – 5.35 (m, $1H_{CH\text{-}int.alkene}$), 5.28 – 5.13 (m, $1H_{CH\text{-}int.alkene}$), 5.03 – 4.89 (m, $2H_{CH2\text{-}term.alkene}$), 2.37 – 2.25 (m, $1H_{CH}$+$1H_{CH}$), 2.12 (s, $3H_{Me\text{-}ketone}$), 2.03 – 1.82 (m, $2H_{CH2}$), 1.65 (dd, *J* = 6.4, 1.6 Hz, $3H_{Me\text{-}alkene}$), 1.62 – 1.48 (m, $2H_{CH2}$), 0.93 (d, *J* = 6.3 Hz, $3H_{Me\text{-}aliphatic}$).

^{13}C NMR (101 MHz, $CDCl_3$) δ 212.9, 138.3, 134.2, 125.7, 115.1, 58.2, 39.6, 31.9, 30.6, 29.1, 19.2, 18.0.

303: Benzyl((3*R,4*R**,*E*)-3-(but-3-en-1-yl)-4-methylhept-5-en-1-yn-1-yl)dimethylsilane**



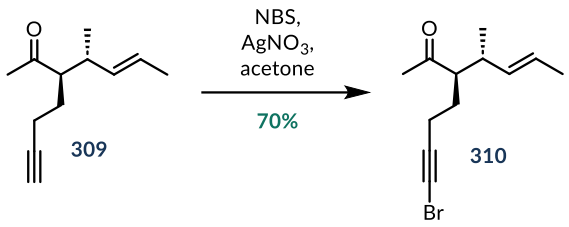
A solution of *i*-Pr_2NH (58 µL, 0.19 mmol, 3.2 eq.) in anhydrous THF (0.5 mL) was cooled to 0 °C under nitrogen atmosphere. *n*-BuLi (2.3 M, 169 µL, 0.39 mmol, 3.0 eq.) was added dropwise at 0 °C and stirred for 5 min at this temperature. The reaction mixture was cooled to −78 °C and a solution of the substrate (21 mg, 0.13 mmol) in anhydrous THF (0.5 mL) was added dropwise and stirred for 25 min at −78 °C. $BnMe_2SiCl$ (36 µL, 0.19 mmol, 1.5 eq.) was added via microsyringe and the reaction mixture was allowed to naturally warm to rt over 4 h. NH_4Cl (sat.) and Et_2O were added and the organic layer was separated, passed through a Pasteur pipette with silica and concentrated (30 °C, 200 mbar). Purification by flash chromatography (hexane/EtOAc 99:1) afforded 32 mg (80%) of clear oil.

^{1}H NMR (400 MHz, $CDCl_3$) δ 7.25 – 7.17 (m, $2H_{Bn}$), 7.14 – 7.02 (m, $3H_{Bn}$), 5.90 – 5.75 (m, $1H_{CH\text{-}term.alkene}$), 5.49 – 5.39 (m, $1H_{CH\text{-}int.alkene}$), 5.37 – 5.30 (m, $1H_{CH\text{-}int.alkene}$), 5.08 – 4.94 (m, $2H_{CH2\text{-}alkene}$), 2.40 – 2.05 (m, $1H_{CH}$+$1H_{CH}$+$2H_{CH2\text{-}Bn}$+$2H_{CH2}$), 1.68 (d, J = 6.2 Hz, $3H_{Me}$), 1.58 – 1.39 (m, $2H_{CH2}$), 1.06 (d, J = 6.7 Hz, $3H_{Me}$), 0.13 (s, $6H_{SiMe}$).

^{13}C NMR (101 MHz, $CDCl_3$) δ 139.5, 138.6, 135.3, 128.5, 128.5, 128.4, 128.2, 114.9, 110.6, 85.2, 40.9, 38.5, 31.8, 31.8, 24.8, 18.1, 18.0, -1.6.

HRMS (ESI) calc. for $C_{21}H_{32}Si$ $[M+H]^+$ 311.2190, found 311.2187.

310: (3*R,4*R**,*E*)-3-(4-Bromobut-3-yn-1-yl)-4-methylhept-5-en-2-one**



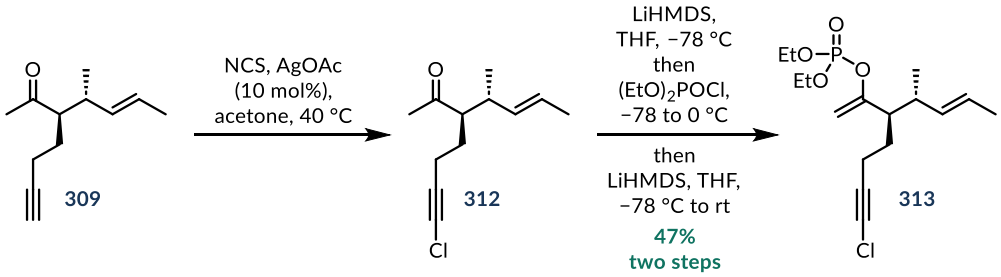
To a solution of ketone (27.0 mg, 0.151 mmol) in ordinary acetone (0.6 mL) under N_2 were added $AgNO_3$ (3.3 mg, 0.019 mmol, 13 mol%) and NBS (35.1 mg, 0.197 mmol, 1.3 eq.). The vial was capped and stirred for 1 h at rt. Solvent was evaporated (100 mbar, 30 °C), pentane was added and evaporated again to remove all acetone. Residual acetone dissolves succinimide side product which reduces the purity of the desired product. Pentane was added again, and the resulting heterogenous mixture was filtered through a SiO_2 filled Pasteur pipette and washed with additional pentane. Evaporation on a rotavap (100 mbar, 30 °C) afforded 27 mg (70%) of oil.

^{1}H NMR (400 MHz, $CDCl_3$) δ 5.52 – 5.36 (m, $1H_{alkene}$), 5.20 (dd, *J* = 15.2, 8.3, $1H_{alkene}$), 2.55 – 2.42 (m, $1H_{CH}$), 2.42 – 2.28 (m, $1H_{CH}$), 2.24 – 2.17 (m, $1H_{CH2\text{-}a}$), 2.16 (s, $3H_{Me\text{-}ketone}$), 2.12 – 2.00 (m, $1H_{CH2\text{-}a}$), 1.83 – 1.61 (m, $2H_{CH2\text{-}b}$), 1.66 (dd, *J* = 6.4, 1.6 Hz, $3H_{Me\text{-}alkene}$), 0.97 (d, *J* = 6.7 Hz, $3H_{Me\text{-}aliphatic}$).

Due to instability of the brominated alkyne, it was used in the next step on the same day, without purification and only ^{1}H NMR was collected. Assigned by analogy to 309.

313: (3*R,4*R**,*E*)-3-(4-Chlorobut-3-yn-1-yl)-4-methylhepta-1,5-dien-2-yl diethyl phosphate**

312: (3*R,4*R**,*E*)-3-(4-Chlorobut-3-yn-1-yl)-4-methylhept-5-en-2-one**



To a vial with ketone (37 mg, 0.21 mmol) under N_2 were quickly added silver(I) acetate (3.5 mg, 0.02 mmol, 10 mol%), acetone (1.1 mL) and N-chlorosuccinamide (33 mg, 0.25 mmol, 1.2 eq.). The vial was capped and stirred at 40 °C overnight. Solvent was completely evaporated (100 mbar, 30 °C). Pentane was added, and the mixture was filtered through a silica filled Pasteur pippette and washed with pentane. Concentration on a rotavap (100 mbar, 30 °C) afforded 53 mg of the crude product which was used in the next step without purification.

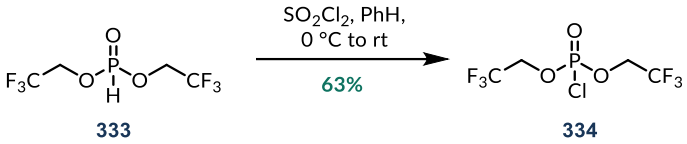
A solution of LiHMDS was prepared by addition of *n*-BuLi (2.3 M, 108 µL, 0.45 mmol, 1.2 eq.) to a solution of HMDS (56 µL, 0.27 mmol, 1.3 eq.) in THF (0.4 mL) at 0 °C. This LiHMDS solution was cooled to −78 °C, and a solution of the crude ketone from the previous step (0.21 mmol if quant. yield of the previous reaction is assumed, 1.0 eq.) in THF (0.3 mL) was added dropwise and stirred for 30 min at −78 °C. Chlorophosphate (33 µL, 0.23 mmol, 1.1 eq.) was added via microsyringe at −78 °C and the reaction mixture was allowed to warm to rt over 2.5 h to form vinyl phosphate. In an unsuccessful attempt to eliminate the phosphate, this solution was added to a freshly prepared LiHMDS [HMDS (108 µL, 0.52 mmol, 2.5 eq.), *n*-BuLi (2.3 M, 207 µL, 0.48 mmol, 2.3 eq.), THF (0.5 mL)] at −78 °C and allowed to warm to rt, however TLC remained unchanged. Sat. aq. NH_4Cl and Et_2O were added, and the organic layer was separated, washed with brine, dried ($MgSO_4$) and concentrated. Purification by flash chromatography (pent/EtOAc 75:25) afforded 34 mg of white solid (47% over two steps). Partial hydrolysis of the vinyl phosphate was observed during chromatography.

^{1}H NMR (500 MHz, $CDCl_3$) δ 5.46 – 5.36 (m, $1H_{CH\text{-}int.alkene}$), 5.22 – 5.14 (m, $1H_{CH\text{-}int.alkene}$), 4.96 (br s, $1H_{CH2\text{-}term.alkene}$), 4.49 (br s, $1H_{CH2\text{-}term.alkene}$), 4.20 – 4.07 (m, $4H_{CH2\text{-}phosphate}$), 2.30 – 2.20 (m, $1H_{CH2\text{-}a}$), 2.17 – 2.06 (m, $1H_{CH2\text{-}a}$+$1H_{CH}$), 1.97 – 1.85 (m, $1H_{CH}$), 1.75 – 1.67 (m, $1H_{CH2\text{-}b}$), 1.65 (d, J = 6.4 Hz, $3H_{Me\text{-}alkene}$), 1.52 – 1.42 (m, $1H_{CH2\text{-}b}$), 1.35 (t, J = 7.1 Hz, $6H_{Me\text{-}phosphate}$), 0.98 (d, J = 6.7 Hz, $3H_{Me\text{-}aliphatic}$).

^{13}C NMR (126 MHz, $CDCl_3$) δ 154.6 (d, $J_{C\text{-}P}$ = 9.5 Hz), 135.1, 125.6, 98.5 (d, $J_{C\text{-}F}$ = 2.7 Hz), 69.5, 64.4 (d, $J_{C\text{-}P}$ = 6.1 Hz), 57.2, 50.4 (d, $J_{C\text{-}F}$ = 7.1 Hz), 39.0, 28.6, 19.7, 18.0, 16.9, 16.2 (d, $J_{C\text{-}F}$ = 6.7 Hz).

HRMS (ESI) calc. for $C_{16}H_{27}{}^{35}ClO_4P$ $[M+H]^+$ 349.1330, found 349.1326.

334: Bis(2,2,2-trifluoroethyl) phosphorochloridate



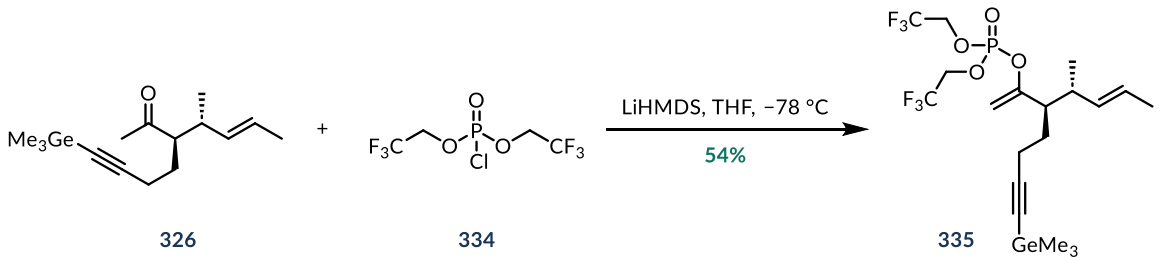
Synthesised according to the literature procedure.[128] A solution of the substrate (1.80 g, 6.58 mmol) in anhydrous benzene (2.0 mL) was cooled to 0 °C under nitrogen atmosphere. $SOCl_2$ (714 µL, 7.90 mmol, 1.2 eq.) was added dropwise and the reaction mixture was stirred for 15 min at 0 °C and then for 2 h at rt. Volatiles were removed under reduced pressure. The product was purified by distillation under reduced pressure (86-88 °C/36 mbar) to give 1.16 g (63%) of clear liquid.

^{1}H NMR (400 MHz, $CDCl_3$) δ 4.57 – 4.46 (m, 1H).

^{31}P NMR (162 MHz, $CDCl_3$) δ 5.72.

Data in agreement with the literature values.[128]

3335: (3*R*,4*R*,*E*)-4-methyl-3-(4-(trimethylgermyl)but-3-yn-1-yl)hepta-1,5-dien-2-yl bis(2,2,2-trifluoroethyl) phosphate



326 334 335

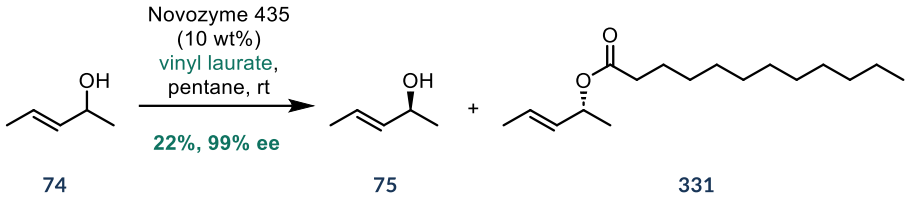
To a solution of HMDS (37 µL, 0.18 mmol, 1.3 eq.) in anhydrous THF (0.4 mL) at −78 °C under nitrogen atmosphere, *n*-BuLi (2.3 M, 71 µL, 0.16 mmol, 1.2 eq.) was added dropwise and the solution was stirred for 10 min at −78 °C. The substrate (40 mg, 0.14 mmol) in anhydrous THF (0.2 mL) was added dropwise and the reaction mixture was stirred for 20 min at −78 °C. Chlorophosphate (42 mg, 0.15 mmol, 1.1 eq.) was added via microsyringe and the reaction mixture was stirred for 30 min at −78 °C. Complete conversion to the product was confirmed by TLC and the reaction was quenched with NH_4Cl (sat.) and allowed to warm to rt. NH_4Cl (sat.) and Et_2O were added and the organic layer was passed through a Pasteur pipette with $MgSO_4$ and concentrated. Purification by flash chromatography (pentane/EtOAc 9:1) afforded 32 mg (54 %) of oil. Chromatography should be performed fast to avoid product decomposition due to prolonged contact with silica.

^{1}H NMR (400 MHz, $CDCl_3$) δ 5.50 – 5.38 (m, $1H_{CH\text{-}alkene}$), 5.18 (ddd, J = 15.2, 8.5, 1.6 Hz, $1H_{CH\text{-}alkene}$), 5.01 – 4.97 (m, $1H_{CH2\text{-}alkene}$), 4.61 (dd, J = 3.0, 2.3 Hz, $1H_{CH2\text{-}alkene}$), 4.48 – 4.36 (m, $4H_{CH2\text{-}phosphate}$), 2.34 – 2.20 (m, $1H_{CH2\text{-}a}$), 2.17 – 2.00 (m, $1H_{CH2\text{-}a}$+$1H_{CH}$+$1H_{CH}$), 1.80 – 1.70 (m, $1H_{CH2\text{-}b}$), 1.66 (dd, J = 6.4, 1.7 Hz, $3H_{Me}$), 1.53 – 1.38 (m, $1H_{CH2\text{-}b}$), 0.98 (d, J = 6.6 Hz, $3H_{Me}$), 0.32 (s, $9H_{GeMe}$).

^{13}C NMR (101 MHz, $CDCl_3$) δ 155.0 (d, $J_{C\text{-}P}$ = 10 Hz), 134.7, 125.8, 122.3 (qd, $J_{C\text{-}F}$ = 278 Hz, $J_{C\text{-}P}$ = 9.8 Hz), 105.3, 99.8 (d, $J_{C\text{-}P}$ = 2.8 Hz), 84.7, 65.9 – 62.8 (m), 50.0 (d, $J_{C\text{-}P}$ = 7.0 Hz), 38.7, 28.7, 19.4, 18.0, 17.9, 0.02.

HRMS (ESI) calc. for $C_{19}H_{31}F_6{}^{74}GeO_4P$ $[M+H]^+$ 541.0992, found 541.0981.

75: (*S*,*E*)-pent-3-en-2-ol



The title compound could be prepared following the literature procedure,[60] using vinyl acetate with Novozym 435, with the resulting acetate by-product separated by chromatography to give the desired alcohol in 39% yield, 99% ee. An alternative method which avoids chromatography by using vinyl laurate and distillation for purification is reported here to give the enantiopure alcohol in 22% yield, 99% ee.

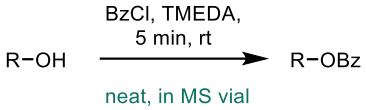
To a mixture of alcohol (1.76 g, 20 mmol), vinyl laurate (27 mL, 102 mmol, 5.0 eq.) and pentane (12 mL) was added Novozym 435 (176 mg, 10 wt%) and the mixture was stirred for 1 h at rt. Residual enzyme was removed by filtration through cotton wool and pentane was removed on a rotary evaporator (150 mbar, 30 °C). Conversion was determined by quantitative NMR before purification. Ratio of alcohol (δ 4.25) to ester (δ 5.31) was 43:57. Distillation under reduced pressure (50-60 °C/30 mbar) afforded 0.39 g (22%, 99% ee) of the desired enantioenriched alcohol as a clear liquid.

^{1}H NMR (400 MHz, $CDCl_3$) δ 5.72 – 5.59 (m, $1H_{alkene}$), 5.53 (ddq, J = 15.3, 6.5, 1.5 Hz, $1H_{alkene}$), 4.25 (qu, J = 6.5 Hz, $1H_{CH}$), 1.68 (d, J = 6.5 Hz, $3H_{Me}$), 1.25 (d, J = 6.5 Hz, $3H_{Me}$).

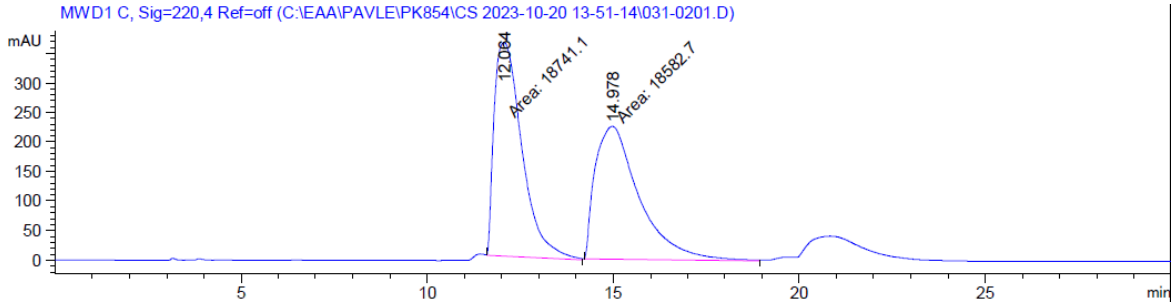
Data in agreement with the literature values.[60] Stereochemistry was assigned by analogy to the literature where vinyl acetate was used as acyl donor. Ester 331 was never isolated and characterised, except for an observed chemical shift at 5.31 ppm.

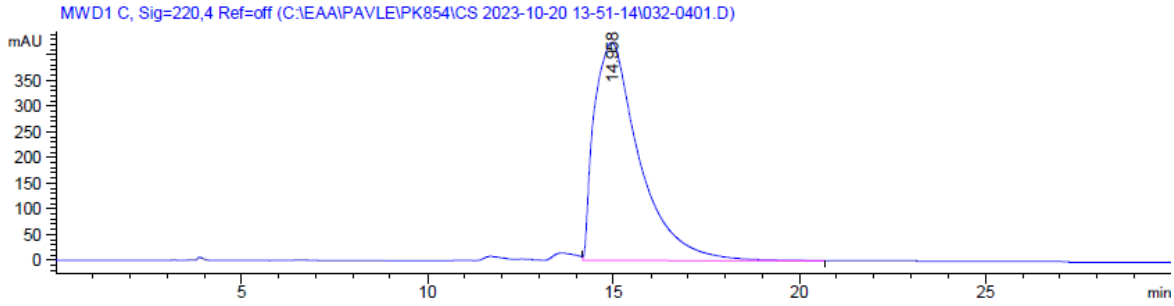
HPLC sample preparation. A sample for a chiral UV-HPLC analysis was prepared in the following way. A reaction mixture aliquot (40 µL) was mixed in a vial with TMEDA (50-100 µL) and benzoyl chloride (50-100 µL). The mixture was allowed to stand for 5-10 min at rt. Hexane

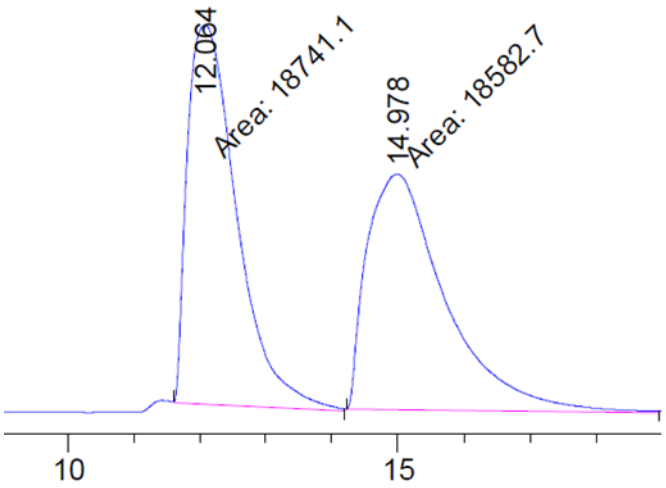
was added to the total volume of 1 mL, and the white precipitate was removed by filtration through a microfilter (PTFE, 0.2 µm) to give a clear solution ready for analysis.



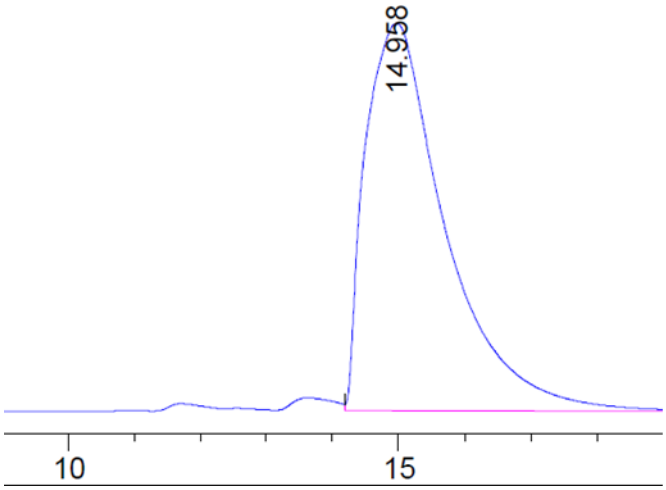
HPLC analysis. Chiralpak IB 5 µm, 4.6×150 mm, 0.5% IPA in hexane, flow 1 mL/min, injection volume 5 µL, detection wavelength 220 nm.





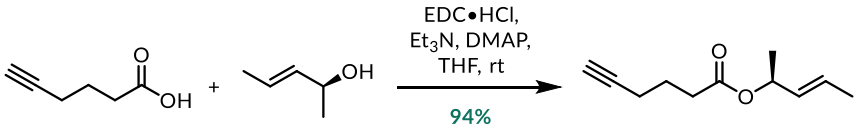


Peak #	RetTime [min]	Area %
1	12.064	50.2123
2	14.978	49.7877



Peak #	RetTime [min]	Area %
1	14.958	100.0000

307: (*S*,*E*)-pent-3-en-2-yl hex-5-ynoate



75 307

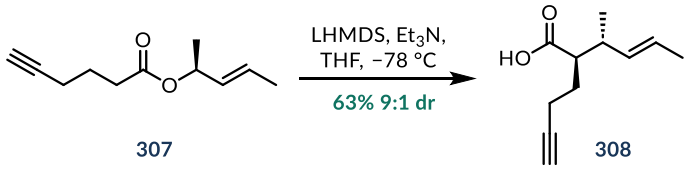
To a mixture of 5-hexynoic acid (250 mg, 2.23 mmol) and alcohol (250 mg, 2.90 mmol, 1.3 eq.) was added anhydrous THF (3.3 mL) under nitrogen atmosphere. EDC·HCl (641 mg, 3.34 mmol, 1.5 eq.), Et_3N (622 µL, 4.46 mmol, 2.0 eq.) and DMAP (27 mg, 0.22 mmol, 10 mol%) were added and the reaction mixture was stirred overnight at rt. 1 M HCl and Et_2O were added and the organic layer was washed with $NaHCO_3$ (sat.), brine, dried ($MgSO_4$) and concentrated (30 °C, 200 mbar) to afford 381 mg (94%) of yellow oil.

^{1}H NMR (200 MHz, $CDCl_3$) δ 5.84 – 5.61 (m, $1H_{alkene}$), 5.57 – 5.39 (m, $1H_{alkene}$), 5.33 (qu, *J* = 5.7 Hz, $1H_{CH}$), 2.52 – 2.35 (m, 2H), 2.32 – 2.17 (m, 2H), 1.96 (t, *J* = 2.6 Hz, 1H), 1.91 – 1.78 (m, 1H), 1.75 – 1.64 (m, 2H), 1.28 (d, *J* = 6.4 Hz, 3H).

^{13}C NMR (126 MHz, $CDCl_3$) δ 172.5, 130.9, 128.3, 83.5, 71.3, 69.2, 33.5, 23.8, 20.5, 18.0, 17.8.

HRMS (ESI) calc. for $C_{11}H_{18}O_2$ $[M+H]^+$ 181.1223, found 181.1223.

308: (2*R*,3*R*,*E*)-2-(but-3-yn-1-yl)-3-methylhex-4-enoic acid



A flask with HMDS (3.39 mL, 16.3 mmol, 3.1 eq.) and anhydrous toluene (118 mL) was cooled to −78 °C under nitrogen atmosphere. *n*-BuLi (2.3 M, 6.73 mL, 15.5 mmol, 3.0 eq.) was added dropwise and the mixture was stirred for 10 min at −78 °C. Anhydrous Et_3N (21 mL) was added fast dropwise, followed by slow addition of the substrate (930 mg, 5.16 mmol) in anhydrous toluene (18 mL) over 1 h. This slow addition prevents local excess of the starting ester in presence of its enolate, which results in an undesired Claisen condensation reaction. The reaction mixture was left in dry ice/acetone bath to naturally warm for 5 h, after which it was put in an ice-bath and allowed to warm to 0 °C over additional 2 h for complete conversion. The acid product was purified by an acid-base extraction procedure. First, $NaHCO_3$ and Et_2O were added and the water layer was separated and acidified with conc. HCl to pH ≤ 2. This was then extracted with Et_2O (×2) and the combined ether layers were dried ($MgSO_4$) and concentrated to obtain 587 mg (63%) of yellow oil as a 9:1 mixture of diastereomers.

^{1}H NMR (500 MHz, $CDCl_3$) δ 5.48 (dq, *J* = 15.2, 6.4 Hz, $1H_{alkene}$), 5.24 (ddd, *J* = 15.2, 8.3, 1.7 Hz, $1H_{alkene}$), 2.44 – 2.32 (m, $1H_{CH}$+$1H_{CH}$), 2.32 – 2.23 (m, $1H_{CH2}$), 2.21 – 2.12 (m, $1H_{CH2}$), 1.96 (t, *J* = 2.6 Hz, $1H_{alkyne}$), 1.81 – 1.75 (m, $2H_{CH2}$), 1.67 (dd, *J* = 6.4, 1.7 Hz, $3H_{Me}$), 1.04 (d, *J* = 6.4 Hz, $3H_{Me}$).

^{13}C NMR (126 MHz, $CDCl_3$) δ 181.3, 133.5, 126.4, 83.6, 69.0, 50.5, 39.6, 28.8, 19.2, 18.0, 17.0.

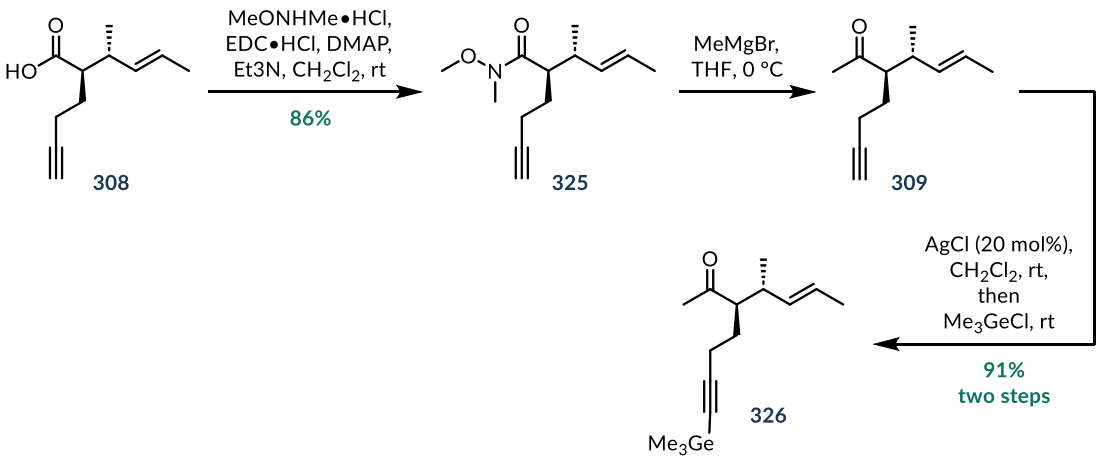
HRMS (ESI) calc. for $C_{11}H_{16}O_2$ $[M+H]^+$ 179.1077, found 179.1072.

The stereochemistry of the double bond was assigned based on the chair-like transition state model of Claisen rearrangement and by analogy to 274 and a close literature example (Figure 76b).

326: (3*R*,4*R*,*E*)-4-methyl-3-(4-(trimethylgermyl)but-3-yn-1-yl)hept-5-en-2-one

309: (3*R*,4*R*,*E*)-3-(but-3-yn-1-yl)-4-methylhept-5-en-2-one

325: (2*R*,3*R*,*E*)-2-(but-3-yn-1-yl)-*N*-methoxy-*N*,3-dimethylhex-4-enamide



To a solution of acid (900 mg, 4.99 mmol) in anhydrous CH_2Cl_2 (45 mL) under nitrogen atmosphere were added MeNHOMe·HCl (584 mg, 5.99 mmol, 1.2 eq.), EDC·HCl (1.15 g, 5.99 mmol, 1.2 eq.) and DMAP (61 mg, 0.50 mmol, 10 mol%). The mixture was cooled to 0 °C and Et_3N (1.74 mL, 12.5 mmol, 2.5 eq.) was added fast dropwise. The reaction mixture was stirred overnight at rt. 1 M HCl and Et_2O were added and the organic layer was washed with $NaHCO_3$ (sat.), brine, dried ($MgSO_4$) and concentrated to afford 0.96 g (86%) of the product that was of sufficient purity to be used in the next step without purification.

A solution of the substrate (960 mg, 4.30 mmol) in anhydrous THF (18 mL) was cooled to 0 °C under nitrogen atmosphere. MeMgBr (2.7 M, 7.8 mL, 21.5 mmol, 5.0 eq.) was added over 7 min at 0 °C and the reaction mixture was stirred for 3 h at rt. The reaction was carefully quenched with NH_4Cl (sat.). Et_2O and NH4Cl (sat.) were added and the organic layer was washed with brine, dried ($MgSO_4$) and concentrated (0 °C, 200 mbar). The product was not concentrated to dryness on high-vac due to its volatility and was used as-is.

To a flask containing the substrate (450 mg, 2.52 mmol, crude from previous step) and AgCl (73 mg, 0.51 mmol, 20 mol%) was added anhydrous CH_2Cl_2 (12 mL) under nitrogen atmosphere.

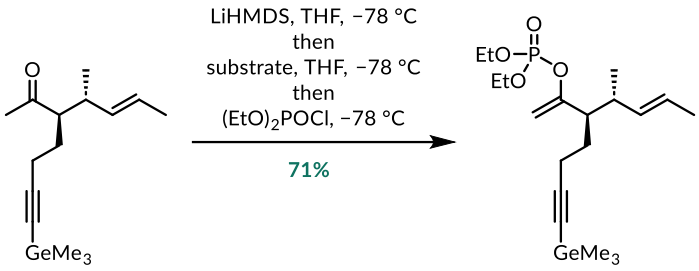
DBU (457 µL, 3.03 mmol, 1.2 eq.) was slowly added and the mixture was stirred for 2 h at rt. Me_3GeCl (373 µL, 3.03 mmol, 1.2 eq.) was added and the reaction mixture was stirred for an additional 1 h at rt to achieve full conversion. NH_4Cl (sat.) and Et_2O were added and the organic layer was washed with brine, dried ($MgSO_4$) and concentrated to afford 683 mg (92%) of yellow solid that was of sufficient purity to be used without purification.

^{1}H NMR (400 MHz, $CDCl_3$) δ 5.52 – 5.35 (m, $1H_{alkene}$), 5.21 (ddd, *J* = 15.2, 8.3, 1.6 Hz, $1H_{alkene}$), 2.56 – 2.47 (m, $1H_{CH}$), 2.40 – 2.31 (m, $1H_{CH}$), 2.24 – 2.04 (m, $2H_{CH2}$), 2.17 (s, $3H_{Me}$), 1.80 – 1.62 (m, $2H_{CH2}$+$3H_{Me}$), 0.97 (d, *J* = 6.7 Hz, $3H_{Me}$), 0.33 (s, $9H_{GeMe}$).

^{13}C NMR (101 MHz, $CDCl_3$) δ 212.4, 133.9, 125.8, 105.1, 85.2, 57.4, 39.3, 31.2, 28.4, 19.1, 18.4, 18.0, 0.0.

HRMS (ESI) calc. for $C_{15}H_{28}{}^{74}GeO$ $[M+H]^+$ 297.1268, found 297.1263.

328: diethyl ((3*R*,4*R*,*E*)-4-methyl-3-(4-(trimethylgermyl)but-3-yn-1-yl)hepta-1,5-dien-2-yl) phosphate



326 328

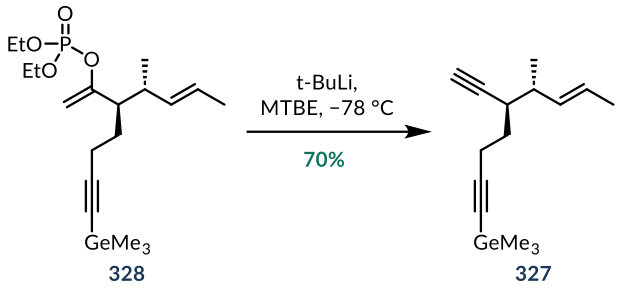
A solution of HMDS (21 µL, 0.101 mmol, 1.3 eq.) in anhydrous THF (0.4 mL) was cooled to −78 °C under nitrogen atmosphere. *n*-BuLi (2.3 M, 41 µL, 0.094 mmol, 1.2 eq.) was added dropwise and the mixture was stirred for 10 min at −78 °C. A solution of the substrate (23 mg, 0.078 mmol) in anhydrous THF (0.1 mL) was added dropwise and the reaction mixture was stirred for 30 min at −78 °C. Chlorophosphate (12 µL, 0.086 mmol, 1.1 eq.) was added via microsyringe and the reaction mixture was stirred for 1 h at −78 °C, quenched with NH_4Cl (sat.) and allowed to warm to rt. NH_4Cl (sat.) and Et_2O were added and the organic layer was passed through a Pasteur pipette with $MgSO_4$ and concentrated. Purification by flash chromatography (pentane/EtOAc 75:25) afforded 24 mg (71%) of amorphous solid. Chromatography should be conducted as quickly as possible to avoid product decomposition in prolonged contact with silica.

^{1}H NMR (400 MHz, $CDCl_3$) δ 5.49 – 5.33 (m, 1H$_{int.alkene}$), 5.24 – 5.14 (m, 1H$_{int.alkene}$), 4.96 (s br, 1H$_{CH2\text{-}alkene}$), 4.48 (s br, 1H$_{CH2\text{-}alkene}$), 4.22 – 4.10 (m, 4H$_{CH2\text{-}phosphate}$), 2.35 – 2.23 (m, 1H$_{CH2\text{-}a}$), 2.19 – 2.05 (m, 1H$_{CH2\text{-}a}$+1H$_{CH}$), 2.00 – 1.90 (m, 1H$_{CH}$), 1.78 – 1.68 (m, 1H$_{CH2\text{-}b}$), 1.65 (d, *J* = 6.5 Hz, 3H$_{Me}$), 1.54 – 1.45 (m, 1H$_{CH2\text{-}b}$), 1.35 (t, *J* = 7.1 Hz, 6H$_{Me\text{-}phosphate}$), 0.98 (d, *J* = 6.6 Hz, 3H$_{Me}$), 0.31 (s, 9H$_{GeMe}$).

^{13}C NMR (101 MHz, $CDCl_3$) δ 154.7, 135.2, 125.3, 105.8, 98.2, 84.2, 64.3, 50.3, 38.7, 28.9, 19.6, 18.0, 18.0, 16.2, 0.0.

HRMS (ESI) calc. for $C_{19}H_{37}{}^{74}GeO_4P$ $[M+H]^+$ 433.1558, found 433.1544.

327: ((5*R*,6*R*,*E*)-5-Ethynyl-6-methylnon-7-en-1-yn-1-yl)trimethylgermane

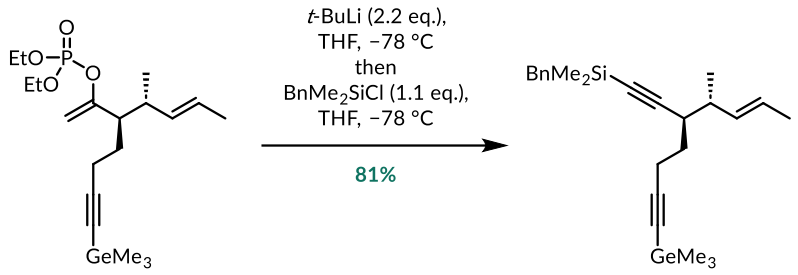


To a solution of phosphate (11.8 mg, 0.027 mmol) in anhydrous MTBE (0.4 mL) under N_2 and at −78 °C was dropwise added *t*-BuLi (1.1 M in pentane, 76 µL, 0.082 mmol, 3.0 eq.) and the reaction mixture was stirred for 15 min at −78 °C. Sat. aq. NH_4Cl and Et_2O were added, the reaction was warmed to rt, and the organic layer was separated, washed with brine, dried ($MgSO_4$) and concentrated (30 °C, 100 mbar). Purification by flash chromatography (Hex/EtOAc 97:3) afforded 5.3 mg (70%) of clear oil. Mass spectrometry analysis using electrospray ionisation was unsuccessful, likely due to the lack of ionisable functional groups.

^{1}H NMR (400 MHz, $CDCl_3$) δ 5.52 – 5.41 (m, $1H_{alkene}$), 5.36 (ddd, *J* = 15.2, 7.8, 1.5 Hz, $1H_{alkene}$), 2.52 – 2.42 (m, $1H_{CH2\text{-}a}$), 2.41 – 2.26 (m, $1H_{CH}$+$1H_{CH2\text{-}a}$), 2.24 – 2.11 (m, $1H_{CH}$), 2.07 (d, *J* = 2.4 Hz, $1H_{alkyne}$), 1.77 – 1.69 (m, $1H_{CH2\text{-}b}$), 1.67 (dd, *J* = 6.0, 1.1 Hz, $3H_{Me\text{-}alkene}$), 1.64 – 1.56 (m, $1H_{CH2\text{-}b}$), 1.08 (d, *J* = 6.8 Hz, $3H_{Me\text{-}aliphatic}$), 0.32 (s, $9H_{GeMe3}$).

^{13}C NMR (101 MHz, $CDCl_3$) δ 134.9, 125.1, 105.5, 85.7, 84.5, 70.9, 40.4, 37.1, 32.2, 22.5, 18.2, 18.1, 17.8, 0.1.

329: benzyldimethyl((3*R*,4*R*,*E*)-4-methyl-3-(4-(trimethylgermyl)but-3-yn-1-yl)hept-5-en-1-yn-1-yl)silane



328 329

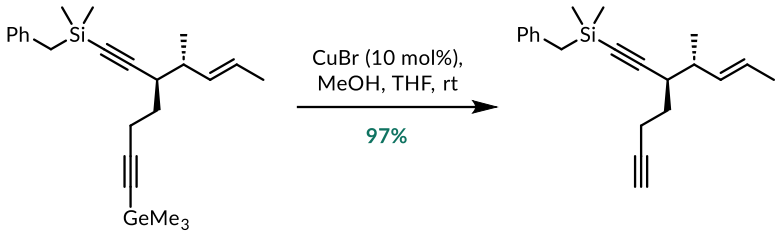
A solution of the substrate (298 mg, 0.69 mmol) in anhydrouos THF (11 mL) was cooled to −78 °C under nitrogen atmosphere. *t*-BuLi (1.7 M, 895 µL, 1.52 mmol, 2.2 eq.) was added dropwise and the reaction mixture was stirred for 10 min at −78 °C. Conversion of vinyl phosphate to alkyne was confirmed by TLC. $BnMe_2SiCl$ (141 µL, 0.76 mmol, 1.1 eq.) was added dropwise and the reaction mixture was stirred for 30 min at −78 °C. The reaction was quenched by addition of NH_4Cl (sat.) at −78 °C and allowed to warm to rt. NH_4Cl (sat.) and Et_2O were added and the organic layer was washed with brine, dried ($MgSO_4$) and concentrated. Purification by flash chromatography (hexane/Et_2O 98:2) afforded 238 mg (81%) of colourless oil. Excess of silyl chloride should be avoided as it results in formation of impurities that are difficult to separate.

^{1}H NMR (400 MHz, $CDCl_3$) δ 7.25 – 7.19 (m, $2H_{Bn}$), 7.13 – 7.04 (m, $3H_{Bn}$), 2.49 – 2.09 (m, $1H_{CH}$+$1H_{CH}$+$2H_{CH2\text{-}Bn}$+$2H_{CH2}$), 1.67 (d, J = 5.9 Hz, $3H_{Me}$), 1.60 – 1.54 (m, $2H_{CH2}$), 1.05 (d, J = 6.8 Hz, $3H_{Me}$), 0.34 (s, $9H_{GeMe}$), 0.11 (s, $6H_{SiMe}$).

^{13}C NMR (101 MHz, $CDCl_3$) δ 139.4, 135.0, 128.5, 128.2, 125.0, 124.4, 109.9, 105.8, 85.6, 84.3, 40.6, 38.4, 32.2, 29.9, 26.7, 18.3, 18.1, 0.1, -1.6.

HRMS (ESI) calc. for $C_{24}H_{38}{}^{74}GeSi$ $[M+H]^+$ 427.1871, found 427.1863.

Diyne fragment: benzyl((3*R*,4*R*,*E*)-3-(but-3-yn-1-yl)-4-methylhept-5-en-1-yn-1-yl)dimethylsilane



329 Diyne fragment

To a solution of the substrate (100 mg, 0.235 mmol) in THF (2.8 mL) and MeOH (2.8 mL) was added CuBr (3.4 mg, 0.024 mmol, 10 mol%) and the reaction mixture was stirred for 3h at rt. NH_4Cl (sat.) and Et_2O were added and the organic layer was washed with brine, dried ($MgSO_4$) and concentrated (30 °C, 150 mbar). Purification by flash chromatography (hexane/Et_2O 99:1) afforded 71 mg (97%) of clear oil.

^{1}H NMR (400 MHz, $CDCl_3$) δ 7.25 – 7.18 (m, $2H_{Bn}$), 7.11 – 7.06 (m, $3H_{Bn}$), 5.48 – 5.38 (m, $1H_{alkene}$), 5.31 (ddd, *J* = 15.2, 8.1, 1.5 Hz, $1H_{alkene}$), 2.41 – 2.32 (m, $1H_{CH}$+$1H_{CH2}$), 2.29 – 2.20 (m, $1H_{CH2}$), 2.18 (s, $2H_{Bn}$), 2.13 (q, *J* = 6.9 Hz, $1H_{CH}$), 1.96 (t, *J* = 2.7 Hz, $1H_{alkyne}$), 1.74 – 1.64 (m, $1H_{CH2}$+$3H_{Me}$), 1.60 – 1.50 (m, $1H_{CH2}$), 1.06 (d, *J* = 6.9 Hz, $3H_{Me}$), 0.12 (s, $6H_{SiMe}$).

^{13}C NMR (101 MHz, $CDCl_3$) δ 139.4, 134.9, 128.5, 128.2, 125.2, 124.4, 109.6, 85.8, 84.4, 68.5, 40.8, 38.2, 31.8, 26.7, 18.2, 18.1, 16.8, -1.6.

HRMS (ESI) calc. for $C_{21}H_{30}Si$ $[M+H]^+$ 309.2033, found 309.2030.

Data in agreement with the literature values.[40]

References

(1) Johnson, J. S. Counting steps. *Nature Synthesis* **2023**, *2* (1), 6-8. DOI: https://doi.org/10.1038/s44160-022-00204-3.

(2) Baran, P. S. Natural Product Total Synthesis: As Exciting as Ever and Here To Stay. *Journal of the American Chemical Society* **2018**, *140* (14), 4751-4755. DOI: https://doi.org/10.1021/jacs.8b02266.

(3) Nicolaou, K. C.; Sorenson, E. *Classics in total synthesis*; Wiley-VCH Verlag, 1996.

(4) Newhouse, T.; Baran, P. S.; Hoffmann, R. W. The economies of synthesis. *Chemical Society Reviews* **2009**, *38* (11), 3010-3021, 10.1039/B821200G. DOI: https://doi.org/10.1039/B821200G.

(5) Peters, D. S.; Pitts, C. R.; McClymont, K. S.; Stratton, T. P.; Bi, C.; Baran, P. S. Ideality in Context: Motivations for Total Synthesis. *Accounts of Chemical Research* **2021**, *54* (3), 605-617. DOI: https://doi.org/10.1021/acs.accounts.0c00821.

(6) Shenvi, R. A. Natural Product Synthesis in the 21st Century: Beyond the Mountain Top. *ACS Central Science* **2024**, *10* (3), 519-528. DOI: https://doi.org/10.1021/acscentsci.3c01518.

(7) Gao, Y.; Ma, D. In Pursuit of Synthetic Efficiency: Convergent Approaches. *Accounts of Chemical Research* **2021**, *54* (3), 569-582. DOI: https://doi.org/10.1021/acs.accounts.0c00727.

(8) Corey, E. J.; Cheng, X.-M. *The logic of chemical synthesis*; John Wiley & Sons, 1989.

(9) Burns, N. Z.; Baran, P. S.; Hoffmann, R. W. Redox Economy in Organic Synthesis. *Angewandte Chemie International Edition* **2009**, *48* (16), 2854-2867. DOI: https://doi.org/https://doi.org/10.1002/anie.200806086.

(10) Hendrickson, J. B. Systematic synthesis design. IV. Numerical codification of construction reactions. *Journal of the American Chemical Society* **1975**, *97* (20), 5784-5800. DOI: https://doi.org/10.1021/ja00853a023.

(11) Gaich, T.; Baran, P. S. Aiming for the Ideal Synthesis. *The Journal of Organic Chemistry* **2010**, *75* (14), 4657-4673. DOI: https://doi.org/10.1021/jo1006812.

(12) Kuttruff, C. A.; Eastgate, M. D.; Baran, P. S. Natural product synthesis in the age of scalability. *Natural Product Reports* **2014**, *31* (4), 419-432, 10.1039/C3NP70090A. DOI: https://doi.org/10.1039/C3NP70090A.

(13) Anastas, P. T.; Warner, J. *Green chemistry: Theory and practice*; Oxford University Press, 2000.

(14) Winterton, N. Green chemistry: deliverance or distraction? *Clean Technologies and Environmental Policy* **2016**, *18* (4), 991-1001. DOI: https://doi.org/10.1007/s10098-016-1118-y.

(15) Jimenez-Gonzalez, C.; Ponder, C. S.; Broxterman, Q. B.; Manley, J. B. Using the Right Green Yardstick: Why Process Mass Intensity Is Used in the Pharmaceutical Industry To Drive More Sustainable Processes. *Organic Process Research & Development* **2011**, *15* (4), 912-917. DOI: https://doi.org/10.1021/op200097d.

(16) Environmental Protection, A. *Methylene Chloride; Regulation Under the Toxic Substances Control Act (TSCA)*; United States Government, Washington, D.C., 2024. https://www.govinfo.gov/content/pkg/FR-2024-05-08/pdf/2024-09606.pdf.

(17) Xiao, W.-L.; Li, R.-T.; Huang, S.-X.; Pu, J.-X.; Sun, H.-D. Triterpenoids from the Schisandraceae family. *Natural Product Reports* **2008**, *25* (5), 871-891, 10.1039/B719905H. DOI: https://doi.org/10.1039/B719905H.

(18) Shi, Y.-M.; Xiao, W.-L.; Pu, J.-X.; Sun, H.-D. Triterpenoids from the Schisandraceae family: an update. *Natural Product Reports* **2015**, *32* (3), 367-410, 10.1039/C4NP00117F. DOI: https://doi.org/10.1039/C4NP00117F.

(19) Zhang, Y.-Q.; Liu, Y.; Zhang, Z.-P.; Wu, D.-D.; Zhuang, L.-X.; Algradi, A. M.; Kuang, H.-X.; Yang, B.-Y. Schisandraceae triterpenoids: A review of phytochemistry, bioactivities and synthesis. *Fitoterapia* **2022**, *161*, 105230. DOI: https://doi.org/https://doi.org/10.1016/j.fitote.2022.105230.

(20) Zhang, Y.-D.; Tang, Y.-F.; Luo, T.-P.; Shen, J.; Chen, J.-H.; Yang, Z. Application of RCM Reaction in the Construction of ABC Ring of Micrandilactone A. *Organic Letters* **2006**, *8* (1), 107-110. DOI: https://doi.org/10.1021/ol052630h.

(21) Tang, Y.; Zhang, Y.; Dai, M.; Luo, T.; Deng, L.; Chen, J.; Yang, Z. A Highly Efficient Synthesis of the FGH Ring of Micrandilactone A. Application of Thioureas as Ligands in the Co-catalyzed

Pauson−Khand Reaction and Pd-Catalyzed Carbonylative Annulation. *Organic Letters* **2005**, *7* (5), 885-888. DOI: https://doi.org/10.1021/ol047394+.

(22) Fischer, D.; Theodorakis, E. A. Studies on the Synthesis of Schisandraceae Natural Products: Exploring a Cyclopropylcarbinol Ring Expansion Strategy. *European Journal of Organic Chemistry* **2007**, *2007* (25), 4193-4196. DOI: https://doi.org/https://doi.org/10.1002/ejoc.200700336.

(23) Maity, S.; Matcha, K.; Ghosh, S. Synthetic Studies on Schisandra nortriterpenoids. Stereocontrolled Synthesis of Enantiopure C-5-epi ABC Ring Systems of Micrandilactone A and Lancifodilactone G Using RCM. *The Journal of Organic Chemistry* **2010**, *75* (12), 4192-4200. DOI: https://doi.org/10.1021/jo1006448.

(24) Lai, K. W.; Paquette, L. A. Stereocontrolled Synthesis of the Sterically Encumbered F Ring of Lancifodilactone G. *Organic Letters* **2008**, *10* (11), 2115-2118. DOI: https://doi.org/10.1021/ol800419v.

(25) Paquette, L. A.; Wah Lai, K. Pinacol Macrocyclization-Based Route to the Polyfused Medium-Sized CDE Ring System of Lancifodilactone G. *Organic Letters* **2008**, *10* (17), 3781-3784. DOI: https://doi.org/10.1021/ol8014607.

(26) Paquette, L. A.; Lai, K. W. Studies Directed toward the Total Synthesis of Lancifodilactone G: An Expeditious Route to the ABC Subunit. *Organic Letters* **2008**, *10* (11), 2111-2113. DOI: https://doi.org/10.1021/ol800418m.

(27) Cordonnier, M.-C. A.; Jennifer Kan, S. B.; Anderson, E. A. A palladium-mediated cascade cyclisation approach to the CDE cores of rubriflordilactone A and lancifodilactone G. *Chemical Communications* **2008**, (44), 5818-5820, 10.1039/B814360A. DOI: https://doi.org/10.1039/B814360A.

(28) Wang, Q.; Chen, C. An Approach to the Core Skeleton of Lancifodilactone F. *Organic Letters* **2008**, *10* (6), 1223-1226. DOI: https://doi.org/10.1021/ol800111j.

(29) Mehta, G.; Bhat, B. A.; Suresha Kumara, T. H. Studies directed towards the synthesis of schisanartane and related complex nortriterpenoids: construction of models of the peripheral ABC and FGH segments of rubrifloradilactone C. *Tetrahedron Letters* **2010**, *51* (31), 4069-4072. DOI: https://doi.org/https://doi.org/10.1016/j.tetlet.2010.05.130.

(30) Xiao, Q.; Ren, W.-W.; Chen, Z.-X.; Sun, T.-W.; Li, Y.; Ye, Q.-D.; Gong, J.-X.; Meng, F.-K.; You, L.; Liu, Y.-F.; et al. Diastereoselective Total Synthesis of (±)-Schindilactone A. *Angewandte Chemie International Edition* **2011**, *50* (32), 7373-7377. DOI: https://doi.org/https://doi.org/10.1002/anie.201103088.

(31) Firoj Hossain, M.; Matcha, K.; Ghosh, S. Synthetic studies toward nortriterpenoids of schisandraceae family. Approach to the construction of functionalized C/D and A/B ring units of micrandilactone C and rubrifloradilactone B. *Tetrahedron Letters* **2011**, *52* (48), 6473-6476. DOI: https://doi.org/https://doi.org/10.1016/j.tetlet.2011.09.104.

(32) Goh, S. S.; Baars, H.; Gockel, B.; Anderson, E. A. Metal-Catalyzed Syntheses of Abridged CDE Rings of Rubriflordilactones A and B. *Organic Letters* **2012**, *14* (24), 6278-6281. DOI: https://doi.org/10.1021/ol303041j.

(33) Gockel, B.; Goh, S. S.; Puttock, E. J.; Baars, H.; Chaubet, G.; Anderson, E. A. Enantioselective Synthesis of the Predominant AB Ring System of the Schisandra Nortriterpenoid Natural Products. *Organic Letters* **2014**, *16* (17), 4480-4483. DOI: https://doi.org/10.1021/ol502027m.

(34) Peng, Y.; Duan, S.-M.; Wang, Y.-W. Concise synthesis of the DEFG ring system in rubriflordilactone B. *Tetrahedron Letters* **2015**, *56* (30), 4509-4511. DOI: https://doi.org/https://doi.org/10.1016/j.tetlet.2015.05.117.

(35) Roth, H. G. Investigations Toward The Application Of Organic Photoredox Catalysis To The Synthesis Of Natural Products. Dissertation, 2019.

(36) Wang, Y.; Zhang, Y.; Li, Z.; Yang, Z.; Xie, Z. A highly efficient synthesis of the DEFG-ring system of rubriflordilactone B. *Organic Chemistry Frontiers* **2017**, *4* (1), 47-51, 10.1039/C6QO00241B. DOI: https://doi.org/10.1039/C6QO00241B.

(37) Wang, Y.; Li, Z.; Lv, L.; Xie, Z. Synthetic Study of Rubriflordilactone B: Highly Stereoselective Construction of the C-5-epi ABCDE Ring System. *Organic Letters* **2016**, *18* (4), 792-795. DOI: https://doi.org/10.1021/acs.orglett.6b00057.

(38) Pozo, J. d.; Zhang, S.; Romiti, F.; Xu, S.; Conger, R. P.; Hoveyda, A. H. Streamlined Catalytic Enantioselective Synthesis of α-Substituted β,γ-Unsaturated Ketones and Either of the Corresponding Tertiary Homoallylic Alcohol Diastereomers. *Journal of the American Chemical Society* **2020**, *142* (42), 18200-18212. DOI: https://doi.org/10.1021/jacs.0c08732.

(39) Li, J.; Yang, P.; Yao, M.; Deng, J.; Li, A. Total Synthesis of Rubriflordilactone A. *Journal of the American Chemical Society* **2014**, *136* (47), 16477-16480. DOI: https://doi.org/10.1021/ja5092563.

(40) Goh, S. S.; Chaubet, G.; Gockel, B.; Cordonnier, M.-C. A.; Baars, H.; Phillips, A. W.; Anderson, E. A. Total Synthesis of (+)-Rubriflordilactone A. *Angewandte Chemie International Edition* **2015**, *54* (43), 12618-12621. DOI: https://doi.org/https://doi.org/10.1002/anie.201506366.

(41) Zheng, X.; Guo, X.; Wang, H.; Zhou, P.-P.; Chen, X. Total Synthesis of (±)-Rubriflordilactone A. *Journal of the American Chemical Society* **2024**, *146* (11), 7198-7203. DOI: https://doi.org/10.1021/jacs.4c01033.

(42) Yang, P.; Yao, M.; Li, J.; Li, Y.; Li, A. Total Synthesis of Rubriflordilactone B. *Angewandte Chemie International Edition* **2016**, *55* (24), 6964-6968. DOI: https://doi.org/https://doi.org/10.1002/anie.201601915.

(43) Mohammad, M.; Chintalapudi, V.; Carney, J. M.; Mansfield, S. J.; Sanderson, P.; Christensen, K. E.; Anderson, E. A. Convergent Total Syntheses of (−)-Rubriflordilactone B and (−)-pseudo-Rubriflordilactone B. *Angewandte Chemie International Edition* **2019**, *58* (50), 18177-18181. DOI: https://doi.org/https://doi.org/10.1002/anie.201908917.

(44) You, L.; Liang, X.-T.; Xu, L.-M.; Wang, Y.-F.; Zhang, J.-J.; Su, Q.; Li, Y.-H.; Zhang, B.; Yang, S.-L.; Chen, J.-H.; et al. Asymmetric Total Synthesis of Propindilactone G. *Journal of the American Chemical Society* **2015**, *137* (32), 10120-10123. DOI: https://doi.org/10.1021/jacs.5b06480.

(45) Wang, Y.; Chen, B.; He, X.; Gui, J. Bioinspired Synthesis of Nortriterpenoid Propindilactone G. *Journal of the American Chemical Society* **2020**, *142* (11), 5007-5012. DOI: https://doi.org/10.1021/jacs.0c00363.

(46) Liu, D.-D.; Sun, T.-W.; Wang, K.-Y.; Lu, Y.; Zhang, S.-L.; Li, Y.-H.; Jiang, Y.-L.; Chen, J.-H.; Yang, Z. Asymmetric Total Synthesis of Lancifodilactone G Acetate. *Journal of the American Chemical Society* **2017**, *139* (16), 5732-5735. DOI: https://doi.org/10.1021/jacs.7b02561.

(47) Wang, L.; Wang, H.; Li, Y.; Tang, P. Total Synthesis of Schilancitrilactones B and C. *Angewandte Chemie International Edition* **2015**, *54* (19), 5732-5735. DOI: https://doi.org/https://doi.org/10.1002/anie.201501169.

(48) Wang, H.; Zhang, X.; Tang, P. Total syntheses of schilancidilactones A and B, schilancitrilactone A, and 20-epi-schilancitrilactone A via late-stage nickel-catalyzed cross

coupling. *Chemical Science* **2017**, *8* (10), 7246-7250, 10.1039/C7SC03293E. DOI: https://doi.org/10.1039/C7SC03293E.

(49) Jiang, Y.-L.; Yu, H.-X.; Li, Y.; Qu, P.; Han, Y.-X.; Chen, J.-H.; Yang, Z. Asymmetric Total Synthesis of Pre-schisanartanin C. *Journal of the American Chemical Society* **2020**, *142* (1), 573-580. DOI: https://doi.org/10.1021/jacs.9b11872.

(50) Tang, Y.; Deng, L.; Zhang, Y.; Dong, G.; Chen, J.; Yang, Z. Tetramethyl Thiourea/Co2(CO)8-Catalyzed Pauson−Khand Reaction under Balloon Pressure of CO. *Organic Letters* **2005**, *7*(4), 593-595. DOI: https://doi.org/10.1021/ol047651a.

(51) Nicolaou, K. C.; Bulger, P. G.; Sarlah, D. Metathesis Reactions in Total Synthesis. *Angewandte Chemie International Edition* **2005**, *44* (29), 4490-4527. DOI: https://doi.org/https://doi.org/10.1002/anie.200500369.

(52) Mendoza, S. D.; Rombola, M.; Tao, Y.; Zuend, S. J.; Gotz, R.; McLaughlin, M. J.; Reisman, S. E. Expanding the Chiral Monoterpene Pool: Enantioselective Diels-Alder Reactions of α-Acyloxy Enones. *Org. Lett.* **2022**, *24* (21), 3802-3806. DOI: https://doi.org/10.1021/acs.orglett.2c01343.

(53) Shevick, S. L.; Freeman, S. M.; Tong, G.; Russo, R. J.; Bohn, L. M.; Shenvi, R. A. Asymmetric syntheses of (+)- and (-)-collybolide enable reevaluation of kappa-opioid receptor agonism. *ChemRxiv* **2021**, 1-6.

(54) Knol, J.; Feringa, B. L. Direct Coupling Procedure for the Synthesis of N-Acyl-2-oxazolidinones Derived from α,β-Unsaturated Carboxylic Acids. *Synthetic Communications* **1996**, *26* (2), 261-268. DOI: https://doi.org/10.1080/00397919608003613.

(55) Sakakura, A.; Kondo, R.; Matsumura, Y.; Akakura, M.; Ishihara, K. Rational Design of Highly Effective Asymmetric Diels−Alder Catalysts Bearing 4,4′-Sulfonamidomethyl Groups. *Journal of the American Chemical Society* **2009**, *131* (49), 17762-17764. DOI: https://doi.org/10.1021/ja906098b.

(56) Tokuyama, H.; Yokoshima, S.; Yamashita, T.; Fukuyama, T. A novel ketone synthesis by a palladium-catalyzed reaction of thiol esters and organozinc reagents. *Tetrahedron Letters* **1998**, *39* (20), 3189-3192. DOI: https://doi.org/https://doi.org/10.1016/S0040-4039(98)00456-0.

(57) Smith, A. B.; Kürti, L.; Davulcu, A. H.; Cho, Y. S.; Ohmoto, K. Indole Diterpene Synthetic Studies: Development of a Second-Generation Synthetic Strategy for (+)-Nodulisporic Acids A

and B. *The Journal of Organic Chemistry* **2007**, *72* (13), 4611-4620. DOI: https://doi.org/10.1021/jo062423a.

(58) Liras, S.; Lynch, C. L.; Fryer, A. M.; Vu, B. T.; Martin, S. F. Applications of Vinylogous Mannich Reactions. Total Syntheses of the Ergot Alkaloids Rugulovasines A and B and Setoclavine. *Journal of the American Chemical Society* **2001**, *123* (25), 5918-5924. DOI: https://doi.org/10.1021/ja010577w.

(59) Ando, K. Highly Selective Synthesis of Z-Unsaturated Esters by Using New Horner−Emmons Reagents, Ethyl (Diarylphosphono)acetates. *The Journal of Organic Chemistry* **1997**, *62* (7), 1934-1939. DOI: https://doi.org/10.1021/jo970057c.

(60) Pulis, A. P.; Aggarwal, V. K. Synthesis of Enantioenriched Tertiary Boronic Esters from Secondary Allylic Carbamates. Application to the Synthesis of C30 Botryococcene. *Journal of the American Chemical Society* **2012**, *134* (17), 7570-7574. DOI: https://doi.org/10.1021/ja303022d.

(61) Miura, K.; Hondo, T.; Takahashi, T.; Hosomi, A. Acid-catalyzed cyclization of vinylsilanes bearing a hydroxy group. Benzyldimethylsilyl group as an effective promoter and novel hydroxy surrogate1. *Tetrahedron Letters* **2000**, *41* (13), 2129-2132. DOI: https://doi.org/https://doi.org/10.1016/S0040-4039(00)00091-5.

(62) Comins, D. L.; Brown, J. D. Ortho metalation directed by .alpha.-amino alkoxides. *The Journal of Organic Chemistry* **1984**, *49* (6), 1078-1083. DOI: https://doi.org/10.1021/jo00180a024.

(63) Corey, E. J.; Kim, C. U.; Takeda, M. A method for selective conversion of allylic and benzylic alcohols to halides under neutral conditions. *Tetrahedron Letters* **1972**, *13* (42), 4339-4342. DOI: https://doi.org/https://doi.org/10.1016/S0040-4039(01)94310-2.

(64) Bhunia, A.; Bergander, K.; Daniliuc, C. G.; Studer, A. Fe-Catalyzed Anaerobic Mukaiyama-Type Hydration of Alkenes using Nitroarenes. *Angewandte Chemie International Edition* **2021**, *60* (15), 8313-8320. DOI: https://doi.org/https://doi.org/10.1002/anie.202015740.

(65) Johnson, C. R.; Braun, M. P. A two-step, three-component synthesis of PGE1: utilization of .alpha.-iodo enones in Pd(0)-catalyzed cross-couplings of organoboranes. *Journal of the American Chemical Society* **1993**, *115* (23), 11014-11015. DOI: https://doi.org/10.1021/ja00076a079.

(66) Mohammad, M. Total synthesis of rubriflordilactone B and pseudo-rubriflordilactone B. University of Oxford, 2018.

(67) Cordonnier, M.-C. A.; Kan, S. B. J.; Gockel, B.; Goh, S. S.; Anderson, E. A. Carbopalladation of bromoene-alkynylsilanes: mechanistic insights and synthesis of fused-ring bicyclic silanes and phenols. *Organic Chemistry Frontiers* **2014**, *1* (6), 661-673, 10.1039/C4QO00123K. DOI: https://doi.org/10.1039/C4QO00123K.

(68) Le, C. M.; Menzies, P. J.; Petrone, D. A.; Lautens, M. Synergistic steric effects in the development of a palladium-catalyzed alkyne carbohalogenation: stereodivergent synthesis of vinyl halides. *Angew Chem Int Ed Engl* **2015**, *54* (1), 254-257. DOI: https://doi.org/10.1002/anie.201409248. From NLM.

(69) Blouin, S.; Blond, G.; Donnard, M.; Gulea, M.; Suffert, J. Cyclocarbopalladation as a Key Step in Cascade Reactions: Recent Developments. *Synthesis* **2017**, *49* (08), 1767-1784. DOI: https://doi.org/10.1055/s-0036-1588708.

(70) Negishi, E.-i.; Harring, L. S.; Owczarczyk, Z.; Mohamud, M. M.; Ay, M. Cyclic cascade carbopalladation reactions as a route to benzene and fulvene derivatives. *Tetrahedron Letters* **1992**, *33* (23), 3253-3256. DOI: https://doi.org/https://doi.org/10.1016/S0040-4039(00)92060-4.

(71) Suffert, J.; Salem, B.; Klotz, P. Cascade cyclization: Carbopalladative cyclization followed by electrocyclic closure as a route to complex polycycles. *Journal of the American Chemical Society* **2001**, *123* (48), 12107-12108. DOI: https://doi.org/Doi 10.1021/Ja0170495.

(72) Salem, B.; Suffert, J. A 4-exo-dig cyclocarbopalladation/8 pi electrocyclization cascade: Expeditious access to the tricyclic core structures of the ophiobolins and aleurodiscal. *Angewandte Chemie-International Edition* **2004**, *43* (21), 2826-2830. DOI: https://doi.org/10.1002/anie.200453773|ISSN 1433-7851.

(73) Salem, B.; Delort, E.; Klotz, P.; Suffert, J. Cyclocarbopalladation: 5-Exo-dig Cyclization versus Direct Stille Cross-Coupling Reaction. The Influence of the α,β-Propargylic Substitution. *Organic Letters* **2003**, *5* (13), 2307-2310. DOI: https://doi.org/10.1021/ol034647a.

(74) Kan, S. B. J.; Anderson, E. A. A Cascade Palladium-Mediated Cross-Coupling/Electrocyclization Approach to the Construction of Fused Bi- and Tricyclic Rings. *Organic Letters* **2008**, *10* (11), 2323-2326. DOI: https://doi.org/10.1021/ol8007952.

(75) Greenaway, R. L.; Campbell, C. D.; Holton, O. T.; Russell, C. A.; Anderson, E. A. Palladium-Catalyzed Cascade Cyclization of Ynamides to Azabicycles. *Chemistry – A European Journal* **2011**, *17* (51), 14366-14370. DOI: https://doi.org/https://doi.org/10.1002/chem.201102880.

(76) Hofmeister, H.; Annen, K.; Laurent, H.; Wiechert, R. A Novel Entry to 17α-Bromo- and 17α-Iodoethynyl Steroids. *Angewandte Chemie International Edition in English* **1984**, *23* (9), 727-729. DOI: https://doi.org/https://doi.org/10.1002/anie.198407271.

(77) Zhang, Y.; Hsung, R. P.; Tracey, M. R.; Kurtz, K. C. M.; Vera, E. L. Copper Sulfate-Pentahydrate-1,10-Phenanthroline Catalyzed Amidations of Alkynyl Bromides. Synthesis of Heteroaromatic Amine Substituted Ynamides. *Organic Letters* **2004**, *6* (7), 1151-1154. DOI: https://doi.org/10.1021/ol049827e.

(78) Krieger, J.; Smeilus, T.; Kaiser, M.; Seo, E.-J.; Efferth, T.; Giannis, A. Total Synthesis and Biological Investigation of (−)-Artemisinin: The Antimalarial Activity of Artemisinin Is not Stereospecific. *Angewandte Chemie International Edition* **2018**, *57* (27), 8293-8296. DOI: https://doi.org/https://doi.org/10.1002/anie.201802015.

(79) Ohmura, T.; Yamamoto, Y.; Miyaura, N. Rhodium- or Iridium-Catalyzed trans-Hydroboration of Terminal Alkynes, Giving (Z)-1-Alkenylboron Compounds. *Journal of the American Chemical Society* **2000**, *122* (20), 4990-4991. DOI: https://doi.org/10.1021/ja0002823.

(80) Mansfield, S. J.; Campbell, C. D.; Jones, M. W.; Anderson, E. A. A robust and modular synthesis of ynamides. *Chemical Communications* **2015**, *51* (16), 3316-3319, 10.1039/C4CC07876D. DOI: https://doi.org/10.1039/C4CC07876D.

(81) Goh, S. S.; Chaubet, G.; Gockel, B.; Cordonnier, M. C.; Baars, H.; Phillips, A. W.; Anderson, E. A. Total Synthesis of (+)-Rubriflordilactone A. *Angew Chem Int Ed Engl* **2015**, *54* (43), 12618-12621. DOI: https://doi.org/10.1002/anie.201506366.

(82) Pozo, J. D.; Zhang, S.; Romiti, F.; Xu, S.; Conger, R. P.; Hoveyda, A. H. Streamlined Catalytic Enantioselective Synthesis of α-Substituted β,γ-Unsaturated Ketones and Either of the Corresponding Tertiary Homoallylic Alcohol Diastereomers. *J Am Chem Soc* **2020**, *142* (42), 18200-18212. DOI: https://doi.org/10.1021/jacs.0c08732. From NLM.

(83) Chen, M. S.; White, M. C. Combined Effects on Selectivity in Fe-Catalyzed Methylene Oxidation. *Science* **2010**, *327* (5965), 566-571. DOI: https://doi.org/10.1126/science.1183602.

(84) Kula, J. Synthesis of new terpenoidal tetrahydrofuran and tetrahydropyran derivatives. *Liebigs Annalen der Chemie* **1983**, *1983* (5), 890-893. DOI: https://doi.org/https://doi.org/10.1002/jlac.198319830515.

(85) Chapuis, C.; Barthe, M.; Cantatore, C.; Saint-Léger, C.; Wyss, P. Analogues of α-Campholenal (=(1R)-2,2,3-Trimethylcyclopent-3-ene-1-acetaldehyde) as Building Blocks for (+)-β-Necrodol (=(1S,3S)-2,2,3-Trimethyl-4-methylenecyclopentanemethanol) and Sandalwood-like Alcohols. *Helvetica Chimica Acta* **2006**, *89* (11), 2638-2653. DOI: https://doi.org/https://doi.org/10.1002/hlca.200690236.

(86) Wolk, J. L.; Goldschmidt, Z.; Dunkelblum, E. A Short Stereoselective Synthesis of (+)-cis-Planococcyl Acetate, Sex Pheromone of the Citrus Mealybug Planococcus citri (Risso). *Synthesis* **1986**, *1986* (04), 347-348.

(87) Asensio, G.; Castellano, G.; Mello, R.; González Núñez, M. E. Oxyfunctionalization of Aliphatic Esters by Methyl(trifluoromethyl)dioxirane. *The Journal of Organic Chemistry* **1996**, *61* (16), 5564-5566. DOI: https://doi.org/10.1021/jo9604189.

(88) Laudadio, G.; Govaerts, S.; Wang, Y.; Ravelli, D.; Koolman, H. F.; Fagnoni, M.; Djuric, S. W.; Noël, T. Selective C(sp(3))-H Aerobic Oxidation Enabled by Decatungstate Photocatalysis in Flow. *Angew Chem Int Ed Engl* **2018**, *57* (15), 4078-4082. DOI: https://doi.org/10.1002/anie.201800818. From NLM.

(89) Chen, M. S.; White, M. C. A predictably selective aliphatic C-H oxidation reaction for complex molecule synthesis. *Science* **2007**, *318* (5851), 783-787. DOI: https://doi.org/10.1126/science.1148597. From NLM.

(90) Gormisky, P. E.; White, M. C. Catalyst-controlled aliphatic C-H oxidations with a predictive model for site-selectivity. *J Am Chem Soc* **2013**, *135* (38), 14052-14055. DOI: https://doi.org/10.1021/ja407388y. From NLM.

(91) Saito, M.; Kawamata, Y.; Meanwell, M.; Navratil, R.; Chiodi, D.; Carlson, E.; Hu, P.; Chen, L.; Udyavara, S.; Kingston, C.; et al. N-Ammonium Ylide Mediators for Electrochemical C-H Oxidation. *J Am Chem Soc* **2021**, *143* (20), 7859-7867. DOI: https://doi.org/10.1021/jacs.1c03780. From NLM.

(92) Kawamata, Y.; Yan, M.; Liu, Z.; Bao, D. H.; Chen, J.; Starr, J. T.; Baran, P. S. Scalable, Electrochemical Oxidation of Unactivated C-H Bonds. *J Am Chem Soc* **2017**, *139* (22), 7448-7451. DOI: https://doi.org/10.1021/jacs.7b03539. From NLM.

(93) Mack, J. B. C.; Gipson, J. D.; Du Bois, J.; Sigman, M. S. Ruthenium-Catalyzed C-H Hydroxylation in Aqueous Acid Enables Selective Functionalization of Amine Derivatives. *J Am Chem Soc* **2017**, *139* (28), 9503-9506. DOI: https://doi.org/10.1021/jacs.7b05469. From NLM.

(94) Still, W. C.; Gennari, C. Direct synthesis of Z-unsaturated esters. A useful modification of the horner-emmons olefination. *Tetrahedron Letters* **1983**, *24* (41), 4405-4408. DOI: https://doi.org/https://doi.org/10.1016/S0040-4039(00)85909-2.

(95) Walters, J. C.; Tierno, A. F.; Dubin, A. H.; Wengryniuk, S. E. (Poly)cationic λ3-Iodane-Mediated Oxidative Ring Expansion of Secondary Alcohols. *European Journal of Organic Chemistry* **2018**, *2018* (12), 1460-1464. DOI: https://doi.org/https://doi.org/10.1002/ejoc.201800118.

(96) Schiaffo, C. E.; Dussault, P. H. Ozonolysis in Solvent/Water Mixtures: Direct Conversion of Alkenes to Aldehydes and Ketones. *The Journal of Organic Chemistry* **2008**, *73* (12), 4688-4690. DOI: https://doi.org/10.1021/jo800323x.

(97) Ruffoni, A.; Hampton, C.; Simonetti, M.; Leonori, D. Photoexcited nitroarenes for the oxidative cleavage of alkenes. *Nature* **2022**, *610* (7930), 81-86. DOI: https://doi.org/10.1038/s41586-022-05211-0.

(98) Hayashi, M.; Yamada, K.; Arikita, O. Practical and catalytic synthesis of 1,5-anhydrohex-1-en-3-uloses. *Tetrahedron* **1999**, *55* (28), 8331-8340. DOI: https://doi.org/https://doi.org/10.1016/S0040-4020(99)00426-3.

(99) Jefford, C. W.; Sledeski, A. W.; Patrick, L.; Boukouvalas, J. The alkylation of silyl enol ethers with SN1-unreactive iodides in the presence of silver trifluoroacetate. *Tetrahedron Letters* **1992**, *33* (14), 1855-1858. DOI: https://doi.org/https://doi.org/10.1016/S0040-4039(00)74160-8.

(100) Kuwajima, I.; Nakamura, E.; Shimizu, M. Fluoride-mediated reactions of enol silyl ethers. Regiospecific monoalkylation of ketones. *Journal of the American Chemical Society* **1982**, *104* (4), 1025-1030. DOI: https://doi.org/10.1021/ja00368a018.

(101) Cox, D. P.; Terpinski, J.; Lawrynowicz, W. "Anhydrous" tetrabutylammonium fluoride: a mild but highly efficient source of nucleophilic fluoride ion. *The Journal of Organic Chemistry* **1984**, *49* (17), 3216-3219. DOI: https://doi.org/10.1021/jo00191a035.

(102) Denmark, S. E.; Edwards, J. P. A comparison of (chloromethyl)- and (iodomethyl)zinc cyclopropanation reagents. *The Journal of Organic Chemistry* **1991**, *56* (25), 6974-6981. DOI: https://doi.org/10.1021/jo00025a007.

(103) Pham, P. V.; Nagib, D. A.; MacMillan, D. W. C. Photoredox Catalysis: A Mild, Operationally Simple Approach to the Synthesis of α-Trifluoromethyl Carbonyl Compounds. *Angewandte Chemie International Edition* **2011**, *50* (27), 6119-6122. DOI: https://doi.org/https://doi.org/10.1002/anie.201101861.

(104) Zhang, P.; Le, C. C.; MacMillan, D. W. C. Silyl Radical Activation of Alkyl Halides in Metallaphotoredox Catalysis: A Unique Pathway for Cross-Electrophile Coupling. *Journal of the American Chemical Society* **2016**, *138* (26), 8084-8087. DOI: https://doi.org/10.1021/jacs.6b04818.

(105) Chapleur, Y. A short route to 2-C-alkyl-2-deoxy-sugars from D-mannose. *Journal of the Chemical Society, Chemical Communications* **1983**, (3), 141-142, 10.1039/C39830000141. DOI: https://doi.org/10.1039/C39830000141.

(106) Albano, E. L.; Horton, D. Synthesis of methyl 2,3,6-trideoxy-.alpha.-D-erythro-hexopyranoside (methyl .alpha.-amicetoside). *The Journal of Organic Chemistry* **1969**, *34* (11), 3519-3522. DOI: https://doi.org/10.1021/jo01263a064.

(107) Wang, B.; Hansen, T. M.; Wang, T.; Wu, D.; Weyer, L.; Ying, L.; Engler, M. M.; Sanville, M.; Leitheiser, C.; Christmann, M.; et al. Total Synthesis of Phorboxazole A via de Novo Oxazole Formation: Strategy and Component Assembly. *Journal of the American Chemical Society* **2011**, *133* (5), 1484-1505. DOI: https://doi.org/10.1021/ja108906e.

(108) Nicolaou, K. C.; Skokotas, G.; Furuya, S.; Suemune, H.; Nicolaou, D. C. Golfomycin A, a Novel Designed Molecule with DNA-Cleaving Properties and Antitumor Activity. *Angewandte Chemie International Edition in English* **1990**, *29* (9), 1064-1067. DOI: https://doi.org/https://doi.org/10.1002/anie.199010641.

(109) Grandjean, J.-M. M.; Nicewicz, D. A. Synthesis of Highly Substituted Tetrahydrofurans by Catalytic Polar-Radical-Crossover Cycloadditions of Alkenes and Alkenols. *Angewandte*

Chemie International Edition **2013**, *52* (14), 3967-3971. DOI: https://doi.org/https://doi.org/10.1002/anie.201210111.

(110) Beckwith, A. L. J.; Lawrence, T.; Serelis, A. K. Stereoselectivity of ring closure of substituted hex-5-enyl radicals. *Journal of the Chemical Society, Chemical Communications* **1980**, (11), 484-485, 10.1039/C39800000484. DOI: https://doi.org/10.1039/C39800000484.

(111) Capella, L.; Montevecchi, P. C.; Navacchia, M. L. Cyclizations and Rearrangements of Samarium Diiodide-Generated Vinyl Radicals. *The Journal of Organic Chemistry* **1995**, *60* (23), 7424-7432. DOI: https://doi.org/10.1021/jo00128a013.

(112) Nguyen, J. D.; D'Amato, E. M.; Narayanam, J. M. R.; Stephenson, C. R. J. Engaging unactivated alkyl, alkenyl and aryl iodides in visible-light-mediated free radical reactions. *Nature Chemistry* **2012**, *4* (10), 854-859. DOI: https://doi.org/10.1038/nchem.1452.

(113) MacKenzie, I. A.; Wang, L.; Onuska, N. P. R.; Williams, O. F.; Begam, K.; Moran, A. M.; Dunietz, B. D.; Nicewicz, D. A. Discovery and characterization of an acridine radical photoreductant. *Nature* **2020**, *580* (7801), 76-80. DOI: https://doi.org/10.1038/s41586-020-2131-1.

(114) Goh, S. Total synthesis of rubriflordilactone A. University of Oxford, 2015.

(115) Müller, S.; Liepold, B.; Roth, G. J.; Bestmann, H. J. An Improved One-pot Procedure for the Synthesis of Alkynes from Aldehydes. *Synlett* **1996**, *1996* (06), 521-522. DOI: https://doi.org/10.1055/s-1996-5474.

(116) Eschenmoser, A.; Felix, D.; Ohloff, G. Eine neuartige Fragmentierung cyclischer α, ß-ungesättigter Carbonylsysteme; Synthese von Exalton und rac-Muscon aus Cyclododecanon Vorläufige Mitteilung. *Helvetica Chimica Acta* **1967**, *50* (2), 708-713. DOI: https://doi.org/https://doi.org/10.1002/hlca.19670500232.

(117) Barczak, N. T.; Jarvo, E. R. Regioselective Silver-Mediated Kondakov–Darzens Olefin Acylation. *Chemistry – A European Journal* **2011**, *17* (46), 12912-12916. DOI: https://doi.org/https://doi.org/10.1002/chem.201102476.

(118) Schmitt, S.; Feidt, E.; Hartmann, D.; Huch, V.; Jauch, J. A Metathesis–Acylation Approach to the Bicyclic Core of Polycyclic Poly-prenylated Acylphloroglucinols. *Synlett* **2014**, *25* (14), 2025-2029. DOI: https://doi.org/10.1055/s-0034-1378380.

(119) Sato, A.; Kinoshita, H.; Shinokubo, H.; Oshima, K. Hydrosilylation of Alkynes with a Cationic Rhodium Species Formed in an Anionic Micellar System. *Organic Letters* **2004**, *6* (13), 2217-2220. DOI: https://doi.org/10.1021/ol049308b.

(120) Sun, W.; Xu, L.; Qin, Y.; Liu, C. Alkyne synthesis through coupling of gem-diborylalkanes with carboxylic acid esters. *Nature Synthesis* **2023**, *2* (5), 413-422. DOI: https://doi.org/10.1038/s44160-023-00243-4.

(121) Negishi, E.; King, A. O.; Klima, W. L.; Patterson, W.; Silveira, A., Jr. Conversion of methyl ketones into terminal acetylenes and (E)-trisubstituted olefins of terpenoid origin. *The Journal of Organic Chemistry* **1980**, *45* (12), 2526-2528. DOI: https://doi.org/10.1021/jo01300a060.

(122) Negishi, E.-i. K., Anthony O. and M. Tour, James Conversion of methyl ketones into terminal alkynes: (E)-buten-3-ynyl-2,6,6-trimethyl-1-cyclohexane. *Organic Synth.* **1986**, *64*, 44. DOI: https://doi.org/10.15227/orgsyn.064.0044.

(123) Burgess, K.; Liu, L. T.; Pal, B. Asymmetric syntheses of optically active .alpha.,.beta.-disubstituted .beta.-amino acids. *The Journal of Organic Chemistry* **1993**, *58* (17), 4758-4763. DOI: https://doi.org/10.1021/jo00069a052.

(124) Ernst, A.; Gobbi, L.; Vasella, A. Orthogonally protected dialkynes. *Tetrahedron Letters* **1996**, *37* (44), 7959-7962. DOI: https://doi.org/https://doi.org/10.1016/0040-4039(96)01838-2.

(125) Li, Y.; Zhao, M.; Wang, J.; Liu, K.; Cai, C. Biofunctionalization of a “Clickable” Organic Layer Photochemically Grafted on Titanium Substrates. *Langmuir* **2011**, *27* (8), 4848-4856. DOI: https://doi.org/10.1021/la104853t.

(126) Oberg, K. M.; Cochran, B. M.; Cook, M. J.; Rovis, T. The Catalytic Alkylative Desymmetrization of Anhydrides in a Formal Synthesis of Ionomycin. *Synthesis* **2018**, *50* (22), 4343-4350. DOI: https://doi.org/10.1055/s-0037-1610108.

(127) Sano, T.; Ohashi, K.; Oriyama, T. Remarkably Fast Acylation of Alcohols with Benzoyl Chloride Promoted by TMEDA. *Synthesis* **1999**, *1999* (07), 1141-1144. DOI: https://doi.org/10.1055/s-1999-3521.

(128) Bowman, R. A.; Stock, J. R.; Jackson, J. A. Improved Synthesis Of Bis(2,2,2-trifluoroethyl) Phosphorochloridate. *Organic Preparations and Procedures International* **1999**, *31* (2), 230-231. DOI: https://doi.org/10.1080/00304949909355721.

(129) Still, W. C.; Kahn, M.; Mitra, A. Rapid chromatographic technique for preparative separations with moderate resolution. *The Journal of Organic Chemistry* **1978**, *43* (14), 2923-2925. DOI: https://doi.org/10.1021/jo00408a041.

(130) Mori, M.; Washioka, Y.; Urayama, T.; Yoshiura, K.; Chiba, K.; Ban, Y. Palladium-catalyzed carbonylation. A new synthesis of .alpha.-methylene .gamma.-, .delta.-, .epsilon.-lactams and lactones including bicyclic lactams of pyrrolizidine and indolizidine skeletons. *J. Org. Chem.* **1983**, *48* (22), 4058-4067. DOI: https://doi.org/10.1021/jo00170a037.

(131) Kan, S. B.; Anderson, E. A. A cascade palladium-mediated cross-coupling/electrocyclization approach to the construction of fused bi- and tricyclic rings. *Org Lett* **2008**, *10* (11), 2323-2326. DOI: https://doi.org/10.1021/ol8007952. From NLM.

(132) Krieger, J.; Smeilus, T.; Kaiser, M.; Seo, E. J.; Efferth, T.; Giannis, A. Total Synthesis and Biological Investigation of (-)-Artemisinin: The Antimalarial Activity of Artemisinin Is not Stereospecific. *Angew. Chem. Int. Ed.* **2018**, *57* (27), 8293-8296. DOI: https://doi.org/10.1002/anie.201802015. From NLM.

(133) Li, M.; Datta, S.; Barber, D. M.; Dixon, D. J. Dual Amine and Palladium Catalysis in Diastereo- and Enantioselective Allene Carbocyclization Reactions. *Organic Letters* **2012**, *14* (24), 6350-6353. DOI: https://doi.org/10.1021/ol303128s.

(134) Liu, Z. L., Renrong; Gu, Yugui. Synthesis of methyl (+)-(1R,3R)-trans-chrysanthemate from (-)-α-pinene. *Huaxue Xuebao* **1987**, *45* (9), 887-892.

(135) Heinrich, M.; Murphy, J. J.; Ilg, M. K.; Letort, A.; Flasz, J. T.; Philipps, P.; Fürstner, A. Chagosensine: A Riddle Wrapped in a Mystery Inside an Enigma. *Journal of the American Chemical Society* **2020**, *142* (13), 6409-6422. DOI: https://doi.org/10.1021/jacs.0c01700.

(136) Kolaříková, V.; Rybáčková, M.; Svoboda, M.; Kvíčala, J. Ring-closing metathesis of prochiral oxaenediynes to racemic 4-alkenyl-2-alkynyl-3,6-dihydro-2H-pyrans. *Beilstein Journal of Organic Chemistry* **2020**, *16*, 2757-2768. DOI: https://doi.org/10.3762/bjoc.16.226.